Chem Soc Rev

# Hydrosulfide Complexes of the Transition Elements: Diverse Roles in Bioinorganic, Cluster, Coordination, and Organometallic Chemistry



| | |
|---|---|
| Journal: | *Chemical Society Reviews* |
| Manuscript ID | CS-SYN-08-2019-000570.R2 |
| Article Type: | Review Article |
| Date Submitted by the Author: | 25-Mar-2020 |
| Complete List of Authors: | Pluth, Michael; University of Oregon, Chemistry and Biochemistry<br>Tonzetich, Zachary; University of Texas at San Antonio, Chemistry |
| | |

# Hydrosulfide Complexes of the Transition Elements: Diverse Roles in Bioinorganic, Cluster, Coordination, and Organometallic Chemistry

*Michael D. Pluth*[a,‡] *and Zachary J. Tonzetich*[b,‡]

[a] Department of Chemistry and Biochemistry, Materials Science Institute, Knight Campus for Accelerating Scientific Impact, Institute of Molecular Biology, University of Oregon, Eugene, OR 97403 USA.

[b] Department of Chemistry, University of Texas at San Antonio, San Antonio, TX 78249 USA.

**Abstract**

Sulfur-based ligands are versatile donors that play important roles in a wide array of subdisciplines of inorganic chemistry including organometallic chemistry, bioinorganic chemistry, and cluster science. Despite the breadth of compounds containing sulfur-based ligands, those containing the simplest mercapto group, hydrosulfide ion ($HS^-$), are significantly less developed. The acceptance of $H_2S/HS^-$ as important biological signaling compounds during the last decade have engendered a renewed interest in the chemistry of $H_2S$ and the hydrosulfide ion. Bioinorganic reactivity of hydrosulfide, however, is only one aspect of its fascinating chemistry, much of which revolves around its interactions with transition metal ions. The coordination of $HS^-$ to *d*-block elements produces a unique class of substances that differ in significant ways from more ubiquitous metal thiolates. This review examines the preparation, structure, spectroscopy, and reactivity of such compounds and the roles they play across several fields of chemistry including biological, organometallic, and coordination chemistry

## 1. Introduction

The chemistry of thiolate ligands has occupied a central place in the consciousness of coordination chemists from the very earliest days of the field.[1-5] These versatile ligands find numerous roles across the subdisciplines of inorganic chemistry from organometallics and bioinorganic chemistry, to cluster science. Yet despite the wealth of compounds reported to date featuring thiolate ligands, those containing the simplest sulfhydryl group, hydrosulfide ion ($HS^-$), have been mostly relegated to the status of curiosities. The lack of prominence of the hydrosulfide ion in inorganic chemistry is especially surprising given that its lighter congener, hydroxide ($HO^-$), is among the most commonly encountered ligands in coordination complexes. Challenges associated with manipulating $HS^-$ account in large part for this discrepancy. Unlike hydroxide, the conjugate acid of hydrosulfide, $H_2S$, is a toxic gas and not a component of typical reaction milieus. Moreover, the ability of sulfur to catenate provides a myriad of decomposition pathways for hydrosulfide complexes that are not relevant in the chemistry of hydroxide. In addition, monometallic metal hydrosulfides often are functional intermediates en route to formation of multimetallic sulfide-bridged complexes, which further complicates isolation and characterization in non-equilibrium mixtures. In many cases, the use of sterically- hindered ligands has enabled the formation of otherwise unisolable complexes. These challenges notwithstanding, the coordination chemistry of hydrosulfide ion and related hydropolysulfides ($HS_n^-$) has played an important, albeit underappreciated, role in the development of several areas of molecular science. Recently, renewed focus has been cast on the chemistry of hydrosulfide ion and related small sulfur-containing molecules as the importance of $H_2S$ as a physiological signaling agent has gained attention.[6-12] Biological roles for the hydrosulfide ion, however, encompass only one aspect of its fascinating chemistry. By in large, this chemistry has revolved around its interactions with

transition metal ions. The coordination of $HS^-$ to *d*-block elements produces a unique class of substances that differ in significant ways from more ubiquitous metal thiolates. This review will examine the preparation, structure, spectroscopy, and reactivity of such compounds and the roles they play across several fields of chemistry.

Transition metal hydrosulfide complexes are defined as those substances possessing at least one ligand of formula $HS^-$. They can be distinguished from metal thiolates and metal sulfides by the presence of a hydrogen atom on sulfur. In the present review, we have elected to focus on examples of these compounds that have been isolated and characterized unambiguously, ideally through structural means, with particular emphasis on identification of the sulfur-bound H atom. We also pay mind to complexes of hydrogen sulfide ($H_2S$), as these species share many of the same features as their hydrosulfide counterparts. Not covered here are species generated transiently in the gas phase or in low-temperature matrices. We note that this field was reviewed previously nearly two decades ago in a pair of articles published in 2001.[13, 14] Since that time, several other reviews have appeared which tangentially cover specific aspects of hydrosulfide complexes.[9, 15, 16] However, no comprehensive treatment of this area has appeared in the intervening 19 years to account for new developments in the field and highlight the common themes encountered in the chemistry of this unique class of ligands. In the following contribution, we have elected to organize the review not by element, but instead by the roles played by transition metal hydrosulfide complexes in different areas of chemistry.

## *1. Definition and Basic Properties of Sulfur, $H_2S$, and Hydrosulfide Ligands.*

Sulfur is the 10$^{th}$ most abundant element in the universe and 15$^{th}$ most abundant element in Earth's outer crust.[17] When comparing basic physical properties, sulfur is more polarizable than

oxygen, larger (covalent radius: 106 versus 66 pm), and less electronegative (2.58 versus 3.44; Pauling electronegativity scale).[18] Sulfur has a wide range of accessible oxidation states, ranging from −2 in thiols and $H_2S$ to +6 in sulfate. In its reduced $S^{2-}$ state, sulfur commonly forms bonds with hydrogen, carbon, or electropositive metals to form thioethers, thiols/$H_2S$, or metal sulfides, respectively. Hydrosulfide has a concerted two-electron reduction potential $E°'(HS_2^-, H^+/2HS^-)$ of −0.230 V (versus SHE),[19] which is similar to that for cysteine E°′(cystine/cysteine) = −0.245 V.[20] The one-electron reduction potential for hydrosulfide $E°'(S^{\bullet-}, H^+/HS^-)$ of +0.92 V[21] is also close to that for cysteine ($E°'(RS^{\bullet}, H^+/RSH)$ = ~+0.9 V).[19] In aqueous solution, $H_2S$ acts as a weak acid ($pK_a$ = 6.90 at 25 °C; 6.76 at 37 °C) with the second deprotonation event ($HS^- \leftrightarrow S^{2-} + H^+$) being inaccessible ($pK_a$ = 17-19) under normal biological conditions.[22] At physiological pH (7.4 at 37 °C), $H_2S$ exists primarily as $HS^-$ (~80%), with the remaining 20% in the diprotic, undissociated form. Because $HS^-$ is the main physiological form of $H_2S$, this anionic protonation state is likely to affect much of the observed chemical biology of $H_2S$. In aqueous solutions, the distinct chemistry of $H_2S$ versus $HS^-$ is often difficult to separate due to the rapid equilibration between these two protonation states. To combat this challenge, numerous investigations of biomimetic inorganic compounds in aprotic solvents have used $H_2S$ or organic-soluble forms of $HS^-$, such as $NBu_4SH$,[23] to directly probe the differential reactivity.

The bond S-H bond dissociation energy of $H_2S$ is 90 kcal/mol, which is similar to the metal-sulfur bond strength with many transition metals. This similarity can facilitate the thermodynamic formation metal-sulfur bonds. Moreover, metal sulfides are often highly-insoluble products, with low $K_{sp}$ values including MnS ($7.0 \times 10^{-19}$), FeS ($4.0 \times 10^{-19}$), NiS ($3.0 \times 10^{-21}$), ZnS ($1.6 \times 10^{-23}$), CuS ($8.0 \times 10^{-37}$), and $Cu_2S$ ($1.2 \times 10^{-49}$).[24] The nature of these solubility equilibria coupled with the properties of $H_2S$ discussed above contribute to the difficulty in isolating well-defined metal

hydrosulfide species. Yet these factors also serve to highlight the importance of understanding the interactions, metals, and ligand environments that facilitate stable metal hydrosulfide formation.

*1.2 Binding Modes of $HS^-$.*

The hydrosulfide ion is capable of both terminal and bridging binding modes (both $\mu_2$ and $\mu_3$), which is similar to many X-type ligands. In all cases, the unambiguous characterization of hydrosulfide complexes poses a unique challenge given the difficulty in locating H atoms by X-ray crystallography. This situation is made even more difficult in cases where the complex contains other ligands capable of protonation (e.g. oxos, sulfidos, etc.) or when the oxidation state of the metal is ambiguous or not confirmed directly by complementary spectroscopic methods. For complexes with terminal metal sulfide groups, the metal-sulfur bond distance can help to inform whether the sulfur donor is acting as a –1 (e.g. M-SH, M-SR) or –2 (e.g M=S) ligand. Spectroscopic identification of the S-H unit, when possible, is therefore of great importance. For diamagnetic complexes, the S-H proton resonance appears over a relatively broad chemical shift range and is dependent on the local environment and charge state of the metal. For paramagnetic complexes, the location of the hydrosulfide SH is highly dependent on the metal, spin state, and isotropic shielding. The S-H bond can also often be observed directly using infrared (IR) spectroscopy. In metal hydrosulfides, the $\nu_{S\text{-}H}$ vibrations typically appear between 2450 – 2650 $cm^{-1}$. We note, however, that there are many instances in which the M-SH group is characterized directly by $^1H$ NMR spectroscopy and/or X-ray crystallography, but for which the S-H stretch is not observed by vibrational spectroscopy. This observation suggests that the S-H vibrational mode may be coupled to other modes within the metal complex, thereby making IR spectroscopy alone

insufficient for confirming or excluding the presence of a metal hydrosulfide. Section 4 of this Review discusses the characterization of metal hydrosulfides in more detail.

*1.3 Organization of the Review.*

This review is divided into to two main sections, the first of which focuses on the role of metal hydrosulfides in biological contexts. This section includes a brief discussion of biological examples of structurally-characterized M-SH interactions. The bulk of this section focuses on investigations into the generation of biomimetic metal hydrosulfides to understand trends in reactivity. Also included in this section are transition-metal inspired approaches to sensing $H_2S/HS^-$ through the generation of metal hydrosulfides as an example of pertinent applications of bioinorganic chemistry. The second section focuses on metal hydrosulfides in organometallic, coordination, and cluster chemistry. This section highlights the large diversity of transition metal hydrosulfides and how their chemistry has impacted many areas of inorganic chemistry. The section begins with a description of hydrosulfide complexes in the context of their roles in the production and consumption of molecular hydrogen. Relevance to the chemistry of hydrogen provided much of the early impetus for the study of transition element hydrosulfides given their resemblance to metal-sulfide surfaces employed for hydrodesulfurization, and the potential to catalytically generate $H_2$ from $H_2S$. The section then goes on to describe the chemistry of hydrosulfides in organometallic compounds, coordination complexes, and finally in the preparation and reactivity of metal clusters. The review concludes with a discussion of characterization methods for metal hydrosulfides and a brief outlook of what lies in store for this unique class of compounds.

## 2. Metal Hydrosulfides and Related Species in Biology

*2.1 Subsection Introduction.*

Hydrogen sulfide ($H_2S$) and related reactive sulfur species play important roles in the geochemistry and evolution of life on Earth. During the "iron-sulfur' world and prior to oxygenation of Earth's atmosphere, $H_2S$ was likely a primary energy source for emerging life on Earth.[25-27] Not only can $H_2S$ and other reactive sulfur species provide reducing equivalents for energy production, but they also likely formed some of the first key structural motifs in the form of iron-sulfur and other metal-sulfur clusters.[28, 29] Remnants of these early metal-sulfide species can still be found in contemporary terrestrial biology in which iron and molybdenum sulfides form important cofactors required for electron transfer reactions in different enzymatic systems. In addition to serving a likely role in the energy economy of developing life on earth, $H_2S$ and related reactive sulfur species also provided a source of sulfur in the synthesis of emerging biomolecules. For example, both cysteine and methionine have been detected in products of prebiotic conditions, including those simulated in Miller's 1958 experiments.[30, 31] Similarly, the atmospheric gas carbonyl sulfide (COS), which is often generated near geothermal vents and hot springs, has been implicated in early peptide bond formation between amino acids.[32-34] More recently, interest in biological aspects of $H_2S$ has increased significantly after the initial discovery by Kimura that $H_2S$ functions as an endogenous neuromodulator and a series of reports on the ability of $H_2S$ to relax smooth muscle cells.[35] Further revitalization was catalyzed by the discovery from Roth that inhalation of 20-80 ppm of $H_2S$ inhalation by mice resulted in a decreased metabolic state, often described as "suspended animation," in which the core body temperature, pulse and respiration of the mouse all decreased substantially, and which could be reversed by reintroduction of oxygen.[36]

The high nucleophilicity and metallophilicity of $H_2S$ provide a number of mechanisms by which $H_2S$ can exert biological action. Focusing on the interactions of $H_2S$ with bioinorganic transition metal compounds, two primary modes of reaction include reduction and/or sulfur ligation. Metal reduction by $H_2S$ results in sulfide oxidation to $HS^{\bullet}$ and subsequent formation of oxidized sulfur products, many of which likely result in down-stream signaling processes. As examples of this reactivity, both free hemin and methemoglobin oxidize $H_2S$ to thiosulfate, with the later example also generating Fe-ligated hydropolysulfides.[37, 38] Similarly, myeloperoxidase carries out the catalytic oxidation of $H_2S$ under aerobic conditions to generate sulfane sulfur species, which can result in protein persulfidation.[39] Complementing these interactions between $H_2S$ and oxygen, metal-mediated sulfide oxidation also likely facilitates crosstalk between reactive sulfur and nitrogen species.[40, 41] For example, the heme mediated sulfide oxidation in mitochondria has been implicated in catalyzing HNO formation from nitrite and $H_2S$.[42] Complementing these redox reactions, ligation of $H_2S$ or $HS^-$ to metals to form stable metal hydrosulfides often results in reversible or irreversible inhibition of different pathways involving metalloenzymes. One classic example of this chemistry, key to the above example of $H_2S$-mediated suspended animation, is irreversible binding of $H_2S$ cytochrome c oxidase (CcO), the terminal acceptor in the mitochondrial electron transport chain, and subsequent inhibition.[43] These as well as other mechanisms of action are continuing to emerge and diversify the landscape of biological activity attributed to $H_2S$ and related reactive sulfur species. Rather than focus on these rapidly expanding roles in contemporary biochemistry, biology, and physiology, we refer the interested reader to a number of recent reviews on the topic.[6-12]

*2.2 Iron-Sulfur Clusters.*

Iron-sulfur assemblies in Nature comprise key structural and electron-transfer cofactors required for different biochemical processes.[44-46] Typically supported by cysteine-rich coordination environments and bridging sulfide ligands, iron-sulfur assemblies have significant structural diversity and are readily found in bacteria, archaea, and eukaryotes. Common examples of iron-sulfur clusters include rubredoxin ($Cys_4Fe$), various ferredoxins including $[Fe_2S_2]$, Rieske, $[Fe_3S_4]$, and $[Fe_4S_4]$ cores, as well as higher nuclearity $[Fe_8S_6]$, $[Fe_8S_7]$, $[Fe_8S_8]$, and $[Fe_{16}S_{16}]$ clusters.[47-52] Iron-sulfur clusters provide structural frameworks and also participate in electron transfer and redox reactions during which the interconversion between different iron-sulfur geometric motifs is common.[53] Similarly, iron sulfur clusters have been implicated in iron storage and transport.[54] Inspired by the prevalence and importance of protein-bound iron-sulfur clusters, biomimetic ligand architectures have been used to access iron-sulfur clusters with well-defined coordination environments in biomimetic compounds. In addition to providing insights into the stability, reactivity, and redox properties of iron-sulfur motifs, a number of synthetic iron-sulfur clusters have been prepared that feature terminal hydrosulfide moieties.

*2.2.1. $[Fe_4S_4]$ Hydrosulfide Complexes.* The most simple synthetic analogue of the $[Fe_4S_4]$ ferredoxin core is $[Fe_4S_4(SH)_4]^{2-}$ (**1**), which was first reported by Müller and co-workers by reacting $CpFe(CO)_2I$ with $H_2S$ in a DMF/MeOH/$Et_3N$ solvent mixture under aerobic conditions (Scheme 1).[55] $[CpFe(CO)_2]_2$ can also be used as the iron-containing synthon to access $[Fe_4S_4(SH)_4]^{2-}$ under identical conditions. Although the self-assembly of an $[Fe_4S_4]$ core under aerobic conditions is unusual, the authors highlight the analogous reaction of $FeSO_4{\cdot}7H_2O$ with $H_2S$ in the presence of $PPh_4Br$ to yield $(PPh_4)_2[Fe_4S_4Br_4]$.[56] The isolated $(PPh_4)_2[Fe_4S_4(SH)_4]$ is isostructural to $(PPh_4)_2[Fe_4S_4X_4]$ (X = Cl, Br) and crystalized in the C2/c space group with a tetragonal distortion of the $[Fe_4S_4]$ core from the idealized $T_d$ symmetry to $D_{2d}$. The Mössbauer

parameters (77 K: $\delta$ = 0.45, $\Delta E_Q$ = 0.87 mm/s; 4.5 K: $\delta$ = 0.47, $\Delta E_Q$ = 1.27 mm/s) are consistent with the $[Fe_4S_4]^{2+}$ oxidation state, and X-ray crystallography confirmed the molecular structure with mean Fe-SH bond distance of 2.262 Å, although terminal S-H hydrogens were not explicitly refined. Vibrational analysis of $[Fe_4S_4(SH)_4]^{2-}$ revealed an Fe-S(H) vibration at 342 $cm^{-1}$.

**Scheme 1**. Synthesis and hydrosulfide exchange of $[Fe_4S_4(SH)_4]^{2-}$.

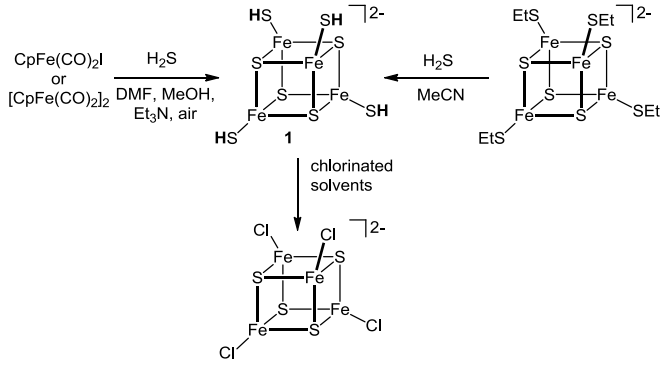


The same $[Fe_4S_4(SH)_4]^{2-}$ cluster was also prepared by Holm and co-workers in higher yields by bubbling $H_2S$ through a solution of $[Fe_4S_4(SEt)_4]^{2-}$ with either $PPh_4^+$, $NBu_4^+$, or $Pr_4N^+$ counterions under anaerobic conditions (Scheme 1).[57-59] The resultant $[Fe_4S_4(SH)_4]^{2-}$ salts were characterized by elemental analysis, X-ray crystallography, and also $^1H$ NMR spectroscopy, which revealed the terminal S-H resonance at $\delta$ = 47.6 ppm. When compared to the earlier $[Fe_4S_4(SH)_4]^{2-}$ structure reported by Müller, X-ray analysis of the $Pr_4N^+$ salt revealed a cubane core structure closer to $T_d$ symmetry rather than the earlier-reported tetragonally distorted $D_{2d}$ symmetry. In efforts to further characterize the $[Fe_4S_4(SH)_4]^{n-}$ system, Holm and co-workers also prepared the more reduced $[Fe_4S_4(SH)_4]^{3-}$ cluster (**2**) by treating $[Fe(PEt_3)_2Cl_2]$ with $Et_4NSH/Na_2S$ in THF to provide $(Et_4N)_3[Fe_4S_4(SH)_4]\cdot Et_4NCl$ (Scheme 2).[59] X-ray analysis of $[Fe_4S_4(SH)_4]^{3-}$ revealed a mean Fe-SH bond distance of 2.317 Å, which as expected is longer than the mean 2.262 Å in the

one-electron oxidized $[Fe_4S_4(SH)_4]^{2-}$. Electrochemical characterization revealed $E_{1/2}$ = −1.08 V in MeCN for the $[Fe_4S_4(SH)_4]^{2-/3-}$ couple, which matches electrochemical data obtained from $[Fe_4S_4(SH)_4]^{2-}$. EPR spectra of $[Fe_4S_4(SH)_4]^{3-}$ showed an $S$ = ½ rhombic pattern at $g$ = 1.92, and also a $S$ = 3/2 signal at $g$ = 5.26, suggesting the presence of multiple spin states in the frozen DMF samples. As a whole, these investigations contributed clear bond metrics for the terminal hydrosulfide analogues in a larger study of $[Fe_4S_4(SR)_4]^{2-}$ and $[Fe_4S_4(SR)_4]^{3-}$ system, which demonstrated terminal hydrosulfide (SH) rather than thiolate (SR; R= alkyl, aryl) capping ligands do not significantly change Fe-S bond metrics of the $[Fe_4S_4]$ core. Importantly, these bond metric analyses were then applied to confirm that exposure of $[Fe_4S_4(SH)_4]^{2-}$ to chlorinated solvents, such as $CH_2Cl_2$, resulted in conversion to $[Fe_4S_4Cl_4]^{2-}$ (Scheme 1), thus providing an additional metric to distinguish the otherwise difficult to differentiate S versus Cl atoms in Fe-SH/Fe-Cl cubane structures.[59]

**Scheme 2.** Synthesis of $[Fe_4S_4(SH)_4]^{3-}$.

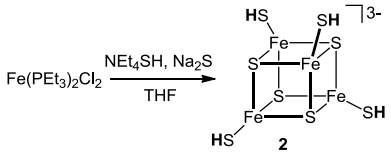


*2.2.2 Site-Differentiated $[Fe_4S_4]$ Platforms.* In the context of building complexity into the $[Fe_4S_4]$ core, iron sulfur clusters bearing 3-fold symmetric site differentiated ligands have also been used to access terminal Fe-SH species (Scheme 3). For example, Holm and co-workers showed that treatment of site differentiated $[Fe_4S_4(LS_3)(SEt)]^{2-}$ with $H_2S$ in pyridine or acetone resulted in formation of the substituted cluster $[Fe_4S_4(LS_3)(SH)]^{2-}$ (**3**), in an equilibrium process ($K_{eq}$ = 120 ± 20 $M^{-1}$; pyridine, 298 K).[60] Further characterization of $[Fe_4S_4(LS_3)(SH)]^{2-}$ revealed a

SH resonance at δ = 46.5 ppm in the $^1$H NMR spectrum, which is characteristic of a terminal Fe-SH moiety, and a UV-vis absorbance with $\lambda_{max}$ = 482 nm (ε = 9,500 $M^{-1}$ $cm^{-1}$; MeCN). Mössbauer spectroscopy revealed δ = 0.46 and $\Delta E_Q$ = 1.15 mm/s (4.2 K) and electrochemical measurements demonstrated $E_{1/2}$ = −1.06 V in MeCN, both of which are similar to the parent $[Fe_4S_4(SH)_4]^{2-}$. In solution, $[Fe_4S_4(LS_3)(SH)]^{2-}$ is in equilibrium with the $\mu$-S double cubane, $\{[Fe_4S_4(LS_3)]_2S\}^{4-}$, and free $H_2S$. Double cubane $\{[Fe_4S_4(LS_3)]_2S\}^{4-}$ was characterized by $^1$H NMR spectroscopy, which showed the disappearance of the characteristic Fe-SH resonance, as well as by Mössbauer spectroscopy, which revealed parameters of δ = 0.47 and $\Delta E_Q$ = 1.15 mm/s, which are similar to those for $[Fe_4S_4(LS_3)(SH)]^{2-}$. Treatment of $\{[Fe_4S_4(LS_3)]_2S\}^{4-}$ with excess $H_2S$ resulted in formation of the parent $[Fe_4S_4(SH)_4]^{2-}$ (**1**) en route to a black, otherwise uncharacterized polymeric product. All of the above site-differentiated clusters were also characterized by $^1$H NMR isotropic shift measurements, which is useful for differentiating otherwise similar iron-sulfur cluster motifs. Similar generation of site differentiated $[Fe_4S_4(LS_3)(SH)]^{2-}$ species have also been reported with differentially-substituted tridentate site-differentiated ligands.[61]

**Scheme 3**. Terminal hydrosulfide $[Fe_4S_4]$ platforms built on site-differentiated ligands.

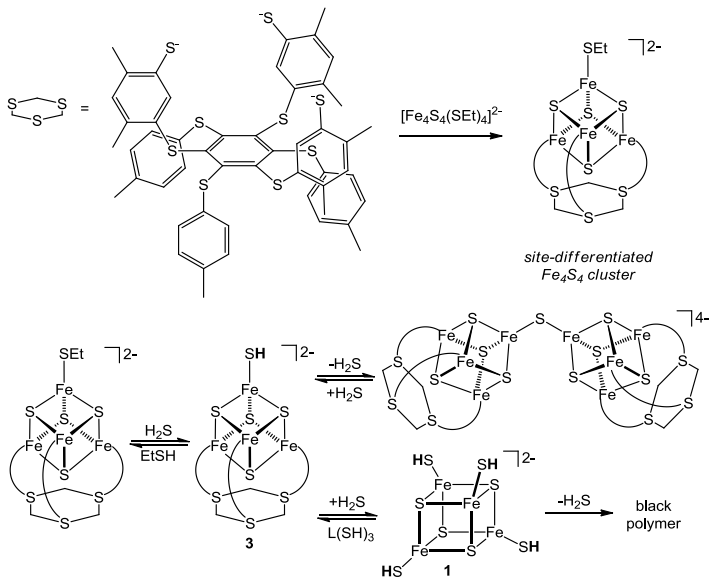


The site differentiated $[Fe_4S_4(LS_3)(SH)]^{2-}$ is also a useful synthon for accessing bridged cubane structures with both salen and porphyrin-based iron systems (Scheme 4). For example, Holm and co-workers showed that treatment of $[Fe_4S_4(LS_3)(SH)]^{2-}$ with $[Fe^{III}(salen)]_2O$ and $[NEt_3H][HS]$ generates the sulfide bridged $[Fe_4S_4(LS_3)\text{-}S\text{-}Fe^{III}(salen)]^{2-}$, which was characterized by $^1H$ NMR and UV-vis spectroscopy (Scheme 4).[60] Similarly, treatment of $[Fe_4S_4(LS_3)(SH)]^{2-}$ with different octaethylporphyrin (OEP) derivatives, including $[Fe^{III}(OEP)]_2O$, $[Fe^{III}(OEP)(OMe)]_2$, $[Fe^{III}(OEP)(OC(Me)=CH_2)]$, and $[Fe^{III}(OEP)(OClO_3)]$, generated sulfide bridged $[Fe_4S_4(LS_3)\text{-}S\text{-}Fe^{III}(OEP)]^{2-}$, which was characterized by $^1H$ NMR and UV-vis spectroscopy as well as isotropic shift measurements. Alternatively, the same $[Fe_4S_4(LS_3)\text{-}S\text{-}Fe^{III}(OEP)]^{2-}$ product can be generated from treatment of the $S_2$-bridged precursor, $\{[Fe_4S_4(LS_3)]_2S_2\}^{4-}$, with $Fe^{II}(OEP)$. Once formed, the bridged $[Fe_4S_4(LS_3)\text{-}S\text{-}Fe^{III}(OEP)]^{2-}$ can be converted to the parent $[Fe_4S_4(LS_3)(SH)]^{2-}$ by treatment with $H_2S$ or $H_2O$, with subsequent extrusion of [Fe(OEP)(SH)] and $[Fe(OEP)]_2O$, respectively.

**Scheme 4**. Reactivity of $[Fe_4S_4(LS_3)(SH)]^{2-}$ (**3**) to access salen- and porphyrin-ligated $[Fe_4S_4]$ adducts.

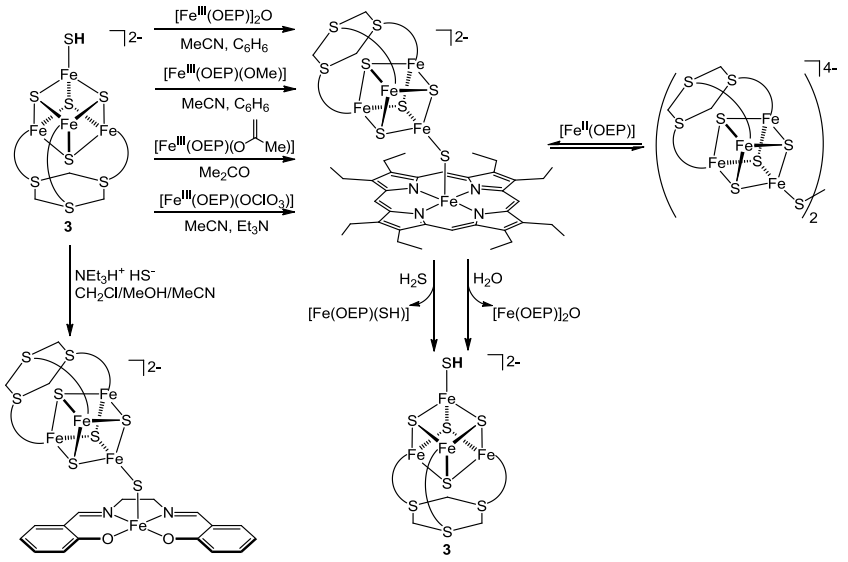


*2.2.3 Heterobimetallic Iron Sulfur Clusters.* In addition to $[Fe_4S_4]$ systems, mixed-metal cuboidal site-differentiated $[NiFe_3S_4]$ compounds with terminal hydrosulfide ligands have been prepared. Using the same tridentate site-differentiated ligand as in **3**, Holm and co-workers demonstrated that treatment of $[(Ph_3P)NiFe_3S_4(LS_3)]^{3-}$ with $NEt_4SH$ in MeCN afforded the ligand substitution product $[(HS)NiFe_3S_4(LS_3)]^{3-}$ (**4**, Scheme 5).[62] The resultant product maintained the $[NiFe_3S_4]^{1+}$ $S$ = 3/2 core and X-ray crystallography revealed a 2.284 Å Ni-S bond distance, with the terminal hydrosulfide ligand disordered over two positions. The S-H resonance was not observed in the $^1$H NMR spectrum of **4**, likely due to the proximity to the Ni center.

**Scheme 5**. Synthesis of $[(HS)NiFe_3S_4(LS_3)]^{3-}$ (**4**).

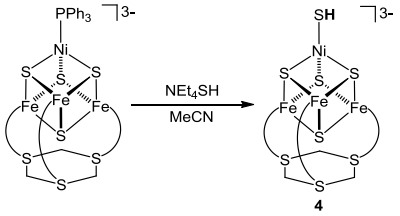


Heterobimetallic iron-sulfur clusters with hydrosulfide ligands have also been prepared using group VI and V elements ligated by trispyrazolylborate (Tp) ligands.[63, 64] For example, Holm and co-workers demonstrated that treatment of $[(Tp)MoFe_3S_4(PEt_3)_3]^+$ with three equiv. of $NEt_4SH$ results in a ligand substitution reaction to form $[(Tp)MoFe_3S_4(SH)_3]^{2-}$ (**5**), which was characterized by X-ray crystallography, with Fe-S bond lengths of 2.293(1) Å and satisfactory elemental analysis (Scheme 6). Electrochemical characterization revealed $E_{1/2}$ = −0.89 V in MeCN. Alternatively, cluster **5** can also be accessed by reduction of $[(Tp)MoFe_3S_4(PEt_3)_3]^+$ with $BH_4^-$ to form edge-bridged double cubane $[(Tp)_2Mo_2Fe_6S_8(PEt_3)_4]$, followed by treatment with excess $HS^-$. By contrast, treatment of $[(Tp)_2Mo_2Fe_6S_8(PEt_3)_4]$ with 3 equiv. of $NEt_4SH$ results in formation of the bis(hydrosulfide) $P^N$-type cluster $[(Tp)_2Mo_2Fe_6S_9(SH)_2]^{3-}$ (**6**), which was characterized by X-ray crystallography, revealing Fe-S bond distances of 2.280(3) and 2.295(3) Å. Electrochemical characterization of **6** demonstrated three distinct redox couples with $E_{1/2}$ = −0.43, −0.71, and −1.09 V in MeCN, and Mössbauer spectroscopy produced an isomer shift of $\delta$ = 0.55 and quadrupole splitting of $\Delta E_Q$ = 0.62 mm/s. Alternatively, cluster **6** can be generated by treatment of $[(Tp)_2Mo_2Fe_6S_8Cl_4]^{4-}$ with excess NaSH. Monocuboidal $[(Tp)MoFe_3S_4(SH)_3]^{2-}$ can also be treated with $[(Tp)_2Mo_2Fe_6S_8(PEt_3)_4]$ to access equilibrium formation of $[(Tp)_2Mo_2Fe_6S_9(SH)_2]^{3-}$ (Scheme 6). A final route to prepare the $[(Tp)_2Mo_2Fe_6S_9(SH)_2]^{3-}$ cluster is by hydroselenide displacement of the analogous $[(Tp)_2Mo_2Fe_6S_9(SeH)_2]^{3-}$ (**7**) with 2 equiv. of $NEt_4SH$. Extrusion of $H_2S$ from the

$[(Tp)_2Mo_2Fe_6S_9(SH)_2]^{3-}$ cluster results in formation sulfide-bridged $\{[(Tp)_2Mo_2Fe_6S_9](\mu_2\text{-}S)\}_2^{5-}$, which was isolated and structurally characterized by X-ray crystallography.

**Scheme 6**. Reactivity and interconversion of mixed $[Fe_3MoS_4]$ clusters containing terminal hydrosulfide ligands.

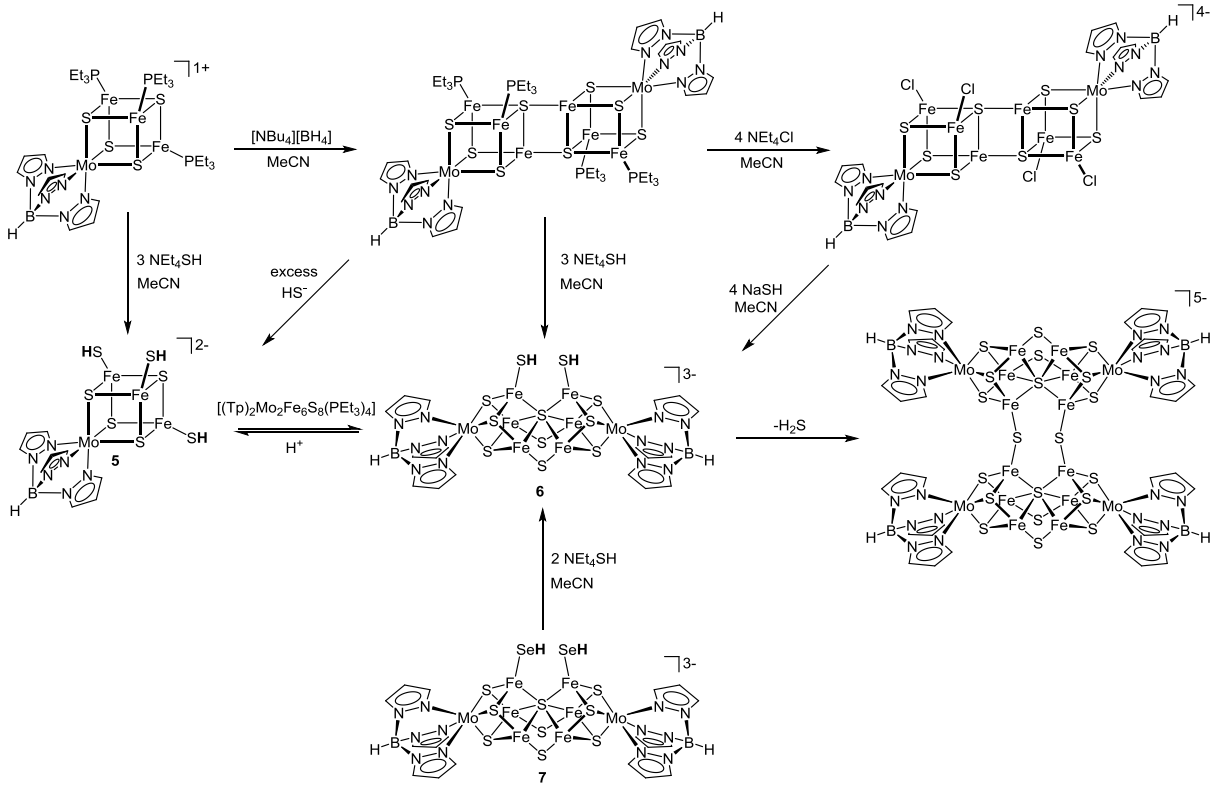


Analogous heterobimetallic $[Fe_3WS_4]$ clusters have also been used to support terminal hydrosulfido ligands. For example, Holm and co-workers showed that reaction of $[(Tp^*)WFe_3S_4Cl_3]^{2-}$ ($Tp^*$ = *tris*(3,5-dimethylpyrazolyl)borate), with excess $PEt_3$, $NBu_4BH_4$, and $NEt_4SH$ enabled the isolation of $[(Tp^*)_2W_2Fe_5S_9Na(SH)(MeCN)]^{3-}$ (**8**), which is analogous to $[(Tp)_2Mo_2Fe_6S_9(SH)_2]^{3-}$ and exhibits a core topology similar to the $P^N$ cluster of nitrogenase

(Scheme 7).[65] The composition of $[(Tp^*)_2W_2Fe_5S_9Na(SH)(MeCN)]^{3-}$ was confirmed by X-ray crystallography, which evinced an Fe-SH bond distance of 2.34 Å.

**Scheme 7**. Synthesis of heterbimetallic $[(Tp^*)_2W_2Fe_5S_9Na(SH)(MeCN)]^{3-}$ (**8**).

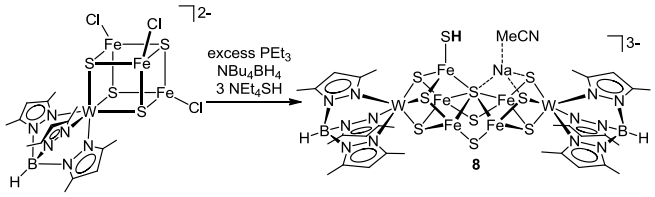


In addition to Mo- and W-heterobimetallic iron-sulfur clusters, heterobimetallic cuboidal vanadium systems have also yielded related hydrosulfide compounds.[66, 67] Holm and co-workers demonstrated that treatment of $[(Tp)VFe_3S_4(PR_3)_3]^{1+}$ (R = Et, Bu) with excess $NEt_4SH$ results in formation of the hydrosulfide product $[(Tp)VFe_3S_4(SH)_3]^{2-}$ (**9**, Scheme 8). This product was characterized by $^1H$ NMR spectroscopy, although the hydrosulfide SH resonance was not observed. Structural characterization by X-ray crystallography revealed a Fe-S hydrosulfide bond distance of 2.297(1) Å. The 1-electron reduced analogue of this cluster can also be accessed through reduction of $[(Tp)VFe_3S_4(PR_3)_3]^{1+}$ with $[Cp_2Co]$ to yield edge-bridged double cubane $[(Tp)_2V_2Fe_6S_8(PEt_3)_4]$, which can be further reacted with excess $NEt_4SH$ to yield $[(Tp)VFe_3S_4(SH)_3]^{3-}$. Structural characterization by X-ray crystallography confirmed the structure and charge state, and the Fe-S hydrosulfide bond was elongated to 2.345(1) Å. To access more complex motifs, treatment of $[(Tp)_2V_2Fe_6S_8(PEt_3)_4]$ with 4 equiv. of $NEt_4SH$ resulted in formation of bis(hydrosulfide) $P^N$-type cluster $[(Tp)_2V_2Fe_6S_9(SH)_2]^{4-}$ (**10**), which was characterized by $^1H$ NMR spectroscopy, although the S-H resonance was again not observed. X-Ray crystallography

confirmed the molecular structure, and the Fe-S hydrosulfide bond length was determined to be 2.327(1) Å.

**Scheme 8.** Heterobimetallic vanadium iron-sulfur clusters with terminal hydrosulfide ligands.

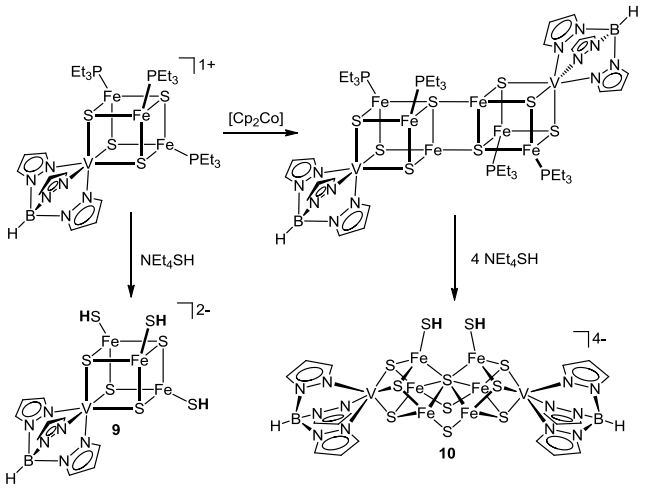


*2.2.4 Other FeS clusters.* Iron hydrosulfide compounds based on [2Fe-2S] core structures have also been reported. Such [2Fe-2S] cores play important roles in a number of enzymatic systems, including certain ferredoxins and Rieske proteins,[51] and related biomimetic clusters have furthered our understanding of how NO interacts with iron sulfur clusters to form mononitrosyl- and di-nitrosyl iron clusters (MNICs and DNICs, respectively).[68-72]

Expanding on chemistry of Roussin's Red Salt (RRS), Beck and Vilsmaier reported that acidification of $Na_2[Fe_2S_2(NO)_4]$ with HCl in water generated $(ON)_2Fe(\mu\text{-}SH)_2Fe(NO)_2$ (**11**), which is the corresponding acid of RRS (Scheme 9).[73] This transformation also occurred in organic solution by treatment of pentane-soluble $[AsPh_4]_2[Fe_2S_2(NO)_4]$ with $HBF_4$ or $CF_3CO_2H$. The $(ON)_2Fe(\mu\text{-}SH)_2Fe(NO)_2$ product was characterized by IR spectroscopy, which revealed an S-H stretch at 2546 $cm^{-1}$ and Fe-S stretch at 350 $cm^{-1}$, and also by mass spectrometry. The RRS acid

could be alkylated directly by treatment with MeI to form $(ON)_2Fe(\mu\text{-}SMe)_2Fe(NO)_2$ and could also be decomposed by the addition of excess HCl to generate the DNIC $[FeCl_2(NO)_2]^-$ and release $H_2S$.

**Scheme 9**. Generation and reactivity of $(ON)_2Fe(\mu\text{-}SH)_2Fe(NO)_2$ (**11**) and related structures.

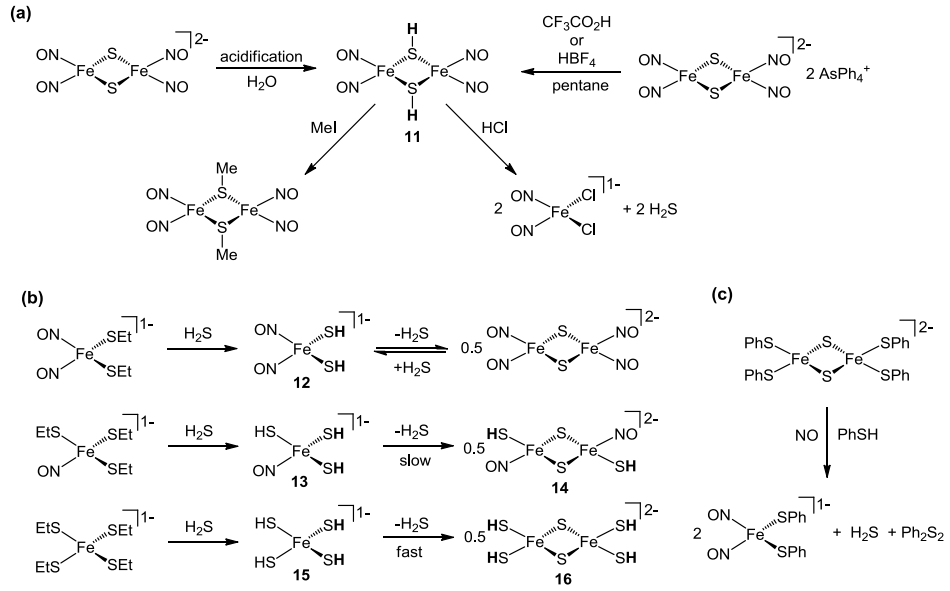


Liaw and co-workers demonstrated that RRS can also be generated from the spontaneous loss of $H_2S$ from the DNIC $[(HS)_2Fe(NO)_2]^-$ (**12**) in water.[74] This reaction is reversible and addition of $H_2S$ to an aqueous solution of $[(HS)_2Fe(NO)_2]^-$ regenerates RRS $[Fe_2S_2(NO)_4]^{2-}$. Alternatively, DNIC **12** can be accessed directly from reaction of $[(EtS)_2Fe(NO)_2]^-$ with $H_2S$ (Scheme 9b). In related chemistry, treatment of $[(EtS)_3Fe(NO)]^-$ with $H_2S$ in THF produces the unstable MNIC, $[(HS)_3Fe(NO)]^-$ (**13**), which spontaneously dimerizes with concomitant extrusion of $H_2S$ to form $[(NO)(HS)Fe(\mu\text{-}S)_2]_2^{2-}$ (**14**). This product was characterized by X-ray crystallography with an Fe-SH bond distance of 2.317 Å, and the S-H resonance was observed at 3.49 ppm in the $^1H$ NMR spectrum. Magnetic characterization of the product revealed that both ferric $\{Fe(NO)\}^7$ motifs are

antiferromagnetically coupled, which was also supported by DFT calculations. Further removing one nitrosyl ligand, the homoleptic tetrahydrosulfide $[(HS)_4Fe]^-$ (**15**) was generated by bubbling $H_2S$ through a solution of $[(EtS)_4Fe]^-$ resulting in an unstable product with EPR signals at $g$ = 9.30 and 4.39 consistent with a high-spin $Fe^{III}$ product. Compound **15** thermally decomposed to generate $[(HS)_2Fe(\mu\text{-}S)]_2^{2-}$ (**16**), which was confirmed by X-ray crystallography with Fe-SH bond distances of 2.3378(9) and 2.3072(9) Å. The $^1H$ NMR spectrum revealed the SH resonance at 36.6 ppm, with an isotropic shift consistent with the general ferric [2Fe-2S] core structure. In related [2Fe-2S] cluster chemistry, Kim and co-workers demonstrated that $[(PhS)_2Fe(\mu\text{-}S)]_2^{2-}$ reacts with NO gas and PhSH to generate the $[(PhS)_2Fe(NO)_2]^-$ DNIC with concomitant release of the oxidized $Ph_2S_2$ disulfide and also $H_2S$ gas, suggesting a possible mechanisms for NO and $H_2S$ crosstalk though FeS cluster chemistry (Scheme 9c).[75]

Although not aimed at biomimetic chemistry, iron carbonyl complexes with bridging hydrosulfide ligands have also been reported. For example, Seyferth and co-workers reported the formation of hydrosulfide-bridged $[Fe_2(CO)_6(\mu\text{-}SH)_2]$ (**17**) by reduction of $[Fe_2(CO)_6(\mu\text{-}S)_2]$ with $LiBEt_3H$ (Scheme 10).[76] More recently, Darensbourg and co-workers also demonstrated that **17** could be generated by protonation of $[Fe_2(CO)_6(\mu\text{-}SAuPPh_3)_2]$ with $HBF_4$.[77] The resultant hydrosulfide bridge product can react with different double-bond containing reactants to alkylate the bridging sulfide ligands. Brief examples of this reactivity are shown in Scheme 10. For example, treatment of **17** with formaldehyde and a primary amine results in formation of sulfide-bridged product $[Fe_2(CO)_6(\mu,\mu\text{-}\{SCH_2\}_2NR)]$. Similarly, treatment of $[(\mu\text{-}SH)_2\{Fe(CO)_3\}_2]$ with terminal olefins results in direct alkylation of both bridging hydrosulfide groups to form $[Fe_2(CO)_6(\mu\text{-}SR)_2]$, whereas treatment with 1,1-disubstituted terminal olefins generates the alkyl-bridged product.[78] Similar reactivity is also observed for alkynes, in which treatment with a

terminal alkyne results in formation of the germinal dithiolate bridging product, whereas treatment with an internal alkyne results in formation of the bridged vinylthiolate, bridging hydrosulfide product (**18**). Further experimental and computational investigations by Franz and co-workers on the S-H bond strengths and S-H bond activation chemistry in $[Fe_2(CO)_6(\mu\text{-}SH)_2]$ and related compounds were later reported.[79]

**Scheme 10.** Formation and general reactivity of $[Fe_2(CO)_6(\mu\text{-}SH)_2]$ (**17**).

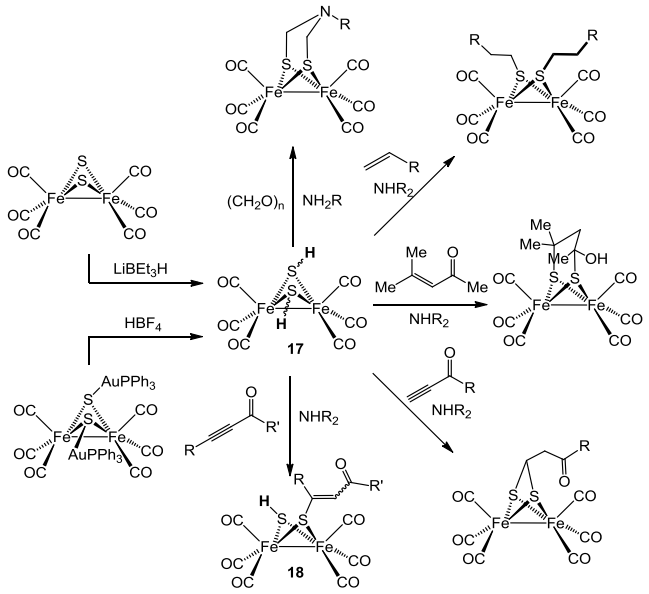


*2.3 Nonheme Diiron and Related Bimetallic Hydrosulfide Complexes*

Majumdar and co-workers recently reported a series of nonheme diiron(II) systems that mediate the desulfurization of aromatic and aliphatic thiols to generate terminal and bridging hydrosulfide complexes. Using dinucleating ligand environments, assembly of the diiron core in the presence of thiols was found to result in C-S bond cleavage to generate products of the form $[Fe_2(BPMP)(SH)_2(MeOH)_2]^+$ (**19**) and $[Fe_2(PhBIMP)(\mu\text{-}SH)(DMF)]^{2+}$ (**20**) (Scheme 11).[80] Both compounds were characterized by X-ray crystallography, X-ray photoelectron spectroscopy, IR

and MS. The *bis*-hydrosulfide **19** has Fe-S bond distances of 2.3832(12) and 2.3771(12) Å, an S-H stretch at 2510 $cm^{-1}$, and is stabilized by hydrogen bonding to co-crystallized MeOH in the X-ray structure. In comparison, the sulfide bridge in **20** has asymmetric Fe-S bond distances of 2.6637(2) and 2.395(2) Å and shows a S-H stretch at 2493 $cm^{-1}$. In a related system, Majumdar and co-workers also reported monohydrosulfide complexes with the *N*-Et-HPTB ligand scaffold by desulfurization of thiols.[81] Although treatment of the iron precursor and ligand with $HS^-$ in the presence of base led to intractable products, treatment with either $^t$BuSH or BnSH resulted in thiol C-S cleavage and formation of the diiron hydrosulfide complex $[Fe_2(N\text{-Et-HPTB})(SH)(H_2O)]^{2+}$ (**21**) as well as the DMF-coordinated $[Fe_2(N\text{-Et-HPTB})(SH)(DMF)_2]^{2+}$ (**22**). In **21**, the Fe-S bond distance is 2.344(4) Å with a $\nu_{SH}$ value of 2515 $cm^{-1}$. In **22**, the Fe-S bond distance is 2.349(2) Å and no IR band for the S-H moiety was detected. Treatment of **21** with $[Cp_2Fe]^+$ resulted in formation of the mixed-valence diiron(II,III)-hydrosulfide $[Fe_2(N\text{-Et-HPTB})(SH)(H_2O)(DMF)_2]^{3+}$ (**23**) which exhibited a $\mu_{eff}$ of 1.78 BM and an inter-valence charge transfer band at 1430 nm ($\varepsilon$ = 310 $M^{-1}cm^{-1}$). Much like the diiron(II) precursor, **23** showed a S-H stretch at 2515 $cm^{-1}$ by IR, but a significantly shorter Fe-S bond distance of 2.183(2) Å.

Using similar ligand scaffolds, Majumdar and co-workers also reported terminal and bridiging nonheme dicobalt(II) hydrosulfide complexes accessed by the C-S bond cleavage of thiols. Treatment of $Co(BF_4)_2$ with dinucleating ligand, base, and thiolate resulted in formation of $[Co_2(N\text{-Et-HPTB})(SH)(H_2O)]^{2+}$ (**24a**) and $[Co_2(N\text{-}CH_2Py\text{-HPTB})(SH)(H_2O)]^{2+}$ (**24b**) depending on the respective ligand used.[82] Both complexes were characterized by X-ray crystallography and exhibited Co-S bond distances of 2.318(3) and 2.232(3) Å for **24a** and **24b**, respectively. Neither complex displayed a $\nu_{SH}$ band by IR. Much like the related Fe(II) structures described above, the hydrosulfides in the Co(II) complexes were stabilized by hydrogen bonding to the adjacent Co-

$OH_2$ moiety. A *bis*-hydrosulfide complex of cobalt was prepared using the BPMP ligand through similar desulfurization chemistry to afford $[Co_2(BPMP)(SH)_2]^+$ (**25**), which was characterized by X-ray crystallography with Co-S distances of 2.330(1) and 2.316(1) Å.[83] Further evidence for the terminal hydrosulfides was provided by the presence of an S-H stretch at 2489 $cm^{-1}$ in the IR spectrum and an observable S-H resonance at 44.13 ppm in the $^1H$ NMR spectrum. In addition to terminal hydrosulfides **24-25**, the bridging hydrosulfide complex, $[Co_2(BPMP)(\mu_2\text{-}SH)(MeCN)]^{2+}$ (**26a**), was also isolated. The X-ray structure of **26a** showed asymmetric Co-S distances of 2.358(1) and 2.717(1) Å, as well as IR and $^1H$ NMR signatures for the S-H moiety at 2493 $cm^{-1}$ and 44.09 ppm, respectively. Using a related PhBIMP ligand, several analogous solvent-coordinated bridging monohydrosulfides of the type $[Co_2(PhBIMP)(\mu_2\text{-}SH)(X)]^{2+}$ (X = DMF, **26b**; MeCN, **26c**) were also characterized with structural and spectroscopic parameters akin to those of **26a**.

**Scheme 11.** Nonheme diiron and dicobalt hydrosulfide complexes.

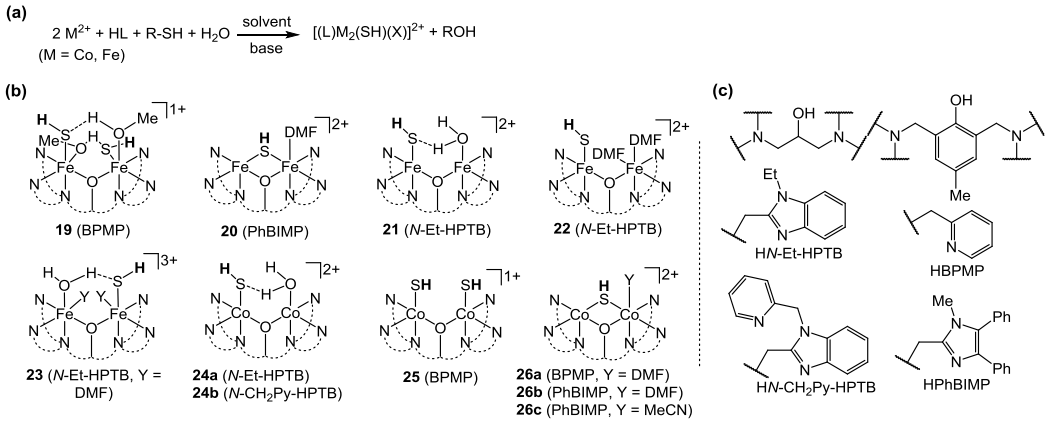


*2.4 Heme-Based Hydrosulfide Complexes.*

Heme subunits provide a broad platform for small molecule binding, and detailed studies of $O_2$, CO, NO, and other small molecules have been reported in both natural and synthetic systems.

Akin to the physical changes in protein structure and activity after $O_2$, CO, or NO binding, reaction with $H_2S$ can generate significant changes in protein activity. For example, cytochrome *c* oxidase (CcO), which contains two heme Fe (*a* and $a_3$) and two Cu ($Cu_A$ and $Cu_B$) centers, is the final acceptor in the mitochondrial respiratory chain and reduces $O_2$ to water.[84, 85] Reaction with $H_2S$ modifies the CcO heme $a_3$ and $Cu_B$ centers resulting in reversible CcO inhibition and a reduction in ATP production, likely contributing to $K_{ATP}$ channel activation. Reactions of $H_2S$ with CcO have revealed a complex concentration dependence, with low $H_2S$ levels stimulating respiration, whereas high $H_2S$ levels result in CcO inhibition. These differing responses can be explained by $H_2S$-mediated reduction to ferric heme $a_3$ at low $H_2S$ concentrations, coordination to and reduction of $Cu_B$ at moderate concentrations, and conformational changes of CcO upon $HS^-$ binding to ferric heme $a_3$ at high concentrations.[6, 86-88] Other common heme targets, including myoglobin (Mb) and hemoglobin (Hb) can react with $H_2S$ to either bind sulfide and/or undergo subsequent redox chemistry (vide infra). Alternatively, reaction of oxy-Mb and oxy-Hb with $H_2S$ results in covalent modification of the heme periphery to generate sulfmyoglobin and sulfhemoglobin, respectively, both of which have lower $O_2$ affinities and thus reduce $O_2$ transport.[89] Prior investigations have exerted significant effort on characterizing binding modes, reaction kinetics, and redox chemistry of $H_2S$, $HS^-$, and related species with hemeproteins, whereas our emphasis in this subsection will focus on structurally-characterized protein-based and small-molecule systems. As a whole, a number of factors contribute to the reactivity of $H_2S$ with hemeproteins, including the accessibility of $H_2S$ to the heme active site, the polarity of the local environment around the heme center, the makeup and orientation of distal site residues, and $H_2S$ concentrations, which influence heme reduction.[90]

*3.4.1 Biological Heme Systems.* One of the best-characterized examples of $H_2S/HS^-$ binding to a natural heme system are the hemoglobins isolated from the gill of the bivalve mollusk *Lucina pectinate*, which harbors chemoautotrophic symbiotic bacteria. Of these hemoglobins, hemoglobin I (HbI) is a sulfide-reactive protein, whereas hemoglobin II (HbII) and hemoglobin III (HbIII) are oxygen-reactive proteins. In the absence of $O_2$, HbI-III all react with $H_2S$ to generate ferric hemoglobin sulfides, as evidenced by the similarity of UV-vis features ($\lambda_{max}$ = 425, 545, 573(sh) nm) to those generated by reaction of ferric whale myoglobin or ferric human hemoglobin with sulfide.[91] Notably, both HbII and HbIII remained oxygenated when $H_2S$ was introduced in the presence of $O_2$. By contrast, HbI reacted with $H_2S$ to generate ferric hemoglobin sulfide, likely through nucleophilic displacement of the bound superoxide anion. The rate of reaction between ferric HbI and $H_2S$ increased significantly from pH 10.5 to 5.5, which suggests that $H_2S$, rather than $HS^-$ is the bound ligand. Furthermore, the pH dependence on rate has an inflection point at 7.0, which qualitatively matches the p$K_a$ of $H_2S$ in water. Further characterization of the ferric HbI sulfide was obtained by EPR spectroscopy displaying a major species with $g$ = 2.67, 2.24, and 1.84,[91] similar to those previously attributed to sperm whale ferric sulfmyoglobin ($g$ = 2.56, 2.25, 1.83).[92]

Complementing solution characterization methods, Bolognesi and co-workers reported the X-ray structures of HbI from *Lucina pectinata* both in the aquo-met and sulfide-bound form, which have helped elucidate $H_2S$ reactivity.[93, 94] The structure of the aquo-met form of HbI revealed an unusual arrangement of four phenylalanine residues near the distal site of the heme center that form a hydrophobic pocket often referred to as the "Phe-cage". In addition, the HbI active site has a glutamine residue (Gln-64) at the distal ligand binding site, which differs from the more common histidine residue found in mammalian Hb, and was found to be oriented toward and likely

hydrogen bonded with a water molecule coordinated to the heme iron. This Gln-64 residue likely facilitates fast sulfide associate rate constants, and hydrogen bonding of bound $H_2S$ to Gln-64 results in stabilization of the bound sulfide and a slow dissociate rate. These conclusions are further supported by later investigations by Negrerie and co-workers who used time-resolved absorption spectroscopy to investigate $H_2S$ photodissociation from both ferrous and ferric HbI.[95] Further structural evidence for $H_2S$ binding in HbI was obtained by soaking aquo-met crystals of HbI with $Na_2S$, which resulted sulfur ligation to the heme center, likely in the form of coordinated $H_2S$ (Figure 1).

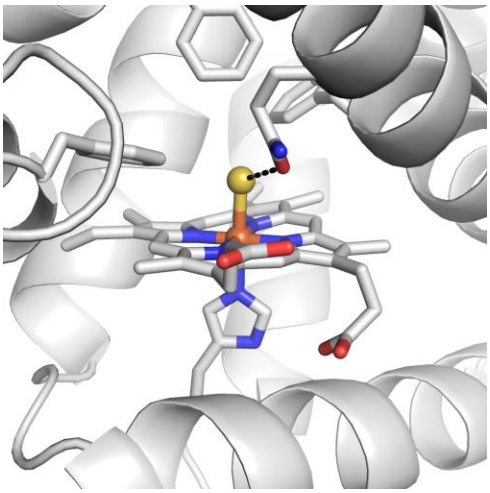

**Figure 1.** X-ray structure of the HbI sulfide adduct from *Lucina pectinata*.[93] PDB: IMOH.

Complementing the sulfide adduct of HbI, the structure of human hemoglobin with a ferric sulfide was recently reported by Banerjee and co-workers (Figure 2).[96] X-ray crystallography revealed sulfide coordination to the low-spin ferric center in both the α- and β-subunits with a 2.2 Å Fe-S bond length. This observed Fe-S distance is constant with the expected 2.24 Å distance for

$HS^-$ coordination rather than 2.50 Å for $H_2S$ coordination based on calculations from the related ferric myoglobin system.[96] The coordinated hydrosulfide is hydrogen bonded to the His-58 nitrogen akin to the observed interaction between the bound sulfide in *L. pectinata* and the Gln-64 residue. Sulfur anomalous dispersion experiments, which confirmed the atomic identity of the sulfide bound to Fe also revealed a second sulfur source not corresponding to Cys or Met residues located near the periphery of the α-subunit and likely hydrogen bonded to Phe-43, Pro-44, and Phe46 carbonyl groups. This second sulfide molecule is located near the PHE path, which has been previously proposed as a transit pathway for CO and $O_2$ to the heme center.

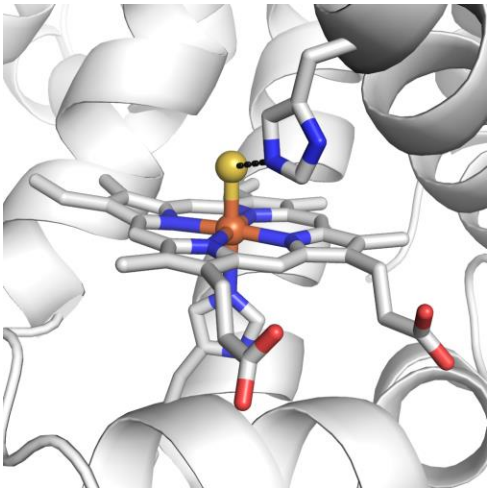

**Figure 2.** X-ray structure of the human myoglobin sulfide adduct.[96] PDB: 5UCU.

In addition to the crystallographically characterized examples of heme-sulfide adducts described above, considerable effort has been paid to understanding how other biological hemes interact with $H_2S$ under different conditions. One of the earliest identified reactions of sulfide with hemoglobin and myoglobin is the formation of a green product due to the covalent modification of the porphyrin ring upon reaction of oxy-Hb or oxy-Mb with $H_2S$ (Figure 3).[97, 98] This sulfheme

formation modifies the electronic structure of the porphyrin, which results in a bathochromic shift in absorbance to ~620 nm, and a reduction in $O_2$ binding affinity.[89, 99] Although the exact mechanism of sulfheme formation remains unclear, this reaction likely proceeds through an oxoferryl intermediate ($Fe^{IV}$=O or $Fe^{IV}$=O $Por^{\cdot+}$) and addition of HS· to the porphyrin. Three general structures of sulfheme modifications have been characterized, including an episulfide (sulfheme-A), a ring-opened episulfide (sulfheme-B), and a thiochlorin structure (sulfheme-C).[100-102] Of these products, the thiochlorin structure has been confirmed crystallographically as a cyanomet-sulfmyoglobin C adduct.[102] In addition to myoglobin and hemoglobin sulfhemes, both sulfcatalase and sulflactoperoxidase have also been observed.[103, 104]

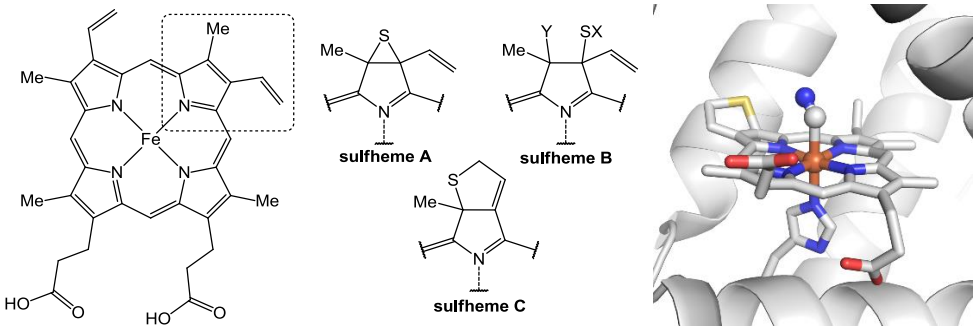


**Figure 3.** Left: Schematic of the iron protoporphyrin moitety and three sulfheme products from covalent modification of the porphyrin ring. Right: X-ray structure showing sulfheme C product formation in a Fe-CN adduct.[101] PDB: 1YMC.

In many of the reported investigations of heme reactivity with $H_2S$, the reaction progress and product formation were assayed by solution-state electronic absorption measurements, EPR spectra, and mass spectrometric evidence for reaction products and intermediates. Rather than summarize each example directly, we refer readers to key references related to different heme

systems including neuroglobins,[105, 106] hemoglobins,[38, 107-109] myoglobins,[110-113] as well as summary reviews.[114-116] One emerging theme that we will note here briefly is that many biological heme systems likely mediate the conversion of $H_2S$ to polysulfides and/or persulfides through sulfide-mediated reduction of the iron center to generate reactive sulfur species. For example, Banerjee and co-workers recently reported that both ferric hemoglobin and myoglobin can oxidize sulfide to thiosulfate through a process that generates Fe-bound hydro(poly)sulfides.[38, 110, 117] Related chemistry to form hydro(poly)sulfides has also been reported in investigations of the addition of $H_2S$ to aqueous solutions of cobalamin.[118] These metal-mediated examples highlight the key interconnectivity of redox-active metals in biology in mediating speciation and redox-state within the reactive sulfur species pool.

*2.4.2 Synthetic and Semi-Synthetic Heme Systems.* In addition to protein-based systems, hydrosulfide binding to semi-synthetic heme systems has also been investigated. For example, Bari and co-workers used the undecapeptide microperoxidase (MP11),[119] which is a heme peptide generated from cytochrome c proteolysis. Addition of $H_2S$ to a pH 6.8 solution of $Fe^{III}$NAcMP11 generated a stable product with an absorbance maximum at 414 nm, which was assigned to the hydrosulfide complex NAcMP11-$Fe^{III}$-SH (**27**), although the precise protonation state of the product was not confirmed directly (Scheme 12). Resonance Raman spectroscopy revealed a new band at 366 $cm^{-1}$, which was assigned to the $Fe^{III}$-SH moiety in a low-spin hexacoordinate heme center. Interestingly, the reactivity of the NAcMP11-$Fe^{III}$ system is different than that of the parent cytochrome c, which is reduced to $Fe^{II}$ by $H_2S$. In addition, Ma, Li, and co-workers reported sulfide binding investigations with a series of deuterohemin-His-peptides to further understand the impacts of the proximal environment on sulfide binding in the absence of distal residues.[120] Stopped-flow kinetic measurements revealed that the deuterohemin-AlaHisThrValGluLys

(DhHP-6) analogue provided significantly faster sulfide association rate constants than the deuterohemin-AlaHis (DhHP-2) system (Scheme 12, **28a-e**). These results suggest that the proximal ligands to the heme center, in this case a Glu residue, play an important role in the sulfide association and binding process, possibly due to hydrogen bonding associations that can facilitate binding.

**Scheme 12.** Semi-synthetic hemes used to investigate reactions with $HS^-$.

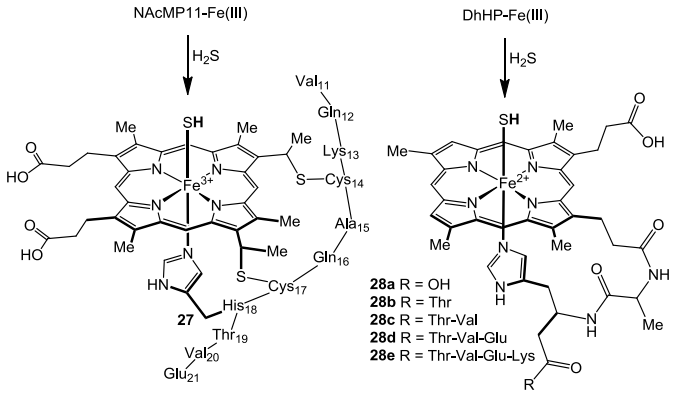


Simple synthetic heme complexes have also been used to investigate sulfide binding. In an early example, Scheidt and co-workers reported the reaction of [$Fe^{III}$(T-p-OMePP)(Cl)] with $S_8$ and $LiBEt_3H$ to afford [$Fe^{III}$(T-p-OMePP)(SH)] (**29**) (Scheme 13).[121] The resultant complex was characterized by UV-Vis spectroscopy, with absorbances at 412 (1.2 x $10^5$ $M^{-1}cm^{-1}$), 523 (1.3 x $10^4$ $M^{-1}cm^{-1}$), and 612 nm (2 x $10^3$ $M^{-1}cm^{-1}$). Magnetic moment measurements were consistent with an S = ½ system, and EPR spectroscopy revealed signals at $g$ = 3.9 and g = 1.74 (4 K). Further characterization by Mössbauer spectroscopy revealed an isomer shift of $\delta$ = 0.30 mm/s and a quadrupole splitting of $\Delta E_Q$ = 2.05 mm/s. X-ray crystallography supported the product identity, with the sulfur atom located 2.30 Å from the Fe center, although the S-H hydrogen was not located by crystallography nor was the S-H stretch observed by IR spectroscopy. This early example

provides a rare report of a stable $Fe^{III}$-SH adduct for synthetic porphyrin systems, but we note that despite the initial characterization, more recent reports have described difficulty in reproducing this initial preparation.[122]

**Scheme 13.** Hydrosulfide adducts of synthetic iron porphyrinates.

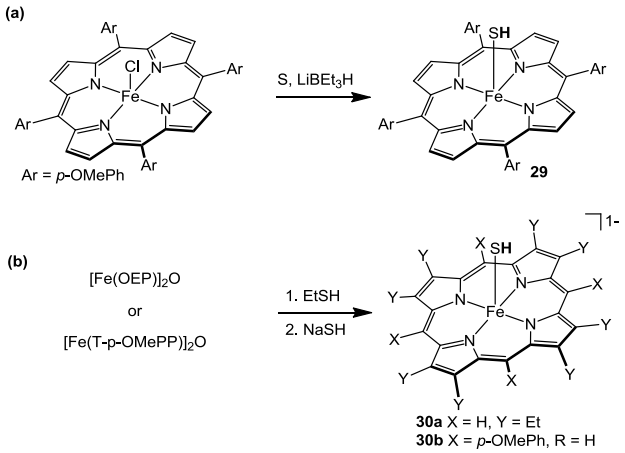


Using more standard sources of hydrosulfide, a number of other investigations have generated synthetic heme hydrosulfide adducts. For example, Scheidt and co-workers later investigated the reaction of NaSH with ferrous octaethylporphyrinates (OEP) and tetra-*p*-methoxyphenylporphyrinates (T-*p*-OMePP) to generate $[Fe^{II}(OEP)(SH)]^-$ (**30a**) and $[Fe^{II}$(T-*p*-OMePP)$(SH)]^-$ (**30b**) (Scheme 13).[123] Initial reduction of $[Fe(OEP)]_2O$ with EtSH, followed by treatment with NaSH, provided the respective hydrosulfide products, both of which were characterized by X-ray crystallography with Fe-S bond distances of 2.3929(5) and 2.3830(5) Å for the two inequivalent porphyrin adducts in $[Fe(OEP)SH]^-$ and 2.388(1) Å in [Fe(T-*p*-OMePP)$(SH)]^-$. Solution binding studies of $[Fe^{II}$(T-*p*-OMePP)] demonstrated an initial association of $HS^-$ to form $[Fe^{II}$(T-p-OMePP)$(SH)]^-$, characterized by a sharp absorbance at 447 nm, which reached maximal intensity after addition of 2.5 equiv. of $HS^-$ per iron. Complex changes in the Q-

band region of the spectra were also observed. On the basis of the solution binding data, the authors proposed the formation of two distinct hydrosulfide species in solution, including the monohydrosulfide $[Fe^{II}(T\text{-}p\text{-}OMePP)(SH)]^-$, with associated Soret bands at 428 and 447 nm and Q bands at 543 and 613 nm, and the *bis*-hydrosulfide $[Fe^{II}(T\text{-}p\text{-}OMePP)(SH)_2]^{2-}$, with associated Soret bands at 418 and 459 nm and Q bands at 585 and 627 nm. A similar proposition of both mono- and bis-hydrosulfide ligation with the $[Fe^{II}(OEP)]$ platform was also proffered. Further characterization of the $[Fe(OEP)(SH)]^-$ species was obtained from Mössbauer spectroscopy. The resultant spectrum was fit to two quadrupole doublets designated as 'a' and 'b' with $\delta$ = 0.95 and 0.89 and $\Delta E_Q$ = 2.81 and 2.14 mm/s (25 K). Both sites were consistent with a high-spin $Fe^{II}$ porphyrin environment.

In similar investigations, Tonzetich and co-workers reported the reaction of $NBu_4SH$ with different $Fe^{II}$ porphyrinates including tetraphenyl porphryinate (TPP), tetramesityl porphyrinate (TMP), and octaflurotetraphenyl porphyrinate ($F_8TPP$) (Scheme 14).[124] In these investigations, treatment of [Fe(TPP)] with $NBu_4SH$ resulted in the reduction of the Q-band absorbance at 540 nm, with the growth of two absorbances at 582 and 625 nm, corresponding to the five-coordinate $[Fe(TPP)(SH)]^-$ (**31a**) species with an associated log($K_a$) value of 5.3(2) and $E_{1/2}$ value of −0.83 V (vs $Fc/Fc^+$). Similar investigations with [Fe(TMP)] revealed comparable changes in the UV-vis spectrum, with a log($K_a$) value of 2.6(2) for formation of $[Fe(TMP)(SH)]^-$ (**31b**). The more electron deficient $[Fe(F_8TPP)]$ analogue revealed formation of a putative hydrosulfide bridged homodimer $[Fe_2(F_8TPP)_2(SH)]^-$ (**32**), which was detected by $^1H$ NMR spectroscopy en-route to formation of the five-coordinate monomeric $[Fe(F_8TPP)(SH)]^-$ (**31c**). Crystallographic characterization of $[Fe(F_8TPP)(SH)]^-$ confirmed the terminal hydrosulfide with an Fe-S distance of 2.323(1) Å. To further probe the reactivity of the ferrous hydrosulfide products, $[Fe(TPP)(SH)]^-$ was treated with

various small molecule reactive species. Chemical oxidation of $[Fe(TPP)(SH)]^-$ with $[FeCp\square][BF_4]$ afforded [Fe(TPP)], intimating that formation of the ferric hydrosulfide adduct [Fe(TPP)(SH)] is immediately followed by reduction. Further treatment of $[Fe(TPP)(SH)]^-$ with 1,2-dimethylimidazole or NO gas resulted in hydrosulfide ligand displacement. Although Fe heme systems have been the primary focus for investigations of $H_2S$ with synthetic porphyrins, recent investigations have also demonstrated stable $Ga^{III}$-SH adducts as structural models for Fe(III) systems.[125]

**Scheme 14.** Iron(II) porphyrin hydrosulfide adducts, including a hydrosulfide-bridged homodimer.

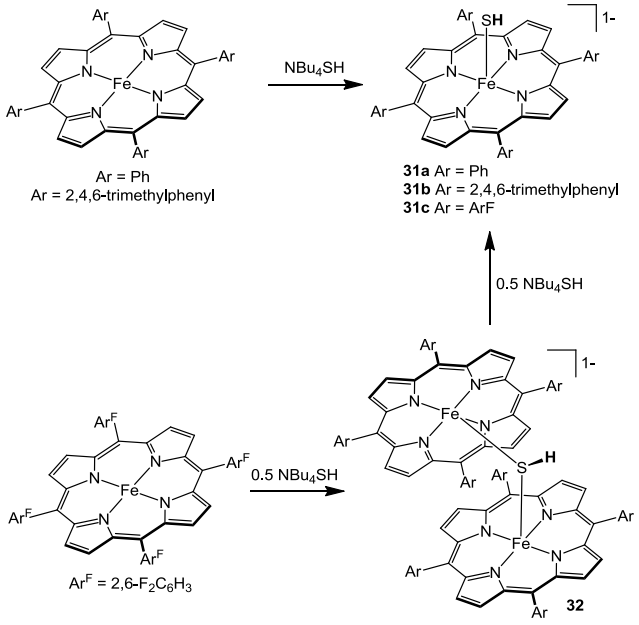


Building from these investigations, Pluth and co-workers used the sterically-protected "picket fence" porphyrin (PfP) system to investigate the reactivity of sulfide with synthetic porphyrins. In these investigation, $[Fe^{III}(PfP)]^-$ reacted with $NBu_4SH$ to generate the ferrous $[Fe^{II}(PfP)(SH)]^-$ (**31d**) product, as evidenced by solution-state UV-Vis measurements and mass spectrometric

investigations (Scheme 15).[126] The same product was observed when [$Fe^{II}$(PfP)] was reacted with $NBu_4SH$, suggesting again that the ferric sulfide product was unstable at room temperature, even within a relatively-hydrophobic cage architecture. In related low-temperature investigations, Dey and co-workers monitored the reduction of $[Fe^{III}(PfP)]^-$ and related species at −80 °C using resonance Raman and EPR spectroscopy.[127] These results supported initial formation of a low-spin $Fe^{III}$-SH intermediate with $\nu_{Fe\text{-}S(H)}$ = 385 $cm^{-1}$ that was stable at low temperatures, but underwent Fe-S homolytic bond cleavage, resulting in $Fe^{II}$ and eventual polysulfide generation. Although the ferrous sulfide product of these reactions was not structurally characterized in either of these investigations, a prior report provided the X-ray structure of $[Fe^{II}(PfP)(SH)]^-$, with an Fe-S distance of 2.3123(8) Å.[128] Although this report provided structural data on the protected ferrous hydrosulfide, no details leading to the formation of the obtained product were provided other than the fact that the crystal was obtained from a solution of chlorobenzene containing [$Fe^{II}$(PfP)], cryptand-222, and potassium thioacetate.

**Scheme 15**. Reaction of hydrosulfide with ferric and ferrous picket fence porphyrin complexes.

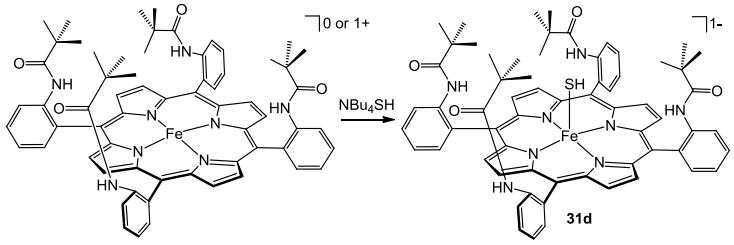


*2.5 Zinc Hydrosulfide Complexes*

The redox inactivity and well-defined coordination environment of bioinorganic zinc complexes has rendered such platforms a viable framework for generation of hydrosulfide species.

Drawing parallels to *Lucina pectinata*, the giant tubeworm *R. pachyptila* lives in sulfide-rich environments near deep sea hydrothermal vents and also has evolved a Hb system to deliver $H_2S$ and $O_2$ to symbiotic sulfide-oxidizing bacteria. Although the $H_2S$ binding and transport by this Hb was initially thought to involve cysteine residues in the protein, recent structural data revealed that the Hb construct is assembled from 24 heme-containing globin chains that generate a hollow cavity with 12 tightly-bound $Zn^{2+}$ ions ligated to histidine and glutamate residues.[129] Zinc chelation studies demonstrated the necessity of the $Zn^{2+}$ ions for $H_2S$ binding and transport. This thiophilicity of $Zn^{2+}$ is also seen in the competitive inhibition of $Zn^{2+}$-containing carbonic anhydrase activity by sulfide, which binds to this $His_3Zn$ active site found in most carbonic anhydrase isoforms.[130, 131] These properties have motivated the development of biomimetic platforms modeled on the 3-fold symmetric $His_3$ coordination environment, and have also provided insights into the coordination behavior of sulfide with different Zn coordination motifs.

*2.5.1 tris-Pyrazolylborate Complexes.* Three-fold symmetric *tris*-pyrazolylborate (Tp) ligands have often been used to mimic the $His_3$ coordination environment found in biological zinc coordination and can provide steric protection of the Zn coordination environment dependent on the Tp ligand substituents. In an early example of Zn-SH generation in Tp scaffolds, Parkin and co-workers demonstrated that reaction of ($Tp^{tBu}$)ZnH with $H_2S$ generates the enthalpically-favored ($Tp^{tBu}$)ZnSH (**33a**) product (Scheme 16).[132] This product was characterized by elemental analysis, MS, and $^1H$ NMR spectroscopy, which revealed a $^1H$ NMR resonance at −0.52 ppm ($C_6D_6$) corresponding to the Zn-SH moiety. Similar investigations by Vahrenkamp and co-workers with the related *tris*(3-*p*-cumenyl-5-methylpyrazolyl)borate ($Tp^{Cum,Me}$) system also provided access to hydrosulfide adducts.[133] Treatment of ($Tp^{Cum,Me}$)Zn-OH with $H_2S$ in $CH_2Cl_2$ resulted in formation of ($Tp^{Cum,Me}$)Zn-SH (**33b**) as well as the accompanying minor impurity ($Tp^{Cum,Me*}$)Zn-SH (**33c**).

This minor impurity was due to the $C_s$-symmetric 3-methyl-5-cumenyl isomer ($Tp^{Cum,Me*}$), which is inseparable from the $C_{3v}$-symmetric $Tp^{Cum,Me}$ ligand. Both Zn-SH products were characterized by X-ray crystallography with Zn-S bond lengths of 2.21 Å. Heating ($Tp^{Cum,Me}$)Zn-SH (**33b**) to 200 °C resulted in formation of the sulfide-bridged product {($Tp^{Cum,Me}$)Zn}$_2$S, which was also characterized by X-ray crystallography.[134]

**Scheme 16.** Zinc *tris*-pyrazolylborate hydrosulfide compounds.

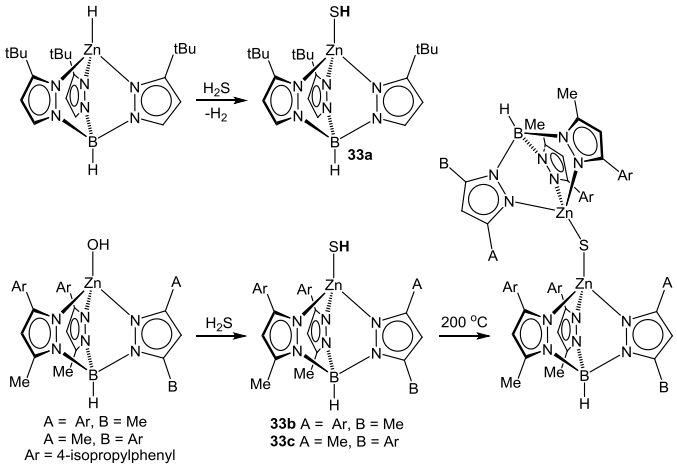


Further investigations by Vahrenkamp and co-workers on related substituted Tp ligand systems including $Tp^{Ph,Me}$, $Tp^{Py,Me}$, $Tp^{Pic,Me}$, and $Tp^{tBu,Me}$ (referred to generally here as Tp*) demonstrated the generality of Tp*Zn-SH (**33d-g**) formation by the reaction of Tp*Zn-OH with $H_2S$ (Scheme 17).[135] The family of Tp*Zn-SH products were characterized by X-ray crystallography, elemental analysis, MS, and $^1$H NMR spectroscopy. The aryl-Tp containing products ($Tp^{Ph,Me}$)ZnSH, ($Tp^{Py,Me}$)ZnSH, and ($Tp^{Pic,Me}$)ZnSH all revealed $^1$H NMR resonances at −2.0 ppm, whereas the alkyl-substituted derivative ($Tp^{tBu,Me}$)ZnSH revealed a resonance at −0.97 ppm. Further investigations into the reactivity of the Tp*ZnSH products showed that these systems did not react directly with esters, phosphates, or $CO_2$, whereas treatment with acidic X-OH organic compounds

including carboxylic acids, trinitrophenol, or hexafluoroacetylacetone resulted in extrusion of $H_2S$ and formation of the Tp*Zn-OX products (Scheme 17). Conversely, treatment of Tp*Zn-SH with different bases did not result in formation of Tp*Zn-$S^-$, but rather extrusion of ZnS and the release of the anionic Tp* ligand. The ligated hydrosulfide could by alkylated by treatment with MeI, which resulted in formation of Tp*Zn-I and MeSH. Rate-order analysis investigations demonstrated that the alkylation proceeds through a clean 2$^{nd}$-order reaction, which is consistent with the direct alkylation of the Tp*Zn-SH while bound to the Zn, followed by release of MeSH. Release of $H_2S$ from the Tp*Zn-SH compounds was possible by treatment with thiols in an entropically-driven exchange process to yield the thiolate-bound Tp*Zn-SR products.

**Scheme 17.** Reactivity of the Tp*Zn-SH with acids, bases, electrophiles, and thiols.

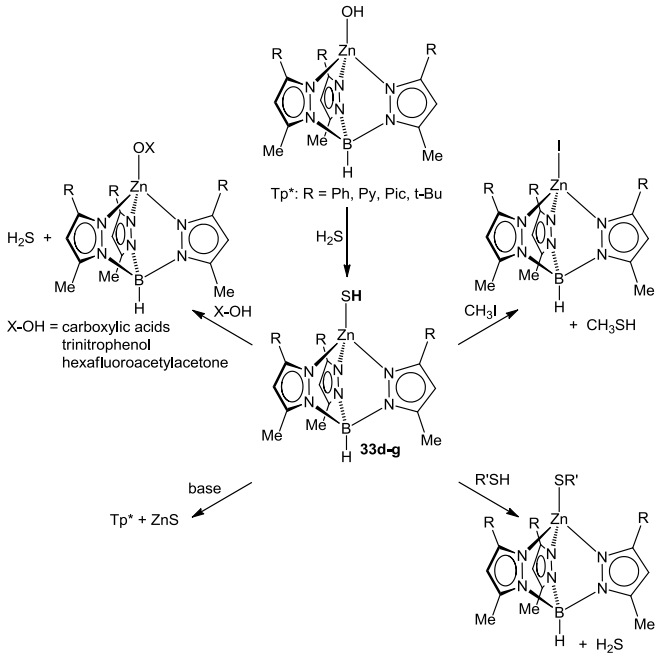


Expanding on ligand exchange reactions and working with similar trispryazolylborate ligands ($Tp^{Ph,Me}$ and $Tp^{iPr,iPr}$), Artaud and co-workers investigated the reaction of persulfide-ligated

TpZn-SSR ($Tp^{iPr,iPr}$, $Tp^{Ph,Me}$) complexes with thiols.[136] In the absence of external base, treatment of TpZn-SSR with a thiol (R'SH) in $CH_2Cl_2$ resulted in thiol/persulfide exchange to yield TpZn-SR and free persulfide (Scheme 18). In the presence of $NEt_3$ as a base, however, formation of TpZnSH (**33d,h**) and mixed organic disulfide and thiol products was observed. In the case of ($Tp^{iPr,iPr}$)ZnSH (**33h**), the product was characterized by X-ray crystallography, elemental analysis, and $^1H$ NMR spectroscopy, which revealed a Zn-SH resonance at −1.43 ppm ($CD_2Cl_2$).

**Scheme 18.** Generation of TpZn-SH products from TpZn-SSH persulfide compounds.

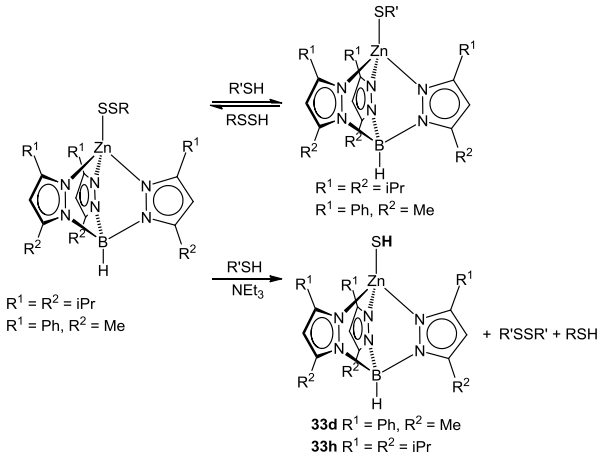


Using the $Tp^{Ph,Me}$ ligand platform, Vahrenkamp and co-workers also investigated the reaction of ($Tp^{Ph,Me}$)Zn-OH with $CS_2$.[137] In the absence of potential nucleophiles, addition of $CS_2$ to ($Tp^{Ph,Me}$)Zn-OH resulted in formation of ($Tp^{Ph,Me}$)Zn-SH (**33d**) and carbonyl sulfide (COS) (Scheme 19). Further product analysis of this reaction also revealed $CO_2$ formation, suggesting that COS can undergo a similar reaction to yield $CO_2$. This reaction is akin to known reactivity of carbonic anhydrase enzymes that can convert COS to $CO_2$ with the liberation of $H_2S$.[34] In the presence of MeOH, however, addition of $CS_2$ to ($Tp^{Ph,Me}$)Zn-OH resulted in formation of the xanthogenate complex ($Tp^{Ph,Me}$)Zn-SC(S)OMe, which is also formed from the addition of $CS_2$ to

pre-formed ($Tp^{Ph,Me}$)Zn-OMe. These results suggest that the $CS_2$ reacts directly with the methoxide complex to yield the observed ($Tp^{Ph,Me}$)Zn-SC(S)OMe product.

**Scheme 19.** Reactivity of ZnTp complexes with $CS_2$.

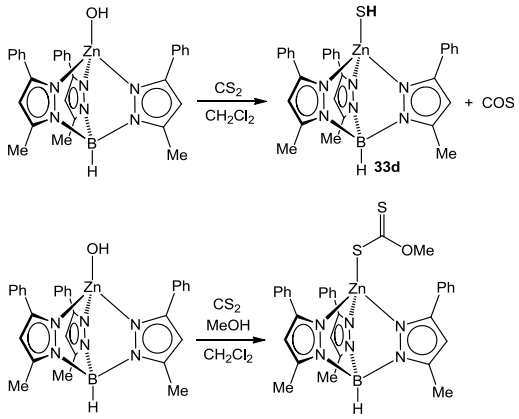


*2.5.2 Other Zn-SH Complexes.* Expanding from the Tp platform, zinc hydrosulfide complexes ligated by the 3-fold symmetric *tris*(thioimidazolyl)hydroborate (Tm) ligand have also been prepared. For example, Parkin and co-workers showed that treatment of the *t*-butyl tris(thioimidazole)hydroborate ($Tm^{tBu}$) complex ($Tm^{tBu}$)Zn-Me with $H_2S$ resulted in formation of ($Tm^{tBu}$)Zn-SH (**34a**) (Scheme 20).[138] Crystallographic characterization confirmed the compound identity, with a Zn-S bond length of 2.265 Å. $^1$H NMR spectroscopy revealed the hydrosulfide resonance at −0.84 ppm. Using similar xylyl-substituted Tm ligands ($Tm^{xyl}$), Vahrenkamp and co-workers demonstrated that treatment of ($Tm^{xyl}$)Zn-OH with $H_2S$ also generates ($Tm^{xyl}$)Zn-SH (**34b**).[139] The resultant ($Tm^{xyl}$)Zn-SH product was characterized by X-ray crystallography, which displayed a Zn-S bond length of 2.258 Å and also by $^1$H NMR spectroscopy, which demonstrated a characteristic Zn-SH resonance at −1.69 ppm in $CDCl_3$.

**Scheme 20.** Zinc hydrosulfide complexes with *tris*(thioimidazolyl)hydroborate ligands.

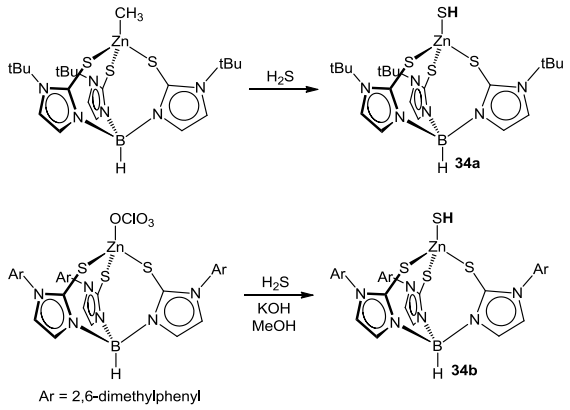


In addition to the anionic Tp and Tm ligands, zinc hydrosulfide adducts have also been accessed with neutral 3-fold symmetric nitrogen-based ligands. For example, Galardon and co-workers demonstrated that the reaction of $[(TPA)Zn(H_2O)]^{2+}$ (TPA = *tris*(2-pyridylmethyl)amine) with KSH in buffered aqueous solution resulted in formation of $[(TPA)Zn(SH)]^{+}$ (**35**) (Scheme 21).[140] The resultant product was characterized by X-ray crystallography, with a Zn-S bond length of 2.306 Å. $^{1}H$ NMR spectroscopy revealed the Zn-SH resonance at −0.86 ppm ($D_2O$). The $[(TPA)Zn(SH)]^{+}$ product was stable in neutral aqueous solution, but released $H_2S$ and reverted to the parent $[(TPA)Zn(H_2O)]^{2+}$ complex in acidic solution. Conversely, deprotonation of the hydrosulfide ligand in basic solution resulted in ZnS extrusion and release of the TPA ligand. Treatment of $[(TPA)Zn(SH)]^{+}$ with the electrophile $MeS\text{-}SO_2Me$ resulted in formation $[(TPA)Zn(SO_2Me)]^{+}$ and dimethyl trisulfide ($Me_2S_3$). The bound hydrosulfide from $[(TPA)Zn(SH)]^{+}$ could also be transferred to other Zn centers. For example, treatment of **35** with $(Tp^{Ph,Me})Zn(OH)$ yielded the dehydration product $[(Tp^{Ph,Me})Zn\text{-}S\text{-}Zn(TPA)]^{+}$ as an intermediate, which could be converted to $(Tp^{Ph,Me})Zn(SH)$ (**33d**) and $[(TPA)Zn(CF_3CO_2)]^{+}$ after the addition of $CF_3CO_2H$.

**Scheme 21.** Generation and reactivity of (TPA)ZnSH compounds.

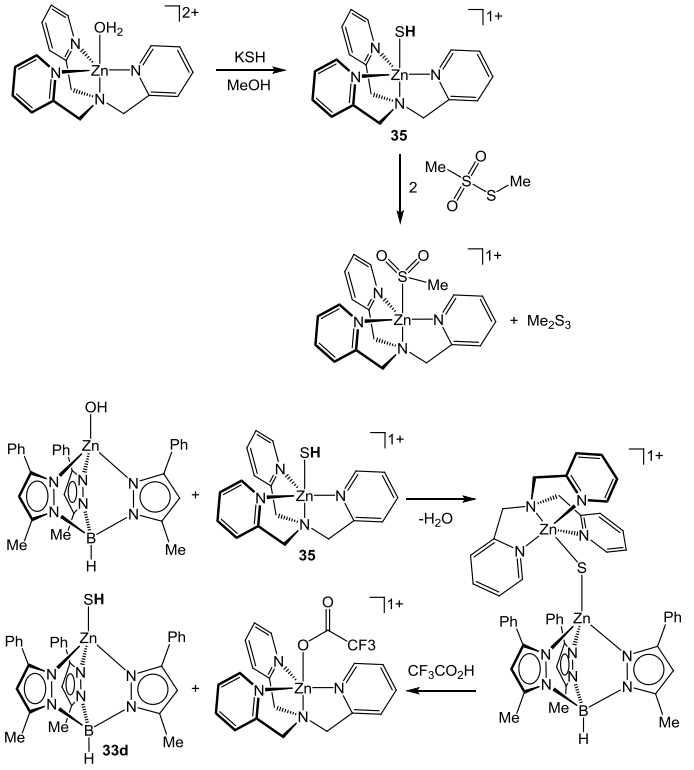


Other 3-fold symmetric ligands with pyridine donors have been investigated as well for the synthesis of Zn-SH complexes. Using *tris*(2-pyridylseleno)methyl (Tpsem) ligands, Parkin and co-workers treated ($\kappa^3$-Tpsem)Zn-N($SiMe_3$)$_2$ with $H_2S$ to form the hydrosulfide complex ($\kappa^3$-Tpsem)ZnSH (**36**, Scheme 22). The resultant product was characterized by X-ray crystallography with a Zn-S bond length of 2.242 Å.[141] Further investigations into the solution behavior of ($\kappa^3$-Tpsem)ZnSH demonstrated that it is in equilibrium with the sulfide bridged complex {($\kappa^3$-Tpsem)Zn}$_2$S, which was also supported by X-ray crystallographic characterization.

**Scheme 22**. Generation and reactivity Tpsem-based Zn-SH compounds.

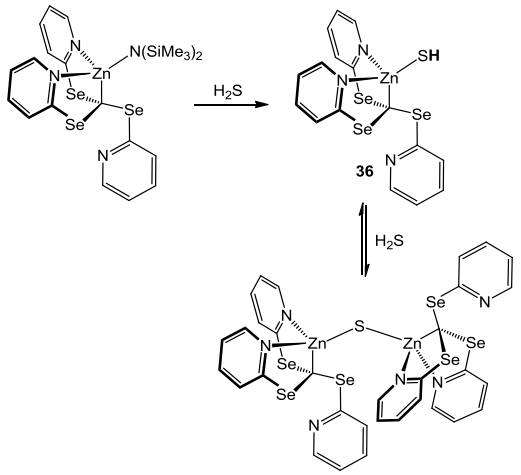


*2.5.3 Reversible Zn-SH Formation.* Complementing the 3-fold symmetric Zn-SH complexes, Gilbertson, Pluth, and co-workers demonstrated that hydrogen bond accepting pyridinediimine (PDI) ligands can also support Zn-SH product formation.[142] Treatment of the parent 2,6-diisopropylphenyl PDI compound ($^{iPr}$PDI)$ZnCl_2$ with $NBu_4SH$ resulted in formation of ZnS and liberation of the free $^{iPr}$PDI ligand. Metal extrusion could be eliminated, however, by replacement of one 2,6-diisopropylphenyl group with a 2-ethyl-diisopropylamine group (didpa). Generation of the corresponding zinc hydrosulfide, (didpa)Zn-SH (**37**), was accompanied by enhanced stabilization by virtue of hydrogen bonding between Zn-SH and the diisopropylamine group on the ligand (Scheme 23). Variable temperature $^1$H NMR experiments revealed conformational rigidity of the ethylene component of the ligand at −35 °C and the appearance of the hydrogen-bonded Zn-S-H---N moiety at 11.05 ppm.

**Scheme 23**. Hydrosulfide stabilization by hydrogen bonding in Zn(pyridinediimine) complexes.

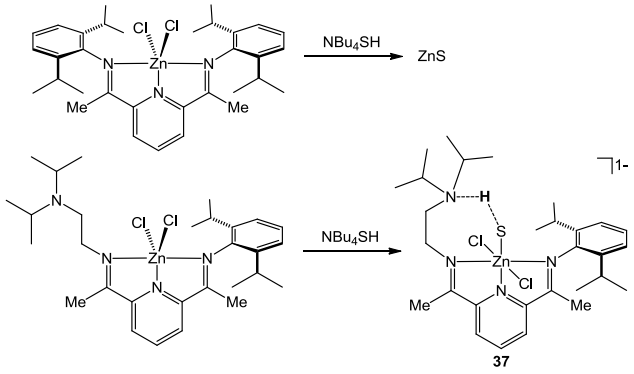


*2.6 Xanthine Oxidase and Related Molybdenum Hydrosulfides.*

Xanthine oxidase (XO) is a key enzyme in purine catabolism that oxidizes hypoxanthine to xanthine and xanthine to uric acid with the concomitant reduction of $NAD^+$ to NADH. The active site of XO contains a sensitive mononuclear $\{Mo^{VI}OS\}$ cofactor ligated to an ene-dithiolate moiety from a coordinated pyranopterin.[143] During the catalytic cycle, this XO active site proceeds through a $LMo^{IV}O(SH)(OR)$ intermediate. As an example of this structural motif, an intermediate was crystallographically-characterized using a slowly reacting substrate, and the resulting Mo-S bond distance of 2.4 Å was found to be consistent with a reduced Mo-SH rather than a Mo=S bond (Figure 4).[144] Structural information was also obtained through treatment of XO with the mechanism-based inhibitor allopurinol, which is oxidized by XO to alloxanthine and subsequently binds tightly to the reduced form of the Mo cofactor.[145] Crystallographic analysis of the allopurinol inhibited state of XO exhibited the $Mo^{IV}O(SH)$ core structure, and the Mo-S distance of 2.4 Å is consistent with a hydrosulfide group rather than a terminal sulfide (Mo=S) moiety (Figure 4).

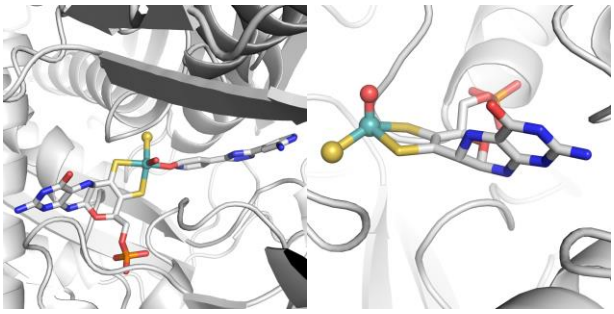

**Figure 4.** X-ray structures of XO with the $Mo^{IV}O(SH)$ core structures. PDB: 1V97 and 3DBJ.

Biomimetic structures related to this $Mo^{IV}O(SH)$ moiety have been targeted in a number of studies. For example, Mitra and Sarkar reported two $[Mo^{IV}O(mnt)(SH)(N\text{-}N)]^-$ species (mnt = maleonitriledithiolate; N-N = 2,2'-dipyridine or 1,10-phenanthroline) by treatment of a thiolate precursor with $H_2S$ (Scheme 24).[146] At short reaction times, monomeric $[Mo^{IV}O(mnt)(SH)(N\text{-}N)]^-$ (**38**) is generated, which can be converted to the $Mo_2$ species (**39**) at longer reaction times. Monomeric $[Mo^{IV}O(mnt)(SH)(N\text{-}N)]^-$ species exhibited SH stretches over the range 2580-2630 $cm^{-1}$. Treatment of **38** with DDQ as an oxidant produced an EPR signal with $g$ = 1.976, which converted to a second signal at $g$ = 1.949 in the presence of moisture. The $[Mo^{IV}O(mnt)(SH)(N\text{-}N)]^-$ products were also characterized by X-ray crystallography, which revealed Mo-SH distances of 2.458 and 2.456 Å for the two structures. In addition to the above example, Sarkar and co-workers also reported that the $[M^{IV}O(mnt)_2]^{2-}$ (M = Mo, W) precursor reacts directly with $H_2S$ to generate the multimetallic $[Mo^{IV}_3(\mu_3\text{-}S)_2(mnt)_6]^{4+}$ or $[W^{V}_2(\mu_2\text{-}S)_2(mnt)_4]^{2+}$ products, likely through the formation of the intermediate hydrosulfide species $[M^{IV}(OH)(SH)(mnt)_2]^{2-}$.[147]

**Scheme 24**. Biomimetic XO compounds featuring hydrosulfide ligands.

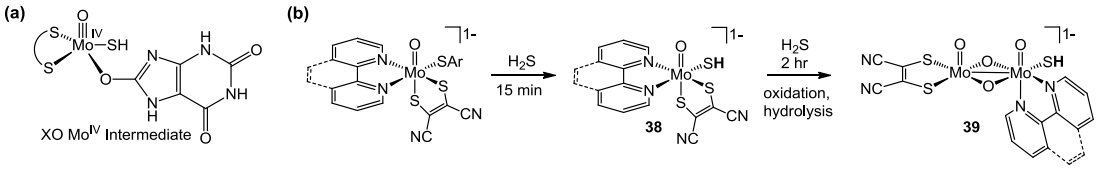


Although not related to the XO system, other biologically-relevant monomeric M-SH species containing bipyridine/phenanthroline-based ligands have been reported for use in biological contexts. For example, Sadler and co-workers reported the generation of a series of half-sandwich Ir hydrosulfide compounds (**40a-d**) and investigated their antiproliferative activity against A2780 ovarian cancer cells (Chart 1).[148] The hydrosulfide compounds shown in Chart 1 were characterized by $^1$H NMR spectroscopy, which revealed characteristic Ir-SH resonances from −1.80 to −2.22. In addition, compound **40a** was also characterized by X-ray crystallography, which demonstrated a M-SH bond distance of 2.388 Å.

**Chart 1.** Examples of $[Cp^*Ir(N_2R)(SH)]^+$ based hydrosulfides.

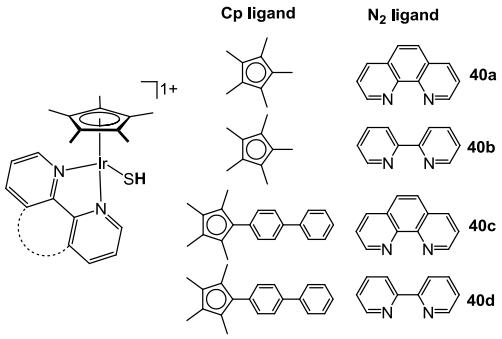


*2.7 Applications of Metal Hydrosulfides to $H_2S$ Sensing*

Motivated by the potential for reversible $H_2S/HS^-$ binding to metal centers, a number of reports have focused on using metal complexes with different optical signatures for the apo- and sulfide-

bound forms as proof-of-concept platforms for reversible $H_2S$ sensing and detection. Readers interested in other activity-based probes for $H_2S$ detection are referred to recent reviews.[149-152] Our focus here is on species that proceed through the generation of metal sulfide intermediates, rather than the large number of systems that have coupled metal extrusion, often in the form of CuS or ZnS, to generate a fluorescence response from quenched fluorophores. We also note that direct binding of $HS^-$ to anion-binding receptors has also recently emerged as a related approach to reversible sulfide binding.[153-155] Here, we focus on recent work aimed at using metals as a reversible binding platform for $H_2S$ detection.

*2.7.1 Chemically-Reversible Responses*. Using a redox-active phthalocyanine, Pluth and co-workers demonstrated that $Co^{II}Pc$ can be reduced by $HS^-$ to generate $[Co^{I}Pc]^-$, which can be reoxidized by air to the parent compound (Scheme 25). This chemically-reversible sequence can be cycled multiple times, and results in conversion from the blue $Co^{II}Pc$ starting compound to the yellow $[Co^{I}Pc]^-$ with shifts in absorbance from 656 to 697 nm and the emergence of a broad absorbance at 467 nm. Using a related approach but with a redox-inactive metal center, Pluth and co-workers also demonstrated that zinc phthalocyanine (ZnPc) could bind $HS^-$ but not $H_2S$.[156] This differential binding of $H_2S$ and $HS^-$ provides a platform for chemically-reversible sulfide binding through metal hydrosulfide formation followed by protonation to release the bound sulfide as $H_2S$. UV-vis investigations showed clean conversion of the ZnPc absorbance at 342 nm to a new absorbance corresponding to $[ZnPc\text{-}SH]^-$ (**41**) at 410 nm, as well as a shift in the Q band absorbance from 665 to 670 nm. Shifts in the aromatic resonances were also observed in the $^1H$ NMR spectrum upon $HS^-$ addition, although the hydrosulfide resonance was not observed directly. Treatment of ZnPc-SH generated *in situ* with acetic acid regenerated the parent ZnPc complex, and this process could be cycled by the successive addition of NaSH and acid. In a related

approach, Milione and co-workers reported the use of Co(II) and Zn(II) heteroscorpionate complexes for $H_2S$ detection.[157] In these systems, changes in the absorbance and fluorescence spectra upon $H_2S$ addition were observed; however, these were attributed to metal extrusion and ligand hydrolysis for Co(II) and Zn(II), respectively.

**Scheme 25**. Chemically-reversible reactions of hydrosulfide ion with $Zn^{II}$ and $Co^{II}$ complexes.

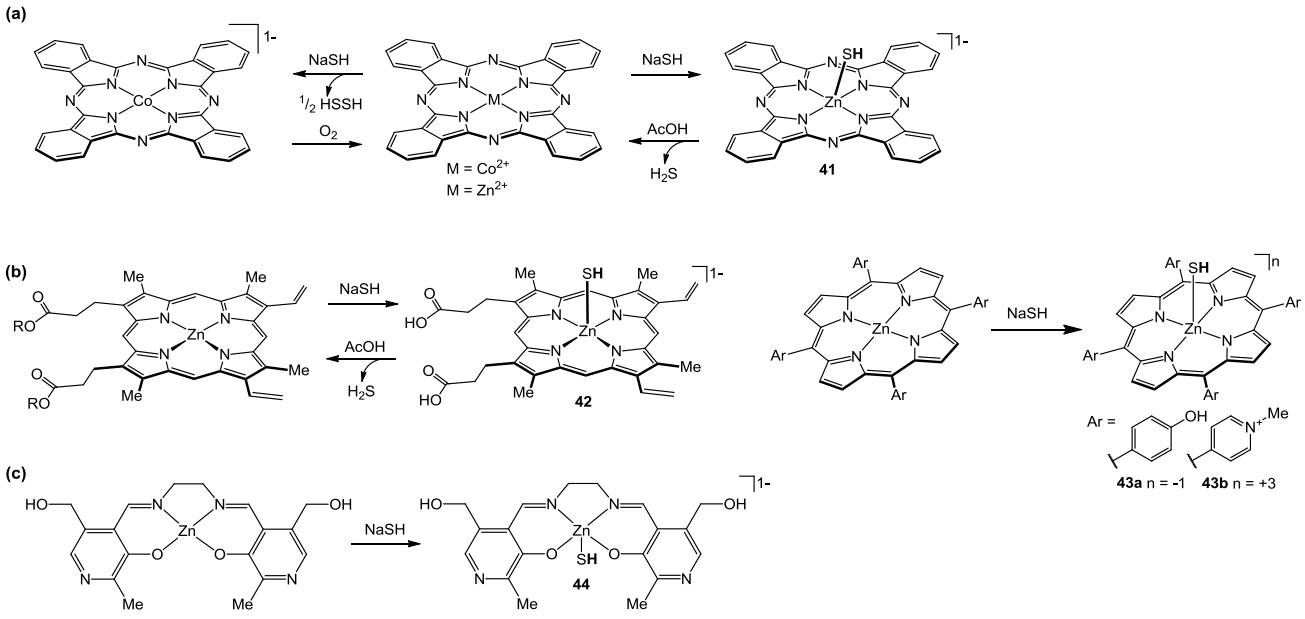


Using protoporphyrin-IX (PPIX) ligands, Strianese and Pluth independently reported the reaction of $H_2S$ and/or $NBu_4SH$ with $[Zn^{II}PPIX]^-$ derivatives (Scheme 25).[158, 159] Working in THF to isolate protonation states, Pluth and co-workers demonstrated that $Zn^{II}PPIX$ reacts with $HS^-$, but not $H_2S$, to form the hydrosulfide adduct, tentatively assigned with the charge state $[Zn^{II}PPIX\text{-}SH]^{2-}$ (**42**) on the basis of the p$K_a$ of the carboxylate moieties on the PPIX ligand. UV-vis investigations showed a shift in the Soret band from 413 to 441 nm and coalescence of the two Q-bands at 544 and 582 nm to a single peak at 563 nm. $^1$H NMR spectroscopy also showed shifts in

the ligand resonances, although the bound hydrosulfide resonance was not observed directly. In similar investigations, Strianese and co-workers investigated the reaction of ZnPPIX and the corresponding methyl ester ligand $ZnPPIX^{Me}$ with NaSH and observed the same reactivity by $^1H$ NMR spectroscopy and also hydrosulfide binding by MS analysis. Using a different porphyrin platform, Strianese and co-workers examined hydrosulfide product formation with zinc complexes of *tetrakis*-(*p*-hydroxyphenyl)tetraphenyl porphyrin (THPP) and *tetrakis*-(*N*-methylpyridyl)porphyrin (TmPyP) under similar conditions.[159, 160] These investigations revealed formation of the Zn-SH adducts (**43a,b**) and chemically-reversible $H_2S$ release upon addition of acid, which matches the reactivity observed for the PPIX systems. One enhancement in this system, however, is the inherent fluorescence of the TmPyP ligand, which allowed for hydrosulfide binding to be translated into a fluorescence response. Treatment of $[(TmPyP)Zn]^{4+}$ with $H_2S$ resulted in a ~2.5-fold upon formation of $[(TmPyP)Zn\text{-}SH]^{3+}$, suggesting the potential for monitoring the chemically-reversible hydrosulfide binding by fluorescence spectroscopy.

The idea of chemically reversible hydrosulfide formation on $Zn^{II}$ platforms was further leveraged by Strianese and co-workers by using a family of pyridoxal-based Zn(II) complexes.[161] Although addition of $H_2S$ to two of the Zn pyridoxal complexes investigated resulted in ZnS formation, use of the pyridoxal derivative shown in Scheme 25 resulted in stable Zn-SH formation (**44**), possibly due to stabilization by hydrogen bond formation with the appended alcohols on the pyridine units. Addition of $H_2S$ resulted in a shift in the fluorescence spectrum of **44** at 500 nm, to a new emission maximum at 380 nm. Fitting of titration data upon addition of NaSH supported a 1:1 binding model and also by MS investigations.

In related investigations, Strianese, Pellecchia and co-workers reported that CuPPIX reacts with sulfide to result in a change in the fluorescence spectrum in water, although the reversibility

of this system was not investigated.[162] The fluorescence signals in the 600-700 nm region of the spectrum changed intensity slightly upon $H_2S$ addition, and a new significant fluorescence band was observed centered at 430 nm, representing a turn-on fluorescence response. MS investigations revealed a $[(CuPPIX)SH]^-$ adduct, suggesting the potential for hydrosulfide coordination to the Cu center. By contrast, Pluth and co-workers reported that in organic solution, $Cu^{II}PPIX$ failed to react with $H_2S$ or $HS^-$, suggesting that proton inventory and/or solvent effects may play an important role in the observed reactivity of sulfide with Cu(II) porphyrin systems.[158]

Although not used for sensing sulfide directly, Galardon and co-workers reported that the reversible coordination of sulfide to a hexadentate Fe(II) complex by utilizing proton transfer and hydrogen bonding chemistry to stabilize the bound hydrosulfide (**45**).[163] In this system in the absence of $H_2S$, the deprotonated carboxamido ligand was coordinated to the Fe(II) center (Scheme 26). After addition of $H_2S$, however, protonation of the carboximido group and coordination of $HS^-$ to the metal center was observed, which was stabilized by an intramolecular hydrogen bond between the sulfur and the amide hydrogen. The presence of this hydrogen bonding interaction was confirmed by IR spectroscopy, which revealed a carbonyl stretch at 1696 $cm^{-1}$ in the protonated amide and by $^1H$ NMR spectroscopy, which displayed an exchangeable proton resonance at −69.2 ppm. Crystallographic characterization of **45** also supported the existence of a strong hydrogen bonding interaction in the solid state, showing an Fe-S bond distance of 2.387 Å and a S-N distance of 3.333 Å.

**Scheme 26**. Reversible binding of $H_2S$ to a $Fe^{II}$ carboximido complex.

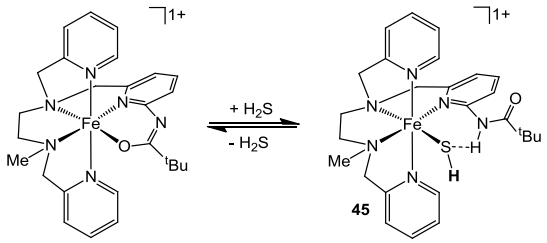


*2.7.2 Fluorophore-Displacement Coupled with Sulfide Binding.* Building from work on the formation of TpZn-SH products, Galardon and co-workers reported fluorophore-ligated zinc systems for $H_2S$ detection.[164] Starting with a coordinated 4-methyl-7-thiocoumarin ZnTp system, treatment with hydrosulfide resulted in fluorophore displacement and formation of a Zn-SH product (**33d**, Scheme 27). This conversion resulted in a clean shift in the UV-vis spectrum from 354 to 383 nm, and an associated reduction in the fluorescence intensity of the coumarin dye.

**Scheme 27**. Displacement of a bound fluorophore from a TpZn platform

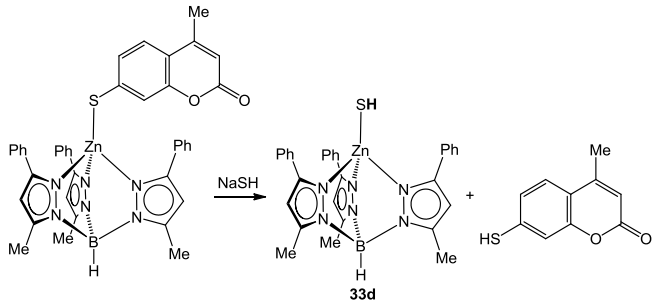


*2.7.3 Heme-Based $H_2S$ Sensing Systems.* The optical changes in the absorption spectrum of myoglobin (see section 3.3.1) upon reaction with $H_2S/HS^-$ have been employed to develop FRET-based fluorescent $H_2S$ sensors. In the absence of $H_2S$, Mb exhibits a Soret band at 409 nm and other weaker absorbances at 503 and 636 nm. Upon reaction with $H_2S$, the Soret band shifts to 421 nm, and the lower-energy absorbances at 503 and 636 nm are quenched with the appearance of

new bands at 543, 581, and 617 nm. By employing dyes that absorb near the different absorbance maxima in the Mb-sulfide adduct, D'Auria and co-workers demonstrated that the fluorescence of the dye can be modulated.[165] As an example of this approach, labeling the N-terminus of Mb with either the dye Cy3 ($\lambda_{max}$ = 550 nm; $\lambda_{em}$ = 570 nm), which overlaps with the 543 nm Mb-sulfide absorbance, or Atto620 ($\lambda_{max}$ = 620 nm; $\lambda_{em}$ = 645 nm), which overlaps with the 617 nm Mb-sulfide absorbance, resulted in fluorescence modulation upon reaction with $H_2S$.

Using a similar approach, Galardon and co-workers leveraged the reversible sulfide binding observed in *Lucina pectinata* by using recombinant HbI (rHBI) to develop a reversible method for $H_2S$ measurement.[166] The authors reasoned that addition of the coumarin-based dye Pacific Blue, which has a maximal absorbance at 404 nm, could take advantage of the change in absorbance of rHbI from 407 to 425 nm upon $H_2S$ binding. In the absence of $H_2S$, rHbI absorbs near the same wavelength as the Pacific Blue dye, thus limiting the dye fluorescence. After addition of $H_2S$, however, the shift in absorbance to 425 nm results in a higher excitation efficiency of the Pacific Blue dye and leads to an enhanced fluorescence response of the dye at 455 nm. Consistent with both the overall design and the reversible binding of $H_2S$ to HbI, the rHb1 / Pacific Blue sensing system was demonstrated to be reversible, as evidenced by repeated cycles with NaSH treatment followed by purging with Ar gas.

*2.7.4 Other Enzyme-Based $H_2S$ Sensing Systems.* Using a similar approach as in the fluorescently-tagged Mb system, other fluorescently-tagged metalloenzymes have also been utilized to detect $H_2S$. For example, peptide deformylase (PDF) from *Escherichia coli* normally has $Fe^{II}$ as its native metal cofactor, but the $Fe^{II}$ can be substituted with other transition metals. Using an Atto620 tagged Co-PDF version of this enzyme, Strianese and co-workers demonstrated that the resultant enzyme-dye conjugate could function as a turn-off fluorescent $H_2S$ reporter.[167]

In the absence of $H_2S$, Co-PDF has absorbances at 560 and 660 nm. These two absorbances are quenched upon addition of $H_2S$, and two new bands appear at 625 and 665 nm, with the 625 nm band having good overlap with the Atto620 fluorophore. This increased absorbance at 625 nm upon $H_2S$ addition results in decreased excitation efficiency of the Atto620 fluorophore and a reduction of fluorescence. Although this reaction was found to be irreversible, the importance of the Co-sulfide interaction was supported by X-ray crystallography of the reaction product of Co-PDF with $H_2S$, which showed sulfide coordination to the metal center with a Co-S bond distance of 2.29 Å. The authors note that exchange of other metals into the PDF platform may also support $H_2S$ sensing. As a proof of concept of this approach, the authors also reported an X-ray structure of the product of Ni-PDF treatment with $H_2S$, which revealed a Ni-S distance of 2.58 Å, although sensing applications were not investigated with the nickel system (Figure 5).

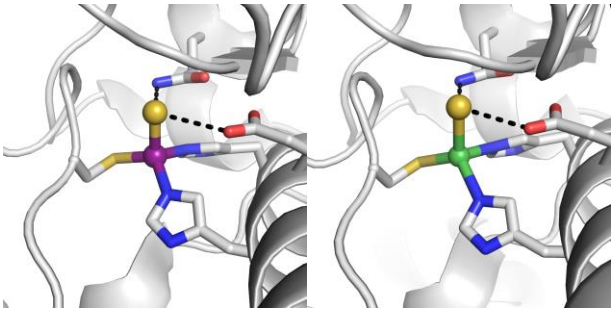

**Figure 5**. X-ray structures of Co(PDF) and Ni(PDF). PDB: 4AZ4, 4AL2.

Using the azurin protein, Strianese and co-workers pursued a similar approach of fluorophore ligation to generate a fluorescence response to sulfide.[168] Treatment of the 14 kDa Cu-containing protein azurin with $H_2S$ was found to result in reduction of the $Cu^{II}$ to $Cu^{I}$ as evidenced by both EPR spectroscopy and X-ray crystallographic analysis before and after reduction of the Cu center. This reduction from $Cu^{II}$ to $Cu^{I}$ was accompanied by a bleaching of the broad charge-transfer

absorbance from 550-650 nm in azurin. Using azurin labeled with the Atto620 fluorescent tag, reduction of $Cu^{II}$ led to an increase in fluorescence, which could be returned to its more quenched state by oxidation back to $Cu^{II}$ with $K_3Fe(CN)_6$, which also supports retention of $Cu^{I}$ in the protein in its reduced state. In addition to the Cu-azurin system, the authors also prepared a Co analogue of azurin, which maintains a broad absorbance in the 300-350 nm region of the spectrum, which increased upon addition of $H_2S$. By using Alexa350 ($\lambda_{max}$ = 346 nm, $\lambda_{em}$ = 442) instead of Atto620 as a fluorescent tag, this change in absorbance in Co-azurin was translated to a fluorescence turn-off response, which could be restored by oxidation with $K_3Fe(CN)_6$.

## 3. Roles in Organometallic and Coordination Chemistry

### *3.1 Subsection Introduction.*

The biological chemistry of hydrosulfide described in the previous sections arises naturally as a consequence of Nature's appropriation of this abundant element during millions of years of evolution. From the standpoint of the synthetic chemist, however, the intrinsic properties of the hydrosulfide ion and its conjugate acid, $H_2S$, render it unideal as a ligand in terms of both kinetic and thermodynamic stability. Nonetheless, these challenges have provided an incentive for intrepid inorganic chemists over the past 50+ years to explore the limits of its coordination chemistry and reactivity with metal ions. Practical considerations as well, such as the desire to mitigate harmful $H_2S$ in the environment by catalytic means, have provided additional impetus to investigate the fundamental reaction chemistry of hydrosulfide. This section will cover aspects of transition metal hydrosulfide complexes in the context of their roles in organometallic chemistry, coordination chemistry, and cluster science. The section begins, however, with a specific focus on the reactivity of $HS^-$ relevant to molecular hydrogen. Parallels between metal hydrides and metal hydrosulfides

are notable and therefore it is no coincidence that an understanding of the former has helped guide the development of the latter.

*3.2 Roles in $H_2$ Chemistry*

The potential for $H_2S$ to serve as a source of $H_2$ equivalents has intrigued coordination chemists for several decades.[169] In this vein, it is worthwhile to appreciate analogies to modern research where the lighter congener of $H_2S$, water, is receiving a great deal of attention as a source of molecular hydrogen in the context of renewable energy. Oxidative addition of the S-H bond to transition metals was envisioned early on as a potential means of activating $H_2S$ toward further chemistry and it remains a popular means of preparing hydrosulfide complexes. In similar fashion, the pronounced acidity of $H_2S$ was also recognized as a convenient means of generating $H_2$ through acid-base chemistry with metal hydrides.

*3.2.1 Oxidative Addition of $H_2S$.* Some of the first examples of $HS^-$ coordination to transition metal ions were reported in the context of studies on oxidative addition. Among the earliest examples of putative hydrosulfide coordination was a brief mention in a 1962 publication by Vaska and co-workers intimating that $H_2S$ is capable of undergoing oxidative addition with *trans*-$[Ir(CO)Cl(PPh_3)_2]$ to generate the Ir(III) hydrosulfide species $[Ir(CO)Cl(PPh_3)_2(SH)H]$ (**46**) (Scheme 28).[170] A similar complex containing the chelating dppe ligand (dppe = *bis*(l,2-diphenylphosphino)ethane) was subsequently reported by Vaska, although as with **46**, the hydrosulfide complex was not isolated.[171, 172] Wilkinson and co-workers later reported similar oxidative addition chemistry of $H_2S$ with $[Ir(CO)Cl(PPh_3)_2]$ and its Rh congener. Although the resulting hydrosulfide species was isolated, direct spectroscopic evidence for the SH ligand was

not forthcoming as an IR peak for the S-H stretch could not be identified.[173] Later work by Pignolet and coworkers provided crystallographic evidence for the composition of **46** along with the bridging hydrosulfide complex $[RhCl(H)(\mu\text{-}SH)(PPh_3)_2]_2$ (**47**), resulting from oxidative addition of $H_2S$ to Wilkinson's catalyst ($[RhCl(PPh_3)_3]$).[174] Working with the related tetraphosphine iridium(I) species, $[Ir(PMe_3)_4]^+$, Milstein and coworkers also observed facile oxidative addition of $H_2S$ to afford *cis*-$[Ir(H)(SH)(PMe_3)_4]^+$ (**48**).[175] Much like **46**, compound **48** failed to demonstrate an observable IR signature. However, the compound was characterized crystallographically and an NMR resonance for the sulfhydryl proton was found at −2.05 ppm showing the expected coupling to both $^{31}P$ and $^{1}H$.

**Scheme 28**. Early examples of M-SH species generated by oxidative addition of $H_2S$.

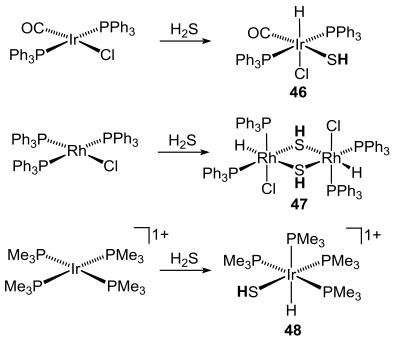


Rhodium(I) compounds were also the subject of early studies by Collman and co-workers who demonstrated oxidative addition of $H_2S$ to generate compound **49**, which contains a macrocyclic $N_4$ ligand (Scheme 29).[176] No IR or NMR features for the S-H ligand were reported, although a Rh-H stretch was identified at 1910 $cm^{-1}$. Hampering characterization was the fact that compound **49** was found to be unstable in solution reverting back to the corresponding Rh(I) species by reductive elimination of $H_2S$. A more robust Rh(III) bis-hydrosulfide complex, **50**, was also

disclosed in the same work arising from hydrolysis of a precursor featuring triethylgermaniumsulfide ligands (Scheme 29). Unlike **49**, both IR and NMR signatures for the SH ligands of **50** were readily apparent at 2580 $cm^{-1}$ and −1.55 ppm, respectively, although rapid exchange between the protons of the sulfhydryls and adventitious water precluded determination of a $^{2}J_{Rh\text{-}H}$ coupling constant.

**Scheme 29.** Mono- and bis-hydrosulfide complexes of a Rh(III) $N_4$ macrocycle.

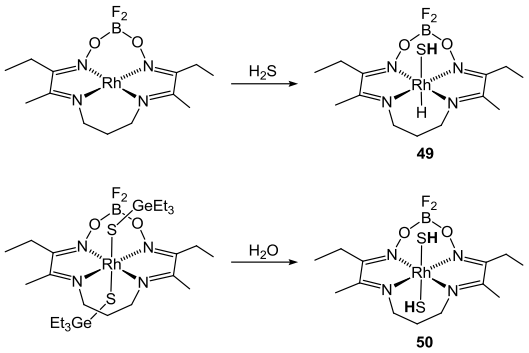


Trivalent Group 9 compounds have likewise been investigated for oxidative addition chemistry. Pignolet and co-workers examined reactions of $H_2S$ with the Ir(III) dihyride complex, $[Ir(H)_2(Me_2CO)_2(PPh_3)_2]^+$.[177] Following up on earlier observations by Crabtree and co-workers,[178] treatment of $[Ir(H)_2(Me_2CO)_2(PPh_3)_2](BF_4)$ with $H_2S$ in acetone was found to primarily give the bimetallic complex $[Ir_2(H)_2(PPh_3)_4(\mu\text{-}SH)_2(\mu\text{-}H)]^+$ (**51**) which could be deprotonated to yield the neutral species $[Ir_2(H)_2(PPh_3)_4(\mu\text{-}S)(\mu\text{-}SH)(\mu\text{-}H)]$ (**52**, Scheme 30). Both **51** and **52** were observed to exist as a mixture of isomers based on the relative stereochemistry of the bridging SH groups. During formation of **51**, a small quantity of the isopropylthiolate-bridged complex $[Ir_2(H)_2(PPh_3)_4(\mu\text{-}S)(\mu\text{-}S^iPr)(\mu\text{-}H)]^+$ was also obtained. Formation of this species was proposed to occur through reaction of acetone with the putative Ir(V) intermediate, $[Ir(SH)(H)_3(PPh_3)_2]^+$ (**53**), arising from oxidative addition of $H_2S$ to $[Ir(H)_2(Me_2CO)_2(PPh_3)_2]^+$. Rauchfuss and co-workers

later demonstrated that **51** could also be prepared by addition of $H_2$ to the iridium sulfide complex, $[Ir_2(\mu\text{-}S)_2(PPh_3)_4]$ (*vide infra*).[179]

**Scheme 30**. Reactions of $H_2S$ with $[Ir(H)_2(Me_2CO)_2(PPh_3)_2]^+$.

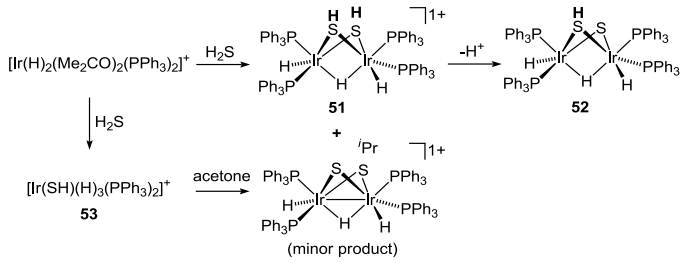


The facile oxidative addition chemistry displayed by $H_2S$ with Ir also prompted early studies with Pt complexes. Pioneering work by Ugo and co-workers examined the interaction of $H_2M$ (M = S, Se, and Te) with "$(Ph_3P)_2Pt$". $H_2S$ was found to add reversibly to $Pt^0$ to afford the cream-colored Pt(II) complex $[Pt(SH)(H)(PPh_3)_2]$ (**54a**) along with a second species proposed to be the $H_2S$ adduct, $[Pt(SH_2)(PPh_3)_2]$ (**55**, Scheme 31).[180] Of particular note, $^1H$ NMR data for **54a** revealed a S-H proton resonance at −1.44 ppm. Such high-field resonances are a hallmark of hydrosulfide complexes of the mid to late transition metals further supporting the composition of **54a**. Low temperature NMR experiments verified the *trans* disposition of the phosphine ligands, although the lack of observable P-H coupling at room temperature suggested a dynamic process at higher temperatures. Later work with analogs of **54a** containing $PBn_3$ (**54b**) $PCy_3$ (**54c**), and $PEt_3$ (**54d**) ligands established unambiguously the composition of such species and provided both NMR and IR evidence for the coordinated SH ligand.[181, 182] To date, no crystal structure has been reported for a species of the type *trans*-$[Pt(H)(SH)(PR_3)_2]$, although Bagdanovic and co-workers have

reported the structure of the related Pd complex, *trans*-[Pd(H)(SH)($PCy_3$)$_2$], which does in fact demonstrate the expected arrangement of the hydride and hydrosulfide ligands.[183]

**Scheme 31.** Synthesis and reactivity of [Pt($PR_3$)$_2$(SH)(H)] species.

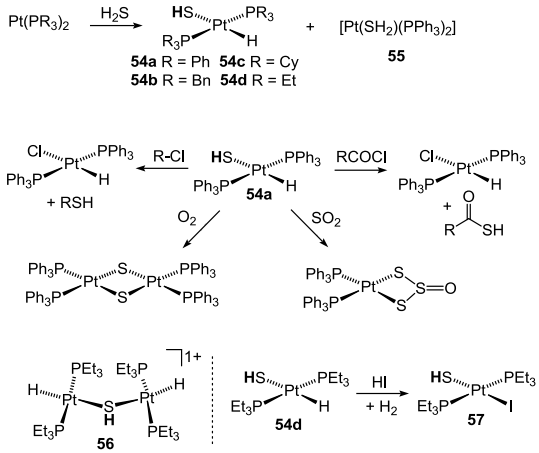


The reactivity of [Pt(SH)(H)($PR_3$)$_2$] was the subject of several subsequent studies. Ugo and co-workers found that **54a** reacts readily with alkyl and acyl halides to produce [Pt(Cl)(H)($PPh_3$)$_2$] and the corresponding thiols and thioesters demonstrating the susceptibility of the hydrosulfide group to attack by electrophiles (Scheme 31).[184] Even more notable, exposure of **54a** to molecular oxygen was found to result in formation of a material with formula "[Pt($PPh_3$)$_2$(S)]$_2$" implying that $H_2S$ can be used as a source of $H_2$ equivalents for reduction of $O_2$. In related chemistry, Shaver and co-workers demonstrated more recently that **54a** reacts with $SO_2$ to generate [Pt($PPh_3$)$_2$($\kappa^2$-$S_2SO$)].[185] This oxotrisulfido species can be regarded as a potential intermediate in the oxidative breakdown of $H_2S$ to elemental sulfur (the Claus process), for which **54a** was shown to be a homogeneous catalyst.

Using compounds related to **54d**, Robertson and co-workers have demonstrated the existence of the hydrosulfide-bridged diplatinum cation *trans*-[Pt($PEt$)$_2$(H)(μ-SH)]$_2$ (**56**).[186] Compound **54d**

was also found to undergo further oxidative addition chemistry with $H_2Se$ but not $H_2S$ to generate new Pt(IV) complexes lacking hydrosulfide ligands.[182] These experiments illustrated the reductive nature of S versus Se leading to facile reductive elimination of $H_2S$ from Pt(IV) intermediates. In a similar vein, exposure of **54d** to HI produced the mixed halide-hydrosulfide species, *trans*-[Pt(I)(SH)($PEt_3$)$_2$] (**57**). Formation of **57** can be envisioned to occur through direct protonation of the hydride ligand, or via oxidative addition of HI and subsequent reductive elimination of $H_2$.

In a modified approach to oxidative addition, the azide precursors [Pd($N_3$)$_2$($PPh_3$)$_2$] and [Pd($N_3$)$_2$($PPh_3$)$_2$] were demonstrated to react with $H_2S$ to produce the bis-hydrosulfide species [M(SH)$_2$($PPh_3$)$_2$] (M = Pd, **58a**; M = Pt, **59a**) (Scheme 32).[187] Formation of **59a** was also reported by Schmidt and co-workers to result from treatment of [$PtCl_2$($PPh_3$)$_2$] with $H_2S$ in the presence of base.[188] The specific geometrical isomers (*cis* vs. *trans*) formed in these reactions were not explicitly noted although subsequent crystallographic studies with **58a** demonstrated that it exists as the *trans* isomer in the solid state,[189] whereas that of **59a** exists as the *cis* isomer (Figure 6).[190] Factors accounting for the different geometrical isomers observed for **58a** and **59a** have never been investigated, and the preparative route employed may account for the particular isomer isolated in each case. For example, the asymmetric unit of **59a** was found to contain a molecule of $CHCl_3$ appearing to engage in a hydrogen-bond with one of the hydrosulfide ligands. Such interactions may provide the neccessary driving force to select for one geometrical isomer over the other in the solid state. The corresponding trialkylphosphine complexes of Pd and Pt featuring P$^i$Bu$_3$ and $PEt_3$ ligands, respectively, were all found to exist as the *trans* isomers in the solid state.[182, 191] The related [M(SH)$_2$(dppe)] complexes (M = Ni, **60a**; Pd, **58b**; Pt, **59b**) were prepared by Schmidt and co-workers via salt metathesis with NaSH and found to display spectroscopic signatures similar to those of **58a** and **59a**.[192] A similar complex, [Pt(dppe)($CH_3$)(SH)] (**61**), was also reported by

Bennet and co-workers through addition of $H_2S$ to the Pt(II) methyl species $[Pt(dppe)(CH_3)(OH)]$.[193]

**Scheme 32.** Generation of Group 10 bis-hydrosulfide species.

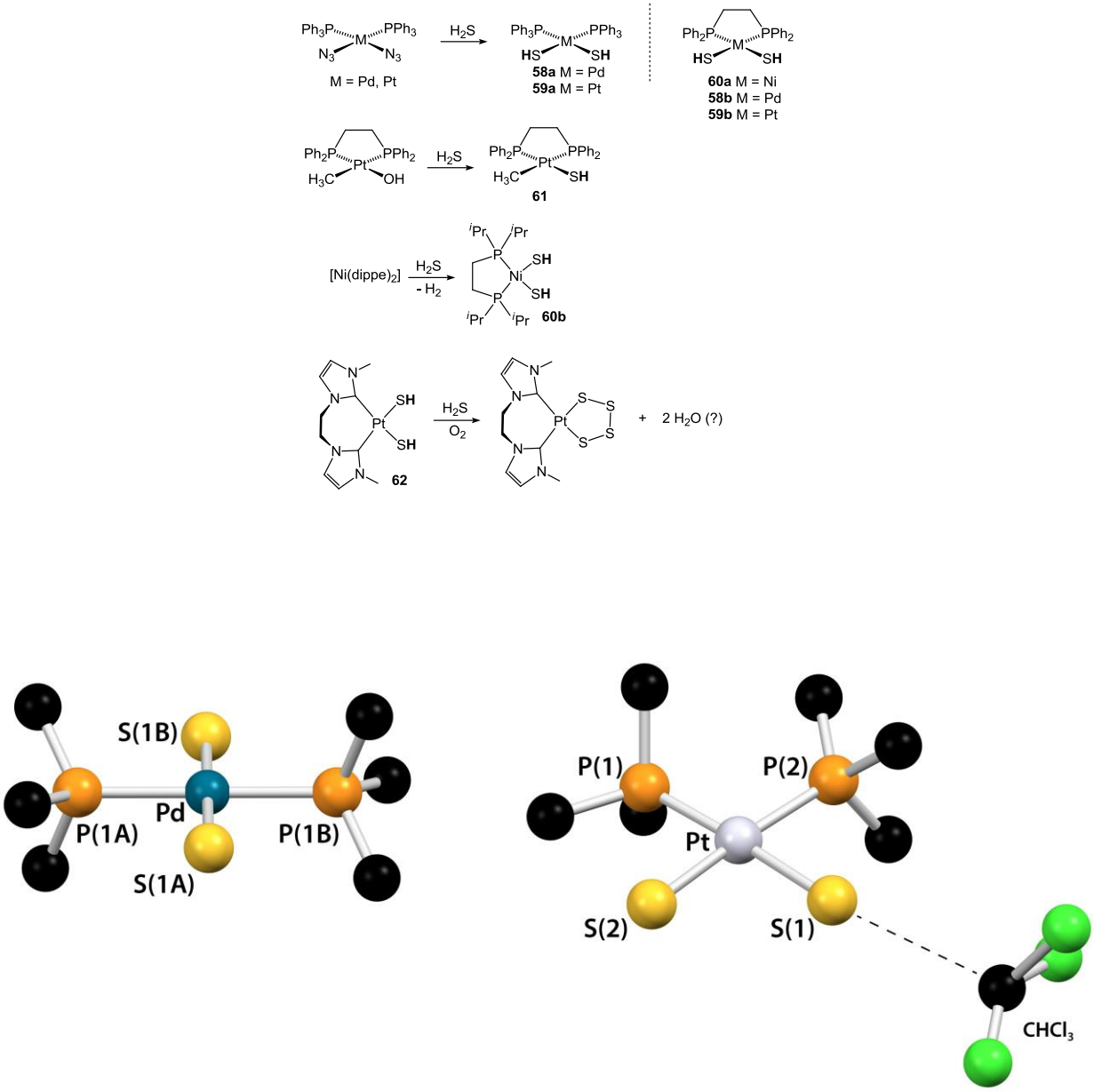

**Figure 6.** Solid-state structures of **58a** (left) and **59a** (right) generated from crystallographic data in references 189 and 190. Hydrogen atoms and phenyl rings of $PPh_3$ are omitted for clarity but co-crystallized $CHCl_3$ with presumed H-bonding interaction is shown for **59a**.

Much more recently, Jones and coworkers have reported the synthesis of [Ni(dippe)$(SH)_2$] (**60b**, dippe = 1,2-bis(diisopropylphosphino)ethane), an analog of **60a** (Scheme 32).[194] Compound **60b** was prepared in the context of desulfurization studies with nickel by oxidative addition of $H_2S$ to the zero-valent complex, [Ni$(dippe)_2$]. As such, **60b** completes the series of bishydrosulfide complexes of the Group 10 metals generated by oxidative addition of $H_2S$. Compound **60b** was further employed as a precursor to sulfide species via comproportionation with a bimetallic Ni(I) hydride. Similarly, Nishioka prepared compound **62**, a chelating NHC variant of **59a**, and demonstrated that it is oxidized by $O_2$ in the presence of $H_2S$ to form a monomeric Pt(*cyclo*-$S_4$) species with $H_2O$ as the presumed by-product (Scheme 32).[195] Such chemistry harkens back to the reaction discussed above concerning **54a** and $O_2$, once again demonstrating the ability of $H_2S$ to serve as a surrogate for $H_2$ in inorganic complexes.

Precious metal systems beyond Ir and Pt have also been the subject of intense investigation regarding the oxidative addition of $H_2S$. For example, James and co-workers reported the facile reaction of $H_2S$ with the zero valent Ru complex [Ru$(CO)_2(PPh_3)_3$] at −35 ºC to give hydrosulfide [Ru$(CO)_2(PPh_3)_2(SH)(H)$] (**63**, Scheme 33).[196] At higher temperatures, **63** reacts further with $H_2S$ to produce $H_2$ and the bis-hydrosulfide [Ru$(CO)_2(PPh_3)_2(HS)_2$] (**64**) through an acid-base process. The *cis,cis,trans* stereochemistry of **63** and **64** and was established through NMR and IR spectroscopy as well as crystallization of **64**.[197] Identical reactions of $H_2S$ with the tricarbonyl precursor, [Ru$(CO)_3(PPh_3)_2$], were found to be significantly less efficient, producing only small

quantities of hydrosulfide **63** and *bis*-hydrosulfide **64** after reflux in tetrahydrofuran.[198] Analogs of **63** and **64** containing the bidentate dppm ligand (**65, 66a,b**) were also prepared by James through treatment of *cis*/*trans*-[Ru(H)$_2$(dppm)$_2$] with $H_2S$.[197] Unlike **63**, compound **66a** was found to exist solely as the *trans*-(H,SH) isomer. By contrast, the *bis*-hydrosulfide was produced as a mixture of *cis* and *trans* isomers (**66a**, **66b**). Later work by James and co-workers reported the crystal structure of **66b** from an improved synthesis of **66a** and **66b** starting from *trans*-[Ru(H)Cl(dppm)$_2$].[199]

**Scheme 33**. Generation of Ru(II) hydrosulfide complexes.

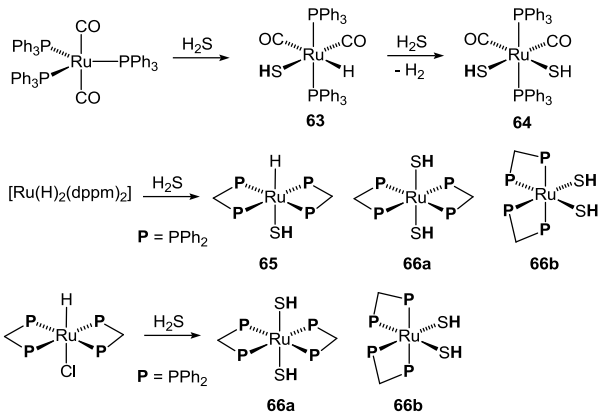


Divalent ruthenium has also been shown to take part in oxidative addition reactions with $H_2S$. Puerta and co-workers reported the reaction of [Cp*RuCl(PEt$_3$)$_2$] with $H_2S$ in the presence of $NaBPh_4$ to afford the cationic Ru(IV) complex [Cp*Ru(SH)(H)(PEt$_3$)$_2$]$^+$ (**67**, Scheme 34).[200] Interestingly, **67** was only observed in the case of the Cp* ligand. Identical reactions with [CpRuCl(PEt$_3$)$_2$] led to formation of the bridging disulfide species [Cp$_2$Ru$_2$(PEt$_3$)$_4$($\mu$-S$_2$)](BPh$_4$)$_2$. Compound **67** was found to convert to a similar disulfide species, [Cp*$_2$Ru$_2$(PEt$_3$)$_4$($\mu$-S$_2$)](BPh$_4$)$_2$,

upon air oxidation with liberation of water. Such a reaction bears a strong resemblance to that described above for **62**.

**Scheme 34.** Reactions of Cp*Ru complexes with $H_2S$.

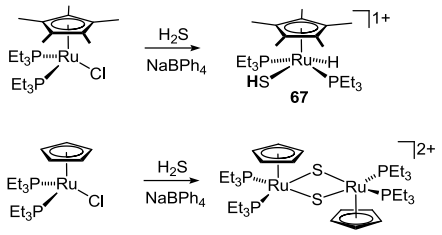


The existence of $H_2S$ adducts as precursors to oxidative addition has continued to intrigue chemists working in this area. In this vein, the chemistry of ruthenium has provided a fertile testing ground for the preparation of such adducts. Sellman and co-workers were the first to crystallographically characterize an $H_2S$ adduct, compound [Ru('$S_4$')($PPh_3$)($SH_2$)] (**68**, '$S_4$' = tetrathiolate ligand), which was prepared by low temperature (−70 ºC) addition of $H_2S$ to the oligomeric Ru(II) complex [Ru($PPh_3$)('$S_4$')]$_n$ (Scheme 35).[201] The stability of **68**, at least in the solid state, was ascribed to significant hydrogen-bonding between $H_2S$ and both a co-crystallized molecule of THF as well as the anionic S atom of the $S_4$ ligand. Unlike the reaction at low temperature, treatment of [Ru($PPh_3$)('$S_4$')]$_n$ with $H_2S$ at ambient temperature proceeded with oxidative addition to generate a mixture of species including the Ru(III) disulfide species, [$Ru_2$($\mu$-$S_2$)($PPh_3$)$_2$($S_4$)$_2$].[202] In similar chemistry, James has also reported several crystallographically-characterized examples of $H_2S$ adducts of Ru(II). In this instance, treatment of halide precursors [$RuX_2$(**P-N**)($PR_3$)] (X = Cl or Br; R = Ph or *p*-tolyl) with $H_2S$ under ambient conditions afforded [$RuX_2$(**P-N**)($PR_3$)($SH_2$)] adducts (**69a-c**, Scheme 35).[203, 204] As with **68**, compounds **69a-c** underwent loss of $H_2S$ upon purging with inert gas or exposure to vacuum.

**Scheme 35.** Coordination of $H_2S$ to Ru complexes.

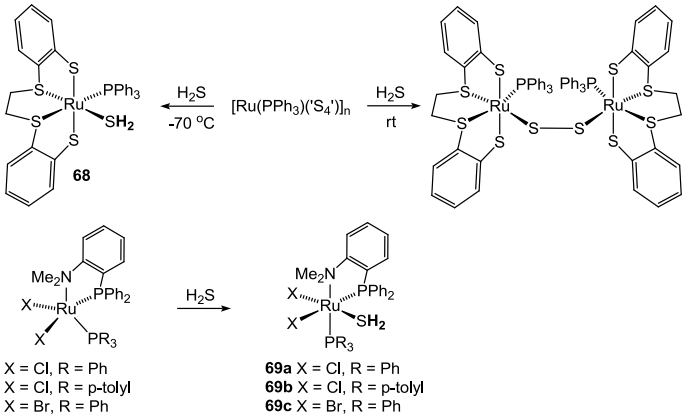


Outside of precious metal systems, oxidative addition of $H_2S$ has likewise been employed in the synthesis of hydrosulfide complexes. In the area of Group 4 chemistry, Bottomley and co-workers were the first to examine the oxidative addition of $H_2S$ to divalent Ti and Zr compounds of the type $[Cp^R_2M(CO)_2]$,[205, 206] although metallocene complexes of hydrosulfide had already been well established for two decades (*vide infra*). Reactions of $[Cp^R_2M(CO)_2]$ with $H_2S$ were found to generate metal-sulfide clusters in the case of Zr and the parent $[Cp_2Ti(CO)_2]$, but when the pentamethylcyclopentadienyl analog $[Cp^*_2Ti(CO)_2]$ was employed, the titanocene hydrosulfide species $[Cp^*_2Ti(SH)_2]$ (**70b**), was isolated (Scheme 36). In all cases, reaction of $H_2S$ with $[Cp^R_2M(CO)_2]$ was found to produce molecular $H_2$ as a byproduct.

**Scheme 36.** Oxidative addition of $H_2S$ to Ti and Zr complexes.

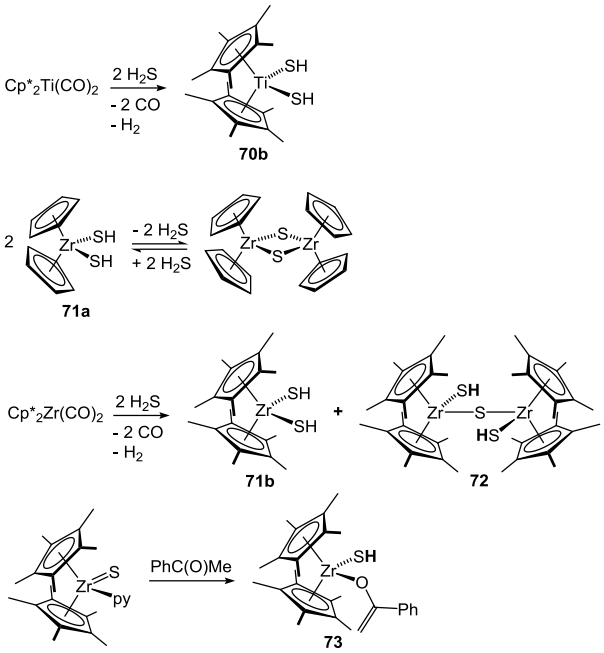


Shaver demonstrated that the Zr analog $[Cp_2Zr(SH)_2]$ (**71a**) containing the parent Cp ligand, exists in equilibrium with $[Cp_2Zr_2(\mu\text{-}S)_2]$ and $H_2S$ in accordance with the reported inability to observe **71a** in reactions of $[Cp_2Zr(CO)_2]$ with $H_2S$.[207] However, in later work with the Cp* ligand, Parkin and co-workers found that treatment of $[Cp^*_2Zr(CO)_2]$ with $H_2S$ does in fact generate small amounts of $[Cp^*_2Zr(SH)_2]$ (**71b**) in contrast to the prior report by Bottomley and co-workers.[208] The major product of the reaction, however, was found to be the bridged-sulfide species $[Cp^*_2Zr_2(SH)_2(\mu\text{-}S)]$ (**72**). Use of $[Cp^*_2Zr(CO)_2]$ also permitted isolation of the terminal sulfide species, $[Cp^*_2Zr(S)(py)]$, which underwent reaction with acetophenone to produce $[Cp^*_2Zr(SH)(OC(CH_2)Ph)]$ (**73**) (Scheme 36).[209]

Parkin and co-workers have also described oxidative addition of $H_2S$ to centers with the masked W(0) species, $[M(\eta^2\text{-}CH_2PMe_2(H)(PMe_3)_4]$ (M = Mo, W) (Scheme 37).[210] The intermediate species, $[W(PMe_3)_4(SH)_2(H)_2]$ (**75**), was detected spectroscopically but was found to lose $H_2$ rapidly to generate the *trans*-$[W(S)_2(PMe_3)_4]$. The corresponding reaction with the Mo

congener [Mo($\eta^2$-$CH_2PMe_2$(H)($PMe_3$)$_4$] produced the analogous sulfide species via *trans*-[Mo(S)$_2$($PMe_3$)$_4$].[211] Interestingly, treatment of [W($\eta^2$-$CH_2PMe_2$(H)($PMe_3$)$_4$] with $H_2Se$ was found to generate the related terminal selenide, *trans*-[W(Se)$_2$($PMe_3$)$_4$], although not through the intermediacy of a hydrogenselenide species.[212]

**Scheme 37**. Oxidative addition of $H_2S$ to Mo and W complexes.

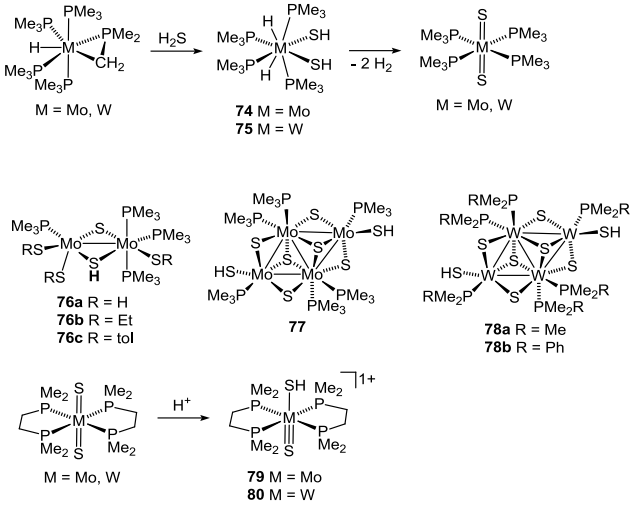


The chemistry of *trans*-[M(S)$_2$($PMe_3$)$_4$] (M = Mo, W) with $H_2S$ and thiols was further investigated by Rauchfuss and found to result in a series of M-S cluster species containing hydrosulfide ligands.[213] In this case, entry to *trans*-[M(S)$_2$($PMe_3$)$_4$] was accomplished by direct treatment of $[MS_4]^-$ with $H_2S$ in the presence of $PMe_3$. Compounds of the type (**76a-c**) were obtained as the initial products of $H_2S$ or thiol reactivity with *trans*-[Mo(S)$_2$($PMe_3$)$_4$] (Scheme 37). Compound **76c** was found to react further with $H_2S$ to give the tetranuclear species, **77**, prepared earlier by Saito and co-workers.[214, 215] Much more recently, Parkin and coworkers have demonstrated that **77** can result from direct treatment of [Mo($PMe_3$)$_6$] with $H_2S$.[216] The tungsten analog of **77**, **78a** was reported by Rauchfuss and coworkers, although intermediate species similar

to **76a-c** were not detected. Of note, the $PMe_2Ph$ variant of **78a**, **78b**, had been reported several years earlier by Hidai from reactions of $[W(N_2)_2(PMe_2Ph)_4]$ with $(Me_3Si)_2S$.[217, 218]

Employing the dimethylphosphinoethane ligand (dmpe), the disulfide species, *trans*-$[M(S)_2(dmpe)_2]$ (M = Mo, W), can be prepared directly from $[MS_4]^-$ and $H_2S$. Rauchfuss examined proton transfer reactions of *trans*-$[M(S)_2(dmpe)_2]$ in non-aqueous media and was able to generate the cationic hydrosulfide species, $[M(S)(SH)(dmpe)_2]^+$ (M = Mo, **79**; W, **80**) (Scheme 37).[219] The p$K_a$ values of the two compounds were estimated at 16.5 and 15.5, respectively, demonstrating a slightly enhanced acidity for the W congener.

The action of $H_2S$ on Group 6 thiometallates to produce hydrosulfide complexes was similarly shown by Rauchfuss and co-workers to take place with $[ReS_4]^-$. In the case of Re, treatment $[ReS_4]^-$ with $H_2S$ in the presence of $PMe_3$ resulted in formation of $[Re(PMe_3)_4(SH)_2(H)]$ (**81**, Scheme 38).[220] Trimethylphosphine sulfide ($S{=}PMe_3$) was observed as a byproduct during the synthesis of **81**, and in fact the hydrosulfide compound could be employed as a catalyst for the formation of $SPMe_3$ from $H_2S$ and $PMe_3$ at room temperature. Treatment of **81** with dmpe afforded the related complex, **82**. Compound **82** is notable in that it possesses inequivalent hydrosulfide ligands. Magnetization transfer experiments with **82** demonstrated that exchange of the two S-H protons is relatively slow on the NMR timescale. Other reported reactions of **81** include its interaction with CO to first produce $[Re(PMe_3)_4(SH)(CO)]$ (**83**) with elimination of $H_2S$, followed by successive displacement of the $PMe_3$ ligands to generate the related carbonyl-hydrosulfide species $[Re(PMe_3)_3(SH)(CO)_2]$ (**84**) and $[Re(PMe_3)_3(SH)(CO)_3]$ (**85**). Both **81** and **82** were found to catalyze a series of H/D exchange reactions involving $H_2/D_2$, $H_2S/D_2$ and protic reagents. In each case **81** was found to be more efficient, likely due to its ability to dissociate $PMe_3$ more readily to afford the $16e^-$ species, $[Re(H)(SH)_2(PR_3)_2]$ (**86**).

**Scheme 38.** Reactivity of Re hydrosulfide complexes.

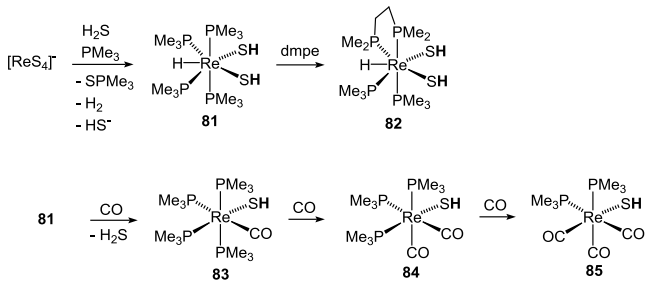


Although the majority of examples of oxidative addition of $H_2S$ involve two-electron processes, one-electron examples have been described. Sacconi and co-workers published an early example of a paramagnetic Ni(I) hydrosulfide complex, **87**, through the reaction of the Ni(0) species, [Ni(**np$_3$**)], with $H_2S$ (Scheme 39).[221] Hydrogen was reported as the byproduct of the reaction in line with many of the two-electron processes described above. Although no crystal structure of **87** was obtained, a $\nu_{SH}$ value of 2545 $cm^{-1}$ was identified by IR spectroscopy and corroborated by a value of 2270 $cm^{-1}$ for the analogous hydroselenide species, [Ni(SeH)(**np$_3$**)] (**88**).

**Scheme 39.** Oxidative addition of $H_2S$ to Ni($np_3$) complexes.

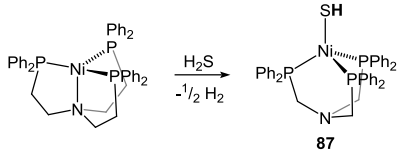


Oxidative addition of $H_2S$ to bimetallic centers has also been examined and found to involve the intermediacy of metal hydrosulfides. Early studies by James and coworkers with bimetallic Pd(I) complexes of the type [$Pd_2X_2(\mu$-P^P)$_2$] (X = halide, P^P = dppm or dppe) demonstrated that

treatment with $H_2S$ led to quantitative formation of $H_2$ and A-frame complexes, $[Pd_2X_2(\mu\text{-}S)(\mu\text{-}P\text{^}P)_2]$.[222, 223] His group later showed that dppm was capable of abstracting sulfur from the A-frame complexes thereby regenerating $[Pd_2X_2(\mu\text{-}P\text{^}P)_2]$ and creating a catalytic cycle for $H_2S$ conversion to $H_2$.[224] Intermediates in route to the A-frame complexes were identified using low temperature NMR spectroscopy and shown to be of the form $[Pd_2X_2(SH)(H)(\mu\text{-}P\text{^}P)_2]$ (**89a-c**) (Chart 2).[225] The chloride analog (**89a**) was postulated to form in similar fashion, although its rapid transformation into the bridging sulfide precluded its definitive characterization. More recently, use of the dmpm (dmpm = dimethylphosphinomethane) ligand has allowed for the intermediate species in the transformation of the chloride analog (**90**) to be observed spectroscopically.[226] An additional likely sulfhydryl-containing species, possibly the $H_2S$ adduct, was observed but could not be positively identified. Related bimetallic zero-valent complexes of Rh and Ir of the type $[M_2(CO)_3(\mu\text{-dppm})_2]$ were also found to oxidatively add $H_2S$ to produce the corresponding A-frame compounds, $[M_2(CO)_2(\mu\text{-}S)(\mu\text{-dppm})_2]$.[227] No intermediates akin to **89** were identified in the case of rhodium, but with iridium, hydrosulfide species **91** was observed by low-temperature NMR spectroscopy (Chart 2).

**Chart 2**. A-frame and related bimetallic hydrosulfide complexes.

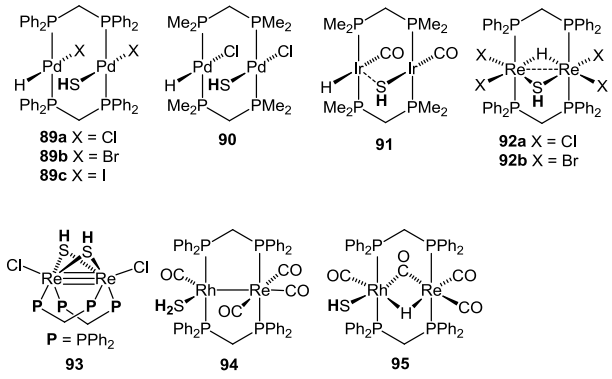

Oxidative addition of $H_2S$ to bimetallic centers has also been demonstrated with species containing formal M-M multiple bonds. Work by Walton and co-workers showed that the dirhenium(II) species, $[Re_2X_4(\mu\text{-dppm})_2]$ (X = Cl, Br), which contains a formal Re-Re triple bond, undergoes reaction with $H_2S$ to produce complexes $[Re_2X_4(\mu\text{-H})(\mu\text{-SH})(\mu\text{-dppm})_2]$ (X = Cl, **92a**; Br, **92b**) (Chart 1).[228] When two of the halide ligands of $[Re_2Cl_4(\mu\text{-dppm})_2]$ were replaced by carboxylates, the related species $[Re_2(O_2CR)_2Cl_2(\mu\text{-dppm})_2]$, was found to take part in a non-redox reaction with $H_2S$ in the presence of acid to produce $[Re_2Cl_2(\mu\text{-SH})_2(\mu\text{-dppm})_2]$ (**93**).[229] The requirement of acid was postulated to stem from the need to convert $[Re_2(O_2CR)_2Cl_2(\mu\text{-dppm})_2]$ to $[Re_2Cl_2(\mu\text{-dppm})_2]^{2+}$ prior to reaction with $H_2S$.[230] The enhanced electrophilicity of $[Re_2Cl_2(\mu\text{-dppm})_2]^{2+}$ over $[Re_2Cl_4(\mu\text{-dppm})_2]$ diverts the chemistry away from oxidative addition and toward proton transfer. Unlike **92a**, compound **93** retained the Re-Re triple bond of the starting material as evidenced by a short Re-Re distance of 2.2577(5) Å. NMR resonances for the bridging SH groups of **93** were not discernable, even at low temperature, likely as a consequence of dynamic motion of the S-H groups in solution which serves to scramble the relative stereochemistry.[231]

In similar fashion to their homobimetallic counterparts, heterobimetallic complexes also react readily with $H_2S$ to give the products of oxidative addition. Cowie and co-workers found that the Rh-Re species, $[RhRe(CO)_4(\mu\text{-dppm})_2]$, produces the A-frame complex, $[RhRe(CO)_4(\mu\text{-S})(\mu\text{-dppm})_2]$, and $H_2$ upon treatment with $H_2S$.[232] Much like the dipalladium species examined by James, intermediates in this process were detected by low temperature NMR and postulated as the $H_2S$ and hydrosulfide adducts, $[Re_2(CO)_4(H_2S)(\mu\text{-dppm})_2]$ (**94**) and $[Re_2(CO)_3(SH)(\mu\text{-CO})(\mu\text{-H})(\mu\text{-dppm})_2]$ (**95**), respectively (Chart 1). The location of the hydrosulfide ligand on Rh in complex **95** was established through heteronuclear $^{31}P$ decoupling experiments. The lighter congener of **95** containing Mn (**96**) was also prepared by Cowie in reactions of $[RhMn(CO)_4(\mu\text{-}$

dppm)$_2$] with $H_2S$ (Scheme 40).[233] In this instance, conversion to the bridging sulfide, [RhMn(CO)$_4$($\mu$-S)($\mu$-dppm)$_2$], was found to require several days permitting isolation of **96**. This work also demonstrated protonation of the bridging sulfide, [RhMn(CO)$_4$($\mu$-S)($\mu$-dppm)$_2$], to afford cationic hydrosulfide [RhMn(CO)$_3$($\mu$-CO)($\mu$-SH)($\mu$-dppm)$_2$]$^+$ (**97**). Compound **97** was found to be active toward the insertion of alkynes into the S-H bond.

**Scheme 40**. Heterobimetallic A-frame complexes.

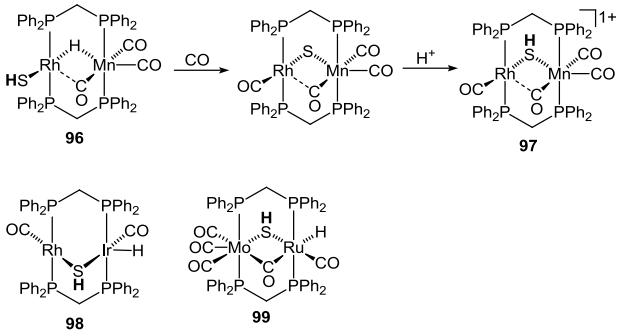


Further underscoring the differences between hetero- and homobimetallic species, Cowie and co-workers were able to isolate the hydrosulfide species [RhIr(CO)$_2$(H)($\mu$-SH)($\mu$-dppm)$_2$] (**98**), by employing the Rh-Ir complex, [RhIr(CO)$_3$($\mu$-dppm)$_2$] (Scheme 40). Compound **98** is analogous to intermediates proposed in the reaction of the homobimetallic $Rh_2$ and $Ir_2$ (**91**) complexes with $H_2S$.[227] Curiously, reaction of [RhIr(CO)$_3$($\mu$-dppm)$_2$] with $H_2S$ terminates with compound **98** instead of proceeding to the sulfide-bridged A-frame complex observed with the homobimetallic species. The unique stability of **98** was proposed to arise from the differing Rh-H vs. Ir-H bond strengths, and the desire of each metal to maintain 16-(Rh) and 18-(Ir) electron counts.

More recently, James and co-workers has demonstrated oxidative addition of $H_2S$ to the Mo-Ru bimetallic species, [MoRu(CO)$_6$($\mu$-dppm)$_2$].[234] As with the examples discussed above, the

ultimate products of the reaction are the bridging sulfide, [MoRu(CO)$_4$($\mu$-S)($\mu$-dppm)$_2$], and molecular hydrogen. Intermediates along the pathway to formation of the sulfide were identified at room temperature, including the isolable compound [MoRu(CO)$_4$($\mu$-CO)($\mu$-SH)($\mu$-dppm)$_2$] (**99**, Scheme 40).

*3.2.2 Addition of $H_2S$ to metal hydrides.* In many of the examples of oxidative addition of $H_2S$ to transition metal centers discussed above, a subsequent proton transfer event occurs between a metal hydride and a second equivalent of $H_2S$ leading to generation of molecular hydrogen. Such a strategy for production of $H_2$ is logical given the acidity of $H_2S$ and the basic nature of most transition metal hydrides. Consequently, such a strategy has been employed to synthesize a number of hydrosulfide complexes.

Early work by Nolte and Singleton described the reaction of $H_2S$ with the ruthenium(II) hydride complex, [RuH(COD)(PMe$_2$Ph)$_3$]$^+$ (COD = 1,4-cyclooctadiene), in methanol to generate **100** and molecular hydrogen (Scheme 41).[235] The triply-bridging nature of the hydrosulfide ligands was proposed through analogy with the structurally characterized hydroxide analog. Both $\nu_{SH}$ and $^1$H NMR resonances for the hydrosulfide ligands were detected spectroscopically further confirming identity of the complex as a hydrosulfide species.

**Scheme 41.** Addition of $H_2S$ to Ru hydride complexes.

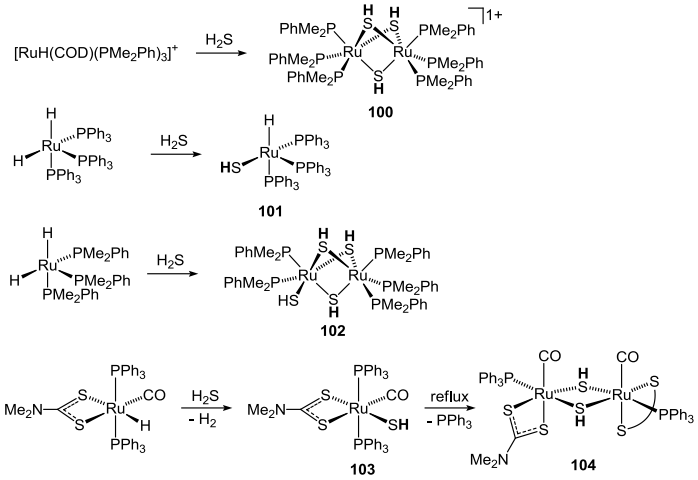


In related chemistry, Yamamoto and co-workers reported the reaction of $H_2S$ with the ruthenium(II) dihydride, $[Ru(H)_2(PPh_3)_2]$ to produce the purple complex **101** (Scheme 41).[236] Hydrogen was evolved quantitatively in the process as expected for simple proton transfer. Compound **101** could also be accessed via reaction of $S_8$ with $[Ru(H)_2(PPh_3)_2]$. Although not prepared via oxidative addition of $H_2S$ to Ru(0) as with **63**, evidence for the facility of such a process was garnered through H/D exchange. Dissolution of **101** in $CH_2Cl_2$ with 4% MeOD was found to result in deuterium incorporation into the hydrosulfide, hydride, and phenyl groups of the phosphine ligands. In the case of the hydride ligand, reversible reductive elimination/oxidative addition of $H_2S$ was invoked to explain the exchange process, much like that observed for **54**.[184] Subsequent work by Yamamoto and co-workers demonstrated that a similar ruthenium(II) dihydride precursor, $[Ru(H)_2(PMe_2Ph)_3]$, containing the smaller $PMe_2Ph$ ligand reacted with $H_2S$ to produce the bimetallic species, **102**. In this instance, a second proton transfer occurs to generate a briding tris(hydrosulfide). Of note, the solid-state structure of **102** was also reported and the authors identified short contacts (within van der Waals radii) between the H atoms of the bridging sulfhydryl groups and the π system of the Ph rings. Compound **102** is conceptually similar to **100**

and the two compounds likely result from their respective reactions due to subtle differences in preparative conditions (i.e. temperature, protic vs. aprotic solvent).

Employing a closely related Ru(II)-hydride containing a thiocarbamate ligand, Matsumoto and co-workers reported analogous protonation chemistry with $H_2S$ to generate **103** (Scheme 41).[237] Refluxing **103** in benzene resulted in loss of $PPh_3$ and formation of the bimetallic species, **104**. Consistent with the presence of a double SH-bridge, the Ru-Ru distance in **104** was found to be slightly longer than that in triply-bridging **103**.

The generation of metal hydrides by reaction with hydrosulfide without formal oxidative addition to the metal center has also been demonstrated. Darensbourg and co-workers reported the reaction of $[M(CO)_5(PR_3)]^+$ (M = Mn, Re; R = tertiary phosphine or phosphite) with NaSH to generate the corresponding metal hydride with loss of carbonyl sulfide (Scheme 42).[238] This reaction was proposed to proceed through nucleophilic attack on the bound CO ligand to generate a transient C(O)SH ligand, which rapidly undergoes $\beta$-H elimination with extrusion of COS. In related chemistry, Ibers and co-workers demonstrated that the reverse process takes place with Rh(I).[239] Reaction of COS with $[Rh(H)(PPh_3)_4]$ produced the Rh(I) hydrosulfide species, **105**, presumably through an intermediate containing a C(O)SH similar to that proposed by Darensbourg.

**Scheme 42.** Transformations of metal hydrosulfides involving COS.

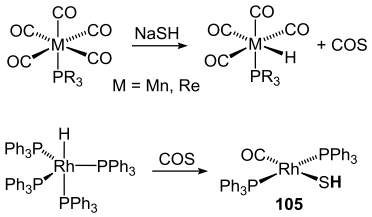

*3.2.3 Addition of $H_2$ to metal-sulfur species*. The interaction of $H_2$ with sulfido and thiolate ligands has also played an important role in the development of hydrosulfide chemistry. Much of this interest has stemmed from its relationship to the hydrodesulfurization process in the refinement of petroleum feedstocks. In work spanning several decades, Rakowski DuBois and coworkers have explored the chemistry of cyclopentadienyl dimolybdenum species containing bridging sulfides.[240] Early work reported the reactions of a series of methyl-cyclopentadienyl Mo sulfido species $[(Me_nCp)MoS_x]_y$ with $H_2$ to produce the Mo(IV) hydrosulfide complexes $[(Me_nCp)_2Mo_2(\mu\text{-}S)_2(\mu\text{-}SH)_2]$ (**106a-c**), with loss of excess sulfur in the form of $H_2S$ (Scheme 43).[241] The authors noted the appearance of at least two isomeric forms of the hydrosulfide products and suggested that these might correspond to *syn* and *anti* arrangements of the S-H groups of the *trans* isomer based on comparison to the structurally characterized SMe analog. Later crystallographic studies of **106c** confirmed the *trans-anti* isomer in the solid state.[242, 243] Compounds of type **106a-c** are active catalysts for the reduction of elemental sulfur by $H_2$ and display H/D exchange with both mixtures of $H_2/D_2$ as well as $H_2/D_2O$. Alkenes, alkynes and isocyanides were also found to react with **106a-c**, producing a series of bridging thiol-derived species with elimination of $H_2$.[244] Compound **106b** was subsequently shown to also serve as an active catalyst for hydrogenation of a variety of nitrogen containing compounds.[245]

**Scheme 43.** Generation of bridging Mo hydrosulfides.

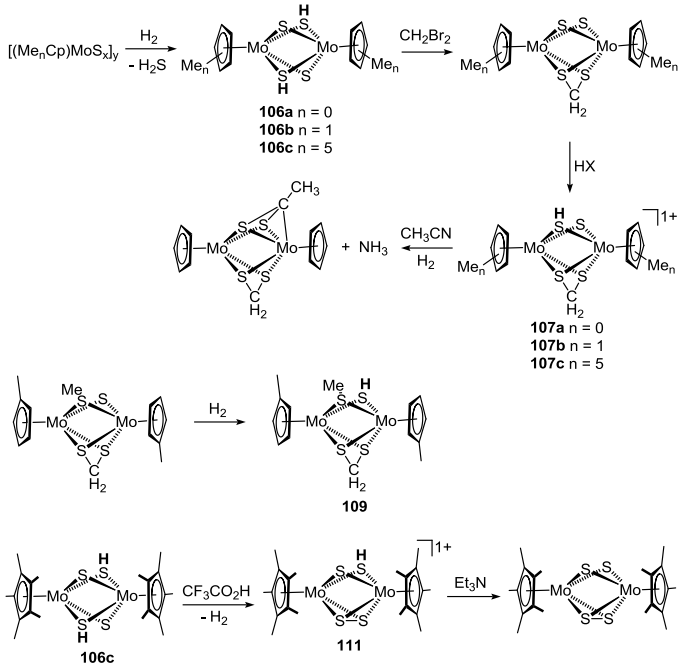


Deprotonation of **106a-c** and treatment with $CH_2Br_2$ results in double alkylation of the sulfur atoms and formation of compounds of the type $[(Me_nCp)_2Mo_2(\mu\text{-}S)_2(\mu\text{-}S_2CH_2)]$.[246] Much like **106a-c**, the $[(Me_nCp)_2Mo_2(\mu\text{-}S)_2(\mu\text{-}S_2CH_2)]$ compounds were found to be active for hydrogen transfer reactions.[245] Protonation of the $[(Me_nCp)_2Mo_2(\mu\text{-}S)_2(\mu\text{-}S_2CH_2)]$ compounds by strong Brønsted acids afforded the cationic hydrosulfide species $[(Me_nCp)_2Mo_2(\mu\text{-}S)(\mu\text{-}SH)(\mu\text{-}S_2CH_2)]$ (**107a-c**) (Scheme 43).[247, 248] In a remarkable transformation, **107a** was shown to cleave the C-N triple bond of acetonitrile in the presence of hydrogen to produce $[(Cp)_2Mo_2(\mu\text{-}S_2CH_2)(\mu\text{-}S_2CCH_3)]$ and $NH_3$. Compound **107a** was also found to be active for the reversible insertion of olefins into the S-H bond.[249] By in large, Markovnikov products were observed as the kinetic regioisomers of insertion, although selected olefins underwent subsequent isomerization. In this sense, the behavior of **107a** with alkenes was noted to provide an interesting homology to classical olefin isomerization reactions mediated by metal hydrides. More recently, Pétillon and co-workers

have extended this chemistry to include isocyanides by demonstrating a double insertion of xylyl isocyanide into the S-H bonds of putative $[Cp_2Mo_2(\mu\text{-}SMe)_2(\mu\text{-}SH)_2]$ (**108**).[250]

In related chemistry, compound **107b** was demonstrated to cleave the C-O bond of selected cyclic and acyclic ethers, with concomitant formation of new bridged hydroxythiolate species.[251] In each case, proton transfer from **107b** to the ether was proposed to initiate C-O cleavage, and work following shortly thereafter determined the p$K_a$ values for the SH group to lie in the range 8 – 10 for the family of **107a-c** compounds.[248] All three complexes of the type **107a-c** undergo autoxidation to produce dicationic tetranuclear clusters of the type $[\{Cp^n{}_2Mo_2(\mu\text{-}S)_2(\mu\text{-}S_2CH_2)\}_2(\mu\text{-}S)]^{2+}$.[248]

In addition to bridging hydrosulfide complexes of Mo(IV), the dimolybdenum(III) species **109** was also reported to form by reaction of the mixed valent complex, $[(Cp^{Me})_2Mo_2(\mu\text{-}S)(\mu\text{-}SMe)(\mu_2\text{-}S_2CH_2)]$, with $H_2$ (Scheme 43).[252] Disproportionation of the mixed-valent species into a small amount of $[(MeCp)_2Mo_2(\mu\text{-}S)_2(\mu\text{-}S_2CH_2)]$ was postulated to catalyze the reaction. Although similar in several respects to **106b**, compound **109** demonstrated quite different reactivity, undergoing alkylation at the hydrosulfide sulfur atom and participating in hydrogen atom transfer with diazo compounds.

In more recent work, compounds of the type **106** have been the subject of studies aimed at quantifying the S-H bond strength. DFT calculations coupled with kinetic studies of hydrogen atom abstraction (HAT) in **106** by benzyl radicals yielded a gas-phase bond dissociation free energy of 73 kcal/mol for the S-H linkage.[253] This value is lower than that for the S-H bond in alkyl and aryl thiols further demonstrating the enhanced reactivity of the SH bonds in these bimetallic species. This reactivity was further parlayed into an electrocatalytic system for proton reduction using $[(Cp)_2Mo_2(\mu\text{-}S)_2(\mu\text{-}S_2CH_2)]$ and related derivatives.[254] Overpotentials as low as

120 mV with nearly 100% current efficiency were observed. Critical to this efficiency was a good match between the p$K_a$ of the acid source and that of compound **107a**. Attendant thermodynamic studies with **107a** permitted determination of a p$K_a$ value of 7.1 ± 0.3 (later corrected to 6.5 ± 0.3[242]), in line with previous studies described above.[248] Reduction of **107a** at the electrode was postulated to produce the mixed-valent species, [$Cp_2Mo_2(\mu$-S)($\mu$-SH)($\mu_2$-$S_2CH_2$)] (**110**), which was calculated to have a S-H bond dissociation free energy of only 50.2 ± 1.3 kcal/mol (later corrected to 49.4 ± 1.3 kcal/mol[242]). Bimolecular elimination of H-H from this mixed-valent species is therefore thermodynamically viable, providing a pathway for hydrogen production.

Further evidence for the dynamic interplay of $H_2$ with complexes of the type **106a** was provided in studies with the Cp* analog, **106c**. In a novel reaction, Franz and coworkers showed that treatment of **106c** with trifluoroacetic acid resulted in elimination of $H_2$ and formation of the cationic species **111** (Scheme 43).[255] Compound **111** was found to undergo smooth deprotonation to afford the sulfide cluster, [$Cp^*_2Mo_2(\mu$-S)$_2$($\mu$-$S_2$)], which was subsequently used to prepare [$Cp^*_2Mo_2(\mu$-S)$_2$($\mu$-SH)($\mu$-SMe)] by successive treatment with methyl lithium and acid. HAT from compound [$Cp^*_2Mo_2(\mu$-S)$_2$($\mu$-SH)($\mu$-SMe)] gave rise to a persistent radical species of formula [$Cp^*_2Mo_2(\mu$-S)$_3$($\mu$-SMe)], which was found to take part in several single-electron processes including dimerization. Treatment of [$Cp^*_2Mo_2(\mu$-S)$_3$($\mu$-SMe)] with $H_2$ was found to regenerate [$Cp^*_2Mo_2(\mu$-S)$_2$($\mu$-SH)($\mu$-SMe)].

The acid-base chemistry and electrochemical behavior of compounds **106c**, **111**, and [$Cp^*_2Mo_2(\mu$-S)$_4$] have been used in the construction of thermodynamic cycles to experimentally determine solution bond dissociation free energies (SBDFEs) for the S-H bonds in this family of Cp*Mo hydrosulfide complexes.[242, 256] Results from these works find SBDFEs that range from 43

to 66 kcal/mol, which are significantly lower than thiols, and once again underscore the pronounced activation of the S-H bond upon coordination to metal centers.

In addition to the extensive work with $CpMoS_x$ clusters, $H_2$ addition to metal-sulfide species has also been examined in several other systems. Bianchini and Meli first reported the synthesis of $[(triphos)_2Rh_2(H)_2(\mu\text{-}SH)_2]^{2+}$ (**112**) via oxidative addition of $H_2S$ to the Rh(I) precursor, $[(triphos)RhCl(C_2H_4)]$. Subsequent work demonstrated that **112** could also be prepared by addition of $H_2$ to a thiocarbonate complex of the type, $[(triphos)Rh(\kappa^2\text{-}S_2CO)]^+$, with extrusion of carbonyl sulfide (COS).[257] Compound **112** was found to reversibly lose $H_2$ under an argon stream to generate the Rh(III) sulfide species $[(triphos)_2Rh_2(\mu\text{-}S)_2]^{2+}$ (Scheme 44). The mechanism of $H_2$ addition to $[(triphos)_2Rh_2(\mu\text{-}S)_2]^{2+}$ was the subject of a detailed computational and experimental study employing para-hydrogen induced polarization.[258] Calculations predicted stepwise formation of a $\eta^2$-dihydrogen complex followed by heterolytic cleavage along the Rh-S bond. NMR experiments found no evidence for a stable dihydrogen complex, but did identify an intermediate species, postulated as either $[(triphos)_2Rh_2(H)(\mu\text{-}S)(\mu\text{-}SH)]^{2+}$ (**113**) or $[(triphos)_2Rh_2(\mu\text{-}H)(\mu\text{-}S)(\mu\text{-}SH)]^{2+}$ (**114**).

**Scheme 44.** Bridging Rh hydrosulfides with tridentate phosphine ligands.

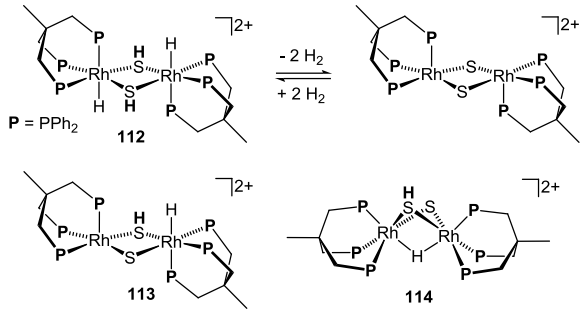

Rauchfuss and co-workers have employed the Ru(II) metallocene hydrosulfide [CpRu($PPh_3$)$_2$(SH)] (**115a**) to demonstrate the interconversion of several sulfur species and molecular hydrogen at the [CpRu($PPh_3$)$_2$]$^+$ fragment (Scheme 45).[259] Compound **115a** was prepared by salt metathesis of [CpRuCl($PPh_3$)$_2$] with NaSH or via sulfur insertion into [CpRu(H)($PPh_3$)$_2$]. Carbonylation of **115a** produced the related complex [CpRu($PPh_3$)(CO)(SH)] (**116**), whereas protonation with triflic acid afforded the $H_2S$ complex [CpRu($PPh_3$)(CO)($SH_2$)]$^+$ (**117a**). Addition of $H_2$ to **117a** resulted in equilibrium formation of the Ru(IV) dihydride, [CpRu(H)$_2$($PPh_3$)$_2$]$^+$, with displacement of $H_2S$. An analog of **115a** containing a 2-(thienylmethyl)cyclopentadienyl ligand (ThiCp) was also prepared and found to undergo protonation in similar fashion to its Cp counterpart. The resulting $H_2S$ complex, [(ThiCp)Ru($SH_2$)($PPh_3$)$_2$]$^+$ (**117b**), was more tolerant to air than **117a**, permitting an analysis of the relative binding affinity of $H_2S$ vs. $H_2$ at the Ru(II) center. Notably, $H_2S$ was found to bind to the [(ThiCp)Ru($PPh_3$)$_2$]$^+$ fragment with slightly greater affinity than $H_2$. Two-electron oxidation of both **115a** and **117a** generated the bridging disulfide species, [$Cp_2Ru_2$($PPh_3$)$_4$($\mu$-$S_2$)], although higher order sulfides were obtained upon treatment with elemental sulfur. Compound **115a** was also found to react with [CpRu($PPh_3$)$_2$](OTf) to produce the metastable bimetallic hydrosulfide, **118**. NMR evidence for formation of **118** was provided in the form of a quintet resonance ($J_{PH}$ = 7 Hz) at −2.3 ppm. A species closely related to **115a** containing Cp* and $PMe_3$ ligands, **115a**, was actually reported several years prior to the studies of Rauchfuss by Bryndza and Bercaw. This compound was prepared in the context of an examination of metal-ligand bond dissociation energies via addition of $H_2S$ to the hydroxo precursor [Cp*Ru($PMe_3$)$_2$(OH)].[260]

**Scheme 45.** Hydrosulfide chemistry of Cp/Cp*Ru complexes.

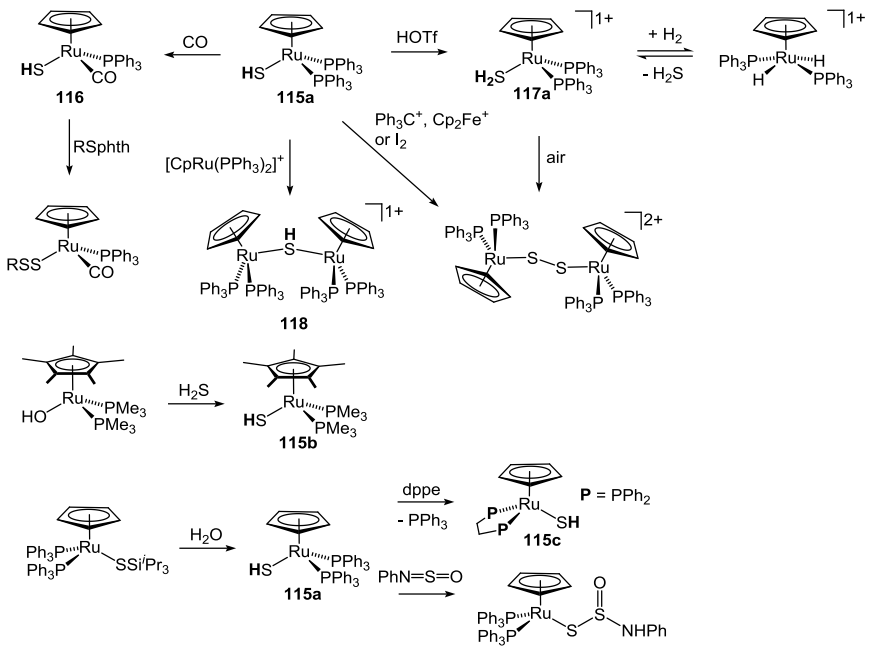


Compound **115a** and its relatives have also been the subject of several subsequent studies. Shaver reported the crystal structure of **116** and demonstrated that the molecule serves as precursor to hydrocarbyldisulfide complexes, such as [CpRu(PPh$_3$)(CO)(SSR)] when treated with sulfur transfer reagents, RSphth (phth = phthalimido; R = 4-tolyl, 1-allyl, *i*-Bu) (Scheme 45). In other work from his laboratory, an alternate synthesis of **115a** was described involving hydrolysis of a triisopropylsilanethiolate ligand.[261] An analog of **115a** containing the dppe ligand, **115c**, was also reported by simple ligand exchange of PPh$_3$. Compounds **115a** and **115c** were found to undergo reaction with *N*-thionylaniline to give unstable products consistent with S-H addition across the S-N bond.

In addition to ruthenium, Rauchfuss and co-workers has also examined the addition of $H_2$ to a formally diiridium(II) species, [Ir$_2$($\mu$-S)$_2$(PPh$_3$)$_4$] (Scheme 46).[179] Hydrogenation of [Ir$_2$($\mu$-S)$_2$(PPh$_3$)$_4$] proceeded through initial addition of $H_2$ to the iridium centers to give [Ir$_2$(H)$_2$($\mu$-S)$_2$(PPh$_3$)$_4$] followed by formation of [Ir$_2$(H)$_2$($\mu$-S)($\mu$-SH)($\mu$-H)(PPh$_3$)$_4$] (**129**). H/D exchange was

observed during transformation of $[Ir_2(H)_2(\mu\text{-}S)_2(PPh_3)_4]$ to **120** intimating that H migration between S and Ir is facile. Very recent computational studies on the reaction have provided additional insight, suggesting that the addition of $H_2$ to $[Ir_2(H)_2(\mu\text{-}S)_2(PPh_3)_4]$ occurs to generate the *bis*-hydrosulfide, **119**, prior to H migration to generate **120**.[262] Consistent with the H/D exchange observed experimentally by Rauchfuss and co-workers, free energy barriers for H migrations between S and Ir in **120** were calculated to be in the surmountable range of 19 to 23 kcal/mol.

**Scheme 46.** Generation of bridging Ir hydrosulfide complexes.

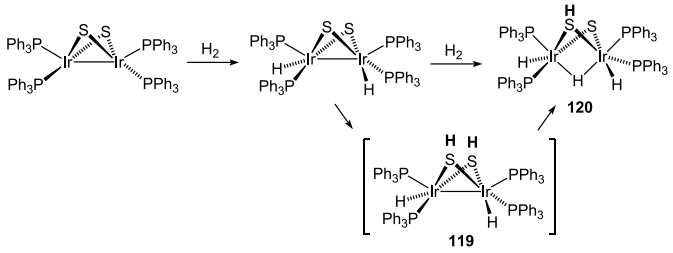


Employing titanocene sulfide species, Andersen and Bergman demonstrated facile $H_2$ activation across the Ti-S bond. $[Cp^*_2Ti(S)(py)]$ was found to react reversibly with molecular hydrogen to produce $[Cp^*_2Ti(SH)(H)]$ (**121**) (Scheme 47).[263] The hydrogen atoms of the hydride and hydrosulfide ligands of **121** were observed to exchange rapidly in solution, consistent with the reversible nature of $H_2$ addition across the Ti=S unit. Exchange of the H atoms with molecular hydrogen was also observed albeit at a slower rate, suggesting that $H_2$ is retained in the coordination sphere of Ti in the form of a dihydrogen complex. The related disulfide complex, $[Cp^*Ti(S_2)]$, was also found to activate $H_2$, in this case forming **70b**.

**Scheme 47.** $H_2$ activation across Ti-S bonds.

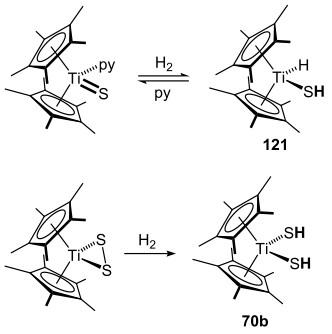


In recent work, Hillhouse and Jordan have described activation of $H_2$ across a Ni(II) sulfide dimer. Reaction of $[(IPr)_2Ni_2(\mu\text{-}S)_2]$ (IPr = 1,3-*bis*(2,6-diispopropylphenyl)imidazol-2-ylidene) with $H_2$ at 70 ºC was shown to generate the bridging hydrosulfide species $[(IPr)_2Ni_2(\mu\text{-}SH)_2]$ (**122**), over the course of 24 h (Scheme 48).[264] Compound **122** formally contains Ni(I), and can be alternately synthesized through a salt metathesis reaction of KSH with the halide precursor $[(IPr)_2Ni_2(\mu\text{-}Cl)_2]$. Unlike Ni(I) hydrosulfide **87**, compound **122** features strong Ni-Ni bonding rendering the compound diamagnetic and permitting identification of the S-H proton resonance at −4.81 ppm in the NMR spectrum. Hydrogen atom abstraction from **122** using the 2,4,6-tri-*tert*-butylphenoxy radical (Ar*O·) resulted in complete regeneration of $[(IPr)_2Ni_2(\mu\text{-}S)_2]$ with concomitant formation of the phenol (Ar*OH). Kinetic and computational studies of the hydrogenation reaction of $[(IPr)_2Ni_2(\mu\text{-}S)_2]$ support a mechanism involving initial heterolytic addition of $H_2$ across the Ni-S bond followed by H migration from nickel to sulfur to produce **122**.[265] Such a reaction pathway bears notable similarities to that proposed by Bianchini and Meli for formation of **112** from $[(triphos)_2Rh_2(\mu\text{-}S)_2]^{2+}$ via **113-114**. In addition to $H_2$, $[(IPr)_2Ni_2(\mu\text{-}S)_2]$ was active toward the heterolysis of the B-H bond of pinacolborane to produce hydrosulfide **123**.

In the pursuit of a Cu(I) sulfide species similar to $[(IPr)_2Ni_2(\mu\text{-}S)_2]$, Hillhouse and co-workers also synthesized hydrosulfides **124a,b** (Scheme 48).[266] These compounds were found to react via proton transfer with [(NHC)CuO*t*Bu] (NHC = IPr* or IPr) to produce the desired bridging sulfide, $[(NHC)_2Cu_2(\mu\text{-}S)]$. In case of the smaller IPr ligand, $[(IPr)_2Cu_2(\mu\text{-}S)]$ was observed spectroscopically, but underwent rapid decomposition precluding its isolation. In more recent work, Sadighi and coworkers reported very similar chemistry with an analog of **124** containing a ring-expanded NHC ligand (**125**).[267] Notably, compound **125** was found to react with $NOBF_4$ to afford a mixture of a new cationic Cu(I) complex, ammonium ion, $S_8$, and nitrous oxide. The reaction was postulated to occur through formation and subsequent decomposition of HSNO.

**Scheme 48.** Hydrosulfide complexes of Ni and Cu carbenes.

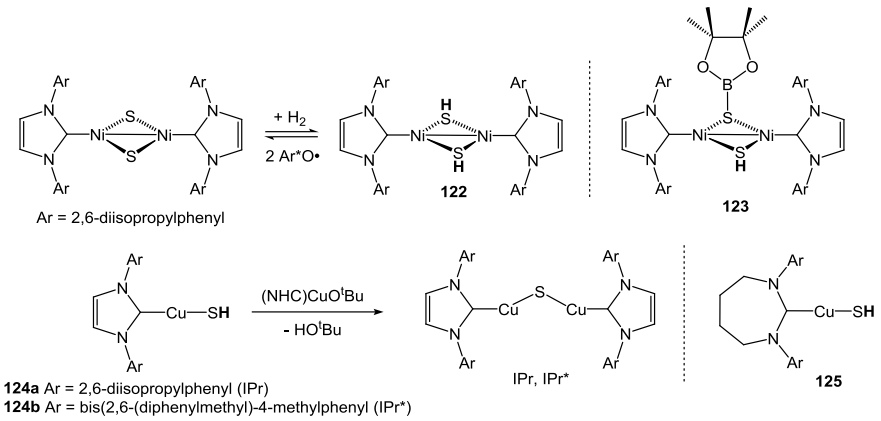


In addition to metal sulfides, hydrosulfide species themselves have also been demonstrated to take part in heterolytic bond activation. Oñate and co-workers reported the reaction of $[Os(P^iPr_3)_2(CO)(H)(SH)]$ (**126**) with boronate esters and 9-BBN to produce dihydrogen complexes containing the corresponding boryl-thiolates $[Os(P^iPr_3)_2(CO)(H)(\eta^2\text{-}H_2)(SBR_2)]$ (Scheme 49).[268] Previous work with **126** and its Ru analog had established the electrophilicity of the metal center

in these hydrosulfide complexes.[269] The reactivity with $HBR_2$ was therefore rationalized in the context of heterolytic activation of the B-H bond to afford $H_2$ and the metal boryl-thiolate. In the case of catechol borate, subsequent loss of hydrogen from the boryl-thiolate species $[Os(P^iPr_3)_2(CO)(H)(\eta^2\text{-}H_2)(SBcat_2)]$ lead to formation of $[Os(P^iPr_3)_2(CO)(SH)(Bcat)]$ (**127**), which possesses a boryl ligand.

**Scheme 49.** Reactivity of Os hydrosulfides.

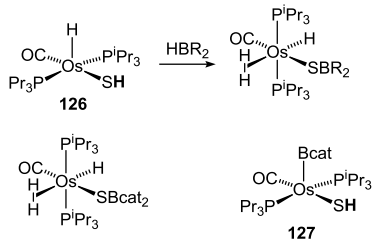


*3.3 Roles in Organometallic Chemistry*

Many of the reactions described in the preceding section concern compounds containing carbon-based ligands. Due to its soft nature, the hydrosulfide ion pairs naturally with organometallic compounds, and its chemistry in this context as both a reactive and supporting ligand has provided fruitful avenues for investigation. This section will examine organometallic compounds of hydrosulfide, which provided the inception point for investigations of $H_2S$ chemistry many years ago and continue to enjoy relevance several decades on.

*3.3.1 Cyclopentadienyl complexes.* The field of organometallic chemistry was revolutionized by the synthesis and interpretation of ferrocene. Since that initial discovery, the cyclopentadienyl ligand has continued to find a vast number of uses across organometallic chemistry. It is therefore unsurprising that much of the organometallic chemistry of hydrosulfide is intimately tied to the Cp ligand and its derivatives. Indeed, many of the examples of hydrosulfide complexes discussed

above in the context of hydrogen chemistry feature the Cp family of ligands. As a class, hydrosulfide compounds containing Cp co-ligands provide a rich collection of molecules that span many transition elements.

Outside of Vaska's early report on the oxidative addition of $H_2S$, the earliest examples of well-characterized hydrosulfide complexes featured Cp ligands. In 1964, Strohmeier and Guttenberger reported the photolysis of $[CpMn(CO)_3]$ in the presence of $H_2S$ to generate a green compound they formulated as $[CpMn(CO)_2(SH_2)]$ (Scheme 50).[270] Little data was provided by way of characterization for the $H_2S$ complex beyond IR stretches for the carbonyl ligands. Subsequent work called into question the composition of the green compound,[271] demonstrating that its true identity is that of the bridging sulfide species, $[Cp_2Mn_2(CO)_4(\mu\text{-}S)]$.[272] As an interesting bookend to the story, however, Lorenz reported nearly three decades later that $[Cp_2Mn_2(CO)_4(\mu\text{-}S)]$ itself undergoes protonation by $HBF_4$ to afford the bridging hydrosulfide complex **128**.[273]

**Scheme 50.** Early cyclopentadienyl complexes of Mn and Ti containing hydrosulfide ligands.

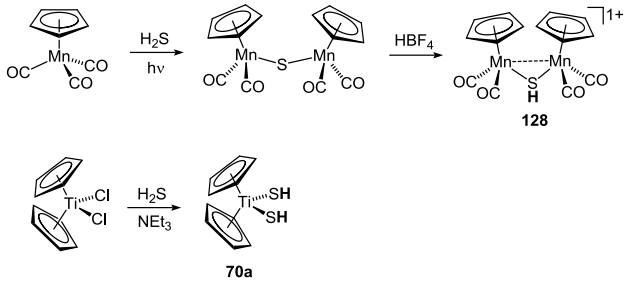


Shortly after the report of putative $[CpMn(CO)_2(SH_2)]$, Köpf and Schmidt reported the synthesis of $[Cp_2Ti(SH)_2]$ (**70a**) (Scheme 50).[274] Compound **70a** represents, in many respects, the first bona fide example of a hydrosulfide complex. The synthesis was accomplished by treatment of $[Cp_2TiCl_2]$ with $H_2S$ in the presence of triethylamine. Unlike many of the hydrosulfide species

discussed above, compound **70a** displays an $^{1}H$ NMR resonance for the SH group downfield of zero at 3.44 ppm. The nature of this resonance was confirmed by its disappearance in $[Cp_2Ti(SD)_2]$ and by reaction of **70a** with dimethylsulfate to generate $[Cp_2Ti(SMe)_2]$. In the context of investigations into the preparation of $[Cp_2MS_5]$ species, Shaver later reported the attempted syntheses of the Zr (**71a**) and Hf analogs of **70a** through an analogous synthetic procedure.[275] The Zr analog was found to be metastable (*vide supra*) but the hafnium analog could not be isolated.

In addition to their role in $H_2$ chemistry discussed above, compounds related to **70a** and **71a** have also been employed to great extent as precursors to metal clusters (*vide infra*) and other complexes bearing sulfide ligands. Bergman and coworkers examined generation of the putative terminal zirconocene sulfide, $[Cp^*_2Zr(S)]$, from hydrosulfide $[Cp^*_2Zr(SH)(I)]$ (**129a**).[276] Compound **129a** was prepared by treatment of the activated "tuck-in" complex, $[Cp^*Zr(\eta^5{:}\eta^1\text{-}C_5Me_4\{CH_2\})(I)]$ with $H_2S$. Dehydrohalogenation of **129a** with $K(N\{SiMe_3\}_2)$ in the presence of pyridine afforded $[Cp^*_2Zr(S)(py)]$ confirming production of the desired $[Cp^*_2Zr(S)]$ (Scheme 51). In a subsequent study aimed at observing formation of $[Cp^*_2Zr(S)]$ by an $\alpha$-elimination route, Bergman targeted the related hydrosulfide $[Cp^*_2Zr(SH)(Ph)]$ (**129b**), by reaction of $[Cp^*Zr(\eta^5{:}\eta^1\text{-}C_5Me_4\{CH_2\})(Ph)]$ with $H_2S$.[277] Compound **129b** was identified spectroscopically but could not be isolated due to its thermal sensitivity leading to mixtures of **79** and **80**.

**Scheme 51.** Reactivity of cyclometallated Zr and Ti complexes toward $H_2S$.

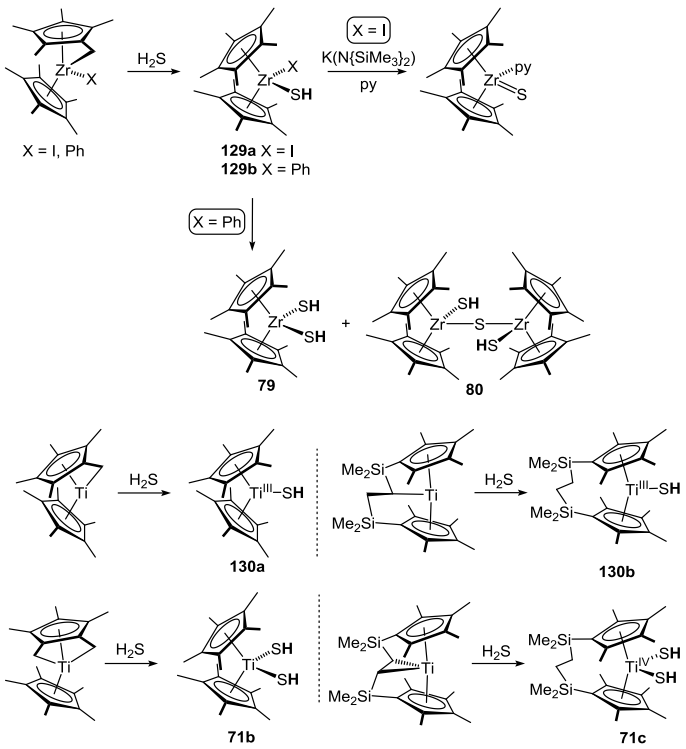


In more recent work, Mach and co-workers have examined the reaction of $H_2S$ with Ti(III) metallocenes through a similar strategy employing "tuck-in" complexes.[278] Reaction of the singly activated titanocene, [Cp*Ti($\eta^5$:$\eta^1$-$C_5Me_4\{CH_2\}$)], with $H_2S$ was found to produce the titanium(III) hydrosulfide [Cp*$_2$Ti(SH)] (**130a**, Scheme 51). Owing to the $d^1$ nature of **130a**, the compound is violet-colored and displays a characteristic EPR spectrum with an isotropic $g$ value of 1.964. Compound **130a** could also be prepared by reaction of [Cp*$_2$TiMe] and $H_2S$ with release of methane. In similar fashion to **130a**, the *ansa*-titanocene **130b** was synthesized by $H_2S$-protonolysis of the activated species, *ansa*-[Ti($\eta^1$:$\eta^5$:$\eta^5$-$C_5Me_4SiMe_2CHCH_2SiMe_2C_5Me_4$)]. Much like **130a**, **130b** is also violet-colored and displays an EPR spectrum typical of Ti(III). Reactions of the **130a** and **130b** with their activated Ti(III) precursors were found to generate bridging Ti(III) sulfides via related protonolysis pathways whereby the hydrosulfide ligand serves as the source of acid equivalents. In the course of their investigations into Ti(III) metallocenes, Mach and

coworkers also demonstrated reaction of $H_2S$ with the doubly activated complexes [Cp*Ti($\eta^4$:$\eta^3$-$C_5Me_3\{CH_2\}_2$)] and [Ti($\eta^2$:$\eta^5$:$\eta^5$-$C_5Me_4SiMe_2CHCHSiMe_2C_5Me_4$)] to afford **71b** and **71c**, respectively. Much like **71b**, diamagnetic **71c** demonstrated $^1$H NMR resonances for the hydrosulfide groups downfield of 0 ppm. Subsequent work has also described derivatives of **71b** and **71c** containing *tert*-butyl-tetramethyl- (**71d**) and benzyl-tetramethylcyclopentadienyl ligands (**71e**).[279]

Shortly after the preparation of $[Cp_2Ti(SH)_2]$ by Köpf and Schmidt, Green and coworkers reported the analogous Mo and W complexes, $[CpM(SH)_2]$ (M = Mo, **131a**; M = W, **131b**) (Scheme 52).[280] The red (Mo) to brown (W) compounds were synthesized by salt metathesis reactions of $[Cp_2MCl_2]$ (M = Mo, W) with NaSH in ethanol and were purified by chromatography on alumina despite decomposing readily in air. The chemical shift of the hydrosulfide protons by NMR was found significantly upfield from those of $[Cp_2Ti(SH)_2]$ consistent with the non-$d^0$ nature of the compounds.

**Scheme 52.** Preparation of Group 6 hydrosulfide compounds containing Cp ligands.

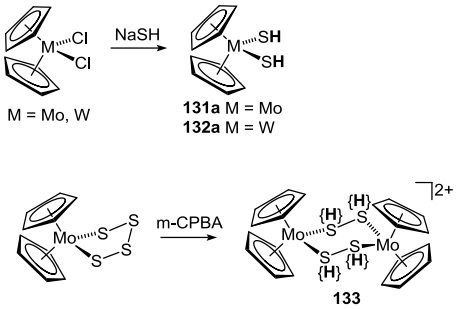


Of relevance to the air-sensitivity of **131a**, Shaver and co-workers have reported the oxidation of $[Cp_2Mo(S_4)]$ by *m*-CPBA to give the protonated disulfide species, $[Cp_2Mo_2(\mu\text{-}S_2H)_2]^{2+}$ (**133**) (Scheme 52).[281] Compound **133** represents a very rare example of a hydropersulfide complex. The

positions of the S-H groups of **133** could not be identified unambiguously by X-ray crystallography, although a broad resonance for the hydropersulfide protons was located by $^1$H NMR spectroscopy at 6.00 ppm. The downfield chemical shift of the S-H protons contrasts that found for **131a**, consistent with their association to a disulfide moiety. Compound **133** was found to undergo deprotonation in the presence of base to afford the monometallic disulfide species, $[Cp_2Mo(S_2)]$, which was found to regenerate **133** upon treatment with a variety of acids.

Also in the area of Group VI cyclopentadienyl chemistry, early work by Beck and co-workers demonstrated the reaction of propylene sulfide with $[CpW(H)(CO)_3]$ to give $[CpW(SH)(CO)_3]$ (**135**, Scheme 53).[282] The synthesis of **135** constitutes a net insertion of an S atom into the W-H bond, and is modeled after the reaction of $[Mn(H)(CO)_5]$ with propylene sulfide to give the bridging hydrosulfide complex $[Mn_2(CO)_8(\mu\text{-}SH)_2]$ **136**.[283] Analogous reactions of propylene sulfide with the Mo congener $[CpMo(H)(CO)_3]$ were reported subsequently and shown to produce $[CpMo(SH)(CO)_3]$ (**134**) in tandem with the sulfide cluster, $[Cp_2Mo_2(S)_2(\mu\text{-}S)_2]$.[284]

**Scheme 53.** Reaction of metal hydrides with propylene sulfide to generate hydrosulfide products.

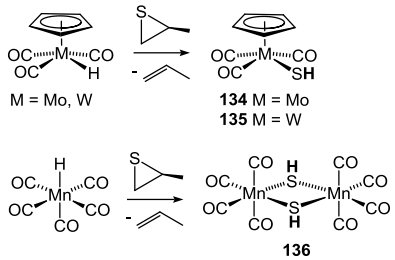


Starting from the cationic precursor, $[CpM(CO)_3]^+$ (M = Mo, W), Beck and co-workers also reported the direct reaction with $H_2S$ to afford the rare hydrogen sulfide adducts $[CpM(CO)_2(SH_2)]^+$ (M = Mo, **137**; M = W, **138**) (Scheme 54).[285] The W congener **138** was

observed to be more thermally robust than its Mo counterpart although both compounds were found to be very moisture sensitive. Characteristic stretches for the $\nu_{SH}$ fundamentals of **137** and **138** were detected by IR spectroscopy, but the corresponding $^1$H NMR resonances could not be identified. In contrast to reactions with $H_2S$, treatment of $[CpW(CO)_3]^+$ with the hydrosulfide ion was found to yield the bimetallic species **139**.

**Scheme 54**. Reactions of $[CpM(CO)_3]^+$ (M = Mo, W) with $H_2S$ and $HS^-$.

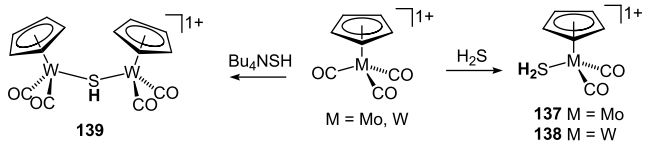


In like fashion to the work of Beck, Herrmann and coworkers reported the synthesis of complexes $[CpM(CO)_3(SH)]$ (M = Cr, **140a**; Mo, **134a**; W, **135a**) as well as the Cp' derivatives (**140b, 134b, 135b**) through reaction of elemental sulfur with $[Cp'M(H)(CO)_3]$ (Cp' = Cp, Cp*; M = Cr, Mo, W) (Scheme 55).[286] This preparative route operates through an identical sulfur-insertion pathway to that described for propylene sulfide but makes use of $S_8$. The corresponding hydroselenide congeners of Mo and W were also prepared by reaction of the hydride precursors with selenium. Later work by Abboud and Hoff expanded upon this sulfur insertion methodology employing the sulfur transfer reagent, $Ph_3Sb{=}S$, to prepare both Cp and Cp* products.[287] Treatment of $[Cp'M(H)(CO)_3]$ with excess $S_8$ was also reported to generate a mixture of species formulated as hydropersulfides, $[Cp'M(S_nH)(CO)_3]$. Unfortunately, unambiguous identification of these intriguing compounds was not possible. Desulfurization of the $[Cp'M(SH)(CO)_3]$ or $[Cp'M(S_nH)(CO)_3]$ compounds was accomplished by addition of $PCy_3$ ultimately affording $[Cp'M(H)(CO)_3]$ and $Cy_3P{=}S$. Solution calorimetry experiments on the insertion and

desulfurization reactions permitted construction of a thermochemical cycle whereby bond dissociation enthalpies (BDEs) for the M-SH bonds in **140, 134-135** could be approximated. The results demonstrated that the W congener possesses the largest BDE (63 kcal/mol) followed by Mo (55 kcal/mol) then Cr (46 kcal/mol). Much more recently, compounds **134** and **135** were used by Mizobe and co-workers to prepare the dppe analogs **141** and **142** via photolytic removal of CO.[288] Treatment of **141** and **142** with $[RhCl(PPh_3)_3]$ was found to afford a series of sulfide-bridged heterobimetallic Mo-Rh complexes.

**Scheme 55**. Generation and chemistry of $CpM(CO)_3(SH)$ (M = Mo, W) complexes.

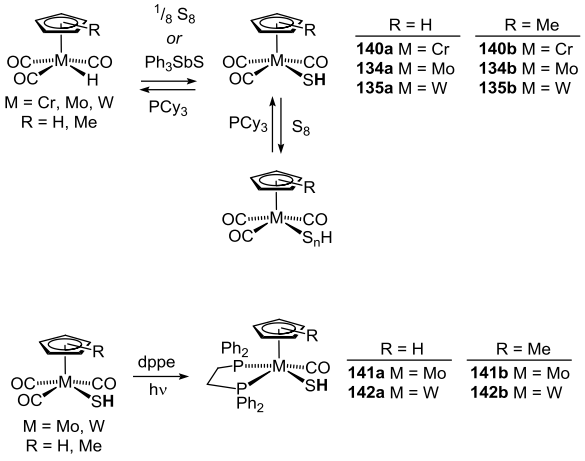


An analog of **135a** containing the fulvalene ligand ($\eta^5$:$\eta^5$-$C_{10}H_8$, Fv) is also known (**143**, Scheme 56). Shaver and co-workers first prepared this species by sulfur insertion into the corresponding hydride, $[FvW_2(CO)_6(H)_2]$.[289] A series of ligand exchange reactions with $[FvW_2(CO)_6(H)_2]$ lead to $[FvW_2(CO)_4(PPh_2Me)_2(SR)_2]$, which was used to synthesize hydrosulfide **144** by thiol exchange with $H_2S$. The crystal structure of **143** was subsequently reported by Hoff and coworkers confirming the *anti* arrangement of the tungsten fragments about the fulvalene ligand.[290] Their study also reported reactions of **143** with both PhN=NPh and

$Cp^*Cr(CO)_3$, which were found to result in H atom abstraction to produce the bridging disulfide, $[FvW_2(CO)_6(\mu\text{-}S_2)]$.

**Scheme 56.** Bimetallic hydrosulfide complexes of W and Mo containing Cp-type ligands.

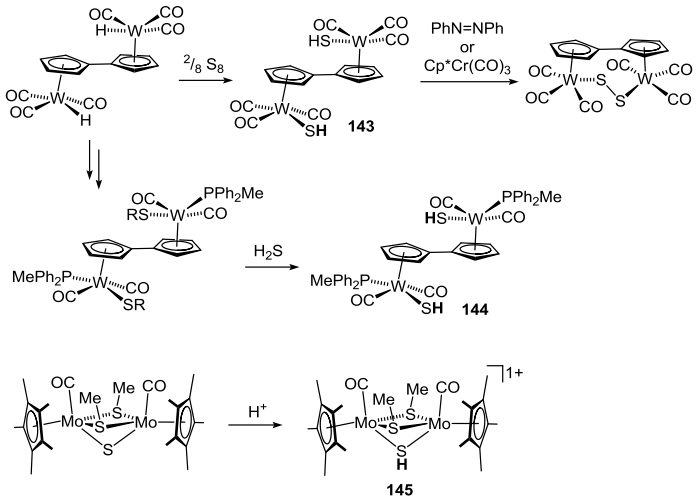


Several additional bimellatic metallocene-hydrosulfide compounds of the Group 6 metals, namely Mo, have been discussed in detail above in the context of their reactivity with molecular hydrogen. An additional example of such a complex, $[Cp^*_2Mo_2(CO)_2(\mu\text{-}SMe)_2(\mu\text{-}SH)$ (**145**), was reported by Pétillon and Muir through protonation of the sulfide-bridged dimolybdenum carbonyl species, $[Cp^*_2Mo_2(CO)_2(\mu\text{-}SMe)_2(\mu\text{-}S)]$ (Scheme 56).[291] Crystallographic analysis of **145** demonstrated that the compound exists as the *cis*-carbonyl isomer and adopts a *syn* arrangement of the SMe ligands.

Among the earliest examples of a crystallographically-characterized hydrosulfide complex was the niobocene compound $[Cp_2Nb(CO)(SH)]$ (**146**). This species was prepared by Kirrilova and coworkers through prolonged boiling of $[Cp_2Nb(CO)H]$ in carbon disulfide (Scheme 57).[292] An intermediate assigned as a thioformate complex was observed, but was found to extrude

carbonyl sulfide under the reaction conditions to give **146**. The crystalline structure of **146** evinced the expected bent metallocene geometry about niobium, with a Nb-S bond distances of 2.54 Å. $^{1}$H NMR resonances for the Cp ligands were noted although no chemical shift value for the hydrosulfide ligand was reported.

**Scheme 57.** Preparation and reactivity of hydrosulfide compounds of Nb and Ta containing Cp ligands.

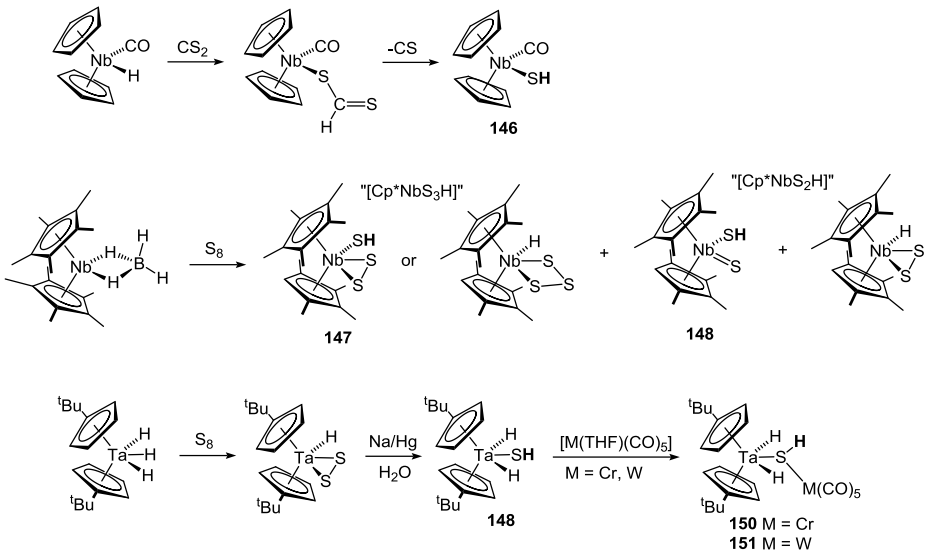


Later work by Wachter and co-workers examined additional metallocenes of the Group 5 metals. Preliminary observations from the reaction of [Cp*$_2$Nb(BH$_4$)] with elemental sulfur identified two compounds of composition [Cp*$_2$NbS$_3$H] and [Cp*$_2$NbS$_2$H] (Scheme 57).[293] Two postulated structures were put forward for [Cp*$_2$NbS$_3$H], one of which, **147**, featured a combination of disulfide and hydrosulfide ligands. $^{1}$H NMR spectra of [Cp*$_2$NbS$_3$H] displayed an upfield resonance at −1.64 ppm, which could not be unambiguously assigned to a hydrosulfide moiety. A subsequent report disclosed the crystal structure of [Cp*$_2$NbS$_3$H], which despite

significant disorder, was consistent with the disulfide-hydrosulfide formulation (**147**).[294] Additional investigations of [Cp*$_2$NbS$_2$H] demonstrated that the compound actually exists as two isomers, [Cp*$_2$Nb(H)(S$_2$)] and [Cp*$_2$Nb(S)(SH)] (**148**), the latter of which was characterized crystallographically.[295] Additionally, [Cp*$_2$Nb(H)(S$_2$)] was found to be capable of generating both **147** and **148** upon thermolysis suggesting that it is formed as an initial species in reactions of [Cp*$_2$Nb(BH$_4$)] with S$_8$. In all cases, prolonged exposure of the niobium compounds to sulfur at elevated temperatures was found to generate metallocene persulfide clusters.

Related reaction of elemental sulfur with [Cp$^{t\mathrm{Bu}}_2$TaH$_3$] was found to produce a molecule of formula [Cp$^{t\mathrm{Bu}}_2$TaS$_2$H] (Scheme 57).[294] Unlike niobium, this species was found to exist solely as the disulfide-hydride, [Cp$^{t\mathrm{Bu}}_2$Ta(H)(S$_2$)]. Although not a hydrosulfide complex, [Cp$^{t\mathrm{Bu}}_2$Ta(H)(S$_2$)] reacts with sodium amalgam in the presence of water to afford the tantalum dihydride-hydrosulfide [Cp$^{t\mathrm{Bu}}_2$Ta(H)$_2$(SH)] (**149**).[296] The symmetric arrangement of the hydrosulfide and hydride ligands in **149** was confirmed by $^1$H NMR spectroscopy, which displayed a lone doublet resonance for the Ta-H groups. Treatment of **149** with [M(CO)$_5$(THF)] (M = Cr, W) produced the hydrosulfide-bridged bimetallic compounds **150** and **151**. The crystal structure of **151** was obtained and demonstrated a considerably longer Ta-S bond of 2.562 Å compared to the distance of 2.274 Å for isomeric [Cp$^{t\mathrm{Bu}}_2$Ta(H)($\mu$-S)W(CO)$_5$], thereby confirming the identities of **150** and **151** as a bona fide hydrosulfides.

Outside of the work with [CpMn(CO)$_3$] described at the beginning of this section, cyclopentadienyl complexes of the Group 7 metals have not been investigated heavily in the context of their interactions with H$_2$S and HS$^-$. In an example from rhenium chemistry, Schenk described the addition of NaSH to the cationic nitrosyl species, [CpRe(NO)(PMePh{C$_{10}$H$_8$N})](BF$_4$), to give [CpRe(NO)(SH)(PMePh{C$_{10}$H$_8$N})] (**152**, Scheme

58).[297] Owing to the chiral nature of the PN ligand in **152**, several diastereomers could be obtained starting from different stereoisomers of the starting material. In all cases, addition of hydrosulfide to [CpRe(NO)(PMePh{$C_{10}H_8N$})]($BF_4$) occurred with retention of stereochemistry. Subsequent reaction of **152** with aldehydes in the presence of $HBF_4$ afforded a series of cationic thioaldehyde complexes.

**Scheme 58.** Re hydrosulfide nitrosyl complexes.

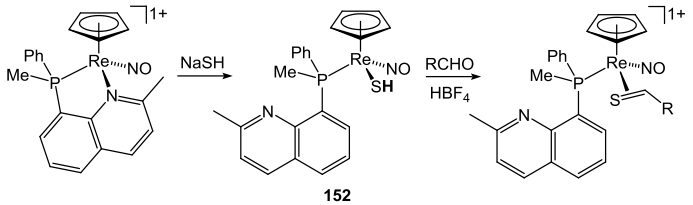


Cyclopentadienyl complexes of Ru bearing hydrosulfide ligands have already been discussed at length in the preceding sections because of their importance to reactions involving molecular hydrogen. Other examples of such species include the bimetallic Ru(II) and Ru(III) compounds **153** and **154**, respectively. [$Cp^*_2Ru_2(\mu\text{-}SH)_2(\mu\text{-}dppm)$] (**153**) was reported by Englert by protonolysis of the methoxy complex, [$Cp^*_2Ru_2(\mu\text{-}OMe)_2(\mu\text{-}dppm)$], with $H_2S$ (Scheme 59).[298] In similar fashion, Hidai prepared **154** by addition of $H_2S$ to either [$Cp^*_4Ru_4(\mu_3\text{-}Cl)_4$] or [$Cp^*_2Ru_2(\mu\text{-}Cl)_2Cl_2$].[299] Compound **154** was subsequently employed to produce a series of cluster compounds (*vide infra*) including the sulfur-bridged cubane, $[Cp^*_4Ru_4(\mu_3\text{-}S)_4]^{2+}$.

**Scheme 59.** Generation and chemistry of bridging hydrosulfide complexes of Ru.

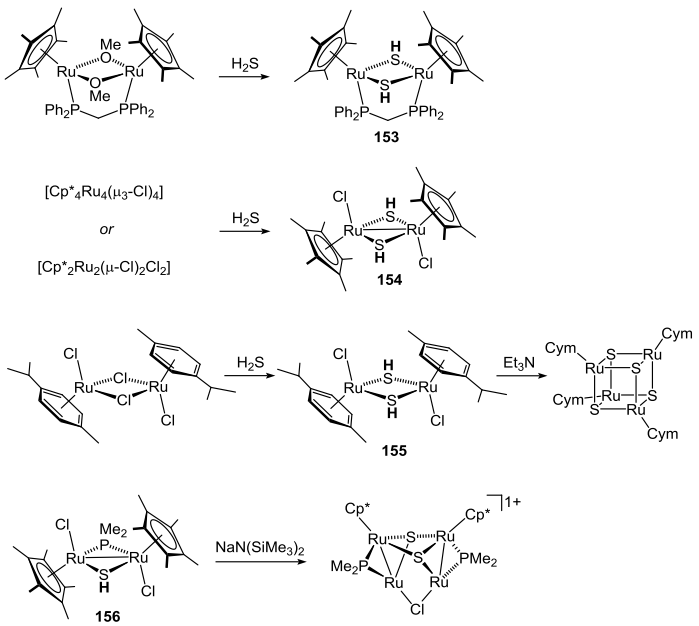


Mizobe and Hidai have also reported the preparation of the arene-derivative [$Cym_2Ru_2(\mu$-$SH)_2Cl_2$] (**155**, Cym = $\eta^6$-cymene).[300] The synthesis of **155** was carried out in identical fashion to that of **154** by treatment of [$Cym_2Ru_2(\mu$-$Cl)_2Cl_2$] with $H_2S$. Unlike **154**, however, compound **155** features Ru(II) as opposed to Ru(III) resulting in a longer Ru-Ru contact being observed in the crystal structure of the selenide analog. Treatment of **155** with $Et_3N$ led to formation of a related tetraruthenium sulfide cluster, [$Cym_4Ru_4(\mu_3$-$S)_4$], containing capping Cym ligands. More recently, Nishibiyashi has described the preparation of **156**, which is an analog of **154** with a phosphide ligand in place of one hydrosulfide.[301] Like **154**, compound **156** serves as a precursor to a tetranuclear ruthenium product, although the resulting cluster retains the bridging phosphide ligands leading to non-cuboidal structure (Scheme 59).

Other examples of cyclopentadienyl complexes containing precious metals have primarily encompassed compounds of Rh and Ir. In the context of studies on [$Cp^*Ir(PMe_3)Cl_2$], Bergman and coworkers reported [$Cp^*Ir(PMe_3)(SH)_2$] (**157a**) via reaction with NaSH in the presence of excess $H_2S$.[302] The related hydride-hydrosulfide complex [$Cp^*Ir(PMe_3)(SH)(H)$] (**158a**), was also

reported from treatment of [Cp*Ir($PMe_3$)H(OEt)] with $H_2S$. Subsequent reactivity of both **157a** and **158a** generated new trivalent iridium species (Scheme 60). In the case of **157a**, reaction with acetone in the presence of catalytic acid afforded a dithiametallocyclobutane complex. With **158a**, treatment with $CS_2$ lead to selective reactivity at the hydride ligand to produce [Cp*Ir($PMe_3$)(SH)(SC(S)H)] (**159**). In all cases, the Ir(III) hydrosulfides displayed identifiable $\nu_{SH}$ modes by IR and $^1$H NMR resonances for the sulfhydryl H atoms upfield of 0 ppm. More recently, Shaver has examined reactions of compound **157a** with thioaniline, $CS_2$, and tolylisothiocyanate.[303] The former two reagents resulted in elimination of $H_2E$ (E = NPh, S) and formation of novel dithiametallacycles. With the isothiocyanate, insertion into the S-H bond was observed to give **160**. Shaver also explored reactions of **157a** and its $PMe_2Ph$ analog **157b** with both thioaniline and tolylisothiocyanate. In contrast to the findings of Bergman and co-workers with $CS_2$, the isothiocyante was found to selectively insert into the S-H bond of **157b** affording [Cp*Ir($PMe_3$)(H)(SC{S}NHtolyl)].

**Scheme 60.** Preparation and reactivity of Cp*Ir hydrosulfide complexes.

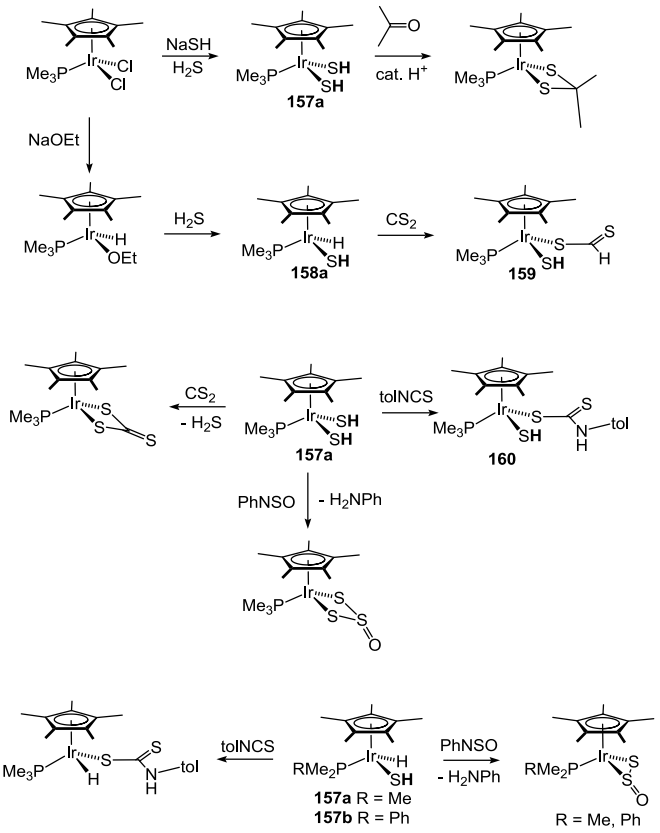


In the area of Rh chemistry, Vázquez de Miguel and Isobe reported the synthesis of $[Cp^*_2Rh_2(\mu\text{-}CH_2)_2(\mu\text{-}SH)]$ (**161**) and $[Cp^*_2Rh_2(\mu\text{-}CH_2)_2(SH)_2]$ (**162**) from $[Cp^*_2Rh_2(\mu\text{-}CH_2)_2Cl_2]$ and hydrogen sulfide (Scheme 61).[304] The H atoms of the methylene ligands in compound **161** were observed as four separate signals at low temperature consistent with the stereochemical activity of both the hydrosulfide proton and the sulfur lone pair, which serve to lower the molecular symmetry. At higher temperatures the signals were found to coalesce leading the authors to posit that the SH ligand undergoes rapid inversion. Compound **162** was prepared from **161** by treatment with additional $H_2S$ in the presence of base, and subsequent addition of acid could be used to regenerate **161**. *Syn* and *anti* isomers of **162** were detected by $^1H$ NMR spectroscopy upon isolation at −20 ºC, although conversion of the *syn* to the *anti* form was noted at room temperature. Both

**161** and **162** were characterized crystallographically, which confirmed the *anti* disposition of the hydrosulfide ligands in the latter.

**Scheme 61.** Group 9 Cp complexes containing bridging hydrosulfide ligands.

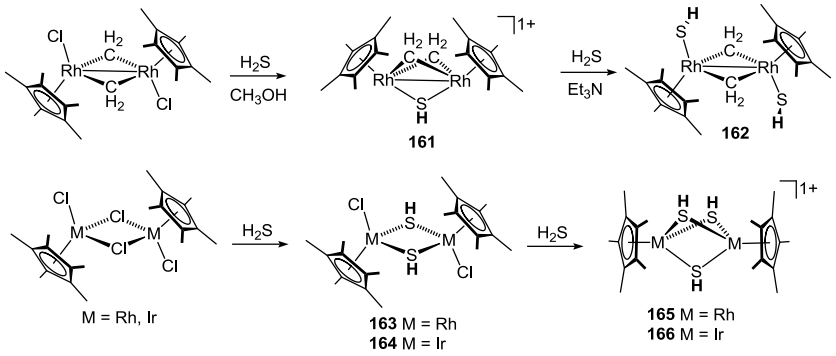


Later work by Hidai and co-workers disclosed the preparation of $[Cp^*_2M_2(\mu\text{-}SH)_2Cl_2]$ (M = Rh: **163**, Ir: **164**), analogs of **154**, through identical treatment of the bridged-chloride precursor, $[Cp^*_2M_2(\mu\text{-}Cl)_2Cl_2]$ (M = Rh, Ir) with $H_2S$ (Scheme 61).[305, 306] Both **163** and **164** were isolated as mixtures of *syn* and *anti* isomers, which could be detected by $^1H$ NMR spectroscopy. Crystallographic analysis of the two complexes, however, revealed that the *anti* isomer is preferred in the solid state. Deprotonation of **163** and **164** with $Et_3N$ resulted in formation of the cubane clusters, $[Cp^*_4M_4(\mu_3\text{-}S)_4]$, through the intermediacy of the transient bimetallic clusters, $[Cp^*_2M_2(\mu\text{-}S)_2]$. Compounds **163** and **164** were also employed in the synthesis of trimetallic sulfide-bridged clusters containing Rh and Pd. Prolonged exposure of $[Cp^*_2M_2(\mu\text{-}Cl)_2Cl_2]$ to $H_2S$ lead to formation of the triply-bridged hydrosulfide complexes $[Cp^*_2M_2(\mu\text{-}SH)_3]^+$ (M = Rh, **165**; Ir, **166**). In the case of the chloride salt of **166**, the crystal structure evinced hydrogen bonding interactions between two of the hydrosulfide ligands and the chloride ion. Identical behavior for **165** was noted in solution as judged by $^1H$ NMR. Upon counterion metathesis with $BPh_4$, the

orientations of the sulfhydryl H atoms in **165** and **166** were found to yield a mixture of stereoisomers.

The Group 10 metals do not provide as fertile ground for cyclopentadienyl chemistry as the earlier metals. Nonetheless, one of the first examples of a Cp-hydrosulfide complex was the nickel(II) species [CpNi($PBu_3$)(SH)] (**167**), prepared by Sato and coworkers. Notably, the compound was prepared under aqueous conditions via addition of NaSH to the ionic precursor, [CpNi($PBu_3$)$_2$]Cl (Scheme 62).[307] In contrast to other Ni(II) hydrosulfide complexes (*vide infra*), the $^1$H NMR spectrum of **167** demonstrated a downfield chemical shift for the SH ligand at 5.25 ppm. Reaction of **167** with phenylacetylene was reported to result in insertion into the S-H bond to generate [CpNi($PBu_3$)(SC{Ph}$CH_2$)], whereas treatment with diphenylacetylene led to loss of the hydrosulfide group and formation of the bimetallic Ni(I) species, [$Cp_2Ni_2$($\mu$-PhCCPh)].[308]

**Scheme 62.** Synthesis of CpNi hydrosulfide complexes.

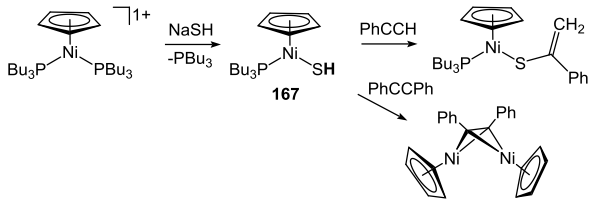


*3.3.2 Carbonyl complexes.* Next to cyclopentadienyl, the ubiquitous carbonyl ligand (CO) has played an equally important role in the development of transition metal hydrosulfide chemistry. In contrast to hydroxide, which is rarely found as a component of carbonyl complexes, the softer hydrosulfide ligand tolerates the lower oxidation states encountered in metal carbonyls. Indeed, many of the compounds discussed in the previous section feature CO ligands in addition to cyclopentadienyl. As with Cp, transition metal hydrosulfide complexes featuring carbonyl co-

ligands trace their origins to the earliest days of the field. Several of these compounds, such as that derived from Vaska's complex, have already been highlighted in the context of hydrogen chemistry.

Compounds of the type $[M(CO)_5(SH)]^{n-}$ (M = Group 6 element, $n$ = 1; M = Group 7 element, $n$ = 0) were the subject of many of the initial investigations concerning the chemistry of metal carbonyl complexes with $HS^-$ and $H_2S$. Among the first examples of such species, Behrens reported the preparation of $[Mo(bipy)(CO)_3(SH)]^-$ (**168**) from the reaction of NaSH with [($\eta^6$-$C_7H_8$)$Mo(CO)_3$] in the presence of 2,2'-bipyridine (Scheme 63).[309] IR spectra of **168** in the solid state demonstrated two CO stretches consistent with the *fac* isomer, but dissolution in $CH_3CN$ was observed to produce a spectrum with three stretches consistent with isomerization to the *mer*.

**Scheme 63.** Synthesis and reactivity of Cr, Mo, and W carbonyl compounds with $H_2S$.

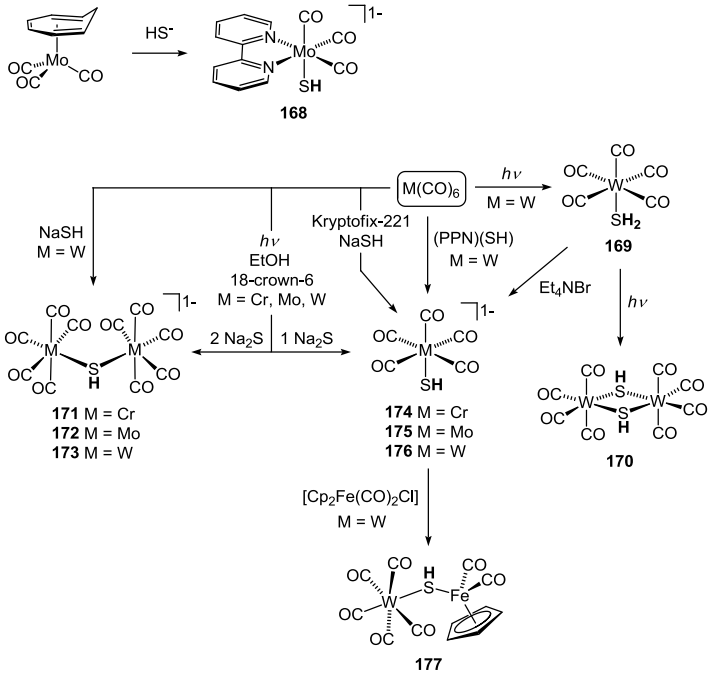

The parent compound to **168**, $[Mo(CO)_5(SH)]^-$ (**175**), was not reported until a decade later by Angelici and Gingerich during the course of investigations into reactions of $[M(CO)_6]$ (M = Cr, Mo, W) with (PPN)(SH).[310] Compound **175** was found to be unstable as its PPN salt and therefore only the W congener $[W(CO)_5(SH)]^-$ (**176**) could be isolated (Scheme 63). Compound **176** had actually been prepared earlier by Heberhold and Süss via a photochemical route involving prior formation of the hydrogen sulfide adduct, $[W(CO)_5(SH_2)]$ (**169**).[311] Notably, further photolysis of **169** was reported to generate the bridging hydrosulfide species, **170**, although little detail was provided to support its composition.[312] Angelici and Gingerich's report included isolation of a related bimetallic species $[W_2(CO)_{10}(\mu\text{-SH})]^-$ (**173**), generated by treatment of $[W(CO)_6]$ with NaSH. Subsequent work by Angelici and Gingerich scrutinized the reactivity of both **176** and **173** with a variety of unsaturated molecules and electrophiles.[313] In many cases, the S-H bond of **176** was found to undergo migratory insertion reactions in like fashion to many of the hydrosulfide complexes described in previous sections. In related work, Höfler reported the heterobimetallic species $[W(CO)_5(\mu\text{-SH})CpFe(CO)_2]$ (**177**), by reaction of **176** with $[CpFe(CO)_2Cl]$.[314]

Later studies by Cooper and McPartlin employing 18-crown-6 encapsulated sodium countercations in a photochemical route from $[M(CO)_6]$ succeeded in isolating all the members of the Group 6 $[M(CO)_5(SH)]^-$ family.[315] Their work also disclosed improved syntheses for the bimetallic species $[M_2(CO)_{10}(\mu\text{-SH})]^-$ (M = Cr, **171**; Mo, **172**; W, **173**). Crystallographic analysis of both **176** and **173** demonstrated that the complexes adopt polymeric structures in the solid state involving Na-O(carbonyl) interactions.[316] Darensbourg and co-workers obtained very similar results by direct reaction of $[M(CO)_6]$ with NaSH in acetonitrile using the cryptand, Kryptofix-221, to give **174-176** in high yield.[317] Use of the cryptand, however, lead to an absence of Na-O(carbonyl) interactions in the solid state structure of the Cr derivative. In like fashion, later

crystallographic studies of the PPN salt of **171** also displayed no cation-ion interactions in the solid state.[318]

The Mn and Re congeners of **174-176** were also the subject of several early investigations. As discussed above in the context of Cp complexes, $[Mn(CO)_4(\mu\text{-}SH)]_2$ (**136**) was prepared by Beck and Höfer by insertion of sulfur into the Mn-H bond of $[MnH(CO)_5]$ (Scheme 53).[283] Vahrenkamp subsequently reported the reaction of Mn and Re carbonyl complexes containing stannylthiolate ligands $[M(CO)_5(SSnMe_3)]$ with HCl to yield $[M_2(CO)_8(\mu\text{-}SH)_2]$ (M = Mn: **136**, Re: **178**) as well as the dimeric and tetrametric hydrosulfides **180** and **181** (Scheme 64).[319] In common with many of the bridging bishydrosulfide complexes discussed in previous sections, compounds **136** and **178** were found to exist as a mixture of *syn* and *anti* isomers corresponding to different orientations of the sulfhydryl H atoms. Treatment of **136** with large pressures of CO generated $[Mn(CO)_4SH]$ (**179**), which was found to rapidly revert to **136** when no longer under pressure consistent with the findings of Beck and Höfer. Although the Re congener of **179** is unknown, its conjugate acid, $[Re(CO)_5(SH_2)]^+$ (**179**), was reported by Beck through the reaction of $[Re(CO)_5(BF_4)]$ and $H_2S$. No NMR data was provided for **179** although an $\nu_{SH}$ peak was identified at 2510 $cm^{-1}$.[320]

**Scheme 64.** Synthesis and reactivity of Mn and Re carbonyl compounds containing hydrosulfide ligands.

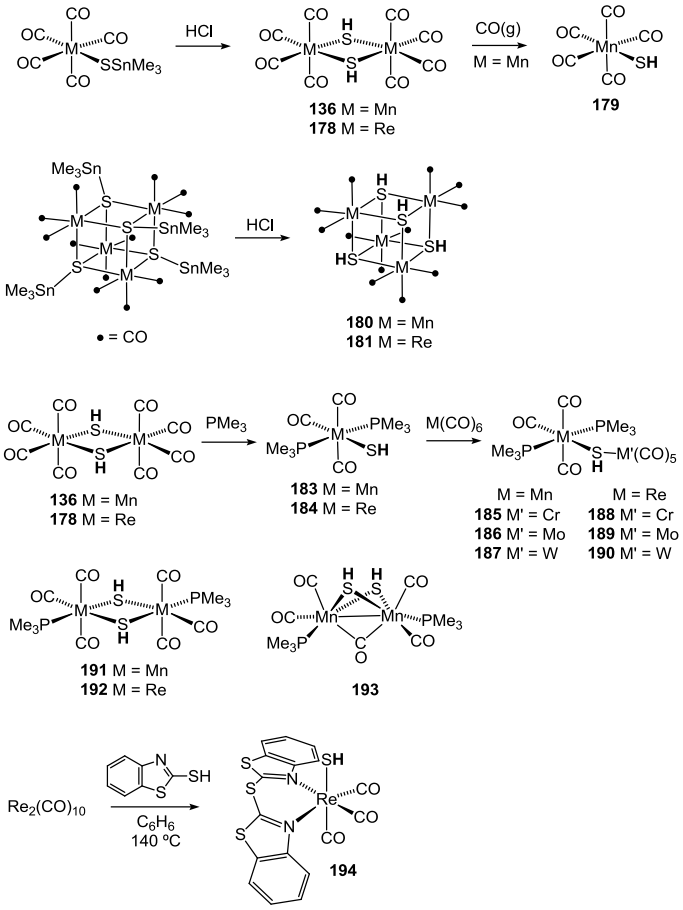


Follow-up work by Vahrenkamp and coworkers succeeded in stabilizing monomeric hydrosulfides of Mn and Re by replacement of two of the carbonyl ligands in **136** and **178** by $PMe_3$ (Scheme 64).[321] Compounds $[M(PMe_3)_2(CO_3)(SH)]$ (M = Mn, **183**; Re, **184**) were found to exist as a mixture of *fac* and *mer-trans* isomers, each of which displayed distinct $^1H$ NMR resonances upfield of 0 ppm. Also reported were bimetallic complexes **191-193**, which were prepared from the corresponding stannylthiolates and HCl in similar fashion to **136** and **178**. *Syn-anti* isomerism involving both the disposition of the hydrosulfide groups and the phosphine ligands was noted for the bimetallic species. Heterobimetallic complexes (**185-190**) containing Group 6 metals were subsequently described by Vahrenkamp through the reaction of **183** and **184** with $[M(CO)_6]$ (M = Cr, Mo, W).[321] As with **183** and **184**, these complexes were found to exist as mixtures of *fac*- and

*mer-trans* isomers. In all cases, assignment of isomers was made possible in large measure due to the diagnostic nature of $^1$H NMR chemical shifts for the sulfhydryl H atoms and CO stretching vibrations for the carbonyl ligands.

In recent work, Tzeng and co-workers isolated compound **194**, another example of a substituted-analog of [Re(CO)$_5$(SH)], from the reaction of 2-mercaptobenzothiazol with Re$_2$(CO)$_9$ under solvothermal conditions (Scheme 64).[322] Production of **194** occurs with coupling of the 2-mercaptobenzothiazol to generate a bidentate benzothiazole ligand. The solid-state structure of **194** was obtained demonstrating a *fac* arrangement of CO ligands, although no $^1$H NMR or IR data was reported for the hydrosulfide ligand.

Groups 6 and 7 provide the greatest number of examples of metal carbonyl complexes containing hydrosulfide ligands. Outside of these groups, transition metal hydrosulfide complexes containing carbonyls usually only feature 1 or 2 CO ligands. Several such compounds have already received mention in previous sections and others will be described in the context of cluster compounds (*vide infra*). In the area of Ru chemistry, an additional early example of a carbonyl-hydrosulfide complex is [Ru$_2$(PPh$_3$)$_2$(CNR)$_2$(CO)$_2$(SH)$_2$($\mu$-SH)$_2$] (**195**) reported by Harris and co-workers (Scheme 65).[323] The identity of the bridging ligands in **195** (iodide vs. hydrosulfide) was never determined as no $\nu_{SH}$ could be observed by IR spectroscopy and the compound proved too insoluble for NMR studies. Nonetheless, the synthetic route to **195** involving modification of the coordinated dithioester [Ru(PPh$_3$)$_2$(CO)(I){C(S)SMe}] by a primary amine represents a novel method of generating hydrosulfide ligands.

**Scheme 65**. Generation of Ru and Os hydrosulfides from carbonyl-containing compounds.

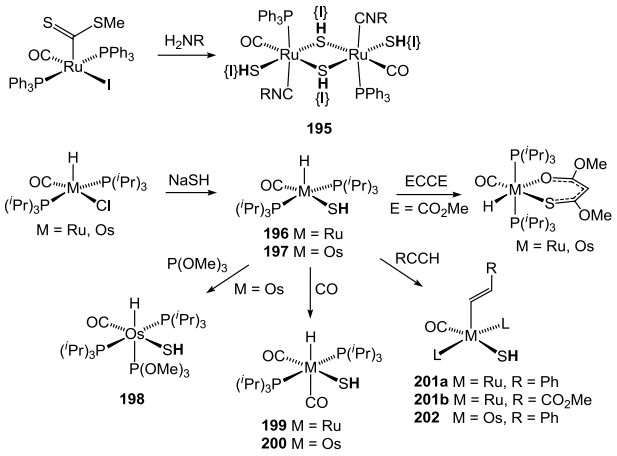


Later work by Esteruelas and co-workers with related five-coordinate complexes of Ru and Os demonstrated the straightforward synthesis of $[M(P^iPr_3)_2(CO)(SH)(H)]$ (M = Ru, **196**; Os, **197**) (Scheme 65).[269] Treatment of either complex with CO lead to the corresponding dicarbonyl species $[M(P^iPr_3)_2(CO)_2(SH)(H)]$ (M = Ru: **199**, Os: **200**). A six-coordinate complex of trimethylphosphite $[Os(P^iPr_3)_2(CO)(SH)(H)\{P(OMe)_3\}]$ (**198**) was also accessible in the case of osmium. Reactions of **196** and **197** with carbon-carbon triple bonds was found to result in reactivity at either the hydrosulfide or hydride ligand depending upon the nature of the alkyne. In the case of acetylenedicarboxylic acid, preferential reactivity occurred at the S-H bond to afford new Ru and Os complexes containing a monothio-β-diketonato ligand. By contrast, use of phenylacetylene or methylpropionate lead to insertion into the M-H bond to afford new hydrosulfide complexes **201** and **202**.

More recently, Macgregor and Whittlesey have examined reactions of $H_2S$ with the Ru(II) carbonyl-dihyride complex $[Ru(IMes)_2(CO)(H)_2(HOEt)]$, which contains bulky IMes ligands.[324] Displacement of the ethanol ligand from $[Ru(IMes)_2(CO)(H)_2(HOEt)]$ was found to occur readily in the presence of 1 atm of $H_2S$ to afford the air-stable hydrogen sulfide adduct $[Ru(IMes)_2(CO)(H)_2(SH_2)]$ (**203**, Scheme 66). The crystal structure of **203** was obtained

confirming both the integrity of the $H_2S$ ligand and the unusual *trans* arrangement of the hydrides. Further reaction of **203** with $H_2S$ lead to extrusion of $H_2$ and formation of the bishydrosulfide complex $[Ru(IMes)_2(CO)(SH)_2]$ (**204**). This 16-electron species was also characterized crystallographically displaying a square-pyramidal geometry about Ru with an apical CO ligand and *trans* hydrosulfides. Addition of hydrogen to a solution of **203** was found to slowly regenerate $[Ru(IMes)_2(CO)_2(H)(SH)]$ (**205**) providing a unique means of constructing an $H_2S$ ligand in the coordination sphere of a metal. Exposure of both **203** and **204** to 1 atm of CO produced the corresponding six-coordinate compounds **205** and **206**, respectively. Unless kept under an atmosphere of carbon monoxide, **205** was found to be unstable with respect to conversion to **204**, presumably through a non-stoichiometric process. The behavior of **205** in this respect is therefore somewhat surprising given its similarity to the stable phosphine analog, **199**, prepared by Esteruelas. In contrast to **205**, **206** was observed to be stable toward loss of CO requiring high temperature and vacuum to regenerate **204**.

**Scheme 66.** Generation of Ru-$SH_2$ and Ru-SH complexes containing IMes ligands.

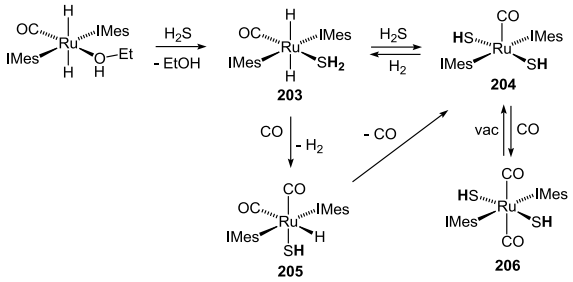


Among the later metals (Groups 9 and 10), carbonyl complexes containing hydrosulfide ligands are much less common, although several feature prominently as components of cluster species and will be discussed below. Two simple examples from Group 9 are the dirhodium

complexes $[Rh_2(PCy_3)_2(CO)_2(\mu\text{-}SH)_2]$ (**207a**) and $[Rh_2(PPh_3)_2(CO)_2(\mu\text{-}SH)_2]$ (**207b**), prepared by Pérez-Torrente and Oro (Scheme 67).[325] These compounds were synthesized from the acac precursors, $[Rh(CO)(PR_3)(acac)]$ (R = Cy, Ph) by treatment with $H_2S$ in THF. Choice of solvent was critical as similar reactions in $CH_2Cl_2$ were found to generate the cluster species, $[Rh_3(\mu\text{-}H)(\mu_3\text{-}S)(CO)_3(PR_3)_3]$. Compounds **207a** and **207b** were found by $^1H$ NMR spectroscopy to exist primarily as the $C_2$-symmetric *anti*-CO isomers with a *syn* disposition of the sulfhydryl groups. Both **207a** and **207b** were found to slowly lose $H_2S$ in solution ultimately forming a trinuclear Rh cluster. Also reported in this study was the all phosphite analog $[Rh_2\{P(OPh_3)\}_2(CO)_2(\mu\text{-}SH)_2]$ (**223**), which was generated from $[Ru(acac)(P\{OPh\}_3)_2]$. Unlike **207a** and **207b**, compound **208** was found to be stable toward formation of cluster species. Crystallographic analysis of **208** confirmed the presence of *syn* hydrosulfide H atoms, in agreement with the solution structures proposed for **207a** and **207b**. Notably, a compound analogous to **208** containing the chelating dippe ligand, **209**, was prepared earlier by Jones from the bridging chloride complex and used to examine the mechanism of S-H inversion.[326] Much like **208**, compound **209** was found to exist as the *syn* isomer in the solid state. However, fluxional behavior was noted in solution corresponding to sampling of several isomeric conformations involving the relative orientation of the sulfhydryls. The mechanism for the isomerization process was found to involve inversion of both sulfur and the $Rh_2S_2$ ring.

**Scheme 67.** Generation of carbonyl-containing Rh hydrosulfide complexes.

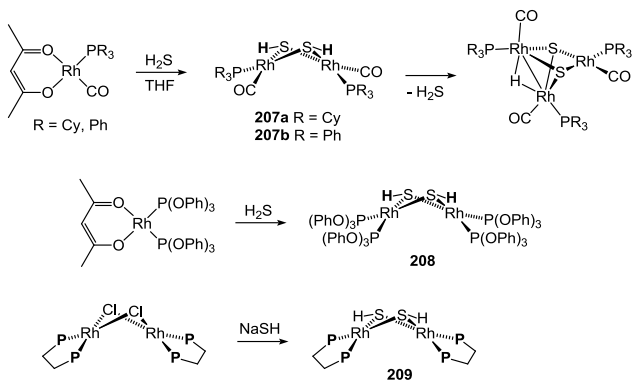


*3.3.3 Other Organometallic Complexes.* Outside of Cp and CO, organometallic compounds featuring hydrosulfide ligands have appeared sporadically but consistently in the literature over the past several decades. By in large these compounds contain hydrocarbyl-derived ligands although the popularity of *N*-heterocyclic carbenes in recent years has provided for additional examples of organometallic hydrosulfides, several of which have already received mention. This section will describe those organometallic species not possessing Cp or CO co-ligands.

The majority of organometallic hydrosulfide compounds from Group 6 have already been discussed as they overwhelmingly contain Cp or CO ligands. In addition to these examples, Luo and Kubas reported the two Mo hydrosulfides, **210a** and **210b**, which contain an aminocarbyne ligand (Scheme 68).[327] The compounds were prepared by thermolysis of hydrido-thiocarbonyl complexes, which were in turn prepared by oxidative addition of thioformamide to $[Mo(N_2)_2(R_2PCH_2CH_2PR_2]$ (R = Ph, Et). Spectroscopic evidence for the hydrosulfide ligands of **210a** and **210b** was provided by both $^1H$ NMR and IR spectroscopy. The solid-state structure of **210a** further corroborated the identity of the compounds as hydrosulfide-carbyne species evincing a short Mo-C distance of 1.830 Å.

**Scheme 68**. Synthesis of an aminocarbyne Mo hydrosulfide.

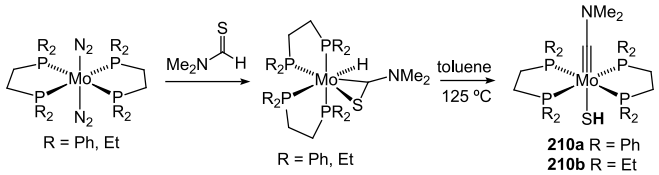


The chelating phosphine platform of **210** has also been employed to stabilize a rare example of an organometallic hydrosulfide of iron. Lörtscher, Venkatesan, and Berke recently described the preparation of **211** in the context of studies involving molecular wires.[328] As with **210**, compound **211** was synthesized from a precursor containing molecular nitrogen ligands (Scheme 69). Unfortunately, the electrochemical behavior and stability of **211** proved unsuitable for use as a transport junction in construction of molecular wires and it was not explored further.

**Scheme 69.** Synthesis of an iron hydrosulfide for use in molecular wires.

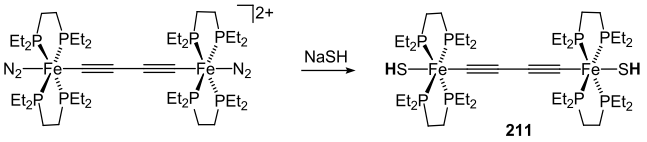


Shapely and co-workers have reported the synthesis of nitride complex, **212**, via deprotection of a silanethiolate ligand on the Ru precursor $[Ru(CH_3)_3(SSiMe_3)N]^-$ with halide ion (Scheme 70).[329] The compound could also be prepared by hydrolysis of the silanethiolate or via a direct salt metathesis reaction between $[Ru(N)(CH_3)_3Br]^-$ and NaSH. The solid-state structure of **212** was determined by X-ray crystallography demonstrating a square-pyramidal geometry about Ru. The compound was found to undergo decomposition at 75 ºC to produce the known trimetallic species, $[Ru_3Me_6(N)_3(\mu_3\text{-}S)_2]$,[330] with elimination of methane.

**Scheme 70.** Synthesis of Ru nitride hydrosulfide complexes.

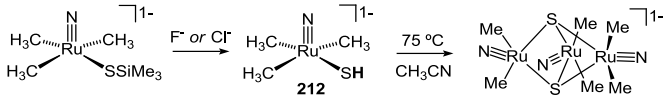


In the area of Group 10 chemistry, Ruiz and coworkers have described a family of bridging hydrosulfide complexes of Pd and Pt containing $C_6F_5$ and $C_6Cl_5$ ligands $[M_2R_4(\mu\text{-}SH)_2]^{2-}$ (M = Pd, Pt; R = $C_6F_5$, $C_6Cl_5$) (Scheme 71).[331] The compounds were generated by reaction of the corresponding hydroxide precursors $[M_2R_4(\mu\text{-}OH)_2]^{2-}$ (M = Pd, Pt; R = $C_6F_5$, $C_6Cl_5$) with $H_2S$. In each case, a single resonance for the sulfhydryl group was apparent by $^1H$ NMR suggesting that isomers resulting from the disposition of the S-H groups are rapidly interconverting in solution. Treatment of **213a** and **214** with $PPh_3$ lead to isolation of the monomeric species, $[M(PPh_3)(R)_2(SH)]^-$ (M = Pd, **215**; Pt, **216**). The *cis* arrangement of the $C_6F_5$ ligands was retained as judged by distinct $^{19}F$ resonances for the two rings. Further reaction of **215** and **216** with [Ag(OTf)($PPh_3$)] afforded the heterobimetallic complexes $[M(PPh_3)(C_6F_5)_2(\mu\text{-}SH)Ag(PPh_3)]$ (M = Pd, **217**; Pt, **218**). Also disclosed in the report by Ruiz and coworkers were compounds **219** and **220**, which are analogs of **213** and **214** featuring $PPh_3$ and imidazolate ligands, respectively (Scheme 71). These species were generated by similar reactions of hydroxide precursors with $H_2S$.

**Scheme 71.** Synthesis and reactivity of organometallic hydrosulfide complexes of Pd and Pt.

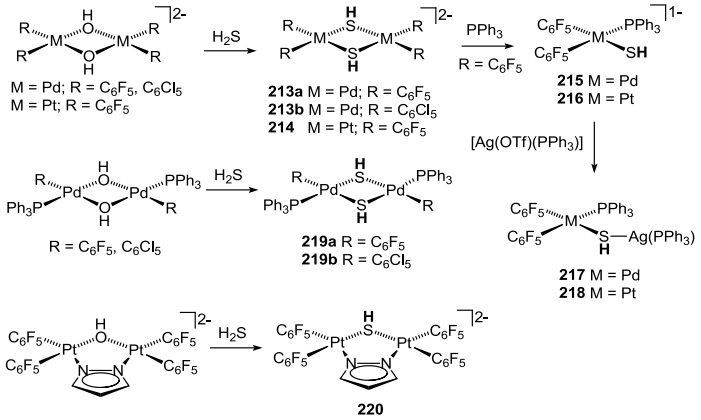


The pentafluorophenyl ligand has also been featured in the chemistry of gold. In work prior to that of Ruiz, Laguna and coworkers demonstrated that gold hydrosulfide compound $[Au(C_6F_5)_3(SH)]^-$ (**221**) could be isolated from the reaction of NaSH with the Au(III) complex, $[Au(C_6F_5)_3Br]^-$ (Scheme 72).[332] No S-H stretch was observed for **221** by IR spectroscopy, but the compound did display a $^1$H NMR resonance for the hydrosulfide ligand at −0.45 ppm. Reaction of **221** with $[Au(C_6F_5)_3(OEt_2)]$ produced the bimetallic species $[Au_2(C_6F_5)_6(\mu\text{-SH})]^-$ (**222**). Unlike **221**, the $^1$H NMR resonance for the hydrosulfide ligand was not found for **222**, although the complex was characterized crystallographically. Compound **222** was further used to prepare sulfide-bridged trimetallic species, $[\{Au(C_6F_5)_3\}_2(\mu_3\text{-S})\{M(PPh_3)\}]^-$ (M = Ag, Au), through reaction with monovalent Ag and Au precursors.

**Scheme 72**. Synthesis and chemistry of Au-SH compounds.

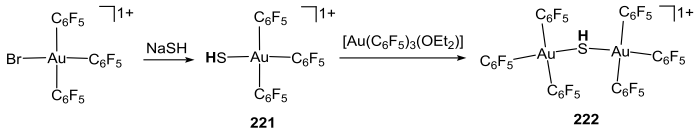

As a final example of organometallic hydrosulfides, we turn to those examples featuring an N-heterocyclic carbene ligand. Sellman and co-workers have prepared the anionic complexes, **223-225**, which feature a chelating dithiolate-carbene ligand ($S_2C$).[333] These compounds were each prepared in identical fashion through the reaction of the dimeric species, $[M_2(S_2C)_2]$ (M = Ni, Pd, Pt), with $Na_2S$ in the presence of 15-crown-5 (Scheme 73). Each of the hydrosulfides was found to demonstrate $^1$H NMR resonances for the S-H group upfield of 0 ppm as well as discernable $\nu_{SH}$ modes near 2500 cm$^{-1}$. Crystallographic analysis of **223** and **224** demonstrated the expected square-planar geometries for the metal atoms with close contacts between the sodium cations and the sulfhydryl groups.

**Scheme 73.** Anionic Ni, Pd, and Pt hydrosulfide complexes.

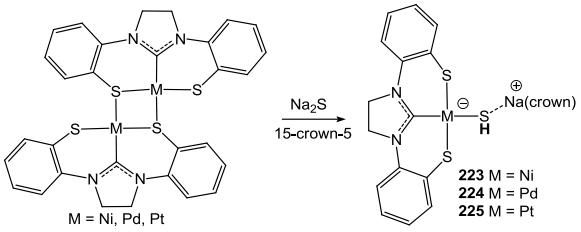


*3.4 Roles in Coordination Chemistry*

Beyond their uses in hydrogen chemistry and organometallic compounds, hydrosulfide ligands have continued to intrigue chemists from the standpoint of their basic coordination chemistry. Perhaps the simplest hydrosulfide complex, $[Cr(SH)(OH_2)_5]^{2+}$ (**226**), was prepared by Taube and Ardon in 1967 by the reaction of Cr(II) salts with sulfur-containing oxidants.[334] This compound, also referred to as the thiolochromium(III) ion, was never isolated, but follow-up solution studies by Sykes supported Taube's formulation and also described the thiocyanate derivative $[Cr(SH)(SCN)(OH_2)_4]^+$ (**227**).[335] A similar solution species, $[Cr^{III}Fe^{II}(\mu\text{-}SSH)(OH_2)]^{4+}$, was

reported in due course by Sykes, although as with **226**, unambiguous characterization was not possible.[336] These early examples notwithstanding, well-defined coordination complexes containing hydrosulfide ligands are well-represented across the transition series. Pnictogen-based ligands (phosphines and amines) feature prominently in their chemistry although examples containing sulfur-donor ligands are also encountered. This section will describe non-organometallic hydrosulfide compounds as they are found in P-, N-, and S-ligated complexes.

*3.4.1 Complexes of P-donor ligands.* Phosphine-derived co-ligands are found in numerous hydrosulfide complexes as evidenced by their frequent appearance in previous sections of this review. Among the phosphine compounds not yet discussed are those of Fe(II), Co(II), and Ni(II) prepared by Sacconi employing the tetradentate *tris*-phosphino ligands, $\mathbf{np_3}$ and $\mathbf{pp_3}$.[337] The Ni(I) complex of $\mathbf{np_3}$ was already mentioned in the context of oxidative addition reactions of $H_2S$, although the divalent metal complexes of both the $\mathbf{np_3}$ and $\mathbf{pp_3}$ ligands with Fe(II), Co(II), and Ni(II) (**228-233**) were reported earlier by the treatment of ethanolic solutions of the aquated metal ions with $H_2S$ in the presence of either the $\mathbf{np_3}$ or $\mathbf{pp_3}$ ligands (Scheme 74). Complexes **228-233** are all low-spin trigonal bipyramidal species, however, the symmetry properties of the Fe(II) species (**228** and **231**) result in paramagnetic triplet ground states. No S-H stretches could be detected by IR spectroscopy but electronic absorption spectra for each of the compounds were in line with their proposed formulations as were the crystal structures of 3-fold symmetric **229**, **231**, and **233**.

**Scheme 74**. Synthesis of Fe, Co, and Ni $\mathbf{np_3}$ and $\mathbf{pp_3}$ hydrosulfide complexes.

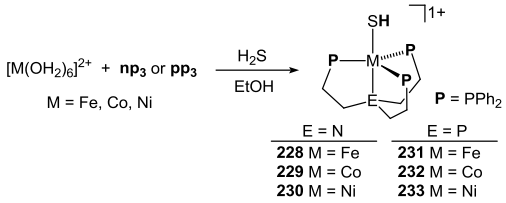


In later work with the **pp$_3$** ligand, Peruzzini and Stoppioni reported the corresponding Rh hydrosulfide species [Rh(**pp$_3$**)(SH)] (**234**).[338] Compound **235** was prepared in similar fashion to **231-233** by reaction of ethanolic solutions of $Na_2S$ with [Rh(**pp$_3$**)(cod)]$^+$ (Scheme 75). The hydroselenide and hydrotelluride derivatives were also synthesized, and crystallographic analysis of all three species demonstrated trigonal planar geometries with apical EH ligands as found for the Fe(II) and Ni(II) congeners. Treatment of **234** with triflic acid produced the hydride-hydrosulfide cation [Rh(**pp$_3$**)(SH)(H)]$^+$ (**235**), which could also be synthesized from the reaction of $H_2S$ with [Rh(**pp$_3$**)(cod)]$^+$. Use of MeOTf in place of triflic acid lead to formation of [Rh(**pp$_3$**)(SMe)(H)]$^+$. Unlike the **pp$_3$** compounds of Fe-Ni discussed above, S-H stretches for the hydrosulfide ligands of **234** and **235** were identified readily by IR spectroscopy ca. 2550 cm$^{-1}$. Likewise, the $^1$H NMR spectrum for both species demonstrated multiplet resonances ($^3J_{HP}$ = 5 – 10 Hz) for the sulfhydryls upfield of 0 ppm. In the case of **234**, the SH resonance was well separated from that due to the rhodium hydride.

**Scheme 75**. Synthesis of **pp$_3$** Rh hydrosulfides.

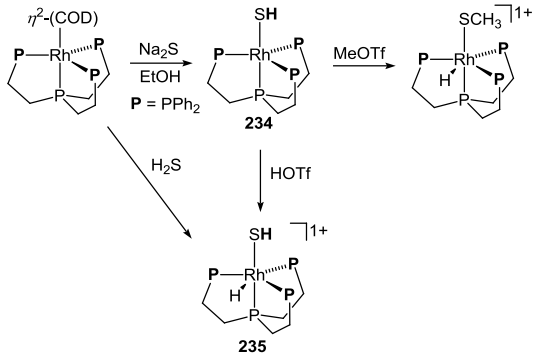


Tridentate phosphine ligands resembling **np$_3$** and **pp**$_3$ were subsequently examined by Sacconi and co-workers with both Ni and Fe. In like fashion to **230** and **233**, complexes **236a-c** were prepared from aqueous Ni(II) salts in the presence of the desired ligand (Scheme 76).[339] In the case of **236a**, protonation of the pendant amino group of **n$_2$p$_2$** was observed. As with **np$_3$** and **pp$_3$**, no S-H stretches could be observed by IR spectroscopy, but the solid-state structure of **236a** was reported. Identical reaction of aqueous Fe(II) with **ppp** afforded the triply-bridging hydrosulfide complex, **237**.[340] The structure of **237**, determined crystallographically, is similar in many respects to that of the Ru complex **100** discussed above. One notable feature of the structure of **237** is the *syn* disposition of the central PPh groups.

**Scheme 76**. Synthesis of Ni and Fe hydrosulfides with tridentate P/N ligands.

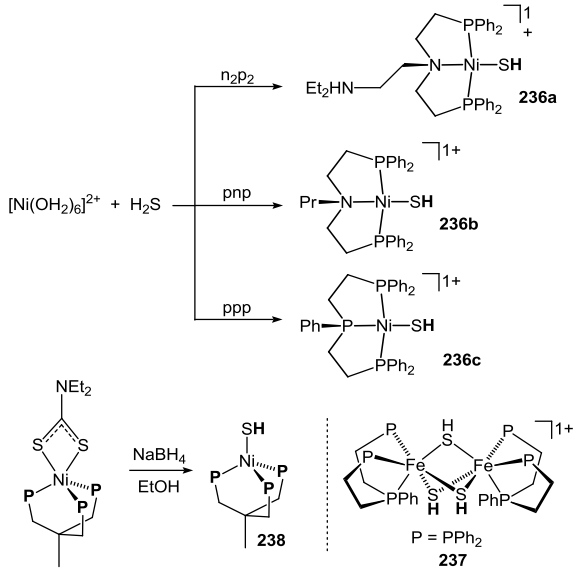


Yet another tridentate phosphine ligand, triphos, has been described earlier in the context of $H_2$ addition to dirhodium sulfide complexes. Prior to this work with rhodium, Bianchini described the reaction of a triphos bound Ni(II) dithiocarbamate with $NaBH_4$ to produce the univalent nickel complex [Ni(triphos)(SH)] (**238**, Scheme 76).[341] Due to the instability of **238** in solution no characterization data was reported, although a crystallographic study confirmed its composition.[342] Similar reactions of $NaBH_4$ with other triphos-Ni(II) species of general formula $[Ni(S_2CX)(triphos)]^+$ (X = SMe, OEt, $PEt_3^+$) were found to yield reduced nickel complexes lacking a hydrosulfide ligand indicating a complex reduction mechanism dependent on the nature of the dithiocarboxylate.

Bidentate phosphine ligands have also been used to great extent to stabilize hydrosulfide complexes, and several examples have been discussed in prior sections. Jones and coworkers reported a rare example of a chromium hydrosulfide supported by the dmpe ligand.[343] Treatment of *trans*-$[CrCl_2(dmpe)_2]$ with NaSH in methanol afforded red, crystalline *trans*-$[Cr(SH)_2(dmpe)_2]$ (**239**, Scheme 77). Reaction conditions were found to be critical during the synthesis of **240**, as

prior exposure of $CrCl_2$ to NaSH before addition of dmpe led to formation of trimetallic sulfide-bridged clusters. Paramagnetic **239** displayed a solution magnetic moment of 2.78 $\mu$B as expected for octahedral Cr(II), and crystallographic analysis of the compound confirmed the *trans* arrangement of the hydrosulfide ligands. The nearly isostructural iron analog, $[Fe(SH)_2(dmpe)_2]$ (**240**), was also reported through an identical synthetic procedure starting from *trans*-$[FeCl_2(dmpe)_2]$. Both compounds demonstrated a $\nu_{SH}$ mode near 2550 $cm^{-1}$, and in the case of the diamagnetic Fe complex, a multiplet $^1H$ NMR resonance at −7.02 ppm was observed for the sulfhydryls.

**Scheme 77.** Synthesis of Cr and Fe *trans* hydrosulfide complexes containing dmpe ligands.

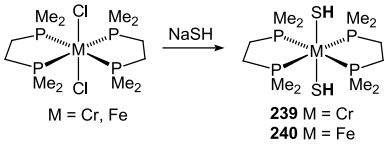


With the related bidentate dcpe ligand, which bears cyclohexyl groups on the phosphine donors, Jones has described the insertion of $S_8$ into the Pt-H bond of [Pt(H)(R)(dcpe)] to give a series of hydrosulfide species of the form [Pt(SH)(R)(dcpe)] (**61b-d**) (Scheme 78).[344] Compound **61b** and **61c** were found to be quite sensitive to excess $S_8$, so an alternative synthetic route involving simple salt metathesis of the halide precursor, [Pt(Cl)(R)(dcpe)], was used to generate larger quantities of material. Treatment of **61b** with halogens ($I_2$ and $Br_2$) resulted in formation of the corresponding dihalides, $[Pt(X)_2(dcpe)]$ through the presumed intermediacy of the Pt(IV) hydrosulfide, $[Pt(Me)(SH)(X)_2(dcpe)]$ (**241**). Similar reaction of **61b** with $H_2S$ produced the bishydrosulfide species $[Pt(SH)_2(dcpe)]$ **59c**, with loss of methane.

**Scheme 78.** Synthesis of Pt *bis*-hydrosulfides

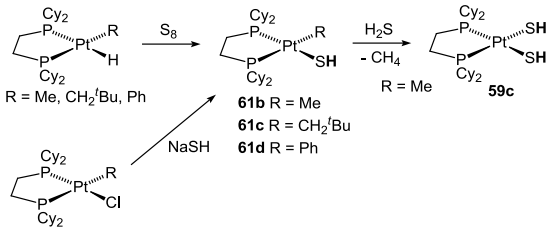


Also in the area of Pt chemistry, Lledós and González-Duarte have employed the dppe and dppp ligands to examine protonation events of the $Pt_2(\mu\text{-}S)_2$ core.[345] Their work builds upon contemporary studies of Hor and Henderson who used a combinatorial ESI-MS approach to identify and prepare $[Pt_2(\mu\text{-}S)(\mu\text{-}HS)(PPh_3)_4]^+$ (**242a**), along with several cluster species derived from $[Pt_2(\mu\text{-}S)_2(PPh_3)_4]$ (Scheme 79).[346, 347] In the work by Lledós and González-Duarte, the related monoprotonated cations, $[Pt_2(\mu\text{-}S)(\mu\text{-}HS)(dppe)_2]^+$ (**241b**) and $[Pt_2(\mu\text{-}S)(\mu\text{-}HS)(dppp)_2]^+$ (**242c**), were synthesized and found to display rapid proton transfer between their sulfur atoms in solution. Subsequent protonation events of **242b** and **242c** with either HCl or $HClO_4$ led to a series of intermediate species, from which the bishydrosulfide complexes $[Pt(SH)_2(dppe)]$ (**59b**) and $[Pt(SH)_2(dppp)]$ (**59d**), were isolated and characterized.

**Scheme 79**. Proton transfer events of phosphine-ligated Pt hydrosulfides.

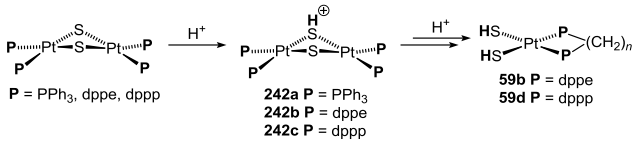


Incorporation of phosphine donors into tridentate pincer type ligands is a popular theme in modern coordination chemistry. Not surprisingly then, such ligands have been used to support

well-defined hydrosulfide complexes. The Ni compounds **236a-c** described above constitute the first examples of hydrosulfide compounds bearing pincer ligands. In more recent work, compounds [($^{Cy}$PNP)Ni(SH)] (**243**) and [(PONOP)Ni(SH)] (**244**) have been prepared in the context of studies dealing with formation and rupture of C-S bonds mediated by nickel (Scheme 80). Tonzetich reported the synthesis of **243** through the protonolysis of the anilide precursor, [($^{Cy}$PNP)Ni(NHPh)], with $H_2S$.[348] In line with many of the compounds discussed above, the hydrosulfide ligand of **243** gave rise to an upfield shifted $^1$H NMR resonance at −2.26 ppm and a $\nu_{SH}$ mode near 2540 cm$^{-1}$. In complementary work by Chen and Zhang, the Ni(II) thiolate complex, [(PONOP)Ni($SCH_2Ph$)], was found to undergo C-S bond cleavage when treated with two equivalents of $BH_3$·THF to generate [(PONOP)Ni(SH)] (**244**).[349] Spectroscopic and structural features of **244** were similar to those of **243**, including a $^1$H NMR resonance for the S-H proton at −1.56 ppm.

**Scheme 80.** Preparation of pincer-containing Ni-SH species.

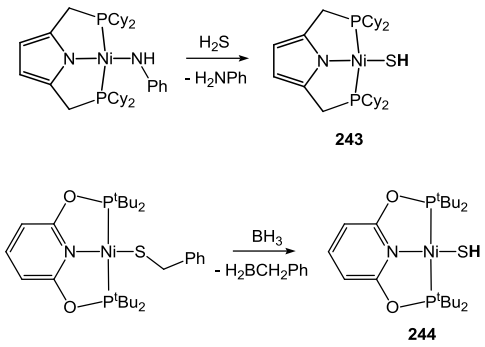


A hydrosulfide complex of a Rh(I) pincer has recently been reported by Braun and co-workers during studies of $SF_6$ activation. The [(POP)Rh(SH)] (**245**) product was isolated in tandem with [(POP)Rh(H)($F_2$)] from the reaction of [(POP)Rh(H)] with $SF_6$ in the presence of $HSiEt_3$ (Scheme

81).[350] The compound could also be prepared directly from [(POP)Rh(H)] by treatment with $H_2S$ in similar fashion to reactions discussed in Section 4.2.2. IR and NMR data for the SH ligand of **245** were comparable to those of **243** and **242**.

**Scheme 81.** Synthesis of a pincer-containing Rh hydrosulfide.

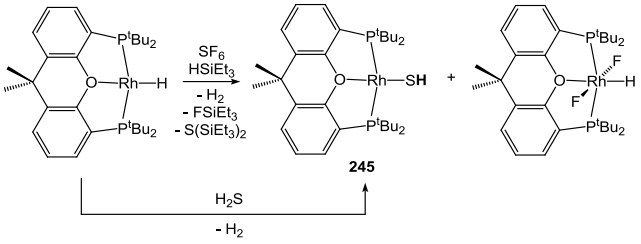


Outside of pincer chemistry, the simple phosphine-ligated Ir(III) hydrosulfide, **246**, has been generated by the treatment of *trans*-$[IrCl_2(PMe_2Ph)_3(OH_2)]^+$ with $H_2S$ (Scheme 82). Compound **246** displayed a characteristic hydrosulfide resonance at −1.08 ppm as a doublet of triplets. Although a $\nu_{SH}$ stretch was not reported, the molecular structure was confirmed by X-ray crystallography.

**Scheme 82.** Generation of an Ir-SH complex.

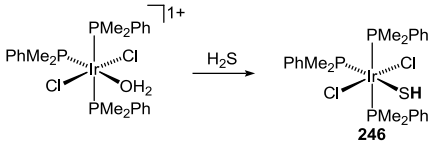


*3.4.2 Complexes of N-donor ligands*. Harder Lewis basic nitrogen-donor ligands do not appear to the same extent in the coordination chemistry of $HS^-$ and $H_2S$ as those of softer phosphines.

Nonetheless, several notable complexes have been prepared using these types of ligands, most frequently as components of chelates. The simplest representative of this class is the coordination complex $[Ru(SH_2)(NH_3)_5]^{2+}$ (**247**) reported by Taube in 1976.[351] This species was generated by treatment of the corresponding aqua complex, $[Ru(OH_2)(NH_3)_5]^{2+}$ with $H_2S$ and isolated as its $BF_4$ salt (Scheme 83). Compound **247** was found to be very susceptible to oxidation resulting in extrusion of $H_2$. The compound was even observed to decompose in a matter of days in a nitrogen-filled glovebox. The related species, **248**, containing an isonicotinamide ligand, was also described and proved more stable toward oxidation than **247**. Ligand exchange processes involving both compounds were scrutinized in detail, as was their electrochemical behavior. From these experiments, an equilibrium constant for substitution of $H_2O$ by $H_2S$ in $[Ru(OH_2)(NH_3)_5]^{2+}$ was calculated at $1.5 \times 10^3$ $M^{-1}$. In addition, the p$K_a$ of the bound $H_2S$ ligand was determined to be 4.0, dropping to −10 upon oxidation to Ru(III).

**Scheme 83.** Synthesis of Ru-$SH_2$ complexes.

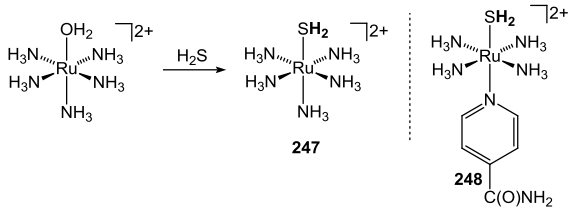


Since Taube's report of **247**, most investigations of hydrosulfide complexes containing *N*-donor ligands have focused on chelating variants. Pohl and coworkers employed the macrocyclic chelate, cyclam (1,4,8,11-tetraazacyclotetradecane), to stabilize a series of Co(II) and Ni(II) hydrosulfide complexes.[352] The linear coordination polymer $[Cu(cyclam)(SH)_2]_n$ (**249**) was obtained from the reaction of $Co(ClO_4)_2 \cdot 6MeCN$ and one equivalent of $HS^-$ in the presence of

cyclam (Scheme 84). Use of two equivalents of $HS^-$ under similar reaction conditions, however, produced the bimetallic species $[Cu_2(cyclam)_2(\mu\text{-}SH)_2][SH]_2$ (**250**). Compound **250** contains hydrosulfide counterions, which form hydrogen bonding contacts with the NH groups of the cyclam ligand in the solid state (Figure 7). The isostructural dinickel analog $[Ni_2(cyclam)_2(\mu\text{-}SH)_2][SH]_2$ (**251**) was also prepared, but from the thermal decomposition of the polymeric trimetallic species **252**. Much like **250** and **251**, the solid-state structure of **252** features hydrogen bonding interactions between the NH groups of the cyclam ligand and a hydrosulfide moiety.

**Scheme 84**. Preparation of cyclam-containing Co and Ni hydrosulfides.

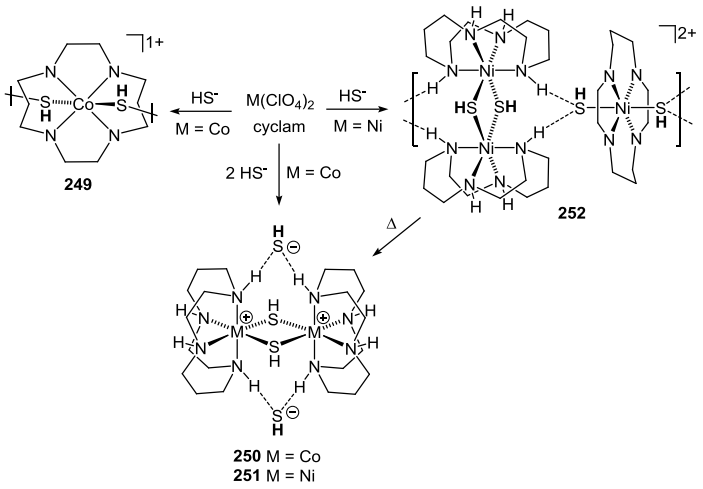

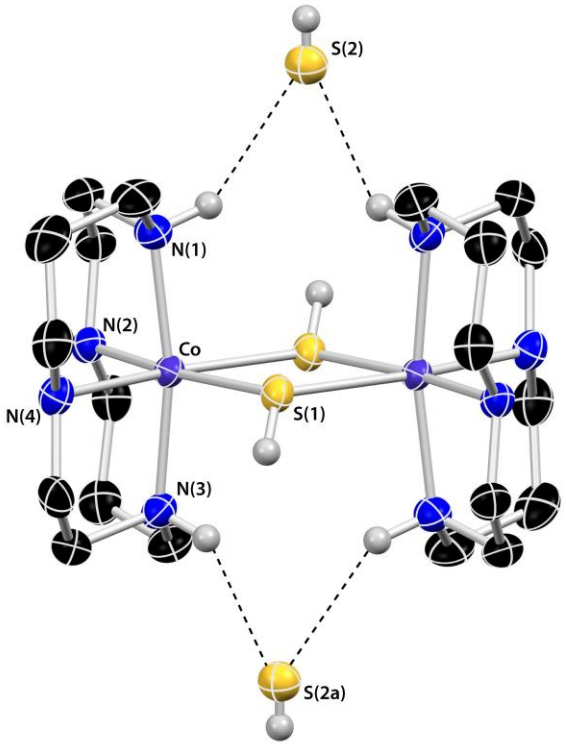


**Figure 7.** Solid-state structure of **250** showing hydrogen bonding interactions between the cyclam NH groups and the hydrosulfide counterion. Imaged generated from crystallographic data in reference 352.

In more recent work, Kersting has used an expanded macrocyclic ligand based on a hexaaza-dithiophenolate motif to prepare the bridging hydrosulfide complex **253** (Scheme 85).[353] The compound was synthesized through either the reaction of elemental sulfur with the borohydride precursor, $[Ni_2L(\mu\text{-}BH_4)]^+$, or through treatment of the perchlorate complex, $[Ni_2L(\mu\text{-}ClO_4)]^+$, with sodium sulfide. The nickel(II) ions of **253** were found to display ferromagnetic exchange resulting in an a pentet ($S$ = 2) ground state for the complex. Electronic absorption studies on **253** along with analogs containing bridging $S_6^{2-}$ and $PhS^-$ ligands permitted a ranking of $\sigma$-donor ability whereby hydrosulfide was found to be the weakest.

**Scheme 85**. Synthesis of a bimetallic Ni-SH complex featuring a macrocyclic N6S2 ligand.

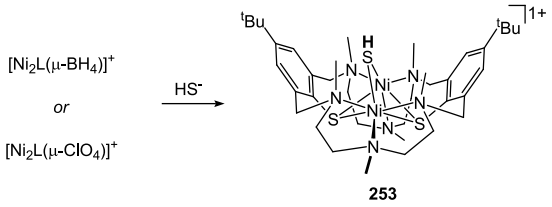


Non-macrocyclic *N*-donor ligands too have found use in the synthesis of hydrosulfide complexes. The simple Cu(II) coordination complex, **254**, was isolated by Gupta and Bhattacharya via the solvent assisted decomposition of the heterometallic Cu-Pb cluster, $[(PPh_3)_3Cu_5(\mu\text{-}SPh)_7Pb]$ (Scheme 86).[354] Also in the area of Cu(II) chemistry, Kurup and co-workers disclosed the use of a chelating **nns** ligand derived from a pyridine thiosemicarbazone to generate the copper(II) hydrosulfide complex **255** (Scheme 86).[355] Curiously, compound **255** was isolated from a reaction targeting the dimeric complex, $[Cu_2(\mathbf{nns})_2]^{2+}$. A decade later, Arnáiz and Javier García-Tojal reported a related bimetallic copper(II) complex, **256**, from the desulfurization reaction of a similar thiosemicarbazone ligand (**nns***).[356] Thus, the original synthesis of **255** by Kurup and coworkers most likely involved an analogous desulfurization process. The monometallic nature of **255** versus **256** is probably a consequence of the bulkier pyrrolidine substituent in the case of **nns**.

**Scheme 86**. Cu(II) hydrosulfide complexes containing *N*-donor ligands.

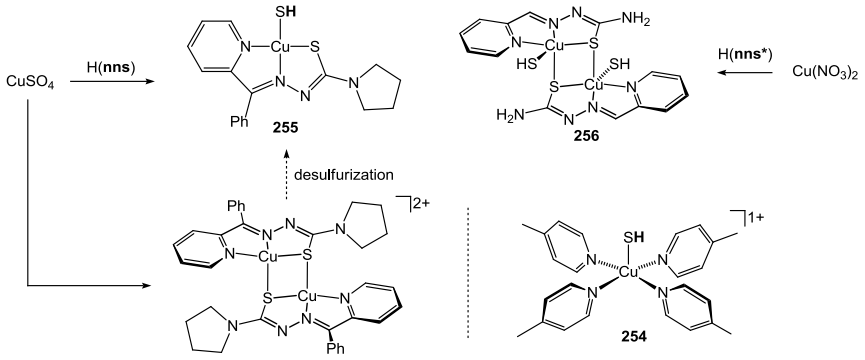

Desulfurization has been applied as well to the preparation of a cobalt(II) hydrosulfide compound. Anacona and co-workers observed the formation of the tetrahedral complex $[Co(quinolone)_2(SH)_2]$ (**257**), from the reaction of hydrated $CoCl_2$ with sulfathiazole in the presence of the *N*-donor quinoline (Scheme 87).[357] The blue paramagnetic complex was obtained in high yield and shown to have superoxide dismutase activity by inhibiting the reduction of nitroblue tetrazolium.

**Scheme 87**. Synthesis of a Co *bis*-hydrosulfide complex containing quinoline ligands.

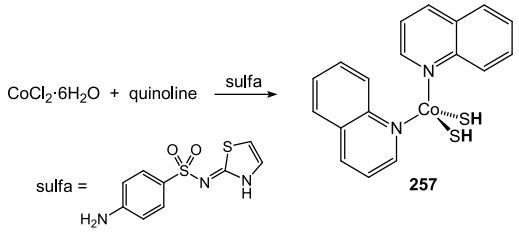


Holm has reported the generation of Ni(II) hydrosulfide complexes supported by tridentate pincer type ligands incorporating a central pyridine donor and flanking acyl units. Employing an SNS type ligand with thiocarboxylate donors, the nickel complex **258** was generated by cleavage of the thiolate bridges of a dimeric precursor (Scheme 88).[358] Refluxing **258** in air led to formation of an unusual $\mu_3$-sulfide-bridged trinickel species. Also described were hydrosulfide complexes **259** and **260**, which contain a reduced version of the SNS ligand. These species were made through identical bridge-cleavage reactions of the corresponding dimeric precursors. Compounds **258-260** all displayed $^1$H NMR resonances for the SH ligand upfield of 0 ppm, similar to the phosphorus-based pincer complexes discussed above. Additional work by Holm concerned with modeling the bimetallic Ni-Fe site of the C-cluster of CO dehydrogenase enzymes reported the nickel hydrosulfide complex **261**, which contains an NNN pincer ligand. This compound was prepared

by simple ligand exchange with the terminal hydroxide precursor.[359] Unlike the hydroxide analogue, however, compound **260** was not used further to construct bimetallic Ni-Fe assemblies.

**Scheme 88.** Preparation of Ni hydrosulfide complexes with amine ligand scaffolds.

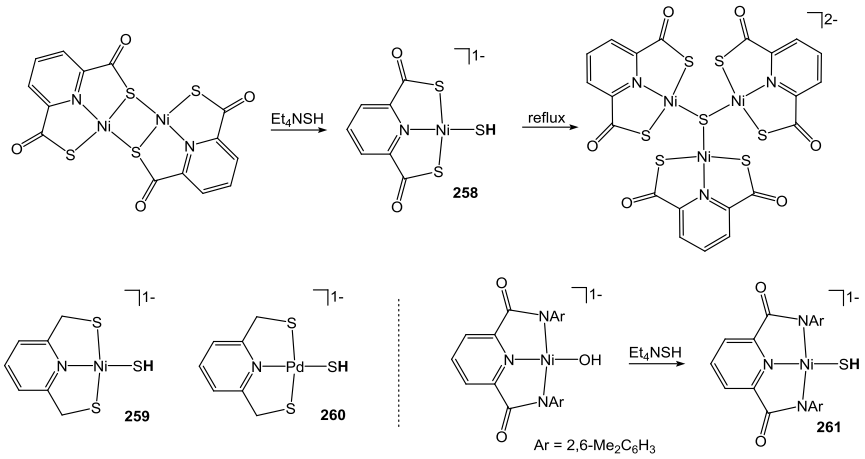


Yet another *N*-based chelate used to stabilize a hydrosulfide complex is the tris-pyrazolyl borate ligand (Tp). Theopold prepared the terminal iron(II) hydrosulfide complex [Tp$^{t\text{Bu,Me}}$Fe(SH)] (**262**), bearing a sterically encumbering Tp$^{t\text{Bu,Me}}$ ligand by protonolysis of the methoxy analog [Tp$^{t\text{Bu,Me}}$Fe(OMe)] with $H_2S$ (Scheme 89).[360] The paramagnetic compound displayed an effective solution magnetic moment of 5.7(1) $\mu_B$ consistent with high-spin iron(II). In contrast to other three-fold symmetric hydrosulfide species discussed in prior sections, the $\nu_{SH}$ mode of **262** was detected by IR spectroscopy as a strong band at 2551 cm$^{-1}$. Crystallographic analysis of **262** confirmed the pseudo-tetrahedral geometry about Fe, revealing an Fe-S bond distance of 2.293 Å.

**Scheme 89.** Synthesis of a Tp$^{t\text{Bu,Me}}$ Fe-SH complex.

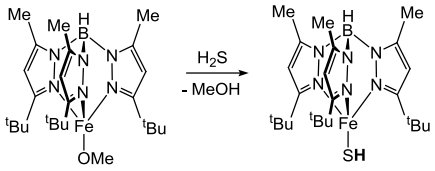


**262**

*3.4.3 Complexes of S-donor ligands.* The final series of coordination complexes to be discussed are those featuring *S*-donor ligands. One of the most fascinating members of this class of compounds is the homoleptic Au(I) hydrosulfide, (PPN)[Au(SH)$_2$] (**263**) reported by Vicente.[361] The only example of a homoleptic hydrosulfide other than [Fe(SH)$_4$]$^-$ (**15**), compound **263** was synthesized by addition of $H_2S$ to (PPN)[Au(acac)$_2$] in dichloromethane. The crystal structure of **263** displayed the expected linear coordination about gold with no significant aurophilic interactions.

Other simple *S*-bound hydrosulfide complexes include the thiometallate species [W(S)$_3$(SH)]$^-$ (**264**) and [Nb(S)$_3$(SH)]$^{2-}$ (**266**). The tungsten congener **126** was reported by Müller and co-workers in 1977 by the action of 40% HF(*aq*) on $WS_4^{2-}$ and isolated as both its $PPh_4^+$ and $AsPh_4^+$ salts.[362] Nearly two decades later Coucouvanis and co-workers reported the niobium analog (**266**) from reaction of the oxo-disulfide species [Nb(S$_2$)$_2$(SH)(O)]$^{2-}$ (**265**), with $PEt_3$ (Scheme 90).[363] Both **265** and **266** displayed assignable $^1$H NMR resonances for the sulfhydryls, although only in the case of **265** was a $\nu_{SH}$ band identified. Crystal structures for **264-266** were determined and each showed the expected tetrahedral geometry about the metal center.[364] A shorter Nb-S bond distance was noted for **265** than **266**, but the molecule was also found to crystallize on a two-fold axis preventing unambiguous assignment of the H atom to a single S center.

**Scheme 90**. Synthesis of *S*-ligated W and Nb hydrosulfides.

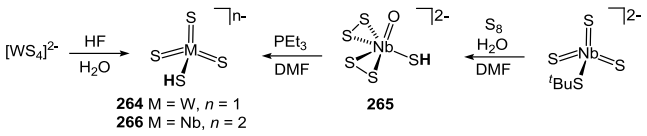


Hydrosulfide complexes containing more sophisticated *S*-bound ligands are also known. Early work by DeSimone and co-workers described the synthesis of several molybdenum complexes containing the macrocyclic polythioether ligand, 1,5,9,13-tetrathiacyclohexadecane ([16]-ane[$S_4$]).[365] Of these complexes, the hydrosulfide species, **267** and **268**, were isolated from the reaction of $[Mo_2(OH_2)_4(OTf)_2]^{2+}$ with [16]-ane[$S_4$] in EtOH (Scheme 91). As in the case of compounds similar to **255** mentioned above, desulfurization of the [16]-ane[$S_4$] ligand was invoked to explain the origin of the hydrosulfide groups in **267** and **268**. The identity of each compound was obtained through X-ray crystallography,[366] but solution characterization of both complexes was limited due to the inability to observe $\nu_{SH}$ modes and the complexity of the $^1$H NMR spectra. Both compounds displayed one-electron cathode processes by cyclic voltammetry, with **268** demonstrating a quasi-reversible couple.

**Scheme 91**. Synthesis of Mo-SH species containing macrocyclic [16]-ane[$S_4$] ligands.

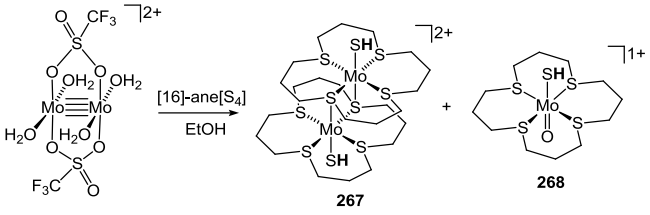


In other work with molybdenum, the hydrosulfide complex $[Mo(SH)(S_2CNEt_2)_3]$ **269** was isolated by Jordanov and co-workers as one of the products of the reaction of $[Cp_4Fe_4S_6]$ with $[Mo(CO)_2(S_2CNEt_2)_2]$ (Scheme 92).[367] Compound **269** was found to be paramagnetic at room

temperature ($S$ = 1), but displayed a diagnostic $\nu_{SH}$ stretch of 2480 $cm^{-1}$ by IR spectroscopy. Crystallographic analysis of **269** confirmed its general composition but could not definitively rule out the possibility that the sulfhydryl group was in fact a terminal sulfide. The identity of **269** as a terminal sulfide complex, however, was argued against on the basis of the aforementioned IR band and the lack of a strong *trans* influence in the Mo-S distance of the dithiocarbamate ligand directly opposite the putative hydrosulfide.

**Scheme 92**. Generation of Mo complexes containing terminal SH ligands.

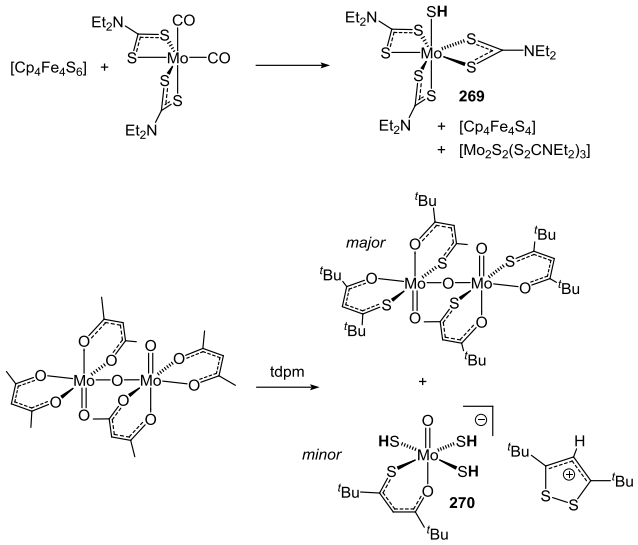


The molybdenum trishydrosulfide complex, **270**, was similarly isolated from a complex mixture by Kamenar and co-workers during investigations of the thiodipivaloylmethane ligand (tpdm). Prolonged reaction of $[Mo_2O_3(OAc)_4]$ and tdpm was found to generate small quantities of **270** in addition to an oxo-bridged complex after 25 days at ambient temperature (Scheme 92).[368] The origin of the hydrosulfide ligands in **270** as well as the dithiolylium counterion was ascribed

to reactivity with $H_2S$ generated by hydrolysis of tpdm by the acetic acid byproduct. Support for the composition of **270**, which represents a very rare example of a Mo(V) hydrosulfide, included an IR peak at 2600 $cm^{-1}$ assigned to $\nu_{SH}$ and an X-ray crystal structure. Notable in the structure of **270** was a hydrogen bonding contact between one of the hydrosulfide ligands and a sulfur atom of the dithiolylium cation.

Examples of hydrosulfide complexes containing non-chelating *S*-donor ligands are quite uncommon. Aside from the complexes discussed at the beginning of this section, additional examples of such compounds include those possessing thiourea-derived ligands. Braun reported the synthesis and crystal structure of the silver(I) hydrosulfide, **271**, which features the 1,1-diethyl-3-benzoylthiourea ligand (Chart 3).[369] In more recent work, Hadjikakou prepared the copper hydrosulfide(I), **272**, which contains 2-mercaptopyrimidine.[370] The pseudo-tetrahedral geometry about copper observed in the solid-state structure of **272** is similar to that of $[Cu(SH)(py)(PPh_3)_2]$ (**273**) prepared earlier by Strauch via photolysis of $[Cu_2(PPh_3)_4(\mu\text{-}C_2S_3O)]$.[371] Complexes **272-273** each feature four-coordinate univalent Group 11 ions with a terminal SH ligand unengaged in any intermolecular interactions. Compound **293** was further shown to inhibit the peroxidation of linoleic acid by lipoxygenase.

**Chart 3.** Ag and Cu hydrosulfide species.

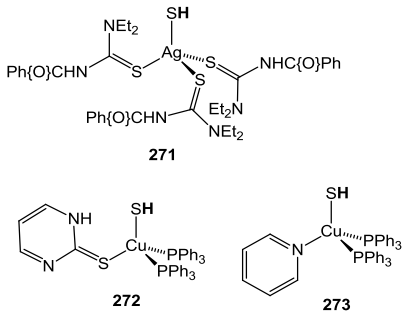

*3.5 Roles in Cluster Chemistry*

Sulfide ligands form the basis of numerous metal cluster compounds found naturally and produced synthetically. It is not surprising then, that the conjugate acid of sulfide, hydrosulfide, also finds a great deal of use in the area of cluster science. Biologically relevant cluster compounds containing hydrosulfide ligands have already received mention in previous sections, as have several synthetic examples relating to the chemistry of organometallic compounds. As the hydrosulfide ion is frequently encountered as a precursor to sulfides in the preparation of metal clusters, this section will focus primarily on those cluster species containing a SH ligand. Metal organic frameworks (MOFs) and coordination polymers containing hydrosulfide ligands will also be treated briefly at the end of this section. In parallel fashion to the sections dealing with organometallic compounds and coordination complexes, the metal clusters will be considered according to their principal supporting ligands.

*3.5.1 Metal cyclopentadienyl clusters.* As noted earlier, the preparation of compound $[Cp_2Ti(SH)_2]$ (**70a**) by Köpf and Schmidt represented a watershed moment in the development of metal hydrosulfide chemistry. Since that initial report, metallocene hydrosulfide compounds have provided a fertile starting point for more elaborate clusters. Rauchfuss reported the use of **70a** and its $Cp^{Me}$ analog, $[Cp^{Me}_2Ti(SH)_2]$ (**70c**), to prepare several heterobimetallic Ti-M (M = Mo, W) compounds containing a double hydrosulfide bridge (**274** and **275**, Scheme 93).[372] These species were synthesized in straightforward fashion from the reaction of **70a** and **70c** with equimolar [($\eta^4$-norbornadiene)$M(CO)_4$] in toluene. $^1$H NMR analysis of **274a** indicated a 2:1 mixture of *syn* to *anti* isomers, which were found to interconvert with an activation barrier of 18 kcal/mol. This interconversion process could also be catalyzed by addition of $Et_3N$. Treatment of **274a** with base led to formation of the putative dianion $[Cp_2Ti(\mu\text{-}S)_2Mo(CO)_4]^{2-}$. This sulfide-bridged species

underwent facile alkylation with MeI to generate [$Cp_2Ti(\mu$-$SMe)_2Mo(CO)_4$] and protonation with HCl to regenerate **274a**. Other transformations observed with **274a** include base-catalyzed reactions with $S_8$ and $Ph_2E_2$ (E = S, Se) to generate a variety of mononuclear titanocene species, and S-H insertion of methyl acrylate to generate compound a heterobimetallic thiolate bridged species.

**Scheme 93.** Synthesis of bimetallic hydrosulfides from $Cp_2Ti(SH)_2$ derivatives.

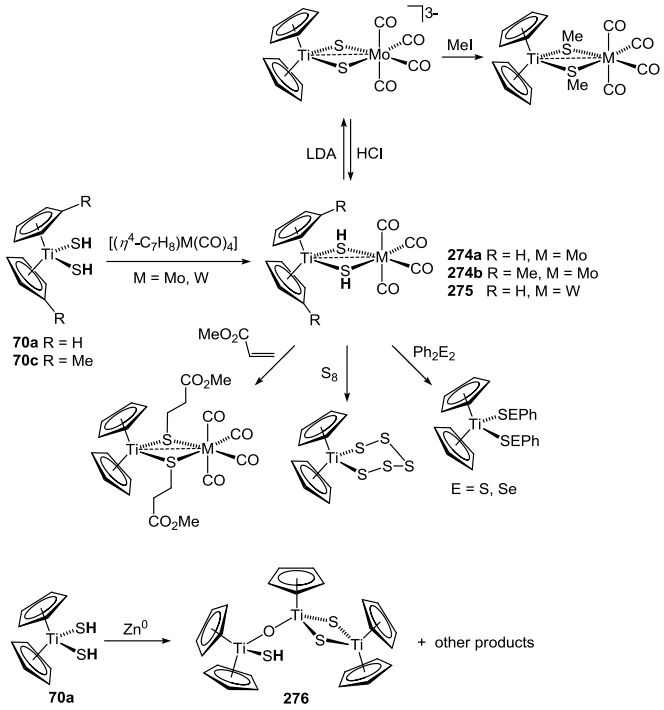


In subsequent work by Bottomley with **70a**, the titanium cluster **276** was isolated as one of the components of the reaction mixture generated upon reduction with Zn powder.[373] Fractional crystallization of **276** from the complicated mixture and analysis by X-ray diffraction permitted identification of this trititanium species, which was formed in tandem with at least four other Ti-sulfide clusters. The genesis of the oxygen atom in **276** was proposed to be the oxide coating of

the Zn powder used in reduction. Interestingly, the mixture of products obtained by reduction of **70a** was similar to that observed upon treatment of $[Cp_2Ti(CO)_2]$ with $H_2S$ in the presence of water (*vide supra*).

Oro and coworkers have utilized **139** to prepare a series of early-late heterobmetallic clusters featuring Rh and Ir. In an early report, the reaction of **70a** with $[Rh_2(\mu\text{-}OMe)_2(tfbb)_2]$ (tfbb = tetrafluorobenzobarrelene) to give $[CpTi\text{-}(\mu_3\text{-}S)_3\text{-}(Rh\{tfbb\})_3]$ was described.[374] Exposure of $[CpTi\text{-}(\mu_3\text{-}S)_3\text{-}(Rh\{tfbb\})_3]$ to CO produced $[CpTi\text{-}(\mu_3\text{-}S)_3\text{-}(Rh\{CO\}_2)_3]$, which was found to undergo further ligand exchange at Rh with $PPh_3$. Identical treatment of **70a** with $[Rh_2(\mu\text{-}OMe)_2(COD)_2]$ led to the analogous cyclooctadiene-bound cluster, $[CpTi\text{-}(\mu_3\text{-}S)_3\text{-}(Rh\{COD\})_3]$.[375] In the absence of rigorously anhydrous conditions, preparation of $[CpTi\text{-}(\mu_3\text{-}S)_3\text{-}(Rh\{COD\})_3]$ was accompanied by the formation of the hexametallic cluster $[(CpTi\text{-}\{\mu_3\text{-}S\}_2\text{-}\{Rh(CO)_2\}\{Rh(CO)\}_2)_2\text{-}\mu_4\text{-}O]$ (Scheme 94). An analog of this hexametallic cluster containing COD ligands on Rh has also been reported recently.[376]

Generalized syntheses for tetrametallic clusters similar to $[CpTi\text{-}(\mu_3\text{-}S)_3\text{-}(Rh\{tfbb\})_3]$ were later developed by employing $[(CpTi\{S\})_2\text{-}(\mu_2\text{-}S)_2]^{2-}$, which is generated by deprotonation of **70a** (Scheme 94).[377] Reaction of $[(CpTi\{S\})_2\text{-}(\mu_2\text{-}S)_2]^{2-}$ with $[M_2(\mu\text{-}Cl)_2(\eta^4\text{-diolefin})_2]$ afforded clusters of the type $[CpTi\text{-}(\mu_3\text{-}S)_3\text{-}(M\{\eta^4\text{-diolefin}\})_3]$ (M = Rh, Ir; diolefin = tfbb, COD, dbd), all of which could be further derivatized with CO and $PR_3$.[378] Work by Oro and coworkers also demonstrated the preparation of the trimetallic clusters through reaction of **70a** with $[M(\mathbf{L_2})(\eta^4\text{-diolefin})]$ ($\mathbf{L_2}$ = acac, 8-oxyquinolinate). Subsequent derivation with CO and $PR_3$ proceeded in identical fashion to clusters of the type $[CpTi\text{-}(\mu_3\text{-}S)_3\text{-}(M\{\eta^4\text{-diolefin}\})_3]$.[379]

**Scheme 94.** Generation of multimetallic products from $Cp_2Ti(SH)_2$.

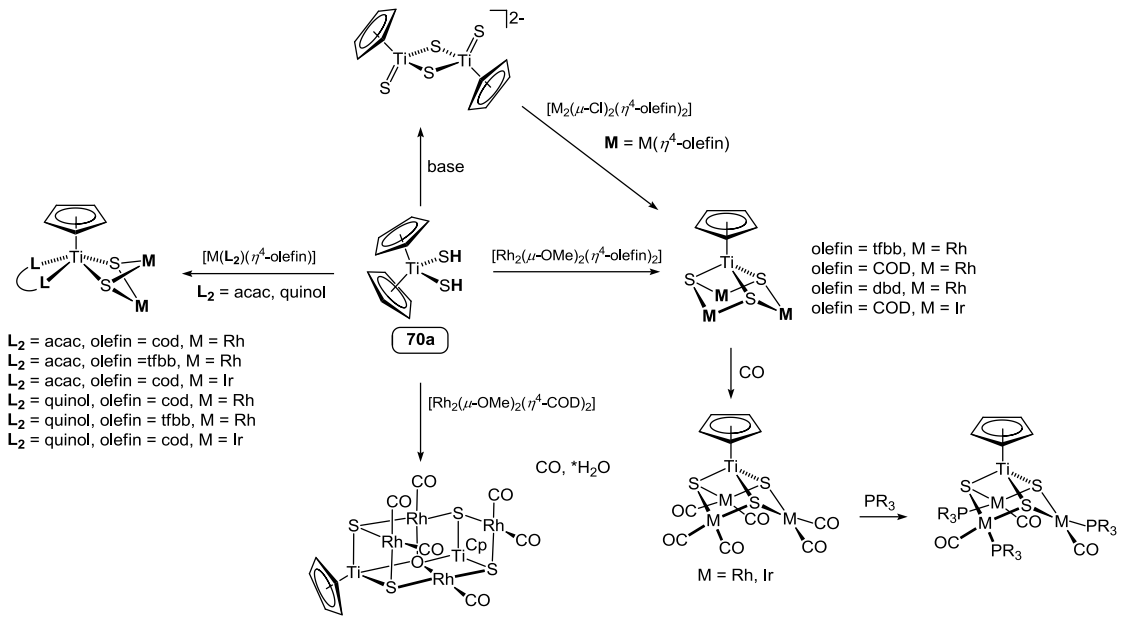


In addition to titanium, Oro and coworkers have explored analogous transformations of a Zr hydrosulfide precurosr.[380] In contrast to the chemistry observed with **70**, reaction of $[Cp_2^{tBu2}Zr(SH)_2]$ (**71c**) with [Rh(acac)($\eta^4$-diolefin)] was found to produce a series of trimetallic clusters retaining both cyclopentadienyl ligands (Scheme 95).[381] Curiously however, reactions of **71c** with the Ir congener, [Ir(acac)($\eta^4$-diolefin)], resulted in loss of $HCp^{tBu2}$ and formation of $[Cp^{tBu2}Zr(acac)\text{-}(\mu_2\text{-}S)_2\text{-}(Ir\{COD\})_2]$. The Ir analog containing both $Cp^{tBu2}$ ligands could be accessed, but only through prior treatment of **71c** with BuLi followed by addition of $[Ir_2(\mu\text{-}Cl)_2(\eta^4\text{-}COD)_2]$. A putative intermediate species, **277**, containing a bridging hydrosulfide ligand, was detected by $^1H$ NMR spectroscopy during preparations of the trimetallic Rh cluster. This species demonstrated a resonance for the sulfhydryl group downfield of 2 ppm. As with Ti, each of the $ZrM_2$ clusters could be further elaborated by substitution of the diolefin ligands for CO and phosphines. In the case of the Rh, phosphine-bound derivatives of $[Cp_2^{tBu2}Ti\text{-}(\mu_3\text{-}S)_2\text{-}(Rh\{nbd\})_2]$ demonstrated activity toward the hydroformylation of 1-octene.

**Scheme 95.** Synthesis of substituted cyclopentadienyl Zr-SH species.

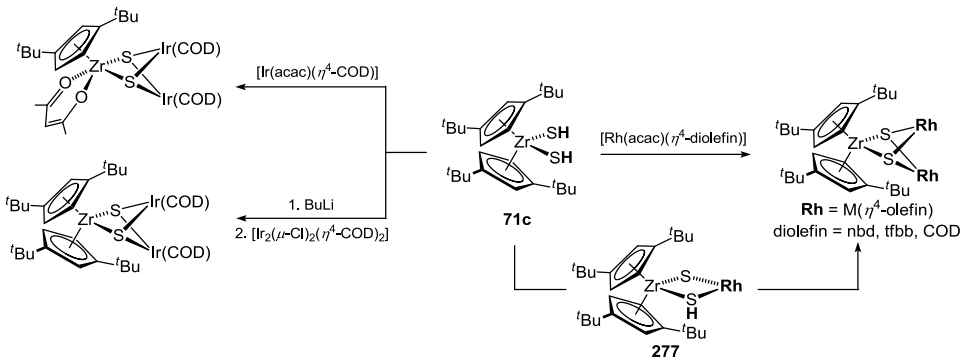


Hidai has also employed **70a** for the preparation of heterobimetallic clusters. Compound **70a** was found to react with the tetraruthenium species, $[Cp^*_4Ru_4(\mu_3\text{-}Cl)_4]$, to give **278** (Scheme 96)[382] The S-H groups of **278** were detected spectroscopically by both IR and $^1H$ NMR and crystallographic analysis of the compound evinced a *syn* disposition for the H atoms of the sulfhydryls. Further treatment of **278** with $Et_3N$ generated the cuboidal cluster $[(CpTi)_2\text{-}(\mu_3\text{-}S)_4\text{-}(RuCp^*)_2]$. Follow-up studies by Hidai on cluster on this cuboidal cluster demonstrated facile oxidation by ferrocenium and HCl to give $[(CpTi)_2\text{-}(\mu_3\text{-}S)_4\text{-}(RuCp^*)_2]^{2+}$ and $[(CpTi)(CpTiCl_2)\text{-}(\mu_3\text{-}S)_4\text{-}(RuCp^*)_2]$, respectively, as well as Cp elimination from the latter to yield $[(CpTi)(TiCl_3)\text{-}(\mu_3\text{-}S)_4\text{-}(RuCp^*)_2]$ (Scheme 96).[383]

Compound **278** has also been demonstrated to serve as a starting point for trimetallic clusters containing $TiRu_2$ and TiRuM motifs.[384] Hidai and co-workers reported the reaction of **278** with $Et_3N$ in the presence of $[RuCl_2(PPh_3)_3]$ to generate $[CpTi\text{-}(\mu_3\text{-}S)_2\text{-}(\mu\text{-}Cl)\text{-}Ru(PPh_3)_2\text{-}(\mu\text{-}Cl)\text{-}RuCp^*$. The synthesis of this trimetallic cluster resembles that of $[(CpTi)_2\text{-}(\mu_3\text{-}S)_4\text{-}(RuCp^*)_2]$ but is thought to involve capture of an unsaturated intermediate cluster by $[RuCl_2(PPh_3)_3]$. A similar strategy involving $[M_2(\mu\text{-}Cl)_2(\eta^4\text{-}COD)_2]$ (M = Rh, Ir) and $[M(PPh_3)_4]$ was therefore utilized to prepare clusters as shown in Scheme 96.

More recently, Bhattacharya has reported the synthesis of a tin hydrosulfide cluster through reaction of **70a** with *n*-BuSnCl(OH)$_2$.[385] Two products were isolated form the reaction, **279** and **280**, each an anion featuring a $[Cp_6Ti_6O_8]^{2+}$ counterion. Crystallographic analysis of the clusters demonstrated similar compositions differing in the ratio of S to Cl.

**Scheme 96.** Cluster syntheses stemming from $[Cp_2Ti(SH)_2]$.

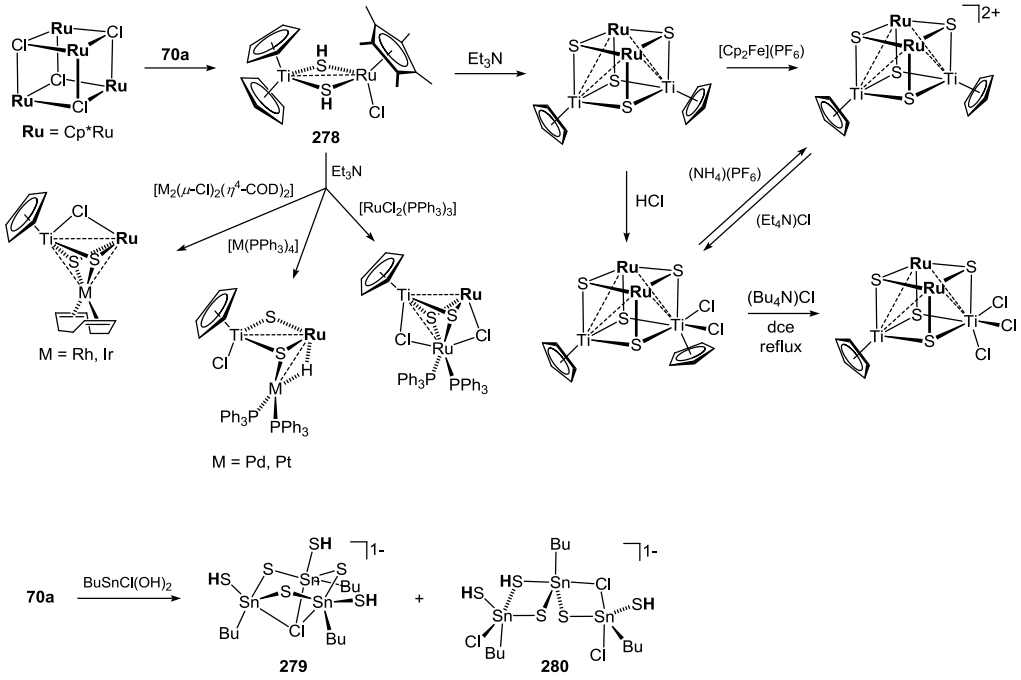


Although not prepared directly from **70a**, additional examples of hydrosulfide clusters incorporating a Group 4 metallocene motif include compounds **281** and **282** reported by Roesky (Scheme 97).[386] These species were synthesized by treatment of the sulfide-bridged compounds, $[(^{Ar}nacnac)Al(\mu\text{-}S)_2MCp_2]$ (M = Ti, Zr), with water. Both compounds were characterized crystallographically, and in the case of **282**, a small quantity of the bishydrosulfide (**283**) was

modeled into the final refinement. Such a species is the presumed intermediate preceding formation of **282**.

**Scheme 97.** Aluminum-containing hydrosulfide complexes.

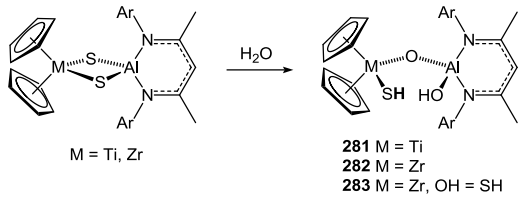


Beyond $[Cp_2Ti(SH)_2]$ and its derivatives, metallocene hydrosulfides of other metals have been applied to the synthesis of cluster compounds. Hidai and co-workers demonstrated that Green's Group 6 metallocenes, $[Cp_2Mo(SH)_2]$ (**131a**) and $[Cp_2W(SH)_2]$ (**132a)**, could be used to prepare bimetallic complexes containing Group 9 metals (Scheme 98).[387] Reaction of either **131a** or **132a** with $[Ir(H)_2(PPh_3)_2(acetone)_2]^+$ under an atmosphere of $H_2$ was found to generate compounds **284** and **285**. Both species demonstrated spectroscopic features consistent with the presence of bridging hydrosulfide ligands, although crystallographic analysis of **284** did not locate the sulfur-bound H atoms precluding its assignment as a *syn* or *anti* isomer. Analogous reactions of **131a** and **131b** with the Rh dihydride, $[Rh(H)_2(PPh_3)_2(acetone)(EtOH)]^+$, resulted in two different bimetallic species. In the case of **131a**, the bridging hydrosulfide compound **186** was produced. The solid-state structure of **286** demonstrated a *syn* disposition for the sulfhydryl groups, which appeared as a singlet resonance by $^1H$ NMR. In contrast to **131a**, reaction of the rhodium dihydride with **132a** afforded the sulfide-bridged complex, $[Cp_2W\text{-}(\mu_2\text{-}S)_2\text{-}Rh(PPh_3)_2]^+$. Exposure of this sulfide-bridge species to 10 atm of $H_2$ produced small quantities of the tungsten congener of **286** as judged by NMR spectroscopy, although the compound was not isolated. Compounds similar to $[Cp_2W\text{-}(\mu_2\text{-}$

S)$_2$-Rh(PPh$_3$)$_2$]$^+$were also detected when **131a** and **132a** were allowed to react with the Rh and Ir dihydrides in the absence of added hydrogen. All four bimetallic complexes, **284-286** and [Cp$_2$W-($\mu_2$-S)$_2$-Rh(PPh$_3$)$_2$]$^+$, were found to be active catalysts for the hydrogenation of alkynes.

**Scheme 98.** Chemistry of Cp$_2$Mo/W(SH)$_2$ species.

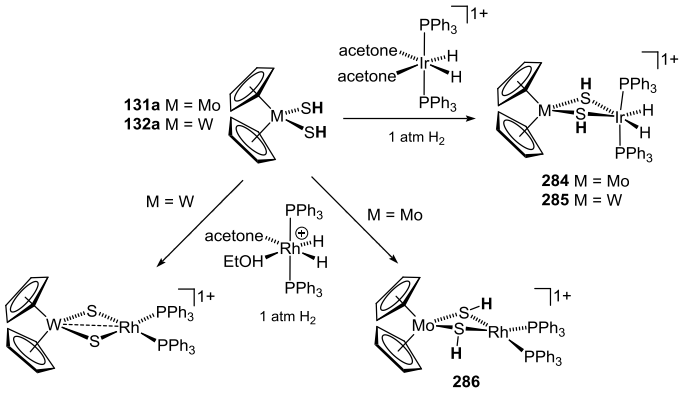


Prior to the work by Hidai with **131a** and **132a**, Curtis and coworkers isolated the unusual cluster species, **287**, which also features a CpMo unit. Compound **287** was obtained in small quantities from the mixture of species produced in the reaction of thiophene with the tetranuclear cluster, [Cp$^{Me}_2$Mo$_2$Fe$_2$S$_2$(CO)$_8$], at 150 ºC. Evidence for the composition of **287** was provided by X-ray crystallography although no $\nu_{SH}$ was detected by IR spectroscopy (Chart 4).

**Chart 4.** A Mo/Fe hydrosulfide cluster

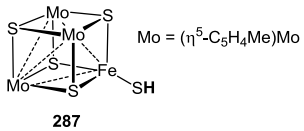

Much like **131a**, a number of homobimetallic hydrosulfides undergo transformations resulting in new cluster compounds. As already noted, thermolysis of $[Cp^*_2Ru_2(\mu\text{-}SH)_2Cl_2]$ (**154**) produces the cuboidal cluster, $[Cp^*_4Ru_4(\mu_3\text{-}S)_4]^{2+}$ (Scheme 59). If instead **154** is treated with $[RhCl(PPh_3)_3]$, the trimetallic cluster, $[\{(Cp^*Ru)_2(\mu\text{-}H)\}\text{-}(\mu_3\text{-}S)_2\text{-}RuCl_2(PPh_3)]$, is obtained.[299] In subsequent work, Hidai also showed that **154** reacts with main group chlorides, $MCl_3$ (M = Sb, Bi), to afford tetrametallic cubanes tetrametallic cubanes displayed in Scheme 99.[388] By employing an analog of **154** containing the ethyltetramethylcyclopentadineyl ligand ($Cp^{Et,Me}$), Hidai later demonstrated that stepwise addition of $MCl_3$ was possible permitting isolation of the hydrosulfide clusters, **288** and **289**.[389] Both an IR and $^1H$ NMR signature was identified for the hydrosulfide groups of **288** and **289**. In the case of NMR, this resonance was found downfield of 5 ppm. Further elaboration of **288** with $[Pd(PPh_3)_4]$ produced a mixture of species containing $Ru_2SbPd$ and $Ru_2SbPd_2$ cores.

**Scheme 99.** Synthesis of hydrosulfide clusters employing $[Cp^*_2Ru_2(\mu\text{-}SH)_2Cl_2]$.

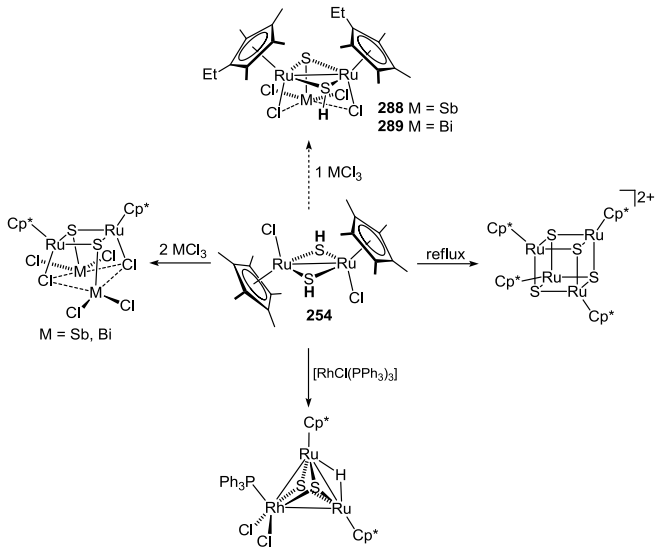


Compounds $[Cp^*_2M_2(\mu\text{-}SH)_2Cl_2]$ (M = Rh, Ir) take part in reactions very similar to those of **154**. Indeed, both species are observed to give to rise to cuboidal clusters and heterometallic

species as shown in Scheme 61. The trishydrosulfide species, **166**, can be engaged similarly in the preparation of homo- and heterometallic clusters, after treatment with excess hydrosulfide (Scheme 100).[390] Compound **166** was found to react with $(Et_4N)(SH)$ to generate the diiridium tetrahydrosulfide **290**. Thermolysis of **290** in solution produced the trimetallic cluster **291**, which underwent further decomposition to give $[Cp^*_4Ir_4(\mu_3\text{-}S)_4]$. The crystal structure of **291** demonstrated interesting aggregation behavior in the solid state stemming from intermolecular S-H-S hydrogen bonding. Both *syn* and *anti* isomers of **291** were noted in solution giving rise to $^1H$ NMR resonances between −1.40 and +0.42 ppm. Subsequent reactions of **291** with $[Cp^*_2Ir_2(\mu\text{-}H)_2Cl_2]$ and $[Pd(PPh_3)_4]$ generated the new cluster compounds **293** and **292**, respectively. Compound **293**, which could also be prepared by treating **166** with $Et_3N$, was the subject of a follow up study by Mizobe and coworkers.[391] The compound was shown to undergo reaction with antimony and bismuth chlorides to produce heterometallic sulfide clusters. Treatment of **293** with $[Pd(PPh_3)_4]$, however, led to formation of **294**, which retained a hydrosulfide ligand.

**Scheme 100.** Synthesis of Ir cluster species from hydrosulfide precursors.

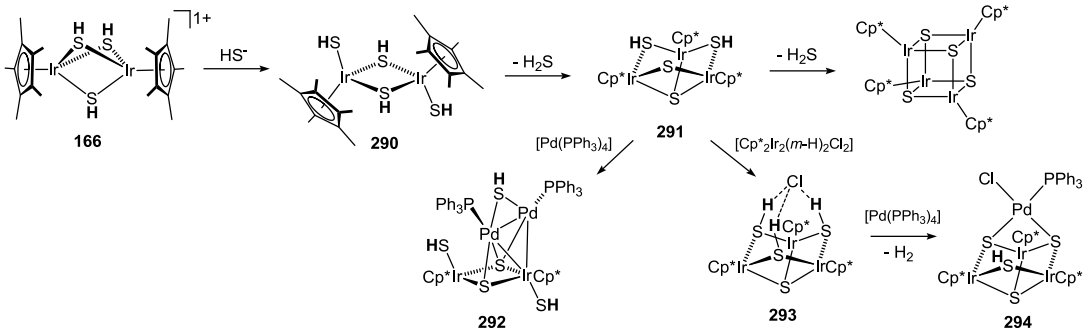


Monometallic hydrosulfides of Rh and Ir have also proved valuable as starting materials in cluster synthesis. Beginning from Rh and Ir complexes $Cp^*M(PMe)(SH)_2$ (M = Rh, **295**; Ir, **157a**),

Hidai and Ishii reported a variety of heterometallic clusters featuring Ti, V, Mo, W and Rh.[392-394] Of these compounds, only the clusters **296** and **297,** generated from reactions with [$Mo(CO)_4$(nbd)], were found to retain hydrosulfide ligands (Scheme 101). Crystallographic characterization of **297** demonstrated a *syn* orientation of the sulfhydryl groups and no fluxional behavior was noted for either cluster in solution.

**Scheme 101.** Synthesis of heterometallic hydrosulfide clusters of Rh, Ir, and Mo.

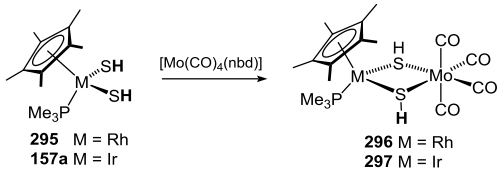


**295** M = Rh
**157a** M = Ir

**296** M = Rh
**297** M = Ir

Two additional examples of metallocene type clusters bearing hydrosulfide ligands are compounds **298** and **299**. The first of these, **298**, was reported by Angelici in the context of studies on iridathiabenzene (Scheme 102).[395] Reduction of an iridathiabenzene moiety by superhydride resulted in ring contraction and formation of **298**. The fidelity of the hydrosulfide ligand was confirmed by both X-ray crystallography and $^1$H NMR spectroscopy. The second cluster, **299**, was prepared by Tatsumi by protonation of a bimetallic sulfide-bridged RuGe complex.[396] Although no crystal structure was obtained for either **299a** or **299b**, vibrational (IR and Raman) and NMR data supported the presence of a sulfhydryl. In the case of the latter, the resonance at -0.33 ppm assigned to the SH ligand was observed to disappear upon treatment with $D_2O$.

**Scheme 102.** Metallocene-based hydrosulfide complexes.

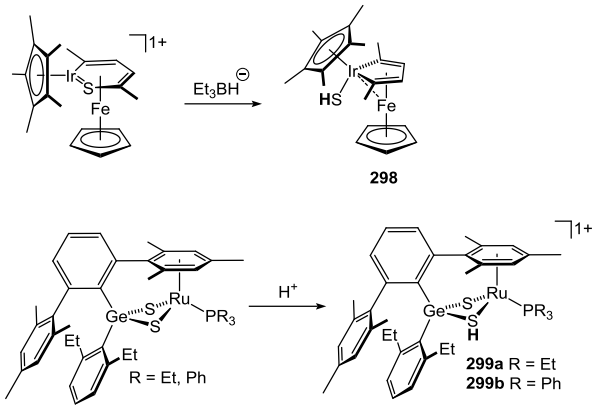


*3.5.2 Metal carbonyl clusters.* Carbonyl ligands feature prominently in the chemistry of *d*-block clusters, so it is therefore unsurprising that they are also found in the context of metal hydrosulfides as well. Numerous examples of cluster compounds containing carbonyl groups, especially of the Group 6 and 8 metals, have been described in earlier parts of this review. Not yet mentioned are clusters $[Mn_2(\mu\text{-H})(\mu\text{-SH})(CO)_6(\mu\text{-P\^P})]$ (P^P = dppm, **300a**; tedip, **300b**), which were prepared by Garcia Alonso and coworkers from the reaction of $[Mn_2(\mu\text{-H})_2(CO)_6(\mu\text{-P\^P})]$ (P^P = dppm, tedip) with elemental sulfur (Scheme 103).[397] Both compounds were found to exist as a mixture of *syn* and *anti* isomers in solution corresponding to the orientation of the SH group with respect to the bridging phosphine. Deprotonation of **300a** with thallium(I) acetate and treatment with $[AuCl(PPh_3)]$ also afforded the trimetallic cluster **301**.

**Scheme 103.** Generation of Mn carbonyl clusters with bridging hydrosulfide ligands.

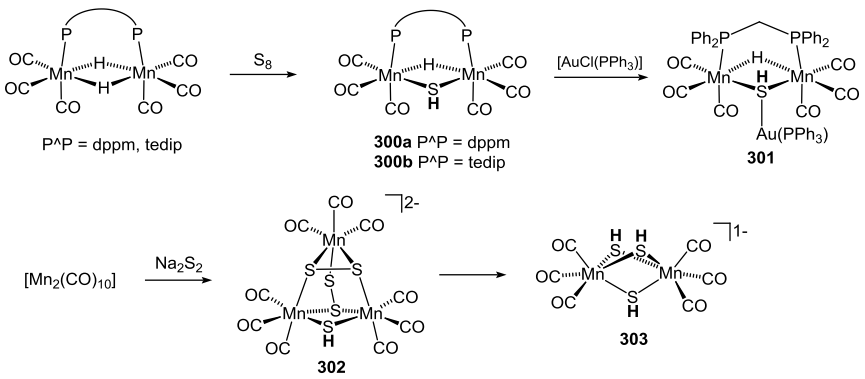


Cluster **301** is reminiscent of the bishydrosulfide species, **192**, originally synthesized by Vahrenkamp (*vide supra*). In this same vein, Huang reported the trishydrosulfide **303** from the reaction of $[Mn_2(CO)_{10}]$ and $Na_2S_2$.[398] Compound **303** was actually the secondary product obtained from the reaction, the initial being the trimanganese cluster, **302**. Both **302** and **303** were characterized crystallographically, but only in the case of **303** were peaks attributable to $\nu_{SH}$ modes detected.

In another example from Group 7 chemistry, Hursthouse described the pentarhenium cluster **304** (Chart 5).[399] Compound **304** was generated by the photochemical reaction of $[Re_2(CO)_{10}]$ with tetramethylthiourea and isolated in modest yield. Also produced in this reaction was the analogous cluster containing hydroxide in place of hydrosulfide. No IR stretch was reported for the hydrosulfide ligand of **304**, but a singlet resonance was observed at 1.85 ppm by NMR spectroscopy. Crystallographic analysis revealed a slightly asymmetry in the Re-S bond lengths involving the bridging hydrosulfide.

Contemporary with the report of **304**, Shapley communicated the synthesis of the heptarhenate cluster **305** (Chart 5).[400] This species was prepared by the action of $H_2S$ on solutions of the analogous carbidoheptarhenate cluster containing a capping Hg-OH group. The bicapped octahedral structure of **305** was found to be similar to that of other $Re_7C(CO)_{21}ML_n$ clusters,

although it represented the first instance of a crystallographically characterized terminal hydrosulfide of mercury.

**Chart 5.**

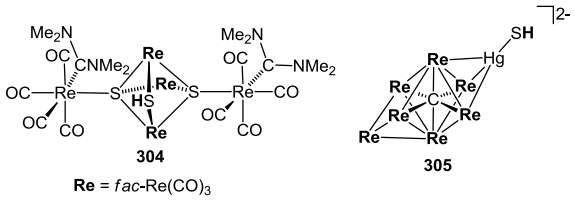


Miguel and coworkers produced a series of homobimetallic and heterobimetallic $M_2$ clusters (M = Mn, Re) containing hydrosulfide by the reductive cleavage of the phosphinoxanthate ligand of $[M_2(CO)_6(\mu\text{-}S_2CPR_3)]$ (R = Cy, $^i$Pr) (Scheme 104).[401, 402] The initial product of reduction in the case of the heterobimetallic system, **306**, was found to be unstable, isomerizing to **309**. Ligand substitution for ammonia in **307-309** led to modified clusters containing phosphine or isocyanide (**310-312**). Intermediate **306** could also be stabilized by similar substitution of the $NH_3$ ligand for the stronger phosphine and isocyanide donors (**313a,b**). $^1$H NMR spectra of all compounds displayed a resonance for the SH group upfield of zero and in those compounds characterized crystallographically, the sulfhydryl was found in a *syn* orientation with respect to the $S_2CHPR_3$ ligand.

**Scheme 104.** Synthesis of Group 7 carbonyl hydrosulfide clusters derived from a phosphinoxanthate ligand.

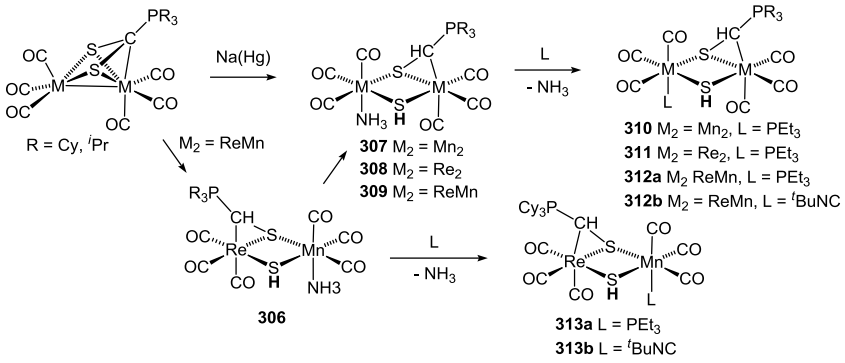


Three additional examples of metal carbonyl clusters containing hydrosulfide ligands involve metals of Group 8. Cockerton and Deeming isolated the hexaruthenium cluster, **314**, in low yield from the thermolysis of $[Ru_3(\mu\text{-H})(\mu_3\text{-pyS})(CO)_9]$ (pyS = pyridine-2-thione) under CO (Chart 6).[403] Crystallography provided the means of identifying **314** although no resonance for the SH group was detected by $^1$H NMR spectroscopy. In related work with a triosmium cluster, Wong described the synthesis of **315a** and **315b** from the reaction of $[Os_3(CO)_{10}(MeCN)_2]$ with 4,6-dimethylpyrimidine-2-thione and bis(4.6-dimethylpyrimidin-2-yl)disulfide, respectively (Chart 6.[404, 405] Both syntheses were accompanied by the formation of other osmium clusters. The solid-state structures of **315a** and **315b** were found to be similar and both compounds were reported to exhibit a $^1$H NMR resonance for the SH group at 2.25 ppm. More recently, Rosales-Hoz and coworkers have prepared **315a** from the reaction of $[Os_3(\mu\text{-H})_2(CO)_{10}]$ with 1,3,5-trithiane.[406]

**Chart 6.**

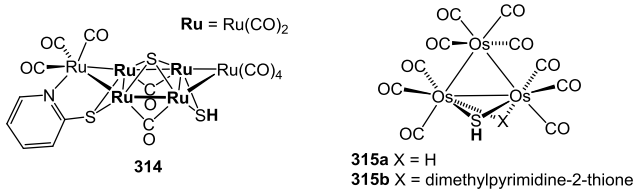

*3.5.3 Metal phosphine clusters.* Much like CO, phosphines are common supporting ligands in metal clusters and several instances of $PR_3$ coordination to multimetallic species containing hydrosulfide ligands have already received attention in this review, primarily in the context of $H_2$ chemistry. The trinickel cluster, **316**, was reported by Ghilardi and coworkers by bubbling of $H_2S$ through a solution of $[Ni(C_2H_4)(PPh_3)_2]$ in the presence of $PEt_3$ (Scheme 105).[407] The cluster was crystallized as its $BPh_4$ salt and subjected to crystallographic analysis. In addition, $^1H$ NMR spectroscopy of **317** demonstrated a doublet resonance for the hydrosulfide group at −1.85 ppm, consistent with a terminal SH bound to a Ni center bearing only one phosphine. Ghilardi and coworkers subsequently reported a related trimetallic cluster of cobalt, **317**, from the reaction of hydrated cobalt(II), $PHEt_2$, and $H_2S$ (Scheme 105).[408] $^1H$ NMR spectroscopy again identified a resonance upfield of 0 ppm for the sulfhydryls, this time as a multiplet consistent with the bridging nature of the SH ligands established by X-ray crystallography.

**Scheme 105.** Synthesis of homotrimetallic Ni and Co hydrosulfide clusters.

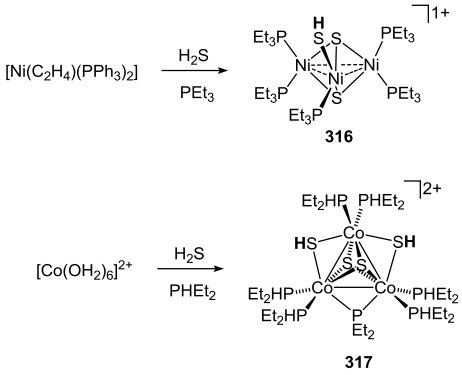


Puddephatt and coworkers obtained NMR evidence for a putative tripalladium cluster, **318**, during reactions of $H_2S$ with $[Pd_3(\mu_3\text{-}CO)(\mu\text{-}dppm)]^{2+}$.[409] Although not structurally characterized, **318** did display a $^1H$ NMR resonance at −2.6 ppm, consistent with a hydrosulfide ligand. Later

work by Chen described two closely related $M_3(\mu\text{-P}\wedge\text{P})_3$ motifs in cations **319** and **320**, both of which contain a pair of capping hydrosulfide groups (Chart 7).[410, 411] Compound **320** was prepared from $[Cu_2(\mu\text{-}Ph_2PNHPPh_2)(MeCN)_2](PF_6)_2$ and the sodium salt of mercaptoacetic acid. Evidence for the composition of **319** and **320** came primarily from X-ray crystallography, as no NMR or IR data was reported for the SH ligands. Superficial similarities between **318**, **319**, and **320** suggest that the former may in fact contain a triply-bridging hydrosulfide ligand. However, the multiplicity of the resonance at −2.6 ppm in **318** corresponding to the sulfhydryl was observed to be a triplet, inconsistent with a symmetrically capping SH ligand. More recently, Zhao has communicated the structure of the tetracopper cluster **321**, which features both triply- and doubly-bridging SH groups.[412] The synthesis of **321** was carried out in similar fashion to that of **320** but with $Li_2S$ as the sulfur source. Chen and co-workers have also described a pair of heterometallic clusters featuring the $M_3(P\wedge P)_3$ unit (**322** and **323**).[413] Both **322** and **323** were isolated as minor species from the reaction of [Pt(bpy)(tdt)] and $[M_2(\mu\text{-dppm})_2(MeCN)_2]^{2+}$ (M = Cu, Ag). Each compound was characterized crystallographically and was further shown to display intense emission in the solid state and in frozen glass at 77 K.

**Chart 7.**

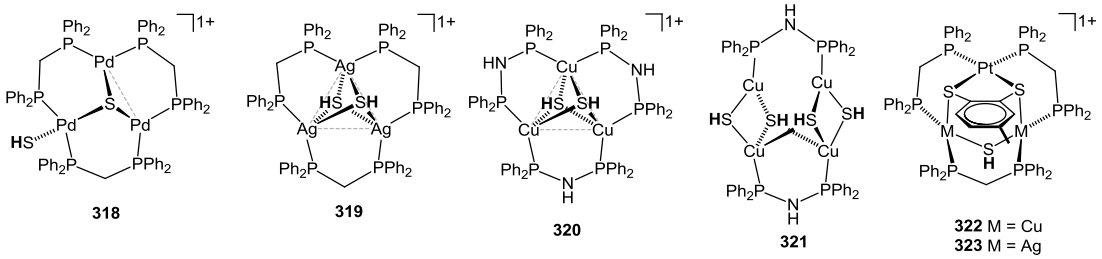

Trimetallic clusters of hydrosulfide have also been accessed by simple salt metathesis reactions of halide species. Llusar and Feliz recently disclosed the synthesis of **324**, a relative of cluster **77**, by reaction of $[Mo_3S_4(dmpe)_3Cl_3]^+$ with NaSH (Scheme 106).[414] The gas phase interaction of **324** with ethanol was examined by mass spectrometry, but no intrinsic reactivity was observed. In prior work, Hidai utilized a similar salt metathesis approach to prepare the heterotrimetallic $RhMo_2$ cluster **325** from the corresponding chloride precursor.[415]

**Scheme 106.** Synthesis of trimetallic Mo and Mo/Rh hydrosulfide clusters.

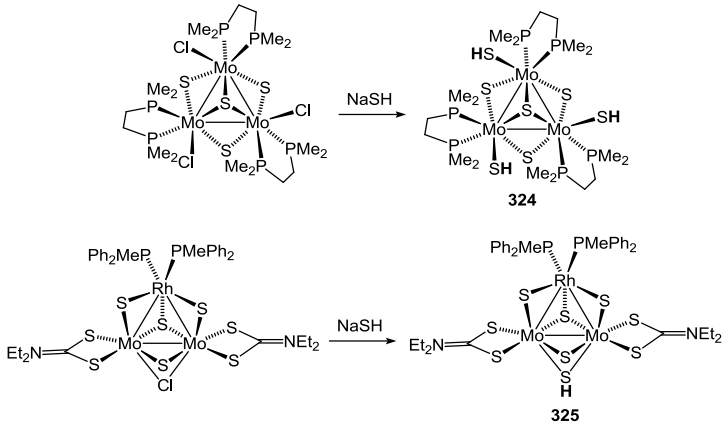


As seen with earlier examples of metallocene *bis*-hydrosulfides, such well-defined species are effective building blocks for more complex cluster compounds. Hidai and Mizobe demonstrated reactions of **58b** and **59b** with Rh and Ir dihydride complexes under an $H_2$ atmosphere to generate clusters **326-329** (Scheme 107).[416] The preference of Ir(III) and Rh(I) in these clusters is identical to that observed previously with compounds built from Mo-based components. Crystallographic analysis of **326-329** failed to locate the H atoms bound to sulfur, but NMR spectra of each compound demonstrated a single multiplet resonance for the hydrosulfide ligands upfield of 0 ppm.

**Scheme 107.** Synthesis of heterobimetallic bridging hydrosulfides.

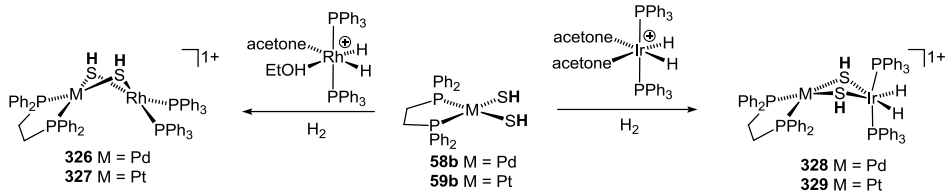


In more recent work, Mizobe has reported the preparation of the Mo(II) bishydrosulfide, **330**, and examined its use for the production of trimetallic clusters (Scheme 108).[417] The synthesis of **330** was accomplished by formal oxidative addition of $H_2S$ to a Mo(0) precursor in very similar fashion to that described for **173** (*vide supra*). Compound **330** was found to display rare trigonal prismatic geometry in the solid state, and unlike many hydrosulfide compounds of Mo, the SH groups of **330** appeared upfield of 0 ppm by $^1$H NMR spectroscopy. Reactions of **330** with [$M_2(\mu$-$Cl)_2(CO)_4$] (M = Rh, Ir) afforded the corresponding $MoM_2$. The Rh analog was isolated in two isomeric forms, both of which were identified by X-ray crystallography. Rapid interconversion of the isomeric forms was found in solution, but resonances for each isomer could be detected at low temperature by $^{31}$P NMR spectroscopy. In both the Rh and Ir clusters, the trigonal prismatic geometry about Mo(II) was maintained.

**Scheme 108**. Synthesis of heterobimetallic Mo and Rh/Ir clusters.

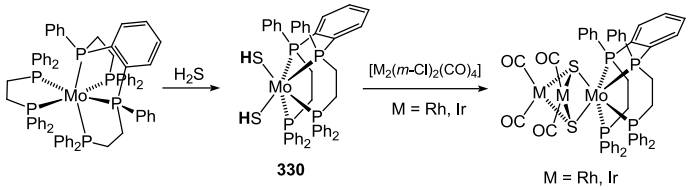

Several additional examples of phosphine-bound metal clusters containing hydrosulfide are known (Chart 8). Fenske and Wirth reported the isolation of **331**, which features six palladium atoms and two hydrosulfide bridges.[418] This cluster was constructed from the reaction of $[Pd(acac)_2]$ and $PPh_3$ in ethanol employing $(S)P(SSiMe_3)_3$ as a sulfur source. The simpler dicopper hydrosulfide, **332**, was reported by Ahmad and coworkers through the treatment of CuCl with $PPh_3$ using mercaptopropanoic acid as the sulfur source.[419] Both **331** and **332** were primarily characterized crystallographically, and no spectroscopic signatures for the hydrosulfide ligands were reported.

**Chart 8.**

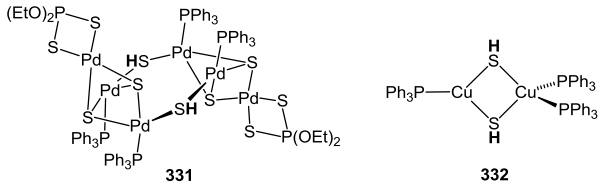


*3.5.4 Other cluster compounds.* Ligands other than Cp, CO, and $PR_3$, have been used to support metal clusters bearing hydrosulfide groups, although examples are less numerous. Nonetheless, these species warrant mention since they add to the rich diversity of hydrosulfide clusters. One of the earliest reports of a metal hydrosulfide cluster was put forward by Morgan and coworkers in 1970.[420] They described the synthesis of **333** from the reaction of $H_2S$ with "sulfatobis(trimethylplatinum(IV))" (Chart 9). Detailed solution characterization of **333** was provided including a $^1H$ NMR resonance for the SH group at −3.29 ppm ($^2J_{PtH}$ = 15.2 Hz) and an IR stretch of 2537 $cm^{-1}$. The structure of **333** was assumed by analogy to the hydroxide analog, $[Pt_4(CH_3)_{12}(\mu_3\text{-}OH)_4]$.

**Chart 9.**

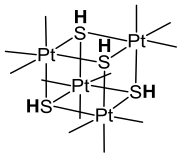


**333**

Sécheresse and coworkers reported the isolation of cluster **334** through acidification of $[WS_4]^{2-}$ (Chart 10).[421] The origin of the oxo ligand in **334** was not explained although the synthesis was conducted aerobically without exclusion of water. The crystal structure of **334** was obtained and the H atoms were assigned to the terminal sulfide groups based on unreported NMR evidence. However, definitive assignment of the H atoms as belonging to terminal hydrosulfides was probably not possible based on the available data. Subsequent work by Sécheresse described the synthesis of the related cluster, $[W_2(S)_2(SH)(S_2)(\mu\text{-}S_2)]^-$ (**335**), through a very similar acidification process of tetrathiotungstate (Chart 9).[422] As with **334**, no diagnostic spectral features were detected for the SH group and crystallography was unable to determine the precise location of the lone H atom.

**Chart 10**.

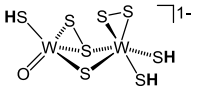


**334**

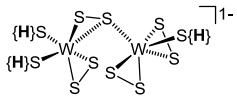


**335**

Working with Mo, Wentworth and Huffman prepared the bimetallic cluster, **336**, by addition of trifluoroacetic acid to the cubane precursor, $[Mo_4(\mu_3\text{-}S)_4(NC_6H_4CH_3)_4(S_2P\{OEt\}_2]$ (Scheme

109).[423] Similar reaction of the cubane with acetic acid did not lead to an analogous cluster demonstrating that the SH group of **336** is somewhat acidic. Crystallographic analysis of **336** demonstrated an *anti* disposition of the sulfhydryl group relative to the imido ligands, which was supported by low temperature NMR spectroscopy, where a 9:1 mixture of isomers was observed.

**Scheme 109.** Synthesis of a bimetallic Mo cluster with bridging hydrosulfide ligand.

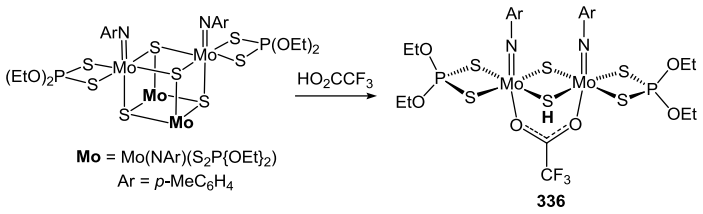


The strategy of protonation of a sulfur vertex was also utilized by Holm to prepare compounds **337a-c** from the corresponding $[Re_6S_8X_6]^{4-}$ (X = Cl, Br, I) clusters (Chart 11).[424] Each compound was characterized crystallographically confirming the addition of a single proton. The *p*Ka of the bromide derivative, **337b**, was estimated to be ca. 20 in acetonitrile making it significantly less acidic than **336**.

**Chart 11.**

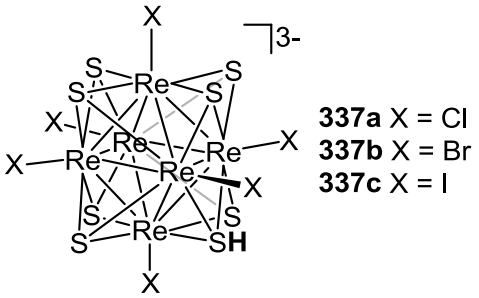

A final example of a hydrosulfide cluster is **338** reported by Jin.[425] This species features a carborane-derived thiolate ligand and was isolated from the 1:1 reaction of the carborane precursor and $[Rh_2(\mu\text{-}Cl)_2(COD)_2]$ (Scheme 110). Notably, this compound is formed by complete extrusion of the Cp*Ir fragment from carborane precursor, which was not observed when the reaction was carried out at different molar ratios of the starting materials. Crystallographic analysis of **338** confirmed its composition but could not delineate the relative orientation of the hydrosulfide ligand with respect to the thiolate. Solution $^1$H NMR characterization of **338** identified a resonance at 0.86 ppm for the hydrosulfide ligand.

**Scheme 110**. Synthesis of Rh hydrosulfide cluster containing a carborane-appended thiolate.

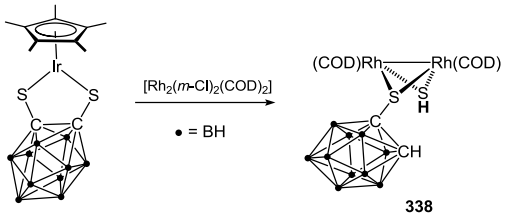


*3.5.5 Coordination polymers and MOFs*. The last class of compounds that will be treated in this review belong to the subset of materials referred to as coordination polymers and metal organic frameworks. Interest in such compounds has exploded over the last two decades, but representative examples containing hydrosulfide ligands remain scarce. One of the first reports of such a species was the cadmium coordination polymer **339** (Chart 12). This species was prepared by Tian and coworkers through a self-assembly process beginning from $CdCl_2$, succinic acid, and thiosemicarbazide.[426] The polymer demonstrated nonlinear optical properties in the form of a strong second harmonic generation response.

**Chart 12.**

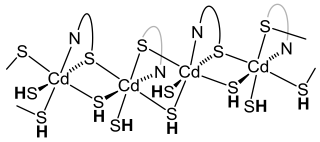

339

Zamora and coworkers also reported a 1D coordination polymer (**340**) built from metal hydrosulfide units.[427] In this case, the monomeric unit consisted of a monocationic cage of nine Cu(I) centers bridged by pyridine-2-thione ligands, in which eight of the metal centers contain a terminal hydrosulfide group (Chart 13). The polymer was prepared by S-S and C-S cleavage of 2,2'-dipyridyldisulfide by Cu(II) under solvothermal microwave heating. X-ray photoelectron spectroscopy of **340** confirmed the monovalent state of each copper center and magnetic measurements were further consistent with a diamagnetic substance. Room temperature measurements on **340** evinced a high electrical conductivity of $1.6 \times 10^{-3}$ $S \cdot cm^{-1}$ placing the polymer among a small group of such materials that display conductivity in the solid state.

**Chart 13.**

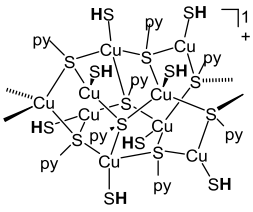

340

py = 2-pyridyl

In addition to 1D coordination polymers, cadmium hydrosulfide species have also found use in the construction of metal organic frameworks (MOFs). Feng described a three-dimensional

MOF framework possessing a four-connected node based on a $N_4Cd(SH)_2$ unit, where the $N_4$ ligation arises form *meso*-4-pyridylporophyrins.[428] Han reported two related MOF structures containing a $N_4Cd(SH)_4$ node built from eclipsed and staggered conformations of tetrapyridylbenzene linker (**341a** and **341b**, Figure 8).[429] The $N_4Cd(SH)_2$ motif was also observed in an anionic boron imidazolate MOF synthesized by Bu and coworkers, where N ligation is provided by imidazole units.[430] In the case, however, the sulfhydryl groups adopt a *cis* disposition with respect to one another. In addition to these examples, the $N_4M(SH)_2$ unit has appeared in MOFs reported by Du, where the metal can be Cd, Mn, Fe, or Co.[431] In this case, use of the *tetrakis*(4-pyridyloxymethylene)methane linker permitted the isolation of a variety of such MOFs which displayed a PtS topology.

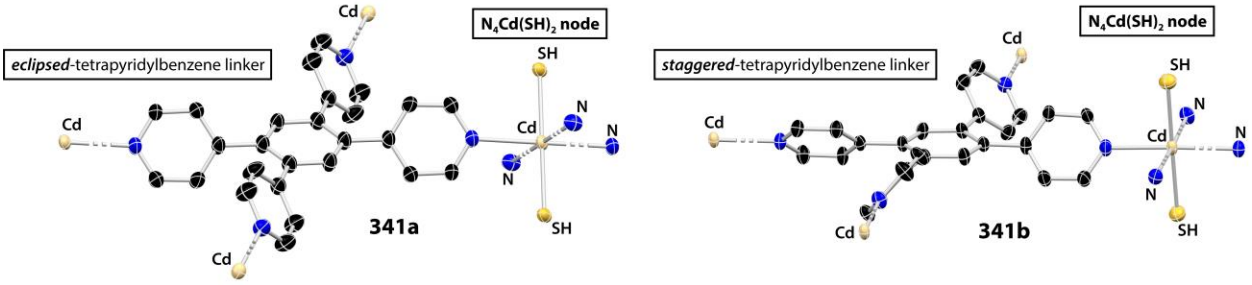


**Figure 8.** Solid-state structures of the $N_4Cd(SH)_2$ nodes in MOFs **341a** and **341b** showing the eclipsed and staggered conformations of the tetraphydridylbenzene unit.

Outside of the $N_4M(SH)_2$ motif, frameworks containing more complex nodes have also been reported in the form of species **342** and **343** (Figure 9).[432, 433] In the case of **342**, the framework is built from a fourteen-connected node composed of $[Cu_{19}I_4(pdt)_{12}(SH)_3]$ units, which give rise to a superoctahedral cluster. The hydrosulfide groups are generated by C-S cleavage of 4-pyridinethiol (pdt) providing an interesting homology to the preparation of copper coordination polymer **340**

from 2,2'-dipyridyldisulfide discussed above. In the case of **343**, the framework is best described as a 2D superlattice comprised of capped-supertetrahedral cadmium clusters of the form $[Cd_{17}(S\text{-}4\text{-tolyl})_{27}(SH)]^{2-}$. The lone hydrosulfide ligand is believed to originate from the co-solvent, carbon disulfide. For both frameworks **342** and **343**, the presence of the suflhydryl group was inferred from X-ray crystallography and charge balance as no IR signature could be identified in either instance.

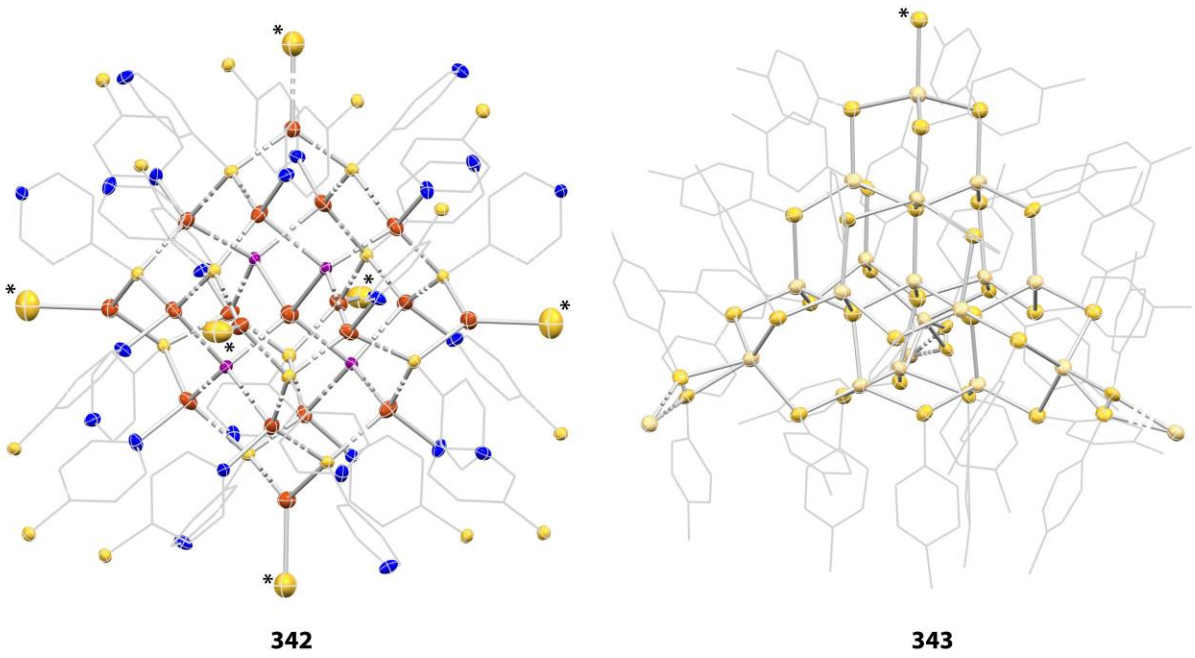


**Figure 9.** Solid-state structures of the cluster nodes comprising frameworks **342** and **343**. Asterisks denote hydrosulfide groups. Carbon atoms are displayed in wireframe. Atom scheme: Cd – beige, Cu – orange, I – purple, N – blue, S – yellow.

## 4. Characterization of Transition Metal Hydrosulfides

One significant challenge in understanding the chemistry of metal hydrosulfide compounds is the inherent difficulty in characterizing the bound hydrosulfide. As discussed for many of the

compounds described in this review, few metal hydrosulfide compounds are characterized by complementary structural and spectroscopic methods. The most robust method of characterization is structural analysis using X-ray crystallography. Such crystallographic methods, however, are not without difficulties. Crystallographic methods prior to the 1990's often were unable to explicitly observe hydrogen atoms due to experimental limitations. In such structures, the presence of hydrogen atoms was often assumed or inferred based on charge balance but may not have been definitively observed in the difference maps. An additional challenge that persists even with more modern diffraction equipment is differentiating -SH from -Cl without complementary spectroscopic evidence to support hydrosulfide formation. Although anomalous dispersion X-ray crystallography experiments can be used to unambiguously identify sulfur from chlorine atoms, such experiments are uncommon for routine structural characterization experiments. To aid researchers in characterizing both terminal and bridging hydrosulfide complexes, we have tabulated the M-S bond distances from structural data described in this review. These data are displayed in Figure 10a and are separated by element and also by bridging/terminal hydrosulfide residues. For certain elements the reported M-S bond distances fit within a fairly narrow range and demonstrate the expected trends in bond length associated with changes in the ionic radii of the metal centers. However, for other elements, in particular Co and Ni, this range can be quite large. This variation, especially for terminal hydrosulfide units, likely reflects the larger uncertainty of experimental M-SH bond distances reported in the literature, which can suffer from both misidentification of the SH group and unassigned partial occupancies. We therefore caution against using these bond distance metrics as *sole* evidence for the formation of M-SH complexes, especially for elements with larger bond distance distributions.

Complementing structural data, IR spectroscopy often provides a useful method to confirm metal hydrosulfide formation through identification of the $\nu_{SH}$ fundamental. One significant limitation of this approach, however, is the apparent infrared inactivity of many, if not most, hydrosulfide complexes. To the best of our knowledge, the origins of this phenomena in metal hydrosulfides have not been investigated in detail, but theoretical studies with simple thiols have demonstrated the overall weaker intensities of S-H oscillators versus C-H and O-H.[434] This factor most likely accounts for part of the difficulty in observing $\nu_{SH}$ modes of bound hydrosulfide. Notwithstanding the sparse nature of this vibrational data, we have assembled SH infrared stretching values for both terminal and bridging metal hydrosulfides from compounds described in this review (Figure 10b). To better clarify the data, SH stretches for compounds in which the S-H unit is well-established to be strongly hydrogen-bonded to nearby acceptors have been omitted. With a few exceptions, the data are clustered about the region 2550 – 2600 $cm^{-1}$, which is as expected given the value for the $\nu_{SH}$ mode in typical thiols (ca. 2700 $cm^{-1}$). Variation within the data, even without accounting for terminal vs. bridging SH coordination, is still less pronounced than that observed for either M-S distances or $^1$H NMR chemical shifts (*vide infra*). Furthermore, the compatibility of IR spectroscopy with paramagnetic compounds ensures that the information in Figure 10b captures a broader swath of known hydrosulfide complexes without an implicit bias towards certain elements, oxidation states, and geometries which favor diamagnetic ground states. Thus, whenever possible, infrared data should be acquired for transition metal hydrosulfide complexes as it provides one of the most unequivocal means of identifying bound SH units.

As a final reference point, we include a comparison of known SH $^1$H NMR resonances arranged by element (Figure 10c). We have excluded most compounds in which the SH proton is significantly shifted (>20 ppm) due to the paramagnetism of the metal center. Unlike the structural

and infrared data discussed above, NMR chemical shifts are subject to a variety of factors that mitigate their usefulness in drawing broad trends. However, two important observations merit discussion. Firstly, diamagnetic complexes containing metals with formally non-zero *d* electron counts are most likely to display chemical shifts for the sulfhydryl H atom upfield of 0 ppm (typically between −1 and −4 ppm). In these instances, the $^{1}$H resonance serves as a reliable diagnostic marker for the bound hydrosulfide ligand. Moreover, the presence of additional H-X coupling can provide added information such as the dynamic motion and relative orientation of the S-H group with respect to other ligands in the complex as discussed for several systems in prior sections of this review. Secondly, for formally $d^0$ complexes the sulfhydryl resonance is more likely to be found downfield of 0 ppm. Such species comprise a smaller subset of hydrosulfide complexes and are mainly relegated to early metal systems in their highest formal oxidation state. Ranges for the sulfhydryl H resonance in these complexes are not as predictable as those for non $d^0$ species and tend to display greater chemical shift dispersion. Taken together, we hope that tabulated metrics in Figure 10 aid researchers in characterizing future metal hydrosulfide complexes, but we again emphasize the importance of obtaining multiple lines of spectroscopic evidence whenever possible.

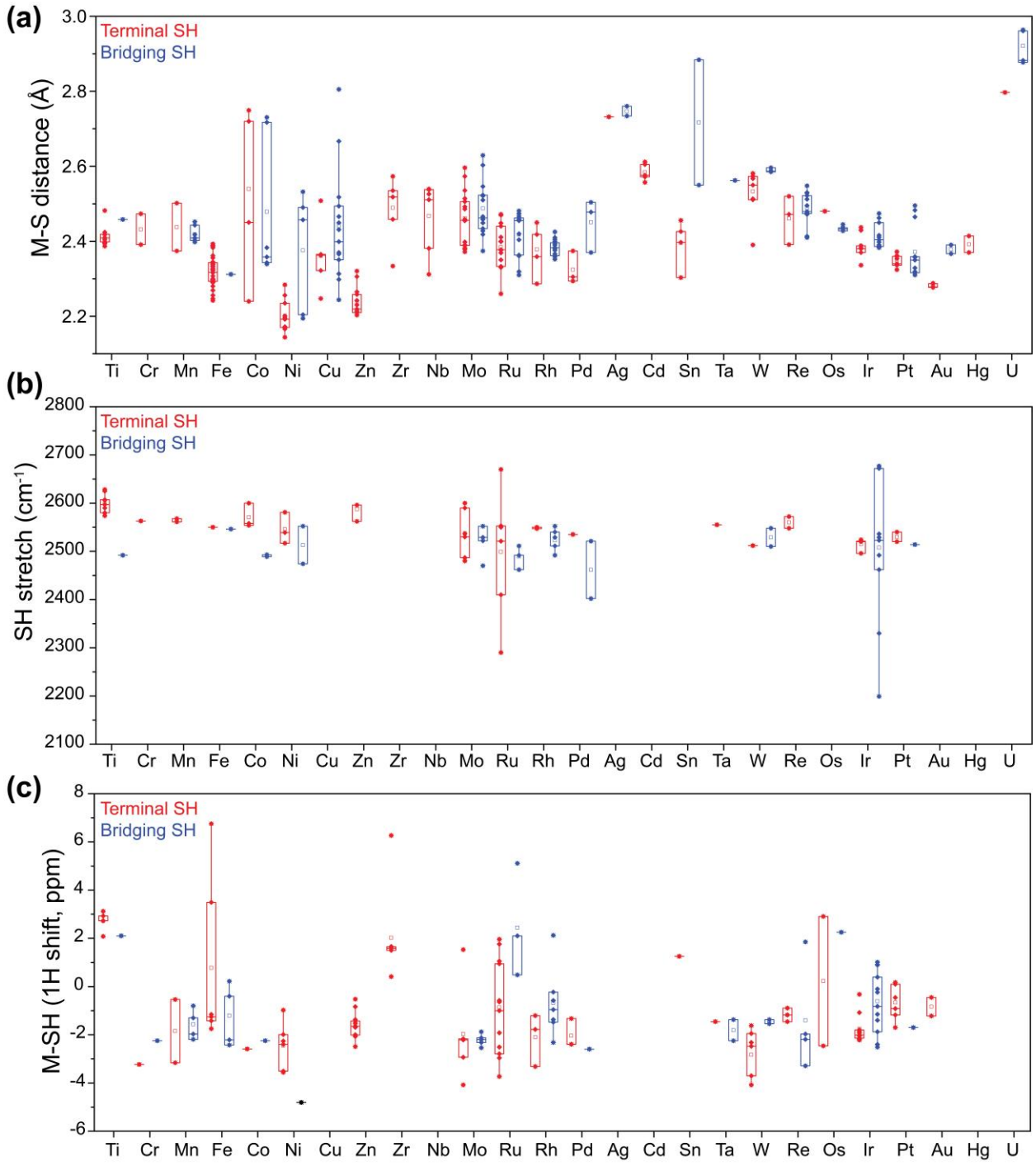


**Figure 10.** (a) Tabulated terminal (red) and bridging (blue) M-SH bond distances for metal hydrosulfides. (b) Tabulated terminal (red) and bridging (blue) M-S-H bond stretches for metal hydrosulfides. (c) Tabulated terminal (red) and bridging (blue) $^{1}$H NMR resonances for metal

hydrosulfides. S-H chemical shifts that are significantly shifted (>20 ppm) due to coordination to paramagnetic metals are excluded for clarity. The box and whisker plots show the individual parameters with solid points. The average is denoted with an open square, and the box corresponds to the middle two quartiles of the pooled data.

## 6. Summary and Outlook

As presented in this Review, molecules containing transition metal hydrosulfide linkages are quite diverse, spanning many elements, coordination environments, and redox states. Through this variety, the hydrosulfide ligand carries out multiple roles across several fields of chemistry. These roles encompass structural motifs and sites of reactivity in compounds ranging from proteins, to small molecule organometallics, to metalloclusters and larger coordination polymers. While early work with metal hydrosulfide complexes focused on simply generating coordination compounds and probing their basic reactivity, more recent chemistry has highlighted the role of these species in biological systems and their potential application in the design of new materials. Despite the disparate nature of these fields and the myriad roles played by the hydrosulfide ion, many aspects of M-SH chemistry remain constant. First and foremost, the hydrosulfide ligand presents unique challenges to both synthesis and characterization not commonly encountered with its lighter congener hydroxide. Therefore, special care must be taken when identifying the presence of M-SH units. Secondly, the inherent redox activity of sulfur renders metal hydrosulfide complexes more amenable to electron-transfer reactions. This facet of M-SH chemistry contributes to the challenges associated with handling these compounds but has also been leveraged to design unique preparative means (e.g. oxidative addition, migratory insertion of $S_8$) and novel functionality relevant to biological identification (sensors). Lastly, it should also be mentioned that

fortuity has played a prominent role in the development of metal hydrosulfide chemistry. Many of the compounds discussed in preceding sections were identified from reactions not designed to create hydrosulfide ligands or even M-S bonds. Nonetheless, these discoveries have helped uncover some of the myriad factors at play in the formation of M-SH units and the corresponding chemistry they are capable of. We anticipate that future research will uncover additional important roles for metal hydrosulfide compounds that bring to bear the unique structural and electronic properties of this class of molecules.

**Biographies**

Michael D. Pluth earned his B.S. in chemistry and applied mathematics from the University of Oregon in 2004 where he conducted undergraduate research with Prof. David Tyler. He earned his PhD in 2008 from UC Berkeley as an NSF predoctoral fellow under the joint direction of Profs. Robert Bergman and Kenneth Raymond in the area of supramolecular chemistry studying proton-catalyzed reactions in supramolecular hosts. Mike then moved to MIT as an NIH NRSA and later NIH Pathway to Independence Postdoctoral Fellow with Prof. Stephen Lippard. Mike began his independent career at the University of Oregon in 2011. His research interests are thematically based on different aspects of molecular recognition and physical organic chemistry, and much of his lab focuses on investigations into reactive sulfur species relevant to biology.

Zachary J. Tonzetich graduated with a B.S. degree in chemistry from the University of Rochester in 2002, where he worked with Prof. Richard Eisenberg on the synthesis of luminescent transition metal complexes. This experience was followed by Ph.D. studies under the tutelage of Prof. Richard Schrock at MIT focused on early metal organometallic chemistry relevant to catalytic transformations of olefins and alkynes. After postdoctoral work with Prof. Stephen

Lippard as an NRSA fellow, Zach began his independent career at UTSA in 2010. His laboratory is broadly interested in synthetic inorganic and organometallic chemistry with an emphasis on catalysis and biomimetic chemistry, especially as it pertains to small sulfur-containing molecules. Zach is also an avid birder and naturalist who enjoys the bountiful species of flora and fauna Texas has to offer.

## Author Information

### Corresponding Author

*pluth@uoregon.edu, zachary.tonzetich@utsa.edu

### Author Contributions

The manuscript was written through contributions of all authors. All authors have given approval to the final version of the manuscript.

‡These authors contributed equally and are listed alphabetically.

### Acknowledgements

The authors thank the Welch Foundation (AX-1772 to ZJT), National Science Foundation (CHE-1454747 to MDP), and Dreyfus Foundation (MDP) for financial support of this work. The authors also thank Dr. Nathanael Lau for assistance with graphical content of protein structures in this manuscript.

## 6. References

1. R. R. Nasaruddin, T. K. Chen, N. Yan and J. P. Xie, *Coord. Chem. Rev.*, 2018, **368**, 60-79.

2. C. Vericat, M. E. Vela, G. Corthey, E. Pensa, E. Cortes, M. H. Fonticelli, F. Ibanez, G. E. Benitez, P. Carro and R. C. Salvarezza, *Rsc Advances*, 2014, **4**, 27730-27754.

3. I. Dance and K. Fisher, *Prog. Inorg. Chem.*, 1994, **41**, 637-803.

4. I. G. Dance, *Polyhedron*, 1986, **5**, 1037-1104.

5. D. W. Stephan and T. T. Nadasdi, *Coord. Chem. Rev.*, 1996, **147**, 147-208.

6. M. R. Filipovic, J. Zivanovic, B. Alvarez and R. Banerjee, *Chem. Rev.*, 2018, **118**, 377-461.

7. H. Kimura, *Antioxid. Redox Signal.*, 2015, **22**, 362-376.

8. G. K. Kolluru, X. G. Shen, S. C. Bir and C. G. Kevil, *Nitric Oxide*, 2013, **35**, 5-20.

9. Q. Li and J. R. Lancaster, *Nitric Oxide*, 2013, **35**, 21-34.

10. K. Ono, T. Akaike, T. Sawa, Y. Kumagai, D. A. Wink, D. J. Tantillo, A. J. Hobbs, P. Nagy, M. Xian, J. Lin and J. M. Fukuto, *Free Radical Biol. Med.*, 2014, **77**, 82-94.

11. R. Wang, *Physiol. Rev.*, 2012, **92**, 791-896.

12. C. Szabo, *Biochem. Pharmacol.*, 2018, **149**, 5-19.

13. S. Kuwata and M. Hidai, *Coord. Chem. Rev.*, 2001, **213**, 211-305.

14. M. Peruzzini, L. Rios Isaac De and A. Romerosa, in *Prog. Inorg. Chem.*, ed. K. D. Karlin, Wiley, 2001, vol. 49, pp. 169-453.

15. A. V. Mishanina, M. Libiad and R. Banerjee, *Nat. Chem. Biol.*, 2015, **11**, 457-464.

16. M. D. Hartle and M. D. Pluth, *Chem. Soc. Rev.*, 2016, **45**, 6108-6117.

17. Y. Ingenbleek, *J. Nutr.*, 2006, **136**, 1641S-1651S.

18. B. Meyer, *Chem. Rev.*, 1976, **76**, 367-388.

19. W. H. Koppenol and P. L. Bounds, *Arch. Biochem. Biophys.*, 2017, **617**, 3-8.

20. K. K. Millis, K. H. Weaver and D. L. Rabenstein, *J. Org. Chem.*, 1993, **58**, 4144-4146.

21. T. N. Das, R. E. Huie, P. Neta and S. Padmaja, *J. Phys. Chem. A*, 1999, **103**, 5221-5226.

22. P. M. May, D. Batka, G. Hefter, E. Konigsberger and D. Rowland, *Chem. Commun.*, 2018, **54**, 1980-1983.

23. M. D. Hartle, D. J. Meininger, L. N. Zakharov, Z. J. Tonzetich and M. D. Pluth, *Dalton Trans.*, 2015, **44**, 19782-19785.

24. A. K. SenGupta, *Ion Exchange in Environmental Processes: Fundamentals, Applications and Sustainable Technology*, John Wiley & Sons, Inc, New Jersey, USA, 2017.

25. K. R. Olson and K. D. Straub, *Physiology*, 2016, **31**, 60-72.

26. G. Wachtershauser, *Microbiol. Rev.*, 1988, **52**, 452-484.

27. G. D. Cody, *Annual Review of Earth and Planetary Sciences*, 2004, **32**, 569-599.

28. M. Cardenas-Rodriguez, A. Chatzi and K. Tokatlidis, *J. Biol. Inorg. Chem.*, 2018, **23**, 509-520.

29. J. J. Braymer and R. Lill, *J. Biol. Chem.*, 2017, **292**, 12754-12763.

30. E. T. Parker, H. J. Cleaves, J. P. Dworkin, D. P. Glavin, M. Callahan, A. Aubrey, A. Lazcano and J. L. Bada, *Proc. Natl. Acad. Sci. USA*, 2011, **108**, 5526-5531.

31. E. T. Parker, H. J. Cleaves, M. P. Callahan, J. P. Dworkin, D. P. Glavin, A. Lazcano and J. L. Bada, *Orig. Life Evol. Biosph.*, 2011, **41**, 201-212.

32. C. Huber and G. Wachtershauser, *Science*, 1998, **281**, 670-672.

33. L. Leman, L. Orgel and M. R. Ghadiri, *Science*, 2004, **306**, 283-286.

34. A. K. Steiger, Y. Zhao and M. D. Pluth, *Antioxid. Redox Signal.*, 2018, **28**, 1516-1532.

35. K. Abe and H. Kimura, *J. Neurosci.*, 1996, **16**, 1066-1071.

36. E. Blackstone, M. Morrison and M. B. Roth, *Science*, 2005, **308**, 518-518.

37. B. Sörbo, *Biochim. Biophys. Acta*, 1958, **27**, 324-329.

38. V. Vitvitsky, P. K. Yadav, A. Kurthen and R. Banerjee, *J. Biol. Chem.*, 2015, **290**, 8310-8320.

39. D. Garai, B. B. Ríos-González, P. G. Furtmüller, J. M. Fukuto, M. Xian, J. López-Garriga, C. Obinger and P. Nagy, *Free Radical Biol. Med.*, 2017, **113**, 551-563.

40. M. M. Cortese-Krott, G. G. C. Kuhnle, A. Dyson, B. O. Fernandez, M. Grman, J. F. DuMond, M. P. Barrow, G. McLeod, H. Nakagawa, K. Ondrias, P. Nagy, S. B. King, J. E. Saavedra, L. K. Keefer, M. Singer, M. Kelm, A. R. Butler and M. Feelisch, *Proceedings of the National Academy of Sciences*, 2015, **112**, E4651-E4660.

41. M. Eberhardt, M. Dux, B. Namer, J. Miljkovic, N. Cordasic, C. Will, T. I. Kichko, J. de la Roche, M. Fischer, S. A. Suárez, D. Bikiel, K. Dorsch, A. Leffler, A. Babes, A. Lampert, J. K. Lennerz, J. Jacobi, M. A. Martí, F. Doctorovich, E. D. Högestätt, P. M. Zygmunt, I. Ivanovic-Burmazovic, K. Messlinger, P. Reeh and M. R. Filipovic, *Nature Communications*, 2014, **5**, 4381.

42. J. L. Miljkovic, I. Kenkel, I. Ivanović-Burmazović and M. R. Filipovic, *Angew. Chem. Int. Ed.*, 2013, **52**, 12061-12064.

43. F. Bouillaud and F. Blachier, *Antioxid. Redox Signal.*, 2011, **15**, 379-391.

44. H. Beinert, *J. Biol. Inorg. Chem.*, 2000, **5**, 2-15.

45. D. C. Johnson, D. R. Dean, A. D. Smith and M. K. Johnson, *Annu. Rev. Biochem*, 2005, **74**, 247-281.

46. R. Lill, *Nature*, 2009, **460**, 831-838.

47. P. V. Rao and R. H. Holm, *Chem. Rev.*, 2004, **104**, 527-559.

48. F. F. de Biani and P. Zanello, *Inorg. Chim. Acta*, 2017, **455**, 319-328.

49. P. Zanello, *Coord. Chem. Rev.*, 2013, **257**, 1777-1805.

50. P. Zanello, *Coord. Chem. Rev.*, 2014, **280**, 54-83.

51. P. Zanello, *Coord. Chem. Rev.*, 2016, **306**, 420-442.

52. P. Zanello, *Coord. Chem. Rev.*, 2017, **335**, 172-227.

53. R. H. Holm and W. Lo, *Chem. Rev.*, 2016, **116**, 13685-13713.

54. B. J. Vaccaro, S. M. Clarkson, J. F. Holden, D. W. Lee, C. H. Wu, F. L. Poole, J. J. H. Cotelesage, M. J. Hackett, S. Mohebbi, J. C. Sun, H. L. Li, M. K. Johnson, G. N. George and M. W. W. Adams, *Nature Communications*, 2017, **8**.

55. A. Muller, N. H. Schladerbeck and H. Bogge, *J. Chem. Soc., Chem. Commun.*, 1987, 35-36.

56. Müller A and N. H. Schladerbeck, *Chimia*, 1985, **39**, 23-24.

57. K. S. Hagen and M. Uddin, *Inorg. Chem.*, 2008, **47**, 11807-11815.

58. H. R. Hoveyda and R. H. Holm, *Inorg. Chem.*, 1997, **36**, 4571-4578.

59. B. M. Segal, H. R. Hoveyda and R. H. Holm, *Inorg. Chem.*, 1998, **37**, 3440-3443.

60. L. S. Cai and R. H. Holm, *J. Am. Chem. Soc.*, 1994, **116**, 7177-7188.

61. T. Terada, T. Wakimoto, T. Nakamura, K. Hirabayashi, K. Tanaka, J. Li, T. Matsumoto and K. Tatsumi, *Chemistry – An Asian Journal*, 2012, **7**, 920-929.

62. J. Sun, C. Tessier and R. H. Holm, *Inorg. Chem.*, 2007, **46**, 2691-2699.

63. Y. Zhang and R. H. Holm, *J. Am. Chem. Soc.*, 2003, **125**, 3910-3920.

64. C. P. Berlinguette and R. H. Holm, *J. Am. Chem. Soc.*, 2006, **128**, 11993-12000.

65. D. Hong, Y. Zhang and R. H. Holm, *Inorg. Chim. Acta*, 2005, **358**, 2303-2311.

66. Y. Zhang, J.-L. Zuo, H.-C. Zhou and R. H. Holm, *J. Am. Chem. Soc.*, 2002, **124**, 14292-14293.

67. J.-L. Zuo, H.-C. Zhou and R. H. Holm, *Inorg. Chem.*, 2003, **42**, 4624-4631.

68. J. C. Crack, J. Green, A. J. Thomson and N. E. Le Brun, *Acc. Chem. Res.*, 2014, **47**, 3196-3205.

69. J. Fitzpatrick and E. Kim, *Acc. Chem. Res.*, 2015, **48**, 2453-2461.

70. L. J. Li and L. L. Li, *Coord. Chem. Rev.*, 2016, **306**, 678-700.

71. J. C. Toledo and O. Augusto, *Chem. Res. Toxicol.*, 2012, **25**, 975-989.

72. M. L. Tsai, C. C. Tsou and W. F. Liaw, *Acc. Chem. Res.*, 2015, **48**, 1184-1193.

73. W. Beck, R. Grenz, F. Götzfried and E. Vilsmaier, *Chem. Ber.*, 1981, **114**, 3184-3187.

74. C.-C. Tsou, W.-C. Chiu, C.-H. Ke, J.-C. Tsai, Y.-M. Wang, M.-H. Chiang and W.-F. Liaw, *J. Am. Chem. Soc.*, 2014, **136**, 9424-9433.

75. C. T. Tran, P. G. Williard and E. Kim, *J. Am. Chem. Soc.*, 2014, **136**, 11874-11877.

76. D. Seyferth and R. S. Henderson, *J. Organomet. Chem.*, 1981, **218**, C34-C36.

77. D. J. Crouthers, S. Ding, J. A. Denny, R. D. Bethel, C.-H. Hsieh, M. B. Hall and M. Y. Darensbourg, *Angew. Chem. Int. Ed.*, 2015, **54**, 11102-11106.

78. D. Seyferth and G. B. Womack, *J. Am. Chem. Soc.*, 1982, **104**, 6839-6841.

79. J. A. Franz, S. J. Lee, T. A. Bowden, M. S. Alnajjar, A. M. Appel, J. C. Birnbaum, T. E. Bitterwolf and M. Dupuis, *J. Am. Chem. Soc.*, 2009, **131**, 15212-15224.

80. T. Ganguly, A. Das and A. Majumdar, *Inorg. Chem.*, 2019, **58**, 9998-10011.

81. N. Pal and A. Majumdar, *Dalton Trans.*, 2019, **48**, 5903-5908.

82. M. Jana and A. Majumdar, *Inorg. Chem.*, 2018, **57**, 617-632.

83. T. Ganguly, A. Das, M. Jana and A. Majumdar, *Inorg. Chem.*, 2018, **57**, 11306-11309.

84. S. Yoshikawa and A. Shimada, *Chem. Rev.*, 2015, **115**, 1936-1989.

85. V. R. I. Kaila, M. I. Verkhovsky and M. Wikstrom, *Chem. Rev.*, 2010, **110**, 7062-7081.

86. P. Nicholls and J. K. Kim, *Can. J. Biochem.*, 1982, **60**, 613-623.

87. B. C. Hill, T. C. Woon, P. Nicholls, J. Peterson, C. Greenwood and A. J. Thomson, *Biochem. J*, 1984, **224**, 591-600.

88. J. Collman, S. Ghosh, A. Dey and R. A. Decreau, *Proc. Natl. Acad. Sci. USA*, 2009, **106**, 22090-22095.

89. R. J. Carrico, W. E. Blumberg and J. Peisach, *J. Biol. Chem.*, 1978, **253**, 7212-7215.

90. R. Pietri, E. Roman-Morales and J. Lopez-Garriga, *Antioxid. Redox Signal.*, 2011, **15**, 393-404.

91. D. W. Kraus and J. B. Wittenberg, *J. Biol. Chem.*, 1990, **265**, 16043-16053.

92. J. A. Berzofsky, J. Peisach and W. E. Blumberg, *J. Biol. Chem.*, 1971, **246**, 3367-3377.

93. M. Rizzi, J. B. Wittenberg, A. Coda, P. Ascenzi and M. Bolognesi, *J. Mol. Biol.*, 1996, **258**, 1-5.

94. M. Rizzi, J. B. Wittenberg, A. Coda, M. Fasano, P. Ascenzi and M. Bolognesi, *J. Mol. Biol.*, 1994, **244**, 86-99.

95. C. Ramos-Alvarez, B.-K. Yoo, R. Pietri, I. Lamarre, J.-L. Martin, J. Lopez-Garriga and M. Negrerie, *Biochemistry*, 2013, **52**, 7007-7021.

96. V. Vitvitsky, P. K. Yadav, S. An, J. Seravalli, U.-S. Cho and R. Banerjee, *J. Biol. Chem.*, 2017, **292**, 5584-5592.

97. D. Keilin, *Proc. R. Soc. Lond. Ser. B. Biol. Sci.*, 1933, **113**, 393-404.

98. B. B. Rios-Gonzalez, E. M. Roman-Morales, R. Pietri and J. Lopez-Garriga, *J. Inorg. Biochem.*, 2014, **133**, 78-86.

99. J. A. Berzofsky, J. Peisach and B. L. Horecker, *J. Biol. Chem.*, 1972, **247**, 3783-3791.

100. M. J. Chatfield, G. N. Lamar and R. J. Kauten, *Biochemistry*, 1987, **26**, 6939-6950.

101. L. L. Bondoc, M. H. Chau, M. A. Price and R. Timkovich, *Biochemistry*, 1986, **25**, 8458-8466.

102. S. V. Evans, B. P. Sishta, A. G. Mauk and G. D. Brayer, *Proc. Natl. Acad. Sci. USA*, 1994, **91**, 4723-4726.

103. P. Nicholls, *Biochem. J*, 1961, **81**, 374-383.

104. S. Nakamura, M. Nakamura, I. Yamazaki and M. Morrison, *J. Biol. Chem.*, 1984, **259**, 7080-7085.

105. T. Brittain, Y. Yosaatmadja and K. Henty, *Iubmb Life*, 2008, **60**, 135-138.

106. M. Ruetz, J. Kumutima, B. E. Lewis, M. R. Filipovic, N. Lehnert, T. L. Stemmler and R. Banerjee, *J. Biol. Chem.*, 2017, **292**, 6512-6528.

107. X. Bailly, R. Leroy, S. Carney, O. Collin, F. Zal, A. Toulmond and D. Jollivet, *Proc. Natl. Acad. Sci. USA*, 2003, **100**, 5885-5890.

108. S. Fernandez-Alberti, D. E. Bacelo, R. C. Binning, J. Echave, M. Chergui and J. Lopez-Garriga, *Biophys. J.*, 2006, **91**, 1698-1709.

109. F. P. Nicoletti, A. Comandini, A. Bonamore, L. Boechi, F. M. Boubeta, A. Feis, G. Smulevich and A. Boffi, *Biochemistry*, 2010, **49**, 2269-2278.

110. T. Bostelaar, V. Vitvitsky, J. Kumutima, B. E. Lewis, P. K. Yadav, T. C. Brunold, M. Filipovic, N. Lehnert, T. L. Stemmler and R. Banerjee, *J. Am. Chem. Soc.*, 2016, **138**, 8476-8488.

111. B. Jensen and A. Fago, *J. Inorg. Biochem.*, 2018, **182**, 133-140.

112. S. H. Libardi, H. Pindstrup, D. R. Cardoso and L. H. Skibsted, *J. Agric. Food. Chem.*, 2013, **61**, 2883-2888.

113. Y. X. Wu and J. Yi, *Prog. Biochem. Biophys.*, 2018, **45**, 865-874.

114. R. Pietri, A. Lewis, R. G. Leon, G. Casabona, L. Kiger, S. R. Yeh, S. Fernandez-Alberti, M. C. Marden, C. L. Cadilla and J. Lopez-Garriga, *Biochemistry*, 2009, **48**, 4881-4894.

115. M. R. Filipovic, J. Zivanovic, B. Alvarez and R. Banerjee, *Chem. Rev.*, 2018, **118**, 1253-1337.

116. O. Kabil and R. Banerjee, *J. Biol. Chem.*, 2010, **285**, 21903-21907.

117. V. Vitvitsky, P. K. Yadav, S. An, J. Seravalli, U. S. Cho and R. Banerjee, *J. Biol. Chem.*, 2017, **292**, 5584-5592.

118. D. S. Salnikov, P. N. Kucherenko, I. A. Dereven'kov, S. V. Makarov and R. van Eldik, *Eur. J. Inorg. Chem.*, 2014, **2014**, 852-862.

119. S. A. Bieza, F. Boubeta, A. Feis, G. Smulevich, D. A. Estrin, L. Boechi and S. E. Bari, *Inorg. Chem.*, 2015, **54**, 527-533.

120. Z. J. Zhao, D. D. Wang, M. Y. Wang, X. L. Sun, L. P. Wang, X. R. Huang, L. Ma and Z. Q. Li, *Rsc Advances*, 2016, **6**, 78858-78864.

121. D. R. English, D. N. Hendrickson, K. S. Suslick, C. W. Eigenbrot and W. R. Scheidt, *J. Am. Chem. Soc.*, 1984, **106**, 7258-7259.

122. A. L. Balch, C. R. Cornman, N. Safari and L. Latos-Grazynski, *Organometallics*, 1990, **9**, 2420-2421.

123. J. W. Pavlik, B. C. Noll, A. G. Oliver, C. E. Schulz and W. R. Scheidt, *Inorg. Chem.*, 2010, **49**, 1017-1026.

124. D. J. Meininger, H. D. Arman and Z. J. Tonzetich, *J. Inorg. Biochem.*, 2017, **167**, 142-149.

125. D. J. Meininger, M. Chee-Garza, H. D. Arman and Z. J. Tonzetich, *Inorg. Chem.*, 2016, **55**, 2421-2426.

126. M. D. Hartle, J. S. Prell and M. D. Pluth, *Dalton Trans.*, 2016, **45**, 4843-4853.

127. K. Mittra, A. Singha and A. Dey, *Inorg. Chem.*, 2017, **56**, 3916-3925.

128. M. Dhifet, M. S. Belkhiria, J. C. Daran and H. Nasri, *Acta Cryst. E.*, 2009, **65**, M967-U1355.

129. J. F. Flores, C. R. Fisher, S. L. Carney, B. N. Green, J. K. Freytag, S. W. Schaeffer and W. E. Royer, *Proc. Natl. Acad. Sci. USA*, 2005, **102**, 2713-2718.

130. G. Parkin, *Chem. Rev.*, 2004, **104**, 699-767.

131. V. M. Krishnamurthy, G. K. Kaufman, A. R. Urbach, I. Gitlin, K. L. Gudiksen, D. B. Weibel and G. M. Whitesides, *Chem. Rev.*, 2008, **108**, 946-1051.

132. A. Looney, R. Han, I. B. Gorrell, M. Cornebise, K. Yoon, G. Parkin and A. L. Rheingold, *Organometallics*, 1995, **14**, 274-288.

133. M. Ruf and H. Vahrenkamp, *Inorg. Chem.*, 1996, **35**, 6571-6578.

134. M. Ruf and H. Vahrenkamp, *J. Chem. Soc. Dalton Trans.*, 1995, 1915-1916.

135. M. Rombach and H. Vahrenkamp, *Inorg. Chem.*, 2001, **40**, 6144-6150.

136. E. Galardon, A. Tomas, M. Selkti, P. Roussel and I. Artaud, *Inorg. Chem.*, 2009, **48**, 5921-5927.

137. M. Brauer, E. Anders, S. Sinnecker, W. Koch, M. Rombach, H. Brombacher and H. Vahrenkamp, *Chem. Commun.*, 2000, 647-648.

138. J. G. Melnick, A. Docrat and G. Parkin, *Chem. Commun.*, 2004, DOI: 10.1039/b412218f, 2870-2871.

139. M. M. Ibrahim, J. Seebacher, G. Steinfeld and H. Vahrenkamp, *Inorg. Chem.*, 2005, **44**, 8531-8538.

140. E. Galardon, A. Tomas, P. Roussel and I. Artaud, *Eur. J. Inorg. Chem.*, 2011, **2011**, 3797-3801.

141. Y. Rong and G. Parkin, *Aust. J. Chem.*, 2013, **66**, 1306-1310.

142. M. D. Hartle, M. Delgado, J. D. Gilbertson and M. D. Pluth, *Chem. Commun.*, 2016, **52**, 7680-7682.

143. R. Hille, J. Hall and P. Basu, *Chem. Rev.*, 2014, **114**, 3963-4038.

144. K. Okamoto, K. Matsumoto, R. Hille, B. T. Eger, E. F. Pai and T. Nishino, *Proc. Natl. Acad. Sci. USA*, 2004, **101**, 7931-7936.

145. K. Okamoto, B. T. Eger, T. Nishino, E. F. Pai and T. Nishino, *Nucleosides Nucleotides & Nucleic Acids*, 2008, **27**, 888-893.

146. J. Mitra and S. Sarkar, *Dalton Trans.*, 2013, **42**, 3050-3058.

147. A. Majumdar, J. Mitra, K. Pal and S. Sarkar, *Inorg. Chem.*, 2008, **47**, 5360-5364.

148. P. Štarha, A. Habtemariam, I. Romero-Canelón, G. J. Clarkson and P. J. Sadler, *Inorg. Chem.*, 2016, **55**, 2324-2331.

149. V. S. Lin, W. Chen, M. Xian and C. J. Chang, *Chem. Soc. Rev.*, 2015, **44**, 4596-4618.

150. K. Shimamoto and K. Hanaoka, *Nitric Oxide*, 2015, **46**, 72-79.

151. Y. Takano, H. Echizen and K. Hanaoka, *Antioxid. Redox Signal.*, 2017, **27**, 669-683.

152. L. Yi and Z. Xi, *Org. Biomol. Chem.*, 2017, **15**, 3828-3839.

153. M. D. Hartle, R. J. Hansen, B. W. Tresca, S. S. Prakel, L. N. Zakharov, M. M. Haley, M. D. Pluth and D. W. Johnson, *Angew. Chem. Int. Ed.*, 2016, **55**, 11480-11484.

154. N. Lau, L. N. Zakharov and M. D. Pluth, *Chem. Commun.*, 2018, **54**, 2337-2340.

155. J. Vazquez and V. Sindelar, *Chem. Commun.*, 2018, **54**, 5859-5862.

156. M. D. Hartle, S. K. Sommer, S. R. Dietrich and M. D. Pluth, *Inorg. Chem.*, 2014, **53**, 7800-7802.

157. M. Strianese, S. Milione, V. Bertolasi, C. Pellecchia and A. Grassi, *Inorg. Chem.*, 2011, **50**, 900-910.

158. M. D. Hartle, M. R. Tillotson, J. S. Prell and M. D. Pluth, *J. Inorg. Biochem.*, 2017, **173**, 152-157.

159. M. Strianese, S. Mirra, M. Lamberti and C. Pellecchia, *Inorg. Chim. Acta*, 2017, **466**, 426-431.

160. M. Strianese, M. Lamberti and C. Pellecchia, *Dalton Trans.*, 2017, **46**, 1872-1877.

161. M. Strianese, M. Lamberti and C. Pellecchia, *Dalton Trans.*, 2018, **47**, 17392-17400.

162. S. Mirra, S. Milione, M. Strianese and C. Pellecchia, *Eur. J. Inorg. Chem.*, 2015, **2015**, 2272-2276.

163. E. Galardon, T. Roger, P. Deschamps, P. Roussel, A. Tomas and I. Artaud, *Inorg. Chem.*, 2012, **51**, 10068-10070.

164. E. Galardon, A. Tomas, P. Roussel and I. Artaud, *Dalton Trans.*, 2009, 9126-9130.

165. M. Strianese, F. De Martino, C. Pellecchia, G. Ruggiero and S. D'Auria, *Protein Pept. Lett.*, 2011, **18**, 282-286.

166. M. Dulac, A. Melet and E. Galardon, *Acs Sensors*, 2018, **3**, 2138-2144.

167. M. Strianese, G. J. Palm, S. Milione, O. Kühl, W. Hinrichs and C. Pellecchia, *Inorg. Chem.*, 2012, **51**, 11220-11222.

168. M. Strianese, G. J. Palm, D. Kohlhause, L. A. Ndamba, L. C. Tabares and C. Pellecchia, *Eur. J. Inorg. Chem.*, 2019, **2019**, 885-891.

169. B. R. James, *Pure Appl. Chem.*, 1997, **69**, 2213-2220.

170. L. Vaska and J. W. DiLuzio, *J. Am. Chem. Soc.*, 1962, **84**, 679-680.

171. L. Vaska and D. L. Catone, *J. Am. Chem. Soc.*, 1966, **88**, 5324-5325.

172. L. Vaska, *J. Am. Chem. Soc.*, 1966, **88**, 5325-5327.

173. H. Singer and G. Wilkinson, *J. Chem. Soc. A.*, 1968, 2516-2520.

174. A. M. Mueting, P. Boyle and L. H. Pignolet, *Inorg. Chem.*, 1984, **23**, 44-48.

175. D. Milstein, J. C. Calabrese and I. D. Williams, *J. Am. Chem. Soc.*, 1986, **108**, 6387-6389.

176. J. P. Collman, R. K. Rothrock and R. A. Stark, *Inorg. Chem.*, 1977, **16**, 437-440.

177. A. M. Mueting, P. D. Boyle, R. Wagner and L. H. Pignolet, *Inorg. Chem.*, 1988, **27**, 271-279.

178. R. H. Crabtree, M. W. Davis, M. F. Mellea and J. M. Mihelcic, *Inorg. Chim. Acta*, 1983, **72**, 223-226.

179. R. C. Linck, R. J. Pafford and T. B. Rauchfuss, *J. Am. Chem. Soc.*, 2001, **123**, 8856-8857.

180. D. Morelli, A. Segre, R. Ugo, G. La Monica, S. Cenini, F. Conti and F. Bonati, *Chemical Communications (London)*, 1967, 524-526.

181. T. Miyamoto, *J. Organomet. Chem.*, 1977, **134**, 335-362.

182. I. M. Blacklaws, E. A. V. Ebsworth, D. W. H. Rankin and H. E. Robertson, *J. Chem. Soc., Dalton Trans.*, 1978, 753-758.

183. B. Bogdanovic, M. Rubach and C. Kruger, *CSD Communication*, 1992, CSD #1262719.

184. R. Ugo, G. La Monica, S. Cenini, A. Segre and F. Conti, *J. Chem. Soc. A.*, 1971, 522-528.

185. A. Shaver, M. El-khateeb and A.-M. Lebuis, *Angew. Chem. Int. Ed. Engl.*, 1996, **35**, 2362-2363.

186. E. A. V. Ebsworth, H. M. Ferrier, B. J. L. Henner, D. W. H. Rankin, F. J. S. Reed, H. E. Robertson and J. D. Whitelock, *Angew. Chem. Int. Ed. Engl.*, 1977, **16**, 482-484.

187. B. Kreutzer, P. Kreutzer and W. Beck, *Z. Naturforsch., Teil B*, 1972, **27**, 461-463.

188. M. Schmidt and G. G. Hoffmann, *J. Organomet. Chem.*, 1977, **124**, C5-C8.

189. N. Singh, B. Singh, K. Thapliyal and M. G. B. Drew, *Inorg. Chim. Acta*, 2010, **363**, 3589-3596.

190. C. E. Briant, G. R. Hughes, P. C. Minshall and D. M. P. Mingos, *J. Organomet. Chem.*, 1980, **202**, C18-C20.

191. C. A. Ghilardi, S. Midollini, F. Nuzzi and A. Orlandini, *Transition Met. Chem.*, 1983, **8**, 73-75.

192. M. Schmidt, G. G. Hoffmann and R. Holler, *Inorg. Chim. Acta*, 1979, **32**, L19-L20.

193. T. G. Appleton and M. A. Bennett, *Inorg. Chem.*, 1978, **17**, 738-747.

194. D. A. Vicic and W. D. Jones, *J. Am. Chem. Soc.*, 1999, **121**, 7606-7617.

195. Y. Maeda, H. Hashimoto and T. Nishioka, *Dalton Trans.*, 2012, **41**, 12038-12047.

196. C.-L. Lee, J. Chisholm, B. R. James, D. A. Nelson and M. A. Lilga, *Inorg. Chim. Acta*, 1986, **121**, L7-L9.

197. P. G. Jessop, C. L. Lee, G. Rastar, B. R. James, C. J. L. Lock and R. Faggiani, *Inorg. Chem.*, 1992, **31**, 4601-4605.

198. P. G. Jessop, S. J. Rettig, C. L. Lee and B. R. James, *Inorg. Chem.*, 1991, **30**, 4617-4627.

199. M. Khorasani-Motlagh, N. Safari, C. B. Pamplin, B. O. Patrick and B. R. James, *Inorg. Chim. Acta*, 2001, **320**, 184-189.

200. A. Coto, M. Jiménez Tenorio, M. C. Puerta and P. Valerga, *Organometallics*, 1998, **17**, 4392-4399.

201. D. Sellman, P. Lechner, F. Knoch and M. Moll, *Angew. Chem. Int. Ed. Engl.*, 1991, **30**, 552-553.

202. D. Sellmann, P. Lechner, F. Knoch and M. Moll, *J. Am. Chem. Soc.*, 1992, **114**, 922-930.

203. D. Chandrika, E. S. Ma, S. J. Rettig, B. R. James and W. R. Cullen, *Inorg. Chem.*, 1997, **36**, 5426-5427.

204. E. S. F. Ma, S. J. Rettig and B. R. James, *Chem. Commun.*, 1999, 2463-2464.

205. F. Bottomley, G. O. Egharevba and P. S. White, *J. Am. Chem. Soc.*, 1985, **107**, 4353-4354.

206. F. Bottomley, D. F. Drummond, G. O. Egharevba and P. S. White, *Organometallics*, 1986, **5**, 1620-1625.

207. A. Shaver and J. M. McCall, *Organometallics*, 1984, **3**, 1823-1829.

208. W. A. Howard and G. Parkin, *Organometallics*, 1993, **12**, 2363-2366.

209. W. A. Howard and G. Parkin, *J. Am. Chem. Soc.*, 1994, **116**, 606-615.

210. D. Rabinovich and G. Parkin, *J. Am. Chem. Soc.*, 1991, **113**, 5904-5905.

211. V. J. Murphy and G. Parkin, *J. Am. Chem. Soc.*, 1995, **117**, 3522-3528.

212. D. Rabinovich and G. Parkin, *Inorg. Chem.*, 1995, **34**, 6341-6361.

213. D. E. Schwarz, T. B. Rauchfuss and S. R. Wilson, *Inorg. Chem.*, 2003, **42**, 2410-2417.

214. K. Tsuge, H. Imoto and T. Saito, *Inorg. Chem.*, 1992, **31**, 4715-4716.

215. K. Tsuge, S. Mita, H. Fujita, H. Imoto and T. Saito, *J. Cluster Sci.*, 1996, **7**, 407-421.

216. A. Sattler and G. Parkin, *Polyhedron*, 2014, **84**, 74-86.

217. S. Kuwata, Y. Mizobe and M. Hidai, *J. Chem. Soc., Chem. Commun.*, 1995, 1057-1058.

218. S. Kuwata, Y. Mizobe and M. Hidai, *J. Chem. Soc., Dalton Trans.*, 1997, 1753-1758.

219. S. J. Smith, C. M. Whaley, T. B. Rauchfuss and S. R. Wilson, *Inorg. Chem.*, 2006, **45**, 679-687.

220. D. E. Schwarz, J. A. Dopke, T. B. Rauchfuss and S. R. Wilson, *Angew. Chem. Int. Ed.*, 2001, **40**, 2351-2353.

221. C. Mealli, S. Midollini and L. Sacconi, *Inorg. Chem.*, 1978, **17**, 632-637.

222. C.-L. Lee, G. Besenyei, B. R. James, D. A. Nelson and M. A. Lilga, *J. Chem. Soc., Chem. Commun.*, 1985, 1175-1176.

223. G. Besenyei, C. L. Lee, J. Gulinski, S. J. Rettig, B. R. James, D. A. Nelson and M. A. Lilga, *Inorg. Chem.*, 1987, **26**, 3622-3628.

224. T. Y. H. Wong, A. F. Barnabas, D. Sallin and B. R. James, *Inorg. Chem.*, 1995, **34**, 2278-2286.

225. A. F. Barnabas, D. Sallin and B. R. James, *Can. J. Chem.*, 1989, **67**, 2009-2015.

226. C. B. Pamplin, S. J. Rettig, B. O. Patrick and B. R. James, *Inorg. Chem.*, 2011, **50**, 8094-8105.

227. R. McDonald and M. Cowie, *Inorg. Chem.*, 1993, **32**, 1671-1680.

228. K.-Y. Shih, P. E. Fanwick and R. A. Walton, *J. Cluster Sci.*, 1991, **2**, 259-270.

229. K.-Y. Shih, P. E. Fanwick and R. A. Walton, *J. Chem. Soc., Chem. Commun.*, 1992, 375-377.

230. R. A. Walton, *Polyhedron*, 1989, **8**, 1689-1693.

231. K. Y. Shih, P. E. Fanwick and R. A. Walton, *Inorg. Chem.*, 1992, **31**, 3663-3668.

232. D. M. Antonelli and M. Cowie, *Inorg. Chem.*, 1990, **29**, 3339-3345.

233. L.-S. Wang, R. McDonald and M. Cowie, *Inorg. Chem.*, 1994, **33**, 3735-3744.

234. M. Khorasani-Motlagh, N. Safari, C. B. Pamplin, B. O. Patrick and B. R. James, *Can. J. Chem.*, 2006, **84**, 330-336.

235. T. V. Ashworth, M. J. Nolte and E. Singleton, *J. Chem. Soc., Chem. Commun.*, 1977, 936-937.

236. K. Osakada, T. Yamamoto and A. Yamamoto, *Inorg. Chim. Acta*, 1984, **90**, L5-L6.

237. M. Kawano, T. Watanabe and K. Matsumoto, *Chem. Lett.*, 1992, **21**, 2389-2392.

238. J. A. Froelich and D. J. Darensbourg, *Inorg. Chem.*, 1977, **16**, 960-962.

239. T. R. Gaffney and J. A. Ibers, *Inorg. Chem.*, 1982, **21**, 2857-2859.

240. M. R. DuBois, *Chem. Rev.*, 1989, **89**, 1-9.

241. M. R. DuBois, M. C. VanDerveer, D. L. DuBois, R. C. Haltiwanger and W. K. Miller, *J. Am. Chem. Soc.*, 1980, **102**, 7456-7461.

242. A. M. Appel, S.-J. Lee, J. A. Franz, D. L. DuBois, M. Rakowski DuBois and B. Twamley, *Organometallics*, 2009, **28**, 749-754.

243. J. H. Shin and G. Parkin, *Polyhedron*, 1994, **13**, 1489-1493.

244. D. L. DuBois, W. K. Miller and M. R. DuBois, *J. Am. Chem. Soc.*, 1981, **103**, 3429-3436.

245. C. J. Casewit, D. E. Coons, L. L. Wright, W. K. Miller and M. R. DuBois, *Organometallics*, 1986, **5**, 951-955.

246. M. McKenna, L. L. Wright, D. J. Miller, L. Tanner, R. C. Haltiwanger and M. R. DuBois, *J. Am. Chem. Soc.*, 1983, **105**, 5329-5337.

247. D. E. Coons, J. C. V. Laurie, R. C. Haltiwanger and M. R. DuBois, *J. Am. Chem. Soc.*, 1987, **109**, 283-285.

248. J. Birnbaum, G. Godziela, M. Maciejewski, T. L. Tonker, R. C. Haltiwanger and M. R. DuBois, *Organometallics*, 1990, **9**, 394-401.

249. J. Birnbaum, J. C. V. Laurie and M. R. DuBois, *Organometallics*, 1990, **9**, 156-164.

250. W. S. Ojo, F. Y. Pétillon, P. Schollhammer and J. Talarmin, *Organometallics*, 2008, **27**, 4207-4222.

251. G. Godziela, T. Tonker and M. R. DuBois, *Organometallics*, 1989, **8**, 2220-2224.

252. C. J. Casewit and M. R. DuBois, *J. Am. Chem. Soc.*, 1986, **108**, 5482-5489.

253. J. A. Franz, J. C. Birnbaum, D. S. Kolwaite, J. C. Linehan, D. M. Camaioni and M. Dupuis, *J. Am. Chem. Soc.*, 2004, **126**, 6680-6691.

254. A. M. Appel, D. L. DuBois and M. R. DuBois, *J. Am. Chem. Soc.*, 2005, **127**, 12717-12726.

255. A. M. Appel, S.-J. Lee, J. A. Franz, D. L. DuBois, M. Rakowski DuBois, J. C. Birnbaum and B. Twamley, *J. Am. Chem. Soc.*, 2008, **130**, 8940-8951.

256. A. M. Appel, S.-J. Lee, J. A. Franz, D. L. DuBois and M. R. DuBois, *J. Am. Chem. Soc.*, 2009, **131**, 5224-5232.

257. C. Bianchini and A. Meli, *Inorg. Chem.*, 1987, **26**, 4268-4271.

258. A. Ienco, M. J. Calhorda, J. Reinhold, F. Reineri, C. Bianchini, M. Peruzzini, F. Vizza and C. Mealli, *J. Am. Chem. Soc.*, 2004, **126**, 11954-11965.

259. J. Amarasekera and T. B. Rauchfuss, *Inorg. Chem.*, 1989, **28**, 3875-3883.

260. H. E. Bryndza, L. K. Fong, R. A. Paciello, W. Tam and J. E. Bercaw, *J. Am. Chem. Soc.*, 1987, **109**, 1444-1456.

261. I. Kovacs, C. Pearson and A. Shaver, *J. Organomet. Chem.*, 2000, **596**, 193-203.

262. A. G. Algarra, *Inorg. Chem.*, 2017, **56**, 186-196.

263. Z. K. Sweeney, J. L. Polse, R. G. Bergman and R. A. Andersen, *Organometallics*, 1999, **18**, 5502-5510.

264. F. Olechnowicz, G. L. Hillhouse and R. F. Jordan, *Inorg. Chem.*, 2015, **54**, 2705-2712.

265. F. Olechnowicz, G. L. Hillhouse, T. R. Cundari and R. F. Jordan, *Inorg. Chem.*, 2017, **56**, 9922-9930.

266. J. Zhai, A. S. Filatov, G. L. Hillhouse and M. D. Hopkins, *Chem. Sci.*, 2016, **7**, 589-595.

267. A. J. Jordan, R. K. Walde, K. M. Schultz, J. Bacsa and J. P. Sadighi, *Inorg. Chem.*, 2019, **58**, 9592-9596.

268. M. A. Esteruelas, A. M. Lopez, M. Mora and E. Onate, *Chem. Commun.*, 2013, **49**, 7543-7545.

269. M. L. Buil, S. Elipe, M. A. Esteruelas, E. Oñate, E. Peinado and N. Ruiz, *Organometallics*, 1997, **16**, 5748-5755.

270. W. Strohmeier and J. F. Guttenberger, *Chem. Ber.*, 1964, **97**, 1871-1876.

271. W. Bathelt, Ph.D. Dissertation Dissertation, Technische Universität München, 1970.

272. M. Höfler and A. Baitz, *Chem. Ber.*, 1976, **109**, 3147-3150.

273. G. Beuter, S. Drobnik, I.-P. Lorenz and A. Lubik, *Chem. Ber.*, 1992, **125**, 2363-2366.

274. H. Köpf and M. Schmidt, *Angew. Chem. Int. Ed. Engl.*, 1965, **4**, 953-953.

275. J. M. McCall and A. Shaver, *J. Organomet. Chem.*, 1980, **193**, C37-C39.

276. M. J. Carney, P. J. Walsh and R. G. Bergman, *J. Am. Chem. Soc.*, 1990, **112**, 6426-6428.

277. M. J. Carney, P. J. Walsh, F. J. Hollander and R. G. Bergman, *Organometallics*, 1992, **11**, 761-777.

278. J. Pinkas, I. Císařová, M. Horáček, J. Kubišta and K. Mach, *Organometallics*, 2011, **30**, 1034-1045.

279. M. Horáček, I. Císařová, R. Gyepes, J. Kubišta, J. Pinkas, M. Lamač and K. Mach, *J. Organomet. Chem.*, 2014, **755**, 141-150.

280. M. L. H. Green and W. E. Lindsell, *J. Chem. Soc. A.*, 1967, 1455-1458.

281. A. Z. Rys, A.-M. Lebuis and A. Shaver, *Inorg. Chem.*, 2006, **45**, 341-344.

282. W. Beck, W. Danzer and G. Thiel, *Angew. Chem. Int. Ed. Engl.*, 1973, **12**, 582-582.

283. W. Beck, W. Danzer and R. Höfer, *Angew. Chem. Int. Ed. Engl.*, 1973, **12**, 77-78.

284. W. Danzer, W. P. Fehlhammer, A. T. Liu, G. Thiel and W. Beck, *Chem. Ber.*, 1982, **115**, 1682-1693.

285. G. Urban, K. Sünkel and W. Beck, *J. Organomet. Chem.*, 1985, **290**, 329-339.

286. R. A. Fischer, H.-J. Kneuper and W. A. Herrmann, *J. Organomet. Chem.*, 1987, **330**, 365-376.

287. A. Bauer, K. B. Capps, B. Wixmerten, K. A. Abboud and C. D. Hoff, *Inorg. Chem.*, 1999, **38**, 2136-2142.

288. K. Iwasa, H. Seino and Y. Mizobe, *J. Organomet. Chem.*, 2009, **694**, 3775-3780.

289. I. Kovács and A. Shaver, *J. Organomet. Chem.*, 1999, **586**, 31-40.

290. K. B. Capps, G. D. Whitener, A. Bauer, K. A. Abboud, I. M. Wasser, K. P. C. Vollhardt and C. D. Hoff, *Inorg. Chem.*, 2002, **41**, 3212-3217.

291. P. Schollhammer, F. Y. Pétillon, R. Pichon, S. Poder-Guillou, J. Talarmin, K. W. Muir and L. Manojlovic-Muir, *Organometallics*, 1995, **14**, 2277-2287.

292. N. I. Kirillova, A. I. Gusev, A. A. Pasynskii and Y. T. Struchkov, *Zh. Strukt. Khim.*, 1973, **14**, 868-874.

293. H. Brunner, U. Klement, J. Wachter, M. Tsunoda, J. C. Leblanc and C. Moise, *Inorg. Chem.*, 1990, **29**, 584-585.

294. H. J. Bach, H. Brunner, J. Wachter, M. M. Kubicki, J. C. Leblanc, C. Moise, F. Volpato, B. Nuber and M. L. Ziegler, *Organometallics*, 1992, **11**, 1403-1407.

295. H. Brunner, G. Gehart, W. Meier, J. Wachter and B. Nuber, *J. Organomet. Chem.*, 1993, **454**, 117-122.

296. S. Challet, O. Blacque, G. Gehart, M. M. Kubicki, J.-C. Leblanc, C. Moise, H. Brunner and J. Wachter, *New J. Chem.*, 1997, **21**, 903-908.

297. F. Bock, F. Fischer, K. Radacki and W. A. Schenk, *Eur. J. Inorg. Chem.*, 2010, **2010**, 391-402.

298. U. Kölle, A. Hörnig and U. Englert, *J. Organomet. Chem.*, 1992, **438**, 309-317.

299. K. Hashizume, Y. Mizobe and M. Hidai, *Organometallics*, 1996, **15**, 3303-3309.

300. H. Seino, Y. Mizobe and M. Hidai, *New J. Chem.*, 2000, **24**, 907-911.

301. Y. Miyake, T. Moriyama, Y. Tanabe, S. Endo and Y. Nishibayashi, *Organometallics*, 2012, **31**, 3292-3299.

302. D. P. Klein, G. M. Kloster and R. G. Bergman, *J. Am. Chem. Soc.*, 1990, **112**, 2022-2024.

303. A. Shaver, B. El Mouatassim, F. Mortini, F. Bélanger-Gariépy and A. Lough, *Organometallics*, 2007, **26**, 4229-4233.

304. Y. Ozawa, A. Vázquez de Miguel and K. Isobe, *J. Organomet. Chem.*, 1992, **433**, 183-188.

305. Z. Tang, Y. Nomura, Y. Ishii, Y. Mizobe and M. Hidai, *Inorg. Chim. Acta*, 1998, **267**, 73-79.

306. Z. Tang, Y. Nomura, Y. Ishii, Y. Mizobe and M. Hidai, *Organometallics*, 1997, **16**, 151-154.

307. M. Sato, F. Sato and T. Yoshida, *J. Organomet. Chem.*, 1971, **31**, 415-419.

308. M. Sato, F. Sato, N. Takemoto and K. Iida, *J. Organomet. Chem.*, 1972, **34**, 205-208.

309. H. Behrens, E. Lindner and G. Lehnert, *J. Organomet. Chem.*, 1970, **22**, 665-676.

310. R. G. W. Gingerich and R. J. Angelici, *J. Am. Chem. Soc.*, 1979, **101**, 5604-5608.

311. M. Herberhold and G. Süss, *Angew. Chem. Int. Ed. Engl.*, 1976, **15**, 366-367.

312. M. Herberhold and G. Suess, *J. Chem. Res. (S)*, 1977, 246.

313. R. J. Angelici and R. G. W. Gingerich, *Organometallics*, 1983, **2**, 89-95.

314. M. Höfler, H. Hausmann and H. A. Heidelberg, *J. Organomet. Chem.*, 1981, **213**, C1-C3.

315. M. K. Cooper, P. A. Duckworth, K. Henrick and M. McPartlin, *J. Chem. Soc., Dalton Trans.*, 1981, 2357-2364.

316. M. K. Cooper, P. A. Duckworth, K. Henrick and M. McPartlin, *J. Organomet. Chem.*, 1981, **212**, C10-C12.

317. D. J. Darensbourg, A. Rokicki and R. Kudaroski, *Organometallics*, 1982, **1**, 1161-1166.

318. R. C. Hynes, K. F. Preston, J. J. Springs and A. J. Williams, *Organometallics*, 1991, **10**, 180-185.

319. V. Küllmer and H. Vahrenkamp, *Chem. Ber.*, 1976, **109**, 1560-1568.

320. K. Raab and W. Beck, *Chem. Ber.*, 1985, **118**, 3830-3848.

321. V. Küllmer and H. Vahrenkamp, *Chem. Ber.*, 1977, **110**, 3799-3809.

322. B.-C. Tzeng, A. Chao and M. Banik, *Dalton Trans.*, 2014, **43**, 11510-11515.

323. R. O. Harris and P. Yaneff, *J. Organomet. Chem.*, 1977, **134**, C40-C42.

324. S. L. Chatwin, R. A. Diggle, R. F. R. Jazzar, S. A. Macgregor, M. F. Mahon and M. K. Whittlesey, *Inorg. Chem.*, 2003, **42**, 7695-7697.

325. J. J. Pérez-Torrente, M. V. Jiménez, M. A. F. Hernandez-Gruel, M. J. Fabra, F. J. Lahoz and L. A. Oro, *Chem. Eur. J.*, 2009, **15**, 12212-12222.

326. S. S. Oster and W. D. Jones, *Inorg. Chim. Acta*, 2004, **357**, 1836-1846.

327. X.-L. Luo, G. J. Kubas, C. J. Burns and R. J. Butcher, *Organometallics*, 1995, **14**, 3370-3376.

328. F. Lissel, F. Schwarz, O. Blacque, H. Riel, E. Lörtscher, K. Venkatesan and H. Berke, *J. Am. Chem. Soc.*, 2014, **136**, 14560-14569.

329. H.-C. Liang and P. A. Shapley, *Organometallics*, 1996, **15**, 1331-1333.

330. P. A. Shapley, H.-C. Liang, J. M. Shusta, J. J. Schwab, N. Zhang and S. R. Wilson, *Organometallics*, 1994, **13**, 3351-3359.

331. J. Ruiz, V. Rodríguez, C. Vicente, J. M. Martí, G. López and J. Pérez, *Inorg. Chem.*, 2001, **40**, 5354-5360.

332. F. Canales, S. Canales, O. Crespo, M. Concepción Gimeno, P. G. Jones and A. Laguna, *Organometallics*, 1998, **17**, 1617-1621.

333. D. Sellmann, C. Allmann, F. Heinemann, F. Knoch and J. Sutter, *J. Organomet. Chem.*, 1997, **541**, 291-305.

334. M. Ardon and H. Taube, *J. Am. Chem. Soc.*, 1967, **89**, 3661-3662.

335. T. Ramasami and A. G. Sykes, *Inorg. Chem.*, 1976, **15**, 1010-1014.

336. T. Ramasami, R. S. Taylor and A. G. Sykes, *J. Chem. Soc., Chem. Commun.*, 1976, 383-384.

337. M. Di Vaira, S. Midollini and L. Sacconi, *Inorg. Chem.*, 1977, **16**, 1518-1524.

338. M. Di Vaira, M. Peruzzini and P. Stoppioni, *Inorg. Chem.*, 1991, **30**, 1001-1007.

339. M. Di Vaira, S. Midollini and L. Sacconi, *Inorg. Chem.*, 1978, **17**, 816-819.

340. M. Di Vaira, S. Midollini and L. Sacconi, *Inorg. Chem.*, 1979, **18**, 3466-3469.

341. C. Bianchini, C. Mealli, A. Meli and G. Scapacci, *Organometallics*, 1983, **2**, 141-143.

342. C. Bianchini, D. Masi, C. Mealli and A. Meli, *Cryst. Struct. Commun.*, 1982, **11**, 1475-1480.

343. A. M. Arif, J. G. Hefner, R. A. Jones and S. U. Koschmieder, *J. Coord. Chem.*, 1991, **23**, 13-19.

344. M. S. Morton, R. J. Lachicotte, D. A. Vicic and W. D. Jones, *Organometallics*, 1999, **18**, 227-234.

345. R. Mas-Ballesté, G. Aullón, P. A. Champkin, W. Clegg, C. Mégret, P. González-Duarte and A. Lledós, *Chem. Eur. J.*, 2003, **9**, 5023-5035.

346. S. W. Audi Fong, W. Teck Yap, J. J. Vittal, T. S. A. Hor, W. Henderson, A. G. Oliver and C. E. F. Rickard, *J. Chem. Soc., Dalton Trans.*, 2001, 1986-2002.

347. S. W. A. Fong, J. J. Vittal, W. Henderson, T. S. A. Hor, A. G. Oliver and C. E. F. Rickard, *Chem. Commun.*, 2001, 421-422.

348. G. T. Venkanna, H. D. Arman and Z. J. Tonzetich, *ACS Catalysis*, 2014, **4**, 2941-2950.

349. J. Zhang, T. Liu, Q.-Q. Ma, S. Li and X. Chen, *Dalton Trans.*, 2018, 6018-6024.

350. M. Wozniak, T. Braun, M. Ahrens, B. Braun-Cula, P. Wittwer, R. Herrmann and R. Laubenstein, *Organometallics*, 2018, **37**, 821-828.

351. C. C. Kuehn and H. Taube, *J. Am. Chem. Soc.*, 1976, **98**, 689-702.

352. R. J. Pleus, H. Waden, W. Saak, D. Haase and S. Pohl, *J. Chem. Soc., Dalton Trans.*, 1999, 2601-2610.

353. V. Lozan and B. Kersting, *Inorg. Chem.*, 2008, **47**, 5386-5393.

354. G. Gupta and S. Bhattacharya, *RSC Advances*, 2015, **5**, 94486-94494.

355. A. Sreekanth and M. R. Prathapachandra Kurup, *Polyhedron*, 2003, **22**, 3321-3332.

356. R. Gil-Garcia, R. Fraile, B. Donnadieu, G. Madariaga, V. Januskaitis, J. Rovira, L. Gonzalez, J. Borras, F. J. Arnaiz and J. Garcia-Tojal, *New J. Chem.*, 2013, **37**, 3568-3580.

357. J. R. Anacona, M. Azocar, O. Nusetti and C. Rodriguez-Barbarin, *Transition Met. Chem.*, 2003, **28**, 24-28.

358. D. Huang, L. Deng, J. Sun and R. H. Holm, *Inorg. Chem.*, 2009, **48**, 6159-6166.

359. D. Huang and R. H. Holm, *J. Am. Chem. Soc.*, 2010, **132**, 4693-4701.

360. F. A. Jové, C. Pariya, M. Scoblete, G. P. A. Yap and K. H. Theopold, *Chem. Eur. J.*, 2011, **17**, 1310-1318.

361. J. Vicente, M.-T. Chicote, P. González-Herrero, P. G. Jones and B. Ahrens, *Angew. Chem. Int. Ed. Engl.*, 1994, **33**, 1852-1853.

362. E. Königer-Ahlborn, A. Müller and H. Schulze, *Z. Anorg. Allg. Chem.*, 1977, **428**, 5-15.

363. B. S. Mandimutsira, S. J. Chen, K. D. Demadis and D. Coucouvanis, *Inorg. Chem.*, 1995, **34**, 2267-2268.

364. M. Parvez, P. M. Boorman and M. Wang, *Acta Cryst. C.*, 1997, **53**, 413-414.

365. J. Cragel, V. B. Pett, M. D. Glick and R. E. DeSimone, *Inorg. Chem.*, 1978, **17**, 2885-2893.

366. R. E. DeSimone and M. D. Glick, *Inorg. Chem.*, 1978, **17**, 3574-3577.

367. N. Dupre, H. M. J. Hendriks and J. Jordanov, *J. Chem. Soc., Dalton Trans.*, 1984, DOI: 10.1039/DT9840001463, 1463-1465.

368. B. Kamenar, B. Korpar-Colig, M. Cindric, M. Penavic and N. Strukan, *J. Chem. Soc., Dalton Trans.*, 1992, 2093-2097.

369. U. Braun, R. Richter, J. Sieler, A. I. Yanovsky and Y. T. Struchkov, *Z. Anorg. Allg. Chem.*, 1985, **529**, 201-208.

370. G. K. Batsala, V. Dokorou, N. Kourkoumelis, M. J. Manos, A. J. Tasiopoulos, T. Mavromoustakos, M. Simčič, S. Golič-Grdadolnik and S. K. Hadjikakou, *Inorg. Chim. Acta*, 2012, **382**, 146-157.

371. P. Strauch, W. Dietzsch and L. Golič, *Z. Anorg. Allg. Chem.*, 1997, **623**, 129-134.

372. C. J. Ruffing and T. B. Rauchfuss, *Organometallics*, 1985, **4**, 524-528.

373. F. Bottomley and R. W. Day, *Can. J. Chem.*, 1992, **70**, 1250-1259.

374. R. Atencio, M. A. Casado, M. A. Ciriano, F. J. Lahoz, J. J. Pérez-Torrente, A. Tiripicchio and L. A. Oro, *J. Organomet. Chem.*, 1996, **514**, 103-110.

375. M. A. Casado, M. A. Ciriano, A. J. Edwards, F. J. Lahoz, J. J. Pérez-Torrente and L. A. Oro, *Organometallics*, 1998, **17**, 3414-3416.

376. M. A. Casado, M. A. Ciriano, F. J. Lahoz, L. A. Oro and J. J. Perez-Torrente, *J. Organomet. Chem.*, 2016, **812**, 123-134.

377. P. J. Lundmark, G. J. Kubas and B. L. Scott, *Organometallics*, 1996, **15**, 3631-3633.

378. M. A. Casado, M. A. Ciriano, A. J. Edwards, F. J. Lahoz, L. A. Oro and J. J. Pérez-Torrente, *Organometallics*, 1999, **18**, 3025-3034.

379. M. A. Casado, J. J. Pérez-Torrente, M. A. Ciriano, A. J. Edwards, F. J. Lahoz and L. A. Oro, *Organometallics*, 1999, **18**, 5299-5310.

380. M. A. F. Hernandez-Gruel, J. J. Pérez-Torrente, M. A. Ciriano, J. A. López, F. J. Lahoz and L. A. Oro, *Eur. J. Inorg. Chem.*, 1999, **1999**, 2047-2050.

381. M. A. F. Hernandez-Gruel, J. J. Perez-Torrente, M. A. Ciriano, A. B. Rivas, F. J. Lahoz, I. T. Dobrinovitch and L. A. Oro, *Organometallics*, 2003, **22**, 1237-1249.

382. S. Kuwata and M. Hidai, *Chem. Lett.*, 1998, **27**, 885-886.

383. S.-i. Kabashima, S. Kuwata and M. Hidai, *J. Am. Chem. Soc.*, 1999, **121**, 7837-7845.

384. S. Kuwata, S. Kabashima, N. Sugiyama, Y. Ishii and M. Hidai, *Inorg. Chem.*, 2001, **40**, 2034-2040.

385. N. Singh and S. Bhattacharya, *Dalton Trans.*, 2011, **40**, 2707-2710.

386. V. Jancik and H. W. Roesky, *Angew. Chem. Int. Ed.*, 2005, **44**, 6016-6018.

387. H. Kato, H. Seino, Y. Mizobe and M. Hidai, *J. Chem. Soc., Dalton Trans.*, 2002, 1494-1499.

388. W. Y. Yeh, H. Seino, T. Amitsuka, S. Ohba, M. Hidai and Y. Mizobe, *J. Organomet. Chem.*, 2004, **689**, 2338-2345.

389. T. Amitsuka, H. Seino, M. Hidai and Y. Mizobe, *Organometallics*, 2006, **25**, 3034-3039.

390. F. Takagi, H. Seino, Y. Mizobe and M. Hidai, *Organometallics*, 2002, **21**, 694-699.

391. A. Shinozaki, H. Seino, M. Hidai and Y. Mizobe, *Organometallics*, 2003, **22**, 4636-4638.

392. S. Kuwata, T. Nagano, A. Matsubayashi, Y. Ishii and M. Hidai, *Inorg. Chem.*, 2002, **41**, 4324-4330.

393. A. Matsubayashi, S. Kuwata, Y. Ishii and M. Hidai, *Chem. Lett.*, 2002, 460-461.

394. K. Arashiba, S. Matsukawa, S. Kuwata, Y. Tanabe, M. Iwasaki and Y. Ishii, *Organometallics*, 2006, **25**, 560-562.

395. J. Chen, V. G. Young Jr and R. J. Angelici, *Inorg. Chim. Acta*, 2005, **358**, 1623-1634.

396. T. Matsumoto, Y. Nakaya and K. Tatsumi, *Organometallics*, 2006, **25**, 4835-4845.

397. F. J. G. Alonso, M. G. Sanz, V. Riera, S. G. Granda and E. P. Carreño, *J. Chem. Soc., Dalton Trans.*, 1992, 545-548.

398. S. D. Huang, C. P. Lai and C. L. Barnes, *Angew. Chem. Int. Ed. Engl.*, 1997, **36**, 1854-1856.

399. K. A. Azam, M. A. Hossain, M. B. Hursthouse, S. E. Kabir, K. M. Abdul Malik and H. Vahrenkamp, *J. Organomet. Chem.*, 1998, **555**, 285-292.

400. U. Brand and J. R. Shapley, *Inorg. Chem.*, 1998, **37**, 5697-5699.

401. J. Li, D. Miguel, M. D. Morales, V. Riera and S. García-Granda, *Organometallics*, 1998, **17**, 3448-3453.

402. D. Miguel, J. Li, D. Morales, V. Riera and S. García-Granda, *Organometallics*, 2001, **20**, 3063-3069.

403. B. R. Cockerton and A. J. Deeming, *Polyhedron*, 1994, **13**, 2085-2088.

404. Y.-K. Au, K.-K. Cheung and W.-T. Wong, *Inorg. Chim. Acta*, 1995, **228**, 267-275.

405. Y.-K. Au, K.-K. Cheung and W.-T. Wong, *J. Chem. Soc., Dalton Trans.*, 1995, 1047-1057.

406. O. R. Reyes-López, M. A. Leyva and M. J. Rosales-Hoz, *J. Mol. Struct.*, 2011, **985**, 134-138.

407. C. A. Ghilardi, S. Midollini, A. Orlandini, C. Battistoni and G. Mattogno, *J. Chem. Soc., Dalton Trans.*, 1984, 939-942.

408. C. A. Ghilardi, S. Midollini, A. Orlandini and G. Scapacci, *J. Chem. Soc., Dalton Trans.*, 1992, 2909-2910.

409. M. C. Jennings, N. C. Payne and R. J. Puddephatt, *Inorg. Chem.*, 1987, **26**, 3776-3781.

410. L. Han, L.-X. Shi, L.-Y. Zhang, Z.-N. Chen and M.-C. Hong, *Inorg. Chem. Commun.*, 2003, **6**, 281-283.

411. Y.-H. Qin, M.-M. Wu and Z.-N. Chen, *Acta Cryst. E.*, 2003, **59**, m317-m318.

412. W.-N. Zhao, L. Han and C.-C. Luo, *Acta Cryst. C.*, 2008, **64**, m280-m282.

413. Y.-D. Chen, Y.-H. Qin, L.-Y. Zhang, L.-X. Shi and Z.-N. Chen, *Inorg. Chem.*, 2004, **43**, 1197-1205.

414. T. F. Beltran, M. Feliz, R. Llusar, V. S. Safont and C. Vicent, *Eur. J. Inorg. Chem.*, 2013, **2013**, 5797-5805.

415. T. Ikada, Y. Mizobe, S. Kuwata and M. Hidai, *J. Chem. Soc. Jpn.*, 2001, **2001**, 493-500.

416. H. Kato, H. Seino, Y. Mizobe and M. Hidai, *Inorg. Chim. Acta*, 2002, **339**, 188-192.

417. K. Iwasa, H. Seino, F. Niikura and Y. Mizobe, *Dalton Trans.*, 2009, 6134-6140.

418. S. Wirth and D. Fenske, *Z. Anorg. Allg. Chem.*, 1999, **625**, 2064-2070.

419. T. Ahmad, T. Rüffer, H. Lang, A. A. Isab and S. Ahmad, *Inorg. Chim. Acta*, 2009, **362**, 2609-2612.

420. R. Graves, J. M. Homan and G. L. Morgan, *Inorg. Chem.*, 1970, **9**, 1592-1593.

421. F. Sécheresse, J. Lefèbvre, J. C. Daran and Y. Jeannin, *Inorg. Chim. Acta*, 1981, **54**, L175-L176.

422. F. Sécheresse, J. M. Manoli and C. Potvin, *Inorg. Chem.*, 1986, **25**, 3967-3971.

423. M. E. Noble, J. C. Huffman and R. A. D. Wentworth, *Inorg. Chem.*, 1983, **22**, 1756-1760.

424. J. R. Long, L. S. McCarty and R. H. Holm, *J. Am. Chem. Soc.*, 1996, **118**, 4603-4616.

425. J.-Q. Wang, S. Cai, G.-X. Jin, L.-H. Weng and M. Herberhold, *Chem. Eur. J.*, 2005, **11**, 7342-7350.

426. S.-L. Li, J.-Y. Wu, Y.-P. Tian, X.-T. Tao, M.-H. Jiang and H.-K. Fun, *Chem. Lett.*, 2005, **34**, 1186-1187.

427. S. Delgado, P. J. Sanz Miguel, J. L. Priego, R. Jiménez-Aparicio, C. J. Gómez-García and F. Zamora, *Inorg. Chem.*, 2008, **47**, 9128-9130.

428. N. Zheng, J. Zhang, X. Bu and P. Feng, *Cryst. Growth Design*, 2007, **7**, 2576-2581.

429. L. Han, W. Zhao, Y. Zhou, X. Li and J. Pan, *Cryst. Growth Design*, 2008, **8**, 3504-3507.

430. J. Zhang, S. Chen and X. Bu, *Dalton Trans.*, 2010, **39**, 2487-2489.

431. J. Zhang, Y.-S. Xue, L.-L. Liang, S.-B. Ren, Y.-Z. Li, H.-B. Du and X.-Z. You, *Inorg. Chem.*, 2010, **49**, 7685-7691.

432. X.-L. Yang, J. Zhang, S.-B. Ren, Y.-Z. Li, W. Huang, H.-B. Du and X.-Z. You, *Inorg. Chem. Commun.*, 2010, **13**, 1337-1339.

433. Z.-M. Hao, R.-Q. Fang, H.-S. Wu and X.-M. Zhang, *Inorg. Chem.*, 2008, **47**, 8197-8203.

434. B. J. Miller, D. L. Howard, J. R. Lane, H. G. Kjaergaard, M. E. Dunn and V. Vaida, *J. Phys. Chem. A*, 2009, **113**, 7576-7583.

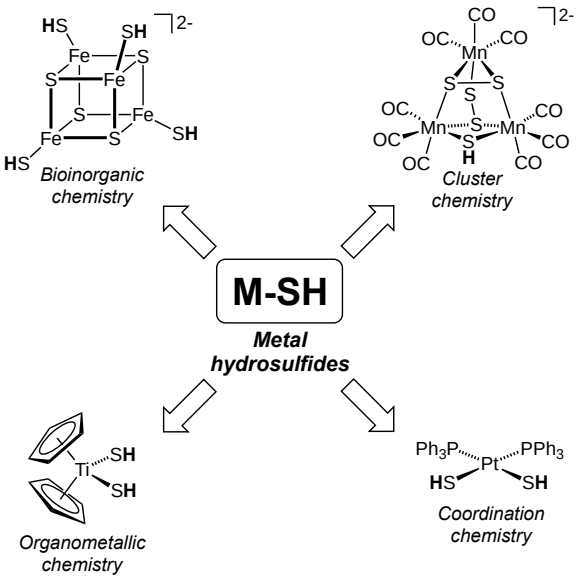
HS
SH
Fe
S
Fe
S
Fe
Fe
S
SH
HS
2-
Bioinorganic chemistry
CO
OC
CO
Mn
S
S
S
S
OC
Mn
S
Mn
CO
OC
S
CO
H
OC
CO
2-
Cluster chemistry
M-SH
Metal hydrosulfides
Ti
SH
SH
Organometallic chemistry
Ph3P
PPh3
Pt
HS
SH
Coordination chemistry